TGF-β family signaling in the regulation of cell plasticity in lung cells and mesothelioma

Jenni Tamminen

Research Programs Unit, Translational Cancer Biology,
Haartman Institute, Transplantation Laboratory
Faculty of Medicine
University of Helsinki
Finland

ACADEMIC DISSERTATION

To be presented, with the permission of the Faculty of Medicine, University of Helsinki, for public examination in Lecture Hall 1, Haartmaninkatu 3, Helsinki on December 19th 2014 at 1 pm

Helsinki, 2014

Thesis supervisor

Docent Katri Koli, Ph.D.

Translational Cancer Biology Research Program

University of Helsinki, Finland

Thesis reviewers

Docent Hannu Koistinen, D.Sc.

Department of Clinical Chemistry

University of Helsinki, Finland

and

Docent Terttu Harju, MD, Ph.D.

Department of Medicine, Respiratory Unit, Oulu University Hospital
Respiratory Research Unit, Medical Research Center Oulu,

Oulu University Hospital and University of Oulu

Finland

Thesis opponent

Professor Maréne Landström

Department of Medical Biosciences

University of Umeå, Sweden

ISBN 978-951-51-0490-8 (paperback)
ISBN 978-951-51-0491-5 (PDF)

Original publications

This thesis is based on the following original publications, which are referred to by their Roman numerals in the text.

I Tamminen JA, Myllärniemi M, Hyytiäinen M, Keski-Oja J and Koli K: Asbestos exposure induces alveolar epithelial cell plasticity through MAPK/Erk signaling. J Cell Biochem. 113: 2234-47, 2012

II Tamminen JA, Parviainen V, Rönty M, Wohl AP, Murray L, Joenväärä S, Varjosalo M, Leppäranta O, Ritvos O, Sengle G, Renkonen R Myllärniemi M and Koli K: Gremlin-1 associates with fibrillin microfibrils *in vivo* and regulates mesothelioma cell survival through transcription factor slug. Oncogenesis 2: e66, 2013

III Tamminen JA, Yin M, Rönty M, Sutinen E, Pasternack A, Ritvos O, Myllärniemi M and Koli K: Overexpression of activin-A and -B in malignant mesothelioma – attenuated Smad3 signaling responses and ERK activation promote cell migration and invasive growth. Manuscript submitted, 2014

Abbreviations

ALK	activin receptor–like kinase
AP-MS	affinity purification-mass spectrometry
ARE	activin response element
ATCC	American Type Culture Collection
BMP	bone morphogenetic protein
CK-7	cytokeratin-7
cDNA	complementary DNA
DAN	differential screening selected gene aberrative in neuroblastoma
DNA	deoxyribonucleic acid
ECM	extracellular matrix
EGF	epidermal growth factor
EGFR	epidermal growth factor receptor
EMT	epithelial-to-mesenchymal transition
ERK	extracellular signal-regulated kinase
FAST-1	fork head activin signal transducer-1
FN	fibronectin
FST	follistatin
FSTL3	follistatin-like 3
ID1	inhibitor of differentiation-1
IκB	inhibitor of κB
IPF	idiopathic pulmonary fibrosis
JNK	c-Jun N-terminal kinase
LC-MS	liquid chromatography-mass spectrometry
LTBP	latent TGF-β binding protein
MAPK	mitogen activated protein kinase
MM	malignant mesothelioma
MMP	matrix metalloproteinase
mRNA	messenger RNA

NF-κB	nuclear factor κ light polypeptide gene enhancer in B-cells1
NHBE	normal human bronchial epithelial cells
PDGF	platelet derived growth factor
PCR	polymerase chain reaction
PBS	phosphate buffered saline
RNA	ribonucleic acid
RT-PCR	reverse transcription PCR
SAEC	small airway epithelial cells
siRNA	small interfering RNA
SDS-PAGE	sodium dodecyl sulfate polyacrylamide gel electrophoresis
α-SMA	α-smooth muscle actin
TBP	TATA binding protein
TBS	tris buffered saline
TGF-β	transforming growth factor-β
TNF-α	tumor necrosis factor-α
WT-1	Wilms' tumor-1
ZO-1	zonula occludens-1
2D	two dimensional
3D	three dimensional

Abstract

The aim of this thesis was to extend the understanding of molecular mechanisms of asbestos exposure related diseases asbestosis (lung fibrosis), lung cancer and mesothelioma. This thesis consists of three parts. The first study investigated the responses that asbestos exposure induced in lung epithelial cells. Epithelial-to-mesenchymal transition (EMT) is implicated in fibrosis and in cancer, both asbestos induced diseases. It was therefore tested whether asbestos fibers induced EMT. In the next two studies, the focus was on mesothelioma. Mesothelioma is an aggressive cancer that is characterized by chemoresistance and local invasion. In these two studies, the aim was to recognize novel potential therapeutic target molecules and pathways involved in chemoresistance and invasion.

By analyzing alterations in cellular protein levels in two (2D) and three dimensional (3D) cell cultures, we found that exposure to asbestos led to loss of epithelial characteristics when lung epithelial cells retained the type II airway epithelial cell phenotype. This loss of epithelial characteristics was found not to depend on TGF-β or Smad signaling cascades. Comparing activities of cancer associated signaling pathways between normal and cancer cells provided us with three candidate pathways. We exposed the cells to asbestos and analyzed the impact of specific inhibitors on epithelial plasticity and phosphorylation levels of intracellular signaling proteins. The MAPK/ERK pathway was found to mediate epithelial plasticity in response to asbestos exposure.

A screen for new gremlin-1 interacting proteins discovered fibrillin-2. This finding was validated in mesothelioma tumor samples in which gremlin-1 and fibrillin-2 were found to co-localize. Primary mesothelioma cells were harvested from pleural effusion samples from mesothelioma patients. These cells recapitulated primary tumor characteristics and overexpressed gremlin-1, fibrillin-2 and transcription factor slug. The association of gremlin-1 with slug was validated *in vitro* and in the tumors. The link between chemoresistant EMT phenotype and high gremlin-1 and slug expression was analyzed using siRNA interference and exposure to chemotherapeutic drugs. Silencing of gremlin-1 downregulated slug, reverted the EMT-phenotype and sensitized the cells to the cytotoxic effect of chemotherapeutic drugs. The concomitant overexpression of gremlin-1 and fibrillin-2 enables gremlin targeting to fibrillin-2 containing fibers in mesothelioma extracellular matrix, where it supports the chemoresistant EMT phenotype through transcription factor slug.

Mesothelioma tumors as well as primary mesothelioma cells and mesothelioma cell lines were found to overexpress activin-A and activin-B. Canonical Smad3 response to activin stimulation was attenuated in mesothelioma cells. Attenuation of the Smad3 response associated with migratory and invasive phenotype analyzed by conventional and live cell imaging in 2D systems as well as in 3D matrigel matrix. Analysis of phosphorylation levels of intracellular signaling proteins revealed that activins induced the MAPK/ERK signaling cascade. Invasion, migration and ERK activation was impaired by sequestering extracellular activins by soluble activin-receptor. Likewise, inhibiting MAPK/ERK upstream kinase impaired migration and invasion. Mesothelioma cells switch from canonical Smad3 signaling to non-canonical MAPK/ERK pathway, and this promotes migration and invasion.

The results presented in this thesis support the concept that pathological EMT is a central mechanism in the development and progression of asbestos induced fibrotic and malignant diseases. They also suggest gremlin-1 and activin-A as new potential therapeutic targets in mesothelioma.

Tiivistelmä

Tämä väitöskirjatyö tutki asbestin aiheuttamien sairauksien molekyylimekanismeja. Asbestialtistus aiheuttaa keuhkojen sidekudostumista (asbestoosi), keuhkosyöpää sekä keuhkopussin syöpää (mesotelioma). Epiteeli-mesenkyymi-transitio (EMT) on tärkeä mekanismi syövän ja sidekudossairauksien etenemisessä. Tämä väitöskirja koostuu kolmesta osasta. Ensimmäisessä osatyössä tutkittiin asbestin aiheuttamia vasteita keuhkon epiteelisoluissa ja testattiin, aiheuttaako asbesti EMT:tä. Kaksi seuraavaa osatyötä keskittyivät mesotelioomaan. Näissä osatöissä etsittiin molekyylejä ja solunsisäisiä viestireittejä, jotka vaikuttavat mesotelioomaan kykyyn tunkeutua aggressiivisesti ympäröiviin kudoksiin ja kykyyn vastustaa solunsalpaajahoitoja.

Asbestille altistettuja keuhkon epiteelisoluja tutkittiin kaksi- (2D) ja kolmiulotteisissa (3D) kasvuympäristöissä. Havaitsimme, että tyypin II keuhkoepiteelisolut, menettävät epiteliaalisia ominaisuuksiaan asbestialtistuksen seurauksena. Tällainen plastisuus viittaa EMT tapahtumiin. Nämä tapahtumat eivät olleet riippuvaisia TGF-β tai Smad- viestireiteistä. Vertailtaessa normaalien keuhkoepiteelisolujen ja syöpäsolujen solunsisäisten viestireittien aktiivisuuksia löydettiin eroja kolmen viestireitin välillä. Näistä reiteistä MAPK/ERK viestireitti osoittautui olevan se, joka aktivoituu asbestialtistuksen seurauksena ja joka sai aikaan epiteeli-mesenkyymi-transitioon viittaavaa plastisuutta keuhkojen epiteelisoluissa.

Systemaattisessa etsinnässä fibrilliini-2 paljastui uudeksi gremliini-1:teen sitoutuvaksi proteiiniksi. Analysoitaessa mesotelioomapotilaiden kudosnäytteitä havaittiin, että sekä gremliiniä että fibrilliiniä ilmennettiin juuri syöpäkudoksessa ja että nämä proteiinit lokalisoituivat hyvin lähelle toisiaan. Mesotelioomapotilaiden pleuranesteestä eristettiin ja kasvatettiin primaarimesotelioomasoluja. Nämä solut yli-ilmensivät gremliiniä, fibrilliiniä sekä transkriptiofaktori slugia syöpäkasvaimen tapaan. Gremliinin ja slugin välinen yhteys varmennettiin syöpäkudosnäytteissä sekä soluviljelmissä. Gremliinin ja slugin välistä yhteyttä sekä niiden merkitystä lääkeresistentissä EMT-fenotyypissä tutkittiin vähentämällä gremliini-1:n ilmenemistä ja altistamalla soluja solunsalpaajille. Gremliinin ilmenemistasojen lasku johti slugin ilmenemistasojen laskuun, EMT-fenotyypin peruuntumiseen ja lisäsi solujen herkkyyttä solunsalpaajille. Gremliini-1:n ja fibrilliini-2:n samanaikainen yli-ilmentäminen mesotelioomassa mahdollistaa gremliini-1:n lokalisaation soluväliaineeseen mesotelioomassa. Gremliini-1 ylläpitää lääkeresistenttiä EMT- fenotyyppiä slugin välityksellä.

Aktiviini-A:ta ja aktiviini-B:tä yli-ilmennetään mesotelioomasyöpäkudoksessa sekä primaari-mesotelioomasoluissa ja solulinjoissa. Havaittiin, että mesotelioomasoluissa kanoninen Smad3 vaste aktiviineille on heikentynyt ja tämä piirre kytkeytyi solun kykyyn invasiiviseen kasvuun 3D ympäristössä ja migraatioon 2D ympäristössä. Analysoimalla signalointiproteiinien fosforylaatiotasoja havaittiin, että aktiviinit aktivoivat mesotelioomasolussa Smad3-reitin sijaan MAPK/ERK-viestireitin ja tämä pystyttiin estämään sitomalla spesifisti solunulkoiset aktiviinit liukoisella aktiviinireseptorilla. Tämä heikensi huomattavasti mesotelioomasolujen migraatiota ja invaasiota. Samoin teki MAPK/ERK-viestireitin salpaus. Havaitsimme, että muutos Smad3-viestireitiltä MAPK/ERK-viestireitille edistää mesotelioomasolujen invasiivisuutta ja migraatiota.

Tämän väitöskirjatyön tulokset tukevat näkemystä, että patologinen EMT on keskeinen mekanismi asbestisairauksien kehittymisessä ja etenemisessä. Tutkimuksen valossa gremliini-1 ja aktiviini-A ovat uusia potentiaalisia kohdemolekyylejä mesotelioomaan hoidossa.

1. Review of the literature

Tissue homeostasis requires tightly regulated interplay between intra- and extracellular environments and involves various cell types. These two environments sustain the balance by reciprocal communication. Disturbance of this balance can lead to a disease. Damage activates tissue repair processes. Organisms have various means to eliminate damaged cells, foreign organisms or materials that try to disturb the balance. These mechanisms include innate and adaptive immune systems. Damaged and aberrant cells are removed by apoptosis. If these surveillance mechanisms fail and the balance is permanently disturbed, the condition can develop into a malignant or fibrotic disease. Often in these diseases developmental genes are reactivated and the cellular processes associated with tissue repair are deregulated. This can promote disease progression.

1.1 Asbestos fibers

Asbestos is a common name for a group of silica fibers. These naturally occurring fibers are strong and flexible; resistant to heat and most chemicals; and have therefore been used for various construction and insulation purposes.

1.1.1 Fiber types and exposure

Asbestos fibers are categorized into serpentine and amphibole fibers. Chrysotile is the only form of serpentine asbestos. These serpentine fibers are curly, whereas amphibole fibers are straight. Amphibole fibers include crocidolite, amosite, anthophyllite, tremolite and actinolite asbestos. Serpentine fibers are cleared from the lung more efficiently than amphiboles, meaning that the biopersistence is greater for amphibole fibers [1, 2]. However, all forms of asbestos are associated with increased risk of malignant as well as non-malignant diseases [3]. Exposure to airborne asbestos fibers is usually work related. However, asbestos is a naturally occurring mineral, and exposure can also happen when people live near natural asbestos deposits. The burden of the asbestos fibers in the lung depends on the amount of fibers deposited and the clearance of the fibers [1].

1.1.2 Cessation of asbestos usage and current exposure

In Finland, the use of new asbestos was ceased in 1988, and the manufacture, import, sale and utilization of asbestos containing products was forbidden in 1992 [4]. Furthermore, the European Union has banned asbestos use since 1999 (1999/77/EY) and this EU directive eliminated the last exceptions for asbestos use in Finland by 2005. Nowadays, in Finland a risk for exposure still remains in demolition and renovation work of old buildings.

1.2 Asbestos exposure related diseases

Asbestos fibers cause genetic and cellular damage and chronic inflammation [5]. Asbestos can cause lung cancer and mesothelioma as well as non-malignant pleural changes, such as pleural plaques, benign pleural effusion, fibrosis of visceral pleura and fibrosis of lung tissue (asbestosis).

1.2.1 Latency

The worldwide asbestos consumption peaked in 1980's [3] and in Finland in 1970's [4]. All asbestos exposure related diseases are preceded by a long latent period of 10-40 years, or even longer [3, 4]. Considering the long latency together with the rather recent termination of asbestos consumption, it is clear that the peak in the incidence of asbestos exposure related diseases is yet to come. In Finland, the peak is expected to occur 2010-2015 [4] and in Europe 2010-2020 [3]. When the view is expanded worldwide, the peak runs further to the future, as many countries have only recently restrained the use of asbestos.

1.2.2 Asbestosis

Asbestosis is an asbestos induced lung fibrosis, which shares common features with another devastating lung disease idiopathic pulmonary fibrosis (IPF) [6]. Histological findings in IPF include usual interstitial pneumonia (UIP) [7]. These lesions are also found in the histology of asbestosis [8]. In asbestosis, also asbestos bodies and fibers are detectable in lung tissue [9, 10]. Both asbestosis and IPF eventually lead to the loss of lung function, and the treatment options are limited. Lung transplantation may rescue a patient with lung fibrosis (http://www.hus.fi/sairaanhoito/sairaanhoitopalvelut/elinsiirrot/keuhkonsiirrot/Sivut/default.aspx, accessed 1.9.2014). In Finland, 20-30 lung transplantations are done each year for different reasons, including lung fibrosis, and the prognosis is usually rather good. After five years of the operation 80% are alive and after ten years 50 %. Both asbestosis and IPF increase the risk for lung cancer [6, 11, 12]. If a patient with asbestosis or IPF is a smoker the cancer risk increases further [11, 13]. Annually, 60-90 new cases of asbestosis are reported in Finland (Finnish Institute of Occupational Health). The progression of the disease and the prognosis differs between the patients. Although not curable, anti-fibrotic drug pirfenidone has shown efficacy and is available for the treatment of IPF in Europe [14]. No comprehensive data is available for pirfenidone treatment in patients with asbestosis.

1.2.3 Lung cancer

The location and histology of asbestos-induced lung cancer (bronchogenic carcinoma) is indistinguishable from lung cancer not related to asbestos exposure [4, 11]. Asbestos-induced lung cancer, however, tends to occur at a younger age. Asbestosis and smoking increases the risk for lung cancer in asbestos exposed individuals [1, 11]. Smoking does this likely through impairment of fiber removal from the lung. Impaired fiber removal is likely also one of the mechanisms by which fibrosis increases the cancer risk. When the carcinogenic fibers remain longer in the airways, the prolonged exposure can contribute to increased cancer risk. No significant differences in the prognosis of non-asbestos-related or asbestos-induced lung cancer have been reported [11]. More than 2000 lung cancers are reported in Finland each year [4] and majority of them have dismal prognosis. After careful staging and defining the histological type of the lung cancer the treatment is designed for the cancer patient according to the Finnish Current Care Guidelines (http://www.kaypahoito.fi/web/english/guidelines/guideline?id=ccs00057, accessed 13.10.2014). Treatment with combinations of surgery (when possible) and radiotherapy with single or multi-drug chemotherapy prolongs survival but is rarely curable.

1.2.4 Molecular mechanisms in asbestosis and asbestos induced lung cancer

In all asbestos exposure related diseases, changes occur in gene expression, epigenetic regulation and in intracellular signaling cascades which contribute to the disease initiation and progression [1]. These changes are brought by the fibers directly, as well as by oxidants that are generated on the surfaces of the fibers and generated and released by the cells. In the lung, asbestos initiated inflammatory reactions and accumulation of alveolar macrophages is followed by a loss of alveolar epithelial cells, fibroblast accumulation and collagen deposition [6]. Fiber deposition in the lungs also induces persistent inflammation [1]. The cellular responses initiating different diseases (asbestosis, lung cancer or mesothelioma) probably overlap. However, there are likely some specific differences that will lead to development of distinct disease. There are probably also genetic differences in the susceptibility to asbestosis among exposed individuals [15, 16].

The cellular responses to asbestos fibers can be different during disease initiation and progression [1]. Common early events in asbestosis and in IPF are injury, repair and apoptosis of alveolar epithelial cells (AEC) and recruitment of inflammatory cells [6, 17]. There are two types of alveolar epithelial cells; type I and type II [18, 19]. The type II cells can differentiate into type I cells. Type I cells make the gas exchange surface of the alveoli and comprise ~90% of the alveolar surface area [6]. The type II cells synthesize, store and release pulmonary surfactant proteins and function as a plastic proliferative repertoire for type I cells [18, 19].

Many of the same factors that direct tissue repair also promote fibrosis [20]. Repeated injury induced by the fibers and aberrant repair leads to persistent and progressive fibrosis. *In vitro* and in rodent models, asbestos induces lytic cell death and apoptosis of epithelial and mesothelial cells and this stimulates wound healing processes including compensatory cell proliferation [2]. Asbestos initiates the accumulation of alveolar macrophages, which produce profibrotic growth factors and cytokines. Implicated in asbestos related lung diseases are various bioactive molecules for example transforming growth factor- β (TGF-β), tumor necrosis factor-α (TNF-α), interleukin-1β (IL-1β) and platelet derived growth factor (PDGF) [1, 6, 20]. The inflammatory cytokines attract inflammatory cells and affect lung epithelium and fibroblasts. Inflammation promotes fibroblast dysfunction and epithelial cell proliferation. Accumulating evidence suggests TNF-α regulated TGF-β1 production to be important in the pathogenesis of asbestosis [1]. PDGF isoforms are implicated in organ fibrosis and also in the development of asbestosis. PDGF binds its specific receptors (PDGFR, α-and β-receptors) on fibroblasts and promotes myofibroblast growth and survival [20]. Asbestos also induces production of reactive oxygen and nitrogen species (ROS and NOS) [6, 21]. ROS are generated at the surfaces of asbestos fibers; they are released by macrophages as a result of unsuccessful phagocytosis of large fibers and ROS can also originate from mitochondria of inflammatory cells or lung epithelial or mesothelial cells. Asbestos induced oxidative stress promotes ROS dependent signaling, pulmonary inflammation, matrix remodeling and degradation as well as fibrogenesis.

After interaction with the cells, asbestos fibers and ROS initiate various signaling cascades and activate transcription factors, including mitogen activated protein kinases (MAPK), activator protein-1 (AP-1), nuclear factor-κB (NF-κB) and protein kinase C (PKC) [1, 2]. AP-1 is a redox sensitive transcription factor and its binding to DNA is increased by asbestos [2, 22, 23] (see also 1.6.1). Asbestos induces proto-oncogenes *c-fos* and *c-jun*, which are subunits of AP-1, in bronchial

epithelial and in pleural mesothelial cells and contributes to their proliferative responses to the fibers. Furthermore, AP-1 proteins are phosphorylated and activated also by MAPkinases [2]. Activation of NF-κB is critical in upregulation of various genes linked to inflammation, proliferation and apoptosis, as well as chemokine and cytokine production [23]. Asbestos induced inflammatory response activates NF-κB in tracheal epithelial cells *in vitro* and *in vivo* leading to transcriptional activation of a number of NF-κB- dependent genes, including the proto-oncogene *c-myc* [23-25]. Cell survival promoting NF-κB can also be activated via the EGFR-(PI3-K)/AKT pathway [23]. Furthermore, asbestos fibers have been reported to directly bind and activate the epidermal growth factor receptor (EGFR) [26] .

Lung epithelial cells communicate with the underlying fibroblasts and smooth muscle cells through paracrine signaling [1]. Epithelial cells produce various factors, including ligands for EGFR. This signaling through EGFR plays an important role in asbestos induced fibrosis by promoting fibroblast proliferation. Also ROS mediate part of their signaling effects through EGFR on fibroblasts and epithelial cells, as well as other cell types. Importantly, asbestos fibers or ROS initiated signaling cascades are significantly different in duration of the signal compared to the endogenous ligand stimulated responses [1]. The components of the downstream signaling cascade can also be different. Accumulating evidence suggests that the EGFR-MEK-MAPK/ERK cascade is an important target for therapeutic intervention in asbestos related lung diseases.

Mutations and altered expression of the tumor suppressor p53 are found in lung cancer and in lung fibrosis [1, 6, 17], whereas in mesothelioma p53 mutations are rare (see below). After asbestos exposure p53 mediates mitochondria-regulated apoptosis in lung epithelial cells [6]. Wild type p53 also promotes cell cycle arrest by transcriptionally activating p21(Cip1/Waf1) [27].

1.2.5 Mesothelioma

Malignant mesothelioma (MM) is a relatively rare tumor but it is among the most aggressive ones [28]. Detection of MM can be difficult [29] and often takes place in late stages of the disease, which in part affects the poor prognosis of the patients [28]. In Finland, 60-80 new mesotheliomas are diagnosed each year (the Finnish Institute of Occupational Health). Majority of mesotheliomas associate with previous, usually work related asbestos exposure but 20-25% of mesotheliomas occur in individuals no apparent exposure, suggesting that there is a genetic susceptibility to mesothelioma or an additional causative agent, or both [28, 30]. Majority of the exposed individuals never develop mesothelioma [17].

Mesothelioma arises from mesothelial cells lining pleura, peritoneum or, in rare cases, pericardium. Histologically mesotheliomas are divided into three subgroups: epithelioid, sarcomatoid and biphasic [29]. Epithelioid mesotheliomas compose of polygonal, oval or cuboidal cells that can resemble non-neoplastic reactive mesothelial cells. Sarcomatoid mesotheliomas generally consist of spindle shaped cells. Biphasic mesotheliomas contain both epithelioid and sarcomatoid areas within the same tumor. Epithelioid mesothelioma is the most frequent subtype, more amenable to treatment and has better prognosis compared to the sarcomatoid or biphasic forms. However, better prognosis means only longer survival with the disease. Unfortunately, mesothelioma is currently incurable. Compared to pleural mesothelioma, the sarcomatoid and biphasic subtypes are rare in peritoneal mesothelioma [31, 32].

Early stage tumors may be surgically removed, but this rarely results in complete resection [28]. Surgery is usually combined with chemotherapy, sometimes also radiotherapy. Inoperable tumors are treated with chemotherapy. Current standard of care for first line chemotherapy is platinium compound (cisplatin or carboplatin) combined with a folate inhibitor (pemetrexed). However, response rates are low and reoccurrences common. The pattern of spread surrounding the lung in the proximity of vital organs (heart, spinal cord), together with usually large surface area of the tumor, limits the delivery of effective therapeutic doses of radiation without significant toxic effects. Clinical trials of new therapeutics have found histone deacetylases and acetyltransferases as well as anti-angionetic agents ineffective [28]. Surprisingly, although EGFR is highly overexpressed in mesothelioma tumors and MAPK/ERKs are strongly implicated in MM, also small molecule EGFR tyrosine kinase inhibitors gefitinib and erlotinib have failed to show clinical effect in MM patients [33, 34]. The overexpression of rather specific proteins and the involvement of chronic inflammation in MM have driven clinical trials that are evaluating the potency of immunotherapies alone or combined with chemotherapies in the treatment of MM. These include dendritic cell (DC)[35] and WT-1 [36] analog peptide vaccines and antibodies targeting mesothelin [37].

1.2.6 Molecular mechanisms in mesothelioma

Suggested mechanisms through which asbestos fibers cause mesothelioma overlap the ones suggested to underlie the pathogenesis of asbestosis and lung cancer. Interestingly, the same signal transduction pathways activated by asbestos are also important in survival and chemoresistance of mesotheliomas and lung cancer [23]. Some of the asbestos activated pathways and mechanisms through which asbestos induces fibrosis and malignant diseases are presented in Figure 1.

Similarly to other asbestos exposure related diseases, ROS likely play a central role also in the pathogenesis of mesothelioma [5, 23]. ROS are produced when macrophages and mesothelial cells engulf asbestos fibers. Asbestos fibers can tangle with the chromosomes and the mitotic spindle, leading to chromosomal abnormalities and aneuploidy of mesothelial and other cells. In addition, asbestos fibers can absorb various proteins and chemicals. This can lead to deprivation of important cellular proteins or to the accumulation of toxic and carcinogenic compounds, or both. Finally, macrophages and mesothelial cells release a variety of growth factors and cytokines in response to asbestos exposure. These include TNF-α, IL-1β, TGF-β and PDGF isoforms. Asbestos exposure also induces necrotic cell death and release of high mobility group box 1 protein (HMGB-1) from mesothelial cells into the extracellular space *in vitro* and *in vivo* [38]. HMGB-1 is a nuclear protein, and its release initiates persistent inflammatory response, secretion of TNF-α, which activates NF-κB. NF-κB can then promote the survival of the mesothelial cells that have accumulated genetic damage due to the asbestos exposure. Based on *in vitro* data and analysis of patient material, high HMGB-1 expression has been suggested to act as prognostic marker for mesothelioma [39] and to support mesothelioma progression [40]. High expression of another high-mobility group A protein with similar functions, HMGA2, is associated with poor prognosis in MM [41].

The most frequently mutated tumor suppressor genes in mesothelioma include cyclin –dependent kinase inhibitor 2A/alternative reading frame (CDKN2A/ARF) (homozygous deletion in ~70% of epithelioid and in ~100% of sarcomatoid type), neurofibromatosis type 2 (NF2) (mutation or

homozygous deletion in 40-50%, not subtype defined) and tumor suppressor BRCA1-associated protein-1 (BAP1) (somatic mutation in ~23 %, not subtype defined) [5, 41, 42]. Furthermore, germ line mutations of BAP1 have also been suggested to genetically predispose to mesothelioma development [43, 44]. Genetic variants of the DNA repair enzyme genes, as well as epigenetic-related genes, may also contribute to the susceptibility difference to mesothelioma [5].

Mesotheliomas display some of the hallmarks of most cancers [28]. Mesothelioma tumors suppress apoptosis, become self-sufficient in mitogenic signaling and capable to cell replication and tissue invasion. However, some oncogenic events commonly seen in other solid tumors are rarely seen in mesothelioma. These include activation of the *RAS* oncogene, commonly seen in lung cancer, and inactivation of the tumor suppressor gene *TP53* [5, 45].

Mesothelioma frequently exhibits localized intracavitary growth and aggressive invasion instead of distal metastasis [28]. Mesotheliomas exhibit various defects in mitogenic signaling pathways as well as disruption of cell cycle control. Furthermore, similarly to other solid tumors, persistent activation of the canonical receptor tyrosine kinase (RTK) Ras/ERK1/2 and the phosphaditylinositol-3-kinase/AKT pathways are common in human mesothelioma and frequently recapitulated in mouse models of MM [28, 46-48]. However, despite constitutive and simultaneous activation of several RTKs, activating mutations of the oncogenes involved in these cascades, such as K-Ras and epidermal growth factor receptor families, are rare in mesothelioma [5].

1.2.7 Complexity and multiplicity of asbestos induced diseases

Although asbestos initiated responses in different cell types clearly overlap, the mechanism by which asbestos induces asbestosis, lung cancer or mesothelioma appears to differ to some extent [1, 6, 29, 30]. In addition to the disease itself, these differences can result from the tissue as well as from the genetic background of the individual.

Historically, chrysotile has been the most commonly used type of asbestos [3, 28] but it has been suggested to be less potent in inducing mesothelioma than amphibole fibers, whereas in lung cancer this trend was reported to be less clear [49]. Crocidolite asbestos has been suggested to be the asbestos type most frequently associated with mesothelioma in humans [50] and to be the most carcinogenic type of asbestos [5]. Interestingly, mesothelioma can also result from exposure to naturally occurring non-asbestos fibers, such as erionite or vermiculite ore [51, 52]. However, no confirmative link between certain fiber type and specific disease has been established [17, 28].

In most studies on asbestos exposure related diseases, majority of the patients are men. One significant reason for this is likely, that most of the jobs with a high risk of exposure, such as car mechanics, working at the construction sites and ship yards have traditionally been occupied by men, not so much by women. There is not enough evidence to firmly link any predisposing factors, such as age, gender or genetics to asbestos exposure related lung cancer [11]. However, in mesothelioma male sex, non-epitheloid cell type and poor performance status indicate poor prognosis [53]. Intriguingly, smoking increases the risk for lung cancer in asbestos exposed individuals [11] but not the risk for mesothelioma [54].

Physical properties of the fiber can affect biopersistence and clearance of the fiber as well as generation of reactive species and initiated cellular signaling responses [5, 23, 28]. However, all types of asbestos fibers induce malignant and nonmalignant diseases [3]. Different doses and exposure times may also have different effect [17]. Asbestos dose can be crucial determinant for triggered inflammation type [6]. Low dose exposure for prolonged time can elicit different type of inflammatory response than high dose exposure for a short period of time. There is likely no safe level of asbestos exposure and the exposure- response relationship appears to be linear [4, 11].

The pathogenesis of asbestos exposure related lung diseases involves various cell types [5, 6]. Extensive research has revealed various pathways and molecular mechanisms underlying asbestos induced lung diseases, but the precise mechanisms and the crosstalk between the implicated pathways in each separate disease are not yet fully understood. The notable difference between mesothelioma and lung cancer in the activation of the Ras- oncogene and in the inactivation of the tumor suppressor p53 emphasizes the complexity of the mechanisms leading from asbestos exposure to the disease [28].

Inside the histological subtypes, mesothelioma exhibits further heterogeneity between and within the tumors [28]. For instance, a recent report [41] identified two subgroups in mesothelioma: C1 with a better prognosis and C2 with a worse prognosis. This was irrespective of the histological subtype. The C2 group was characterized by mesenchymal phenotype (see 1.3). This subgrouping was able to divide epithelioid mesotheliomas into groups of better and worse prognosis. Consistent with their two-component nature, biphasic mesotheliomas were also included in both subgroups. As could be expected, sarcomatoid tumors were all included into the C2 group.

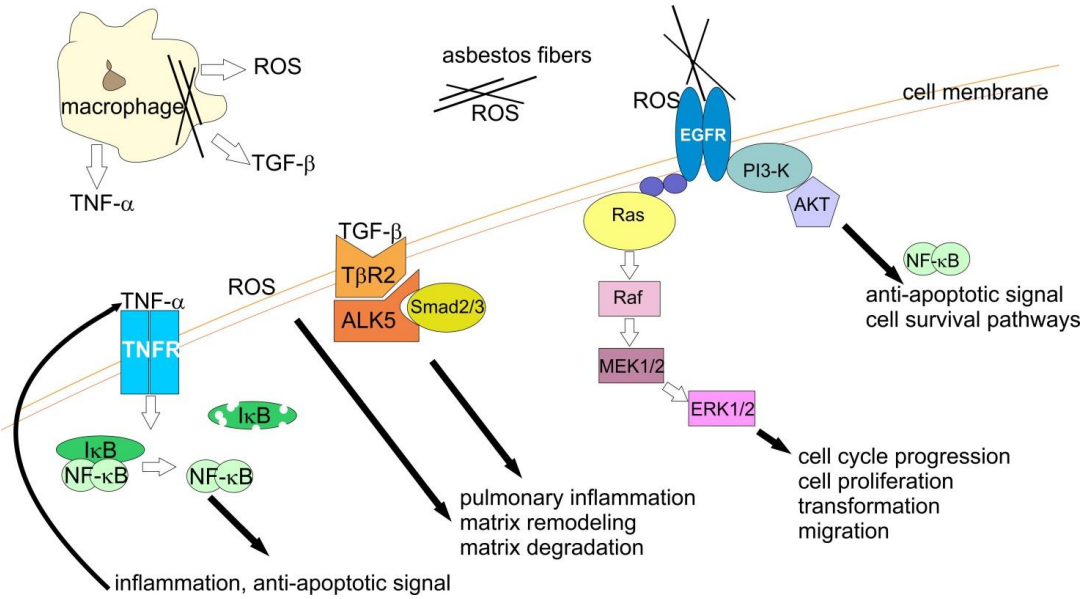

Figure 1. Some of the asbestos evoked disease related responses. Phosphorylation cascades are not shown. Asbestos has pleiotropic effects on epithelial and mesothelial cells as well as other cell types. Asbestos can activate cell signaling pathways through direct interactions with receptors or by inducing generation of reactive oxygen species (ROS) and bioactive molecules. ROS are also generated at the surfaces of asbestos fibers. ROS and growth factors (e.g. TGF-β) and cytokines (e.g. TNF-α) are released by macrophages as a result of unsuccessful phagocytosis of large fibers. TGF-β and TNF-α mediate inflammatory and anti-apoptotic signals through their receptors, TGF-β type 2 (TβR2) and type 1 (ALK5) receptors and TNF-α receptor (TNFR). Asbestos induced oxidative stress and bioactive molecules promote pulmonary inflammation and matrix remodeling and degradation as well as fibrosis. Asbestos also induces activation of nuclear factor- κB (NF-κB), which promotes cell survival and inflammation as well as chemokine and cytokine production. Direct interaction of the fibers with the epidermal growth factor receptor (EGFR) activates the Ras-Raf-extracellular signal–regulated kinase (ERK) pathway, which by stimulating and/or regulating proliferation, differentiation, survival and migration will promote disease progression. Activated EGFR also activates the phosphoinositol-3 kinase (PI3K)/AKT pathway, which promotes cell survival through NF-kB. Adapted and modified from [1, 6, 23, 55].

1.3 Epithelial-to-mesenchymal transition

Epithelial cells can downregulate their epithelial characteristics and acquire mesenchymal traits. Epithelial-to-mesenchymal transition (EMT) is a reprogramming of the cells' gene expression, as well as non-transcriptional changes induced and regulated by extracellular cues [56]. Endothelial and mesothelial cells can also undergo transition to mesenchymal phenotype.

1.3.1 Introduction to EMT

The epithelia has a recognized role as a permeability barrier outlining tissues and organs as a single cell layers or as multilayer tissues [57]. On the contrary, mesenchymal cells are loosely organized in a three dimensional extracellular matrix comprising connective tissues next to the epithelia [58]. During EMT, E-cadherin in adherens junctions, ZO-1 in tight junctions and other intercellular junction proteins are dissoluted, which leads to the loss of apical-basal polarity [56, 59]. The cells reorganize their cytoskeleton and gene expression, and begin to express mesenchymal genes such as N-cadherin, vimentin, fibronectin and α-SMA [58, 60]. During EMT, the Rho GTPases regulate actin dynamics and actin reorganization to stress fibers [56]. The loss of apical-basal polarity and reorganization of the cytoskeletal architecture result in changes in the cell shape; the cells become elongated and they gain front-rear polarity, which enable directional movement.

Depending on the tissue and signaling context, EMT can also be partial [56]. This means that an epithelial cell loses some of its epithelial characteristics while retaining some and simultaneously acquires some mesenchymal traits. Furthermore EMT can be transient in nature and cells that have gone through EMT can revert to their original state by mesenchymal-to-epithelial transition (MET) [58, 61]. Thus, epithelial plasticity covers a wide range of changes in cell behavior and the plasticity of the epithelial phenotype enables the cells to undergo multiple rounds of EMT and MET.

During development, EMT represents an initial differentiation event in the generation of the three germ layers from pluripotent cells [56, 59]. In addition to its crucial role in the formation of the body plan and in the differentiation of various tissues and organs, EMT also contributes to tissue repair and wound healing [58]. Depending on the physical context, EMT can be categorized into three types [56] : type 1 EMT occurs in embryogenesis and development, type 2 EMT is an important contributor in tissue repair and in organ fibrosis and type 3 EMT associates with cancer progression.

1.3.2 Inducers and transcription factors

EMT is crucial for tissue remodeling during embryogenesis and responsible for the formation of various structures in vertebrates, including the cardiac valves, the craniofacial structures, the vertebrate and the lungs [60, 62]. Various signaling pathways have been reported to regulate numerous transcription factors during EMT. TGF-β-Smad3, WNT-β-catenin, PI3-K/AKT and MAPK/ERK cascades and Notch, NF-κB, epidermal growth factor (EGF), fibroblast growth factor (FGF) and bone morphogenetic proteins (BMPs) can initiate EMT [56, 59, 62, 63]. These pathways frequently, but not necessarily, regulate transcription factors snail and slug (see section 1.3.3), which downregulate the expression of epithelial E-cadherin and other cell junction proteins in the initiation of EMT which eventually is accompanied by upregulation of mesenchymal gene expression.

In EMT processes, other activated transcription factors include AP-1 transcription factors, TWIST, zink-finger E-box-binding (ZEB) 1 and ZEB2, which can downregulate epithelial and upregulate mesenchymal gene expression [60, 62]. During EMT processes, it is likely that several transcription factors are activated simultaneously or in a hierarchical manner.

In addition to the direct effects of growth factors and transcription factors on gene expression, numerous splicing and translation factors regulate EMT/MET [62]. Alternative splicing generates proteins with structural and functional differences and can generate isoforms of the same gene with opposing effects on EMT [58]. In addition, non-coding miRNAs that selectively bind mRNA regulate EMT [56, 62]. Binding of a miRNA to mRNA can inhibit mRNA translation or promote mRNA degradation. Furthermore, chromatin regulators control EMT processes epigenetically [62].

1.3.3 Snail family transcription factors

Snail family zink-finger transcription factors are the key inducers of EMT but act also as survival factors and as inducers of cell movement during developmental as well as pathological EMT [63]. In humans, there are three members in the family: snail (*SNAI1*), slug (*SNAI2*) and smuc (*SNAI3*). All three genes are located in different chromosomes in human, *SNAI1* in chromosome 20, *SNAI2* in 8 and *SNAI3* in 16 (http://www.ncbi.nlm.nih.gov/gene accessed 17.10.2014). Although discovered over a decade ago [64], not much is known of about smuc, and it will not be discussed further here. Co-operation between different transcription factors is central in EMT induction [58]. There is increasing evidence of a hierarchy in controlling the expression of the transcription factors snail and slug, which are induced by TGF-β superfamily members. For instance, snail upregulates slug expression in fibrosis [58]. Furthermore, in both developmental as well as in cancer progression associated EMT, snail has been suggested to be expressed at the onset of the transition, whereas slug together with other transcription factors would be subsequently induced to maintain the mesenchymal phenotype [65]. Snail family transcription factors act as repressors for genes supporting epithelial phenotype, the major gene being E-cadherin (*CDH1*) [66]. They also induce genes of mesenchymal phenotype, including vimentin and fibronectin.

1.3.4 Mesothelial-to-mesenchymal transition

The mesothelium has multifaceted functions. It resembles the epithelia as it maintains a protective barrier. However, the components of extracellular matrix, hyaluronan and other lubricants, as well as chemokines and cytokines that mesothelium produces differ from those produced by the epithelium [28]. Mesothelial cells originate from the mesoderm and are histologically different from the cells of true epithelium. Mesotheial cells can undergo an EMT like transition, mesothelial-to-mesenchymal transition (MMT). In peritoneal mesothelial cells, EMT has been reported to be mediated by the ERK/NF-κB/snail cascade [67].

1.3.5 Pathological EMT

Aberrant EMT contributes to organ fibrosis and cancer progression through various mechanisms [58, 61]. EMT provides cells with migratory and invasive properties and pathological EMT prevents apoptosis and senescence, and contributes to immunosuppression and chemoresistance. In addition, EMT also promotes cancer cell dissemination and metastasis [61]. At distant site MET may contribute

to the establishment of the metastasis. Many of the same growth factors, extracellular cues and pathways that co-operate to orchestrate EMT during development and normal tissue repair operate also in pathological EMT [58]. Some features of EMT and its contribution to pathological conditions are presented in Figure 2.

During tissue fibrosis, myofibroblasts accumulate and secrete excess amounts of the altered extracellular matrix (ECM) [58, 68]. This compromises organ function and leads to its failure. In mouse models of fibrosis, part of these myofibroblasts has been shown to originate through pathological activation of interstitial fibroblasts, but a significant part was shown to arise from the epithelial cells through EMT processes [69]. Furthermore, high levels of recognized EMT inducer TGF-β have been found in the fibrotic tissues of patients. Altered ECM can initiate and support EMT and promote the progression of fibrosis and cancer [61].

Cancer invasion can be a synchronized action of both EMT dependent as well as EMT independent mechanisms [61]. EMT is observed in the invasive front of colon carcinoma [70, 71] as well as in other solid tumors [58, 61]. Furthermore, many important EMT drivers, including snail and slug, have been found to correlate with disease relapse and survival in various cancers, indicating that EMT leads to worse prognosis and clinical outcome [58]. In lung cancer and mesothelioma, EMT phenotype and expression of snail or slug, or both, has also been linked to worse prognosis [41, 72, 73].

Constitutive expression of EMT inducers can maintain the mesenchymal phenotype and because this suppresses senescence and apoptosis, the two safeguard mechanism against cancer, it ensures an invasive phenotype and promotes survival of metastatic cells [58]. Tumors with EMT phenotype can resist chemotherapy. In addition, EMT can induce [59, 74] and be induced by the expression of matrix metalloproteinases (MMPs) which degrade the ECM [75] and promote tumor invasion as well as fibrosis. Degradation of ECM can release more EMT driving growth factors and cytokines, which can create a self-amplifying vicious cycle.

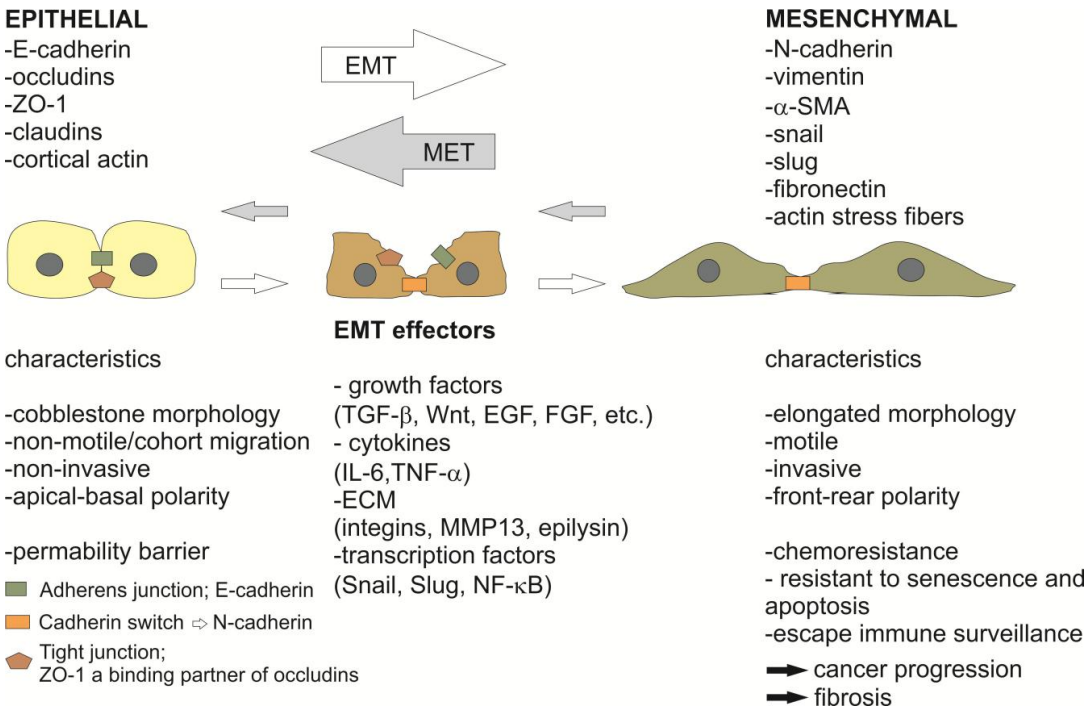

Figure 2. Characteristics of pathological EMT (epithelial-to-mesenchymal transition). During fibrosis or cancer progression, epithelial cells can undergo complete or partial EMT, which can be reversible. Various effectors are able to induce EMT, including growth factors (e.g. TGF-β, Wnt, EGF, FGF), cytokines (e.g. IL-6 and TNF-α) and ECM components. Although not all events in EMT require transcriptional changes, these inducers will also activate transcription factors (including snail, slug and NF-κB) which are responsible for transcriptional reprogramming of the cell undergoing EMT. Some of these transcription factors are also used as markers for mesenchymal phenotype (e.g. snail and slug). During EMT, the cells downregulate epithelial proteins of cellular junctions (e.g. E-cadherin and ZO-1) and reorganize their cortical actin to stress fibers. The cells lose their apical-basal polarity and gain front-rear polarity. A mesenchymal cell will express mesenchymal markers, including N-cadherin and α-smooth muscle actin (α-SMA). During EMT, the cell loses its cobblestone like morphology and stationary character and becomes elongated in morphology and capable of migration and invasion. In addition to the ability to invade, EMT phenotype can gain resistance to senescence and apoptosis, and escape immunosurveillance; thus aberrant cells persist and are not removed from the tissues. EMT phenotype can also support chemoresistance. Adapted and modified from [58, 60, 76, 77].

1.4 Extracellular matrix

In multicellular organisms, cells are surrounded by a complex three dimensional extracellular matrix (ECM) that provides support and strength to the cells within the tissues but also functions as an important regulator of various cellular activities and as a reserve for many growth factors [78].

1.4.1 Structure and function

The composition of the ECM differs depending on the tissue and organs, and it defines the rigidity of the tissue [78]. Therefore, the strength of the bone, flexibility of the skin and other unique characteristics of organs and connective tissues are determined by the ECM and by the cells that produce it. Collagens, structural glycoproteins, proteoglycans and elastins are components of the ECM, and they organize into macromolecular superstructures, such as collagen fibrils, elastic fibrils and microfibrils.

ECM undergoes constant remodeling and reshaping by the cells which degrade and reassemble it [79]. Thereby the cells actively modulate their surrounding environment which directs their own phenotypes. The composition of the ECM is controlled by coordinate and distinct regulation of synthesis and turnover of each separate component [80]. The ECM interacts and signals through cellular receptors [81]. Various receptors have been identified that transduce signals from the ECM to the cytoskeleton and to the nucleus [82]. These include integrins, receptor tyrosine kinases, immunoglobulin superfamily receptors, destroglycan and cell surface proteoglycans. Physical linkages and biochemical signaling generate a bidirectional flow of information between the extracellular and intracellular compartments.

ECM components are bioactive polymers [80]. In addition to its structural role and direct signaling to the cells through cell surface receptors, ECM components can also physically interact with signaling molecules and their regulators [78]. These interactions enable the sequestering of bioactive molecules, which modulates the availability, localization and activity of the signaling molecules including FGF, WNTs, Hedgehogs, TGF-βs and BMPs (see l.7.3 and 1.7.5). Remodeling of the ECM is often a result of cell-matrix crosstalk leading into the release of active ECM components and bioactive peptides as well as the growth factors stored into the ECM [79]. During cancer progression, cancer cells modulate their surroundings, which usually leads to generation of a stiffer ECM, that can facilitate tumor progression and invasion [83].

When tissue is injured, healing processes involve the formation of early remodeling phase of provisional ECM [80, 84]. This provisional ECM contains for example proteoglycans and hyaluronan and it is a loose and highly hydrated environment for cell invasion and repair. During this stage, specific ECM components interact with the cells and control cell behavior critical to the wound healing. In many diseases, something goes wrong after this early repair phase leading to generation of fibrotic ECM. Like cancer ECM, fibrotic ECM is stiffer and altered in composition, compared to the ECM of a heathy tissue [85]. Fibrotic ECM can also contain increased amounts of profibrotic growth factors.

By eliciting structural changes and releasing growth factors and cytokines sequestered into the ECM, the cells and the ECM sustain a reciprocal communication important in normal tissue

development, homeostasis and wound healing [79], but is also a crucial factor in cancer progression [86] and in lung fibrosis (IPF) [8]. Tumor cells and cancer associated fibroblasts modify their surrounding ECM to promote angiogenesis, chemoresistance and metastasis [86]. In lung fibrosis, aberrant wound healing processes lead to deposition of excess and altered ECM [8]. Modification of the altered ECM and release of stored signaling molecules supports inflammation and fibrosis promoting environment.

Basement membrane is a specialized ECM lining the basal face of epithelium and endothelium, and surrounding muscle and fat cells [87]. Basement membrane is mainly comprised of laminins and collagen IV but contains also nidogen and heparin sulfate proteoglycans.

1.4.2 Microfibrils

Fibrillins are large cysteine rich glycoproteins [78, 88, 89]. In human, three fibrillin genes have been identified: *FBN1* (fibrillin-1), *FBN2* (fibrillin-2) and *FBN3* (fibrillin-3) [90], which are scattered in different chromosomes, *FBN1* in chromosome 15, *FBN2* in 5 and *FBN3* in 19 (http://www.ncbi.nlm.nih.gov/gene, accessed on 17.10.2014). Fibrillins-1 and- 2 are ECM proteins, structurally related to fibulins and latent TGF-β binding proteins (LTBPs) [88-90]. LTBPs and fibrillins form a fibrillin-LTBP family of extracellular matrix proteins [91]. This family contains the fibrillins and four different LTBPs [92]. These proteins typically have repeated domain structure that consists of EGF-like repeats and characteristic eight cysteines.

Fibrillin -2 is generally expressed during development and tissue remodeling but consistently in lower amounts than fibrillin-1 [89, 90]. Fibrillin-1 production continues in adult organisms. Fibrillins-1 and -2 have both unique as well as overlapping functions [90, 93]. Fibrillins exert structural functions through the temporal and hierarchical assembly of microfibrils and elastic fibers [90]. The fibrillin monomers organize into microfibrils. The microfibrils are essential for elastic fiber formation.

In addition to their structural role, fibrillins exert indispensable regulatory function to biochemical signaling by sequestering TGF-βs and BMPs, thereby concentrating, targeting and regulating bioavailability of these growth factors. Perturbation of either structural or regulatory function will lead to a disease. Elastic fibers that contain fibrillins are key architectural components of connective tissues, although microfibrils containing fibrillins can also exist without being associated with elastic fibers [90, 94]. The fundamental roles of fibrillins in connective tissues are emphasized by the manifestations of the microfibrillopathies, a group of diseases resulting from abnormalities in the microfibrillar network [95]. Two recognized examples are Marfan syndrome caused by a mutation in fibrillin-1 [96], and congenital contractual arachnotactyly (CCA), which results from fibrillin-2 mutations [97]. Fibrillin mutations lead to disintegration and fragmentation of connective tissues. Some syndrome manifestations can result directly from these structural abnormalities. Due to the indispensable role of the fibrillins in sequestering and in regulation of various growth factors, parts of the manifestations are likely to result from aberrant growth factor activation and signaling. In Marfan syndrome, the extracellular TGF-β protein levels and patient serum TGF-β levels are significantly elevated [98]. Fibrillin-1 mutation impairs the delivery of the large latent complexes to ECM, and abnormal ECM can stimulate aberrant activation of TGF-βs. Considering that also BMPs

are targeted to microfibrils, which contain fibrillins [94, 99], it is likely that the balance of also BMP activities might be disturbed in fibrillin mutation induced syndromes.

1.5 Nuclear factor-κB

The nuclear factor-κB transcription factor family is central in regulating several cellular functions, including inflammation, apoptosis, cell survival and proliferation [100]. NF-κB transcription factors also play a key role in innate and acquired immunity.

1.5.1 NF-κB mechanism of activation

NF-κB signaling occurs via two independent yet interlinked pathways [100, 101] of which only the canonical pathway is discussed here. The NF-κB transcription factor family consists of five subunits: RelA (p65), RelB, c-Rel (Rel), p50 (processed from NF-κB1) and p52 (processed from NF-κB2) [100]. All subunits share the same homologous element the Rel homology region (RHR), which is responsible for dimerization, inhibitor binding, nuclear localization and DNA binding. The genes *RELA*, *RELB*, *REL*, *NFKB1* and *NFKB2* are all located in different chromosomes in human genome (http://www.ncbi.nlm.nih.gov/gene, accessed 1.9.2014). These five subunits form homo- and heterodimers which in most quiescent cells are bound to inhibitory molecules, the IκB (inhibitors of NF-κB) family proteins [101]. Association with the inhibitory proteins sequesters the NF-κB-IκB complexes in the cytoplasm, and because the binding takes place through the DNA binding domains of NF-κBs, it makes them transcriptionally inactive. The activation of NF-κB occurs by release from the IκB molecules. This can be achieved by degradation of the inhibitor. IκB is targeted to proteosomal degradation by polyubiquitination, which requires a specific double phosphorylation of the IκB [102]. This is mediated by an enzyme complex that contains IκB kinases IKK1 (IKKα) or IKK2 (IKKβ) and accessory proteins. IKKs are phosphorylated and activated by NIK (NF-κB inducing kinase) and MAPK3K family kinases (see 1.6) MEKK1, MEKK2 and MEKK3 as well as by TAK1 (TGF-β activating kinase 1). Extracellular signals that can activate NF-κB pathway include LPS (lipopolysaccharides), TNF-α and IL-1 (interleukin-1).

1.5.2 NF-κB in inflammation and cancer

Inflammation, a process of innate immunity, is a response to physical injury, oxidative stress, or other harmful substance, and it is associated with activation of the canonical NF-κB pathway [101]. Inflammation and NF-κB have a dual role in cancer. NF-κB activation is part of the immune defense targeted to eliminate transformed cells. However, this immune defense is not always tight enough or capable to eliminate all aberrant cells. Most malignancies exhibit constitutive activation of NF-κB [100], which enables it to exert various pro-tumorigenic functions. NF-κB can do this because it regulates the expression of pro-inflammatory cytokines (IL-1, IL6), chemokines, growth factors, cell cycle regulators, adhesion molecules, matrix degrading proteases and anti-apoptotic molecules (e.g. B-cell lymphoma 2 gene, Bcl-2) [87]. Importantly, NF-κB can antagonize the apoptotic pathway of the tumor suppressor p53. Tumors can establish elevated NF-κB activity by obtaining mutations that target NF-κB genes (the five subunits) or oncogenes that activate the NF-κB pathway; increased NF-κB activity can also be achieved by increasing the release of activating cytokines, such as TNF-α, into the tumor microenvironment.

1.6 Mitogen activated protein kinases

The mitogen activated protein kinase (MAPK) pathways transduce signals from the cell membrane into the cell and into the nucleus [103]. In response to many different stimuli, MAPK cascades control a range of cellular processes, including growth, differentiation and stress responses.

1.6.1 MAPK cascades

The MAPK family contains extracellular signal-regulated kinase (ERK), c-Jun N-terminal kinase (JNK, often referred to also as the stress activated protein kinase, SAPK) and p38 MAPK [103]. The ERK pathway is activated by mitogenic stimuli by growth factors and cytokines, whereas JNK and p38 MAPKs respond less robustly to growth factor stimulation but are readily activated by stress signals, including TNF-α, IL-1. Whereas the ERK pathway is a central regulator of cell growth, survival and differentiation, the JNK and p38 MAPK pathways contribute to the regulation of stress response and apoptotic cell death. Majority of the MAPK pathways become activated, along with the NF-κB pathway, in response to stress and inflammation [104]. The MAPkinase signaling is highly complex. A core triple kinase cascade is a defining feature of the MAPKs. This means that the phosphorylation, i.e. activation of a MAPK/ERK, JNK or p38 is a result of a sequential, three-membered kinase cascade. The kinase closest to the cell membrane receptor in the cascade is a member of a vast group of kinases called MAPK kinase kinase (MAP3K) [104]. These kinases phosphorylate serines and threonines in a conserved motif in MAPK kinases (MAP2Ks, MKK or MEKs) and induce their activation. MAP2Ks having a dual specificity will phosphorylate threonine and tyrosine residues in a distinct conserved motif in MAPKs, which leads to their activation. MAPK p38 is phosphorylated by MAP2Ks MKK3, MKK4 and MKK6, and JNK is phosphorylated by MKK4 and MKK7. These MAP2Ks, on the other hand, are phosphorylated by a vast group of different MAP3Ks. The most well-known triple phosphorylation signaling cascade for ERK is Ras/Raf/MEK/ERK cascade. It starts from activated cell membrane tyrosine kinase receptor (e.g. EGFR) and a G-protein Ras (Ras oncoprotein), which activates Raf family of MAP3Ks. Raf phosphorylates ERK-spesific MAP2Ks: MEK1 (MAP2K1) and MEK2 (MAP2K2), which phosphorylate and activate ERKs [104, 105]. MEK1 and MEK2 can, however, be activated also by various other MAP3Ks [104]. ERKs can also be activated independently of Ras. Separate MAPKs have distinct but also overlapping targets. They phosphorylate membrane proteins and cytoplasmic proteins, which can act as downstream kinases, and on cytoskeletal proteins [105]. MAPKs phosphorylate and activate transcription factors that upregulate AP-1 (see 1.2.4) component genes [104]. JNKs and p38 are the predominate MAPKs responsible for the recruitment of the AP-1, but also ERKs can regulate AP-1. AP-1 in turn controls a number of cellular processes, including differentiation, proliferation and apoptosis.

The duration and amplitude of the MAPK cascades are regulated by controlling the intracellular localization of the kinases as well as removing the activating phosphorylations [105]. The activated MAPKs can be concentrated in a different intracellular localizations, cellular structures and compartments in the cell which can affect downstream cascades and cellular responses. Furthermore, substantial number of dual specific phosphatases, MAPkinase phosphatases (MKPs), specifically removes one or both phosphorylations. Activities of the MAP kinases are also regulated by targeting them for degradation by ubiquitin proteasome system [106].

1.6.2 Extracellular signal-regulated kinases (ERKs)

There are at least seven ERK genes in human (*ERK1, ERK2, ERK3, ERK4, ERK5, ERK6* and *ERK7=ERK8*, http://www.ncbi.nlm.nih.gov/gene, accessed on 1.9.2014). The most well studied MAPK/EKRs are encoded by the genes *ERK1* and *ERK2* [104], which are located in the chromosomes 16 and 22, respectively (http://www.ncbi.nlm.nih.gov/gene, accessed on 15.10.2014). The Ras/Raf/MEK/ERK is the best studied MAPK pathway [107]. There are more than 160 substrates which ERK1/2 can phosphorylate [108]. In addition, ERKs have also functions that do not depend on kinase activity. For instance, kinase deficient ERK1/2 could upregulate p21 levels and induce cell cycle arrest in response to Raf/MEK activation [109]. Activation by growth factors, hormones and cytokines has been shown to stimulate and regulate proliferation, differentiation, survival, senescence and migration [107, 108]. External stimulus will eventually activate the membrane bound GTPase Ras. Ras, when GTP-bound recruits Raf to the plasma membrane and enables it to phosphorylate MEK1 and MEK2, which are the two only substrates for Rafs. MEKs will further phosphorylate ERKs. Three isoforms of Raf are expressed in mammals (A-, B- and C-Raf) with distinct differences in affinities for both the upstream activator Ras as well as for the target MEKs. As discussed above, ERKs require dual (tyrosine and threonine) phosphorylation in their activation loop to become active. Both ERKs are expressed ubiquitously, but the relative levels of ERK1 and ERK2 in tissues differ [105]. In various cases, the ERKs can also be activated in Ras-independent manner by proinflammatory stimuli, such as cytokines of the TNF-family [104]. This Ras-independent mode of ERK activation plays a significant role in innate immunity and inflammation as well as in cell proliferation. MAPK/ERKs are well recognized activators of cyclin D1 gene transcription [110]. Cyclin D1 functions in a rate limiting role in cell cycle progression through G1. Subsequently, cyclin D1 is overexpressed in various cancers. However, sustained activity of Raf/MEK/ERK pathway can also induce growth inhibitory signaling in many different cell types [108]. MAPK/ERK signaling can induce cell death and cell cycle arrest in response to various signals. A model has been suggested where not only too low but also too high MAPK/ERK activity leads to growth arrest [108]. The thresholds are likely to be different in different cell types.

1.6.3 ERKs and EGFR in pathological conditions

Epidermal growth factor receptor (EGFR, also known as HER1, ERBB1, http://www.ncbi.nlm.nih.gov/gene, accessed on 15.10.2014) is one of the major cell membrane tyrosine kinase receptor activating ERKs. Therefore, changes in MAPK/ERK regulation can result from EGFR overexpression or activating mutations of Ras or Raf [103, 105, 107]. This is frequently observed in human cancers. However, EGFR and Ras mutations may be mutually exclusive [55]. Mouse knockout experiments show that in B-Raf deficient cells growth factor stimulated ERK activation decreases, but this is not the case in A-Raf or C-Raf deficient cells [111-113]. This suggestion of B-Raf as a dominant MAP3K is supported by the observation that B-Raf mutations are far more frequent in human cancers compared to A-Raf or C-Raf mutations [114, 115].

EGFR family tyrosine kinase receptors are frequently upregulated in human cancers [55]. Dimerization of these receptors after ligand (for example EGF) binding will eventually activate the Raf/MEK/ERK or PI3K/AKT pathway, or both. These pathways promote cell cycle progression and

cell proliferation as well as anti-apoptotic signals and survival pathways. ERK activation will also promote transcription of inflammatory cytokine TNF-α and angiogenesis stimulating VEGF (vascular endothelial growth factor). MAPK/ERKs are strongly implicated in the development of radio- and chemoresistance [103, 116].

In addition to these two well characterized mechanisms (hyperactivation of EGFR or Raf), MAPK/ERK may contribute to cancer progression and treatment resistance also through regulating other cascades. MAPK pathways play a central role in regulating the key mediators of fibrosis, namely TGF-β and Smad pathways (see 1.7). There is also significant cross-talk between these pathways. MAPKs are also strongly implicated in EMT processes (see 1.3.2). In addition, MAPK cascades contribute to the development of fibrotic diseases. ERK activation is implicated in EMT in chronic hypoxia-induced renal fibrosis *in vitro* and in rodent models as well as in the samples from patients suffering from chronic kidney disease [117]. In TGF-α mouse model of pulmonary fibrosis, MEK inhibition prevents the progression of established fibrosis [118]. Furthermore, upregulation of EGFR in IPF lungs has been reported [119] and EGFR activation has been suggested to be an important event in the development of pulmonary fibrosis [120]. However, MAPK/ERK activation can also occur independently of EGFR and promote fibrosis. Activation of the MAPK/ERK pathway occur in cancer cells not only by growth factors but also by activating mutations which promote EMT [56].

EGFR also activates PI3-K/AKT pathway which promotes cell survival through NF-κB [23]. PI3-K/AKT activity is frequently elevated in mesothelioma, and this reduces sensitivity to chemotherapeutic drugs [46, 121]. Also hepatocyte growth factor (HGF)/Met receptor and other growth factors (e.g. insulin) can activate the PI3-K/AKT pathway. Activation of AKT increases tumor invasion, antagonizes cell cycle arrest and activates mTOR (mammalian target of rapamycin), a serine/threonine protein kinase that regulates numerous cellular functions, including proliferation, cell survival, transcription and protein synthesis. PRAS40 (proline-rich AKT substrate of 40-kDa) is a substrate for AKT and a regulator of mTOR [122]. mTOR is found in cellular complexes referred as mTOR complex 1 and 2 (mTORC1 and mTORC2). The core component of mTORC1 is the Raptor (regulatory associated protein of mTOR) but also other regulatory proteins are found bound in these complexes, including Rag GTPases, RalA GTPase and PRAS40. PRAS40 associates with the mTOR complex 1 and regulates its activity. PI3-K/AKT phosphorylates PRAS40 and modulates is regulatory effect on mTOR complex 1.

1.7 Transforming growth factor-β superfamily

The transforming growth factor-β superfamily consists of over 30 members in mammals [123]. Members of this superfamily have fundamental roles in the development as well as in the homeostasis of adult organisms. The TGF-β superfamily members are found broadly in both vertebrates and in invertebrates.

1.7.1 Introduction to the TGF-β superfamily

The transforming growth factor (TGF)-β superfamily includes TGF-βs, activins, nodals, BMPs, growth differentiation factors (GDFs) and anti-Müllerian hormone [123]. The TGF-β superfamily members have from 66% to 80% sequence identity and nine strictly conserved cysteines [124]. Ubiquitous expression of these secreted factors starts at development and continues into the adulthood of the organism [123]. TGF-β superfamily members participate in determining the body axis formation and patterning. At cellular level, TGF-β superfamily members control fundamental cellular processes including proliferation, differentiation cell death, cytoskeletal organization, adhesion and migration. Consistent with their fundamental role in normal physiology, aberrant TGF-β superfamily signaling activity is strongly implicated in pathologic conditions such as fibrotic and malignant diseases.

The ligands of the TGF-β superfamily are synthetized as precursor proteins and they are processed and secreted as proproteins where the N-terminal prodomain associates non-covalently with the C-terminal mature active ligand [125]. Within the superfamily the C- terminal active growth factor domains resemble each other but the N-terminal prodomains appear dissimilar. Prodomains differ between TGF-βs and BMPs, whereas activin-A proregion resembles more that of TGF-β [126, 127]. The prodomains facilitate proper folding, dimerization and secretion [126]. Mature ligands are characterized by a structure called the cysteine knot that results from the formation of the three intramolecular disulfide bonds between six highly conserved cysteines [128]. Also a seventh cysteine, that mediates dimerization is conserved in most members [123]. Schematic structures of TGF-βs, BMPs and activin-A are pictured in Figure 3.

TGF-β superfamily members can be divided into two functional groups, the TGF-β-like group contains TGF-βs, activins, nodals and some GDFs; whereas the BMP-like group contains BMPs, most GDFs and anti-Müllerian hormone [123]. Intracellular Smad responses also follow this division so that the TGF-β-like group binding receptors activate receptor Smads (R-Smads) Smad2 and Smad3 and the BMP-like group binding receptors activate R-Smads Smad1, Smad5 and Smad8. The ligand binding and activated Smads (canonical pathways) of some of the TGF-β superfamily members are presented in Figure 4. Some of the reported non-canonical signaling cascades for those growth factors are also shown, as well as some of the extracellular regulators, which will be discussed in sections 1.7.4 and 1.8.

1.7.2 Receptors and signaling through Smads

TGF-β superfamily members transmit their signals through heteromeric complexes of type 1 and type 2 serine/threonine receptors [123, 129-132]. Generally the activated receptor complex is formed

when the ligand dimer binds to two type 2 receptor kinases. Two type 1 receptors are recruited to the complex and phosphorylated after which the Smad cascade is initiated[133-135]. However, the BMPs have higher affinity to type 1 receptors than to type 2 receptors, and BMPs can form receptor complexes also by binding first to the type 1 receptors [136-138]. Typically, the type 1 receptor defines the specificity of the Smad signal [130]. In vertebrates, there are five type 2 and seven type 1 receptors [123]. This relatively small group of receptors can pair up in various combinations to mediate signals for all the members of the TGF-β superfamily. Remarkably, the diversity of over 30 ligands and numerous combinations of receptor signals are mainly funneled to only two intracellular Smad-pathways.

Both the TGF-β-like group and BMP-like group activated R-Smads share the same common partner Smad (co-Smad), Smad4 [123]. Heteromeric partnering with Smad4 is not needed for nuclear localization, but it is essential for initiation of transcriptional regulation [139]. After localization to the nucleus, the R-Smad likely determines target gene specificity and the co-Smad acts to promote transcriptional activity [123]. However, although these Smads bind directly to DNA, the binding is of low affinity, and Smads generally need to recruit binding partners, specific transcription factors and co-activators. In the C- and N- termini of the R-Smads are highly conserved domains called Mad Homology (MH) 1 and MH2 [140]. The MH domains are separated by a linker region of variable length. The MH1 domain mediates DNA binding and MH2 mediates oligomerisation.

In transcription complexes, depending on the interacting transcription factors, different stoichiometries of R-Smads can be found [141]. Smad heterodimers, containing for instance Smad2 and Smad4, or heterotrimers containing two Smad2s and one Smad4, can be found in transcription complexes associated with FAST-1 or FAST-3 transcription factors, respectively. It has been suggested that TGF-β induced transcriptional responses would be primarily mediated by Smad3/Smad4 complexes, whereas activin responses would be mainly mediated by Smad2/Smad4 complexes [139].

Various TGF-β family members induce transcription of inhibitory Smads (I-Smads) [139, 140, 142]. These Smads, Smad6 and Smad7, associate with type 1 receptors, but they lack the MH1 domain and the phosphorylation site (SXS motif) at their C-terminus, which in R-Smad is phosphorylated by type 1 receptors during signal transduction [139, 140]. Thus I-Smads act as inhibitors of the Smad pathways. Whereas R-Smads and Smad4 are expressed in most if not all cells, the expression of the inhibitory Smads is strictly controlled by extracellular signals, which include TGF-β and BMP [143]. Inhibitory Smad, Smad7, besides inhibiting canonical Smad activation induced by TGF-β, also functions as an adaptor protein that facilitates the activation of the non-canonical, non-Smad signaling pathways [144]. Smad6 has been suggested to be specifically induced by BMP signaling and Smad7 by TGF-β and activin signals with similar regulatory distinction [145].

Although the phosphorylation of the SXS motif in R-Smads is the key event in signal transduction, Smad signaling is also fine-tuned through post-translational modifications such as phosphorylation, ubiquitination, SUMOylation (Small-Ubiquitinrelated Modifier) and acetylation [146]. Post-translational modifications of the signaling components control their subcellular localization, activity and duration of the signal. Type 1 receptor phosphorylated R-Smad can be

dephosphorylated or ubiquitinated and targeted to degradation [146]. R-Smads can also be phosphorylated to alternative locations (linker region) by MAPKs and cyclin-dependent kinases (CDKs) which can regulate Smad activity positively or negatively. Interestingly, linker region phosphorylation by MAPKs can have a dual role in the regulation of Smad2 and Smad3 in different contexts. Mitogens and hyperactive Ras stimulated ERK-mediated phosphorylation of Smad3 and Smad2 have been reported to inhibit the nuclear localization of both Smad2 and Smad3 in epithelial cells [147], whereas ERK dependent Smad2 phosphorylation was suggested to enhance Smad2 transcriptional activity in COS7 and in mink lung epithelial cells [148]. MAPK/ERK, p38 and JNK can phosphorylate Smad1, which leads to its cytoplasmic retention [149]. Smad proteins are frequently inactivated in cancer [146].

An additional layer of complexity is brought by the ability of TGF-β superfamily members to bind co-receptors which can regulate ligand/receptor activation, and pseudoreceptors, which lack the kinase domain and inhibit signaling by forming inactive complexes with type 2 receptors [123]. BAMBI (BMP and Activin membrane bound inhibitor) is an example of a pseudoreceptor for TGF-β, BMPs and activins [123, 150]. TGF-β co-receptors betaglycan and endolgin can enhance ligand binding to the receptor complexes when they are membrane bound. However, when the cytoplasmic tail is cleaved, the co-receptor is released to the extracellular space and the soluble co-receptor sequesters the ligands, thus leading to negative regulation [123, 129]. In addition, the access of the ligands of the TGF-β superfamily members to their receptors is controlled by numerous extracellular binding factors. Of these, extracellular regulators of the activins and BMPs will be discussed later.

1.7.3 TGF-βs

There are three isoforms of TGF-β, TGF-β1, TGF-β2 and TGF-β3, which are structurally and functionally very similar (reviewed in [151]). The genes *TGFB1*, *TGFB2* and *TGFB3* are all located in different chromosomes, in the chromosomes 19, 1 and in 14 (http://www.ncbi.nlm.nih.gov/gene, accessed on 15.10.2014). Latent TGF-βs complexes are targeted to fibronectin and fibrillin containing fibers in the ECM [152, 153]. In the three dimensional structure of TGF-β, two monomers are arranged in antiparallel manner and the bioactive dimer is established by a disulfide bond [142, 154].

TGF-βs have various functions in normal physiology. In general, they modulate inflammatory cell function, inhibit cell growth, regulate differentiation and control extracellular matrix production [155]. TGF-βs regulate also development, organogenesis and wound healing [151]. Massive inflammatory response and early death in TGF-β1 null mice emphasizes the critical role of this growth factor in normal tissue homeostasis [156]. However, the amount and activation of TGF-βs must be in delicate balance. Disturbances in this balance can result in a disease but may also be a result of a disease.

Fibrillin rich microfibers enable temporal and spatial extracellular regulation of TGF-β and BMP signaling in a context specific manner (reviewed in [90]). TGF-βs (TGF-β1, TGF-β2 and TGF-β3) are secreted as a small latent complex that contains the bioactive homodimer, which is non-covalently associated with its pro-peptide called small latency associated protein (LAP). This association blocks interaction with the receptors, but the small latent complex can associate covalently with latent TGF-β binding proteins (LTBPs) through specific interactions [153]. LTPBs target TGF-βs to

fibronectin and fibrillin-1 and -2 containing ECM structures [152] where the growth factor can be activated by various mechanisms. LAP associated TGF-β1 can be cleaved by furin endoproteinase in the RXRR sequence [157, 158] while LAP remains associated with TGF-β dimer via non covalent interactions. This is referred as small latent TGF-β. In most cultured cells TGF-βs are secreted as large latent complexes (reviewed in [92]). In large latent complex small latent TGF-βs are covalently associated with one of the four latent TGF-β binding proteins (LTBPs). LTBPs likely have a central role in the processing and secretion of TGF-βs.

Activation of TGF-β can take place through various mechanisms. During activation the non - covalent interactions between TGF-β and LAP need to be disrupted. In vitro activation can take place through proteolysis, enzymatic deglucosylation, acid treatment (reviewed in [92]), by ROS [159] and by plasmin [160]. Young thrombospondin-1 null and TGF-β1 null mice exhibit many similarities in their phenotypes [161]. Thrombospondin-1 can activate latent TGF-β *in vivo*, and this likely occurs through binding induced conformational change in LAP which enables TGF- β to bind its receptors [161]. Furthermore, human LTBP-1 and the LAP isoforms of TGF-β1 and 3 contain an integrin binding sequence arginine-glycine-aspartic acid (RGD) [155, 162] which has been shown to bind integrins α5β1, α5β5, α5β6 and α5β8 [155, 163]. Of these integrins αvβ6 [155] and αvβ8 can activate the latent forms of TGF-β1 in *in vivo* mouse models. The mechanisms suggested by the *in vitro* studies are, however, different: activation by αvβ6 involves cell traction [155], whereas αvβ8 functions through proteolytic cleavage by membrane bound metalloproteinase [163]. Activation of the growth factor on the cell surface offers means to spatially restricted activation [155]. Also active TGF-β can bind to many ECM components [92].

TGF-βs signal through type 2 TGF-β receptors (TβR2), and partnering with ALK5 (TβR1) leads to activation of Smad2 and Smad3 [139]. TβR2 can, however, also partner with ALK1 and activate Smad1 and Smad5. In addition to Smad mediated transcription, TGF-βs can activate also other signaling cascades, including MAPK/ERK, JNK and p38 [139, 144]. Part of these pathways can regulate Smad activation as described for ERKs above but others can also induce responses unrelated to transcription. The mechanism of TGF-β induced ERK activation has been suggested to rely on the dual specificity of the receptors acting as serine/threonine kinases but also as tyrosine kinases [144]. Phosphorylated tyrosine residues can recruit adaptor proteins that facilitate ERK activation. PI3K and mTOR are other non-canonical pathways activated by TGF-β and which have been linked to TGF-β induced EMT.

1.7.3.1 TGF-βs in pathological conditions

Especially TGF-β1 is implicated in EMT and in fibrotic and malignant diseases. This is at least partially due to its capacity to upregulate the production of ECM components and suppress the immune system [153, 164]. Whereas immunostaning of TGF-βs is present but low in normal lung, all TGF-β isoforms are found abundantly expressed in the tissue samples of patients suffering from asbestosis [165]. TGF-βs localize into the extracellular matrix in fibrotic areas. Immunoreactivity was reported to increase as the fibrosis progressed. Due to mutation in the fibrillin-1 gene and impairment of the extracellular sequestering of latent TGF-βs, the extracellular TGF-β protein and serum TGF-β levels are significantly elevated in patients with Marfan syndrome [98]. Elevated levels of TGF-β are also found in the lung tissues of IPF patients [119, 166]. LTBP-1 is also overexpressed and

associates with fibrillin fibers and fibronectin in IPF lungs [167]. Some TGF-β1 polymorphisms have been reported to be associated with increased risk of asbestos induced fibrosis with simultaneous decreased risk to lung cancer [168]. This appears controversial with the established view that lung fibrosis increases the risk for lung cancer [6, 11, 12] (and 1.2). In asthmatic patients serum, TGF-β1 levels are elevated irrespective of the disease severity and glucocorticoid treatment [169].

TGF-β overexpression is a general phenomenon in cancer cells and suggests poor prognosis [151]. TGF-β inhibits the growth of benign cells. During cancer progression, cancer cells lose responsiveness to the growth inhibitory signals of TGF-β and become susceptible to TGF-β induced EMT [142]. One proposed model to explain this paradox suggests that TGF-β induces differential ERK activation in benign and cancer cells through differential recruitment of the tumor suppressor PP2A-B56α (subunit B56α of protein phosphatase2A) [151]. This model suggests that the initial triggering factor would be downregulation of type 1 TGF-β receptor TBR1 (ALK5) in early carcinogenesis, which would also lead to attenuation of Smad2/3 responses and increase the activation of the MAPK/ERK pathway. Activated ERK is a key regulator of cell proliferation as discussed above (1.6.2). Hyperactive Ras induced ERK activation and subsequent phosphorylation of Smad2/3 linker region by MAPK/ERK, which leads to decreased nuclear translocation of the Smads, has also been suggested as one mechanism by which TGF-β induced growth inhibition could be overcome in Ras mutated cancers [147].

Due to the diverse regulatory functions that TGF-βs have in normal physiology, the contribution of TGF-βs in cancer progression is likely more complex than merely the impact on cell proliferation. As a potent inducer of EMT (see 1.3), TGF-β also contributes to migration and invasion of the cancer cells, but TGF-β is also an important regulator of apoptosis. The mechanisms through which TGF-β induces apoptosis are complex, differ between the cells, can be Smad-dependent or independent, and often involve specific transcription factors, such as p53 (reviewed in [142]). As mentioned, I-Smads are transcriptionally regulated by the TGF-β family members, including TGF-β, and induced by Smad signaling [142] (and 1.7.2). Smad7 is essential to TGF-β induced apoptosis in human prostate cancer cell lines, human keratinocytes, human embryonic kidney (HEK) cells and in apoptosis of hepatocellular carcinoma cancer cells [170-173], as well as in the mouse model [173]. The transmitting signaling cascades appear to differ although apoptosis depends on Smad7. Different pathways in Smad7 dependent apoptosis include TGF-β induced p38 activation with subsequent p53 or β-catenin activation [170-172] and suppression of TGF-β and NF-kB activity by Smad7 [173]. In many occasions, TGF-β induced Smad7 appears to function as a common scaffold for recruited apoptosis inducing factors.

1.7.3.2 TGF-βs in mesothelioma

TGF-β1 and TGF-β2 are overexpressed in human mesothelioma [164, 165, 174]. The levels of phosphorylated Smad2, which indicate TGF-β activity, have been found to be elevated in human mesothelioma tumors [164]. Activated Smads localize into the nucleus and were found mainly in the tumor and associated with worse survival. It has been suggested that TGF-β1 localizes predominantly into the stroma and TGF-β2 more into the mesothelioma cells [165]. TGF-βs can promote tumor growth and invasion through regulation of immune functions and angiogenesis, as

well as production of stromal components. In a murine model soluble TGF-β receptor combined with treatment with monoclonal antibodies targeted to regulatory T-cells and cytotoxic T-lymphocytes were effective in clearing the tumors [175]. Inhibitor of TGF-β receptor ALK5 was found to efficiently inhibit growth of the tumors and their reoccurrence after surgical resection in another murine model of mesothelioma [176]. Various clinical trials targeting TGF-β pathway in numerous different cancers are ongoing (reviewed in [140]). A clinical trial for monoclonal antibody targeted to TGF-β in relapsed pleural mesothelioma has been completed 2012, but no publications of the outcome is yet available. (http://clinicaltrials.gov/ct2/show/NCT01112293?term=TGF-beta+mesothelioma&rank=1, accessed on 1.9.2014). A study on a TGF-β blocking antibody on a small patient group (n=13) has been reported [177]. The treatment was well tolerated, but unfortunately not very efficient.

1.7.4 Activins

Activins consist of two β-subunits, which they share with the inhibins [178]. The activin β-subunits are coded by the genes *INHBA* and *INHBB*, and these β-units form homodimers to generate activin-A (two activin-A β-units) or activin-B (two activin-B β-units). Activin-A and –B β-subunits share only 65% sequence homology [179]. Formation of a heterodimer, activin-AB, has also been reported, and this activin would have binding and signaling capacities of both activins. Other activin β-units, βC, βD and βE, have been found, but their biological roles are not very well known [180, 181]. Activin-C and heterodimers activin-AC and -BC have been detected at least *in vitro* and have been suggested to form non-signal transducing receptor complexes and to inhibit or regulate activin signaling by competing for the receptors [182]. Activin Eβ subunit appears to be liver specific [183]. Like the other members of the TGF-β superfamily, activins are homodimers linked with intramolecular disulphide bonds that form the cysteine knot motif [124]. Following the characteristics of the superfamily, activins are synthesized as disulfide linked dimers, which are processed from the mature cytokine by proteolysis or acid hydrolysis [126, 180, 184]. However, unlike many members of the TGF-β superfamily, the activin propeptide sequence has relatively low affinity for the mature dimer and does not interfere with receptor binding [185].

Inhibins antagonize activins by forming a stable inactive complex with the type 2 activin receptors (ActR2A and ActR2B) [181, 186]. This interaction requires betaglycan for sufficient affinity, but when the complex is formed it efficiently sequesters the type 2 receptors and excludes the type 1 receptors. As mentioned earlier (1.7.2) betaglycan participates also in the regulation of TGF-β-signals [129]. Inhibins form when the activin-A and activin-B β-subunits form a heterodimer with an α-subunit (*INHA*), generating inhibin-A (activin-A β-unit+ α-subunit) or inhibin-B (activin-B β-unit+ α-subunit). Inhibins resemble TGF-β superfamily members structurally [181]. The *INHA* and *INHBB* genes are both located in the chromosome 2, whereas *INHBA* is located in chromosome 7 (http://www.ncbi.nlm.nih.gov/gene, accessed on 1.9.2014).

Activins and inhibins were originally discovered because of their ability to stimulate and inhibit the secretion of the follicle stimulating hormone (FSH) from the pituitary [186, 187]. Activins-A and-B are expressed in most, if not all, tissues but especially in the female and male reproductive tracks under normal conditions [180]. In addition to their role in the reproductive track, activins are now recognized as multifunctional regulators of inflammation, immunity, hematopoiesis and angiogenesis [180, 186].

Activins regulate differentiation and proliferation of various cell types and are central in the control of wound healing [180, 186, 188]. Mouse knockout experiments have demonstrated that although activins-A and –B do have some overlapping functions, they do have distinct physiological roles and cannot replace each other [189].

Activin-A gene expression is stimulated by various pro-inflammatory and immunoregulatory pathways, such as TNF-α, IL-1 and MAPKs [180, 190]. The *INHBA* promoter contains one or more binding sites for the stress/inflammatory transcription factor, AP-1 [191, 192]. The *INHBB* promoter also contains similar binding sites suggesting similarities in the regulation [192]. *In vitro* TGF-β1 can induce activin-A expression and reciprocally activin-A can stimulate the expression of TGF-β, but in lesser extent [169].

Activin action starts when activins bind their type 2 receptors ActR2A (ACVR2A) or ActR2B (ACVR2B) [193]. ALK4 (ActR1B) is the major type 1 receptor for activins through which they activate Smad2 and Smad3 [130, 194] . However, activin-B has been reported to activate these Smads also through ALK7 (ActR1C) [195, 196] and Smad1/5/8 through ALK3 (BMPR1A) [197]. Similar to TGF-β, activins also activate MAP kinases. Activin-A has been reported to induce phosphorylation, i.e., activation of MAPK/ERK and p38 [198]. Activin-B induced activation of SAPK/JNK and MAPK/ERK are strongly linked to cell migration and wound healing [199-201].

Follistatin (FST) and follistatin like-3 (FSTL-3) bind activins with high affinity [202] and this binding renders activins unable to bind their receptors [203]. Different sized splice variants are produced from a single follistatin gene (*FST*) [181, 203]. The most common splice variants of follistatin are (FS)-315 and FS-288, which undergo further multiple levels of modifications, including proteolytic processing and glycosylation [203]. Follistatin does not structurally relate to the TGF-β superfamily [181]. FST binds and antagonizes activins but also myostatin and some BMPs [202]. FST does not bind TGF-β or block its effects (reviewed in [180]). FSTL-3 resembles FST and acts as an inhibitory binding protein for activins and BMP-2 [203].

1.7.4.1 Activins in pathological conditions

Aberrant activin activity is implicated in tissue fibrosis. Compared to normal lung, where activin-A expression is relatively low and localized in the bronchiolar epithelium, strong immuostaning of activin-A is found in the tissue samples of patients suffering from lung fibrosis [204]. Activin-A is found in alveolar macrophages, in fibrotic lesions and in hyperplastic smooth muscle cells. Activin-A can stimulate fibroblast proliferation [205, 206] and induce differentiation of lung and renal fibroblasts to myofibroblasts [206, 207] *in vitro*. Activin expression is stimulated *in vitro* by various inflammatory cytokines, such as TNF-α and IL-1 [190]. This together with reciprocal co-operation with TGF- β [169] implies that activin-A and possibly also –B have important roles in the progression of fibrotic diseases. In asthmatic patients with mild asthma and no anti-inflammatory medication, serum activin-A levels are elevated, whereas this is not the case in patents on anti-inflammatory glucocorticoid medication [169].

Activins can be tumor suppressive or tumor promoting depending on the tumor and tissue type [181] . Activin-A has been reported frequently to have a tumor suppressive role in breast and liver cancer [183, 208]. *In vitro* activin-A inhibits growth and induces apoptosis in low grade prostate cancer cell

lines, whereas high grade metastatic prostate cancer cell lines are insensitive to these effects [209]. However, in thoracic cancers activin-A is frequently overexpressed in tumor samples and associated with poor outcome [210, 211]. Activins can contribute to cancer progression also indirectly by modifying the tumor microenvironment through their regulatory action on inflammatory and immune responses and by regulating angiogenesis [188].

1.7.4.2 Activins in mesothelioma

Activin-A is highly overexpressed in human mesothelioma tumors [212]. *In vitro* data suggest that activin-A stimulates mesothelioma cell migration and growth via cyclin D.

1.7.5 Bone morphogenetic proteins

Human *BMP* genes (*BMP2*, *BMP3*, *BMP4*, *BMP5*, *BMP6*, *BMP6*, *BMP7* and *BMP10*) are scattered in different chromosomes in the human genome (http://www.ncbi.nlm.nih.gov/gene, accessed on 1.9.2014). Similar to the other members of the TGF-β superfamily, the C-terminal disulfide linked bioactive dimer of BMPs remains non-covalently associated with its N-terminal prodomain [94, 127]. These prodomains (pds) target the BMPs to the microfibrils in the ECM. BMP prodomains, however, do not likely confer latency to the associated dimers [94]. Quite little is known about the activation of BMPs and the role of the prodomains during BMP activation. BMP-2, -4, -7 and -10 bind to the N-terminal end of both fibrillin-1 and fibrillin-2 [99]. In addition, fibrillins also have alternative binding sites for different BMPs and other growth factors with weaker affinity than the N-terminal universal binding site. The extracellular regulation of BMP bioavailability is less well understood, but it is known to differ from the extracellular regulation of TGF-β signaling [90]. Unlike TGF-βs, BMPs can be directly targeted to the microfibrils through non-covalent interactions between their prodomains and the fibrillins. The type 2 receptors can compete for the binding site and displace the prodomain [94].

BMPs, despite the name, actually differ significantly in their ability to induce bone formation [213]. Different BMPs have various unique functions during development and are expressed in tightly regulated temporal and spatial manner. Mouse knockout studies have shown that knockout of BMP-2, -4 or -7 is lethal due to severe defects in the development of the heart, limb patterning and kidney, respectively (reviewed in [213]). Also neural and cartilage development depends on BMPs [214]. In addition to their indispensable role in embryonic development, BMPs and the signaling cascades they generate are central in maintaining homeostasis and proper functionality in the tissues of adult organisms [215]. BMPs also play an important role in bone formation in adult organisms [214].

BMPs can signal through ActR2A/B+ALK3 as well as ActR2A/B+ALK6 and activate Smad1/5/8 [137, 139, 193]. BMPs activate Smad1/5/8 also when BMP-R2 combines with ALK3, ALK2 or ALK6. Anti-Müllerian hormone type 2 receptor partners with ALK3, ALK2 and ALK6 and induces Smad1/5/8 activation [139]. In development, anti-Müllerian hormone mediates EMT in coleomic epithelium (the epithelium lining the surfaces of body wall and abdominal organs) during Müllerian duct regression [56]. As mentioned (1.7.2) BMPs have higher affinity to type 1 receptors than type 2 receptors and can therefore bind first the type 1 receptor. There are also differences between affinities of distinct BMPs to different receptors [137].

In addition to the canonical Smad1/5/8 response, BMPR2 has been reported to bind and regulate LIM kinase 1 (LIMK1), a downstream effector of GTPase Rho, in a Smad independent manner [216]. Binding and activation of JNKs by BMPR2 has also been reported [217]. In addition, BMP type 1 and type 2 receptors can form complexes with TGF-β-activated kinase 1 (TAK1) via binding partner TAB1, which eventually leads to Smad independent activation of p38/MAPK [213, 218]. Interestingly, TAK-1 mediated p38 and MAPK/JNK activation is also implicated in TGF-β induced growth arrest, apoptosis and EMT [219, 220]. Furthermore, activated ALK3 (BMPR1A) complexes can initiate downstream signaling also through MAPK/ERK, p38 and JNK as well as NF-κB, although the mechanisms are not yet known [150].

As mentioned earlier (1.7.4), inhibins sequester type 2 activin receptors with betaglycan [186]. Considering that, in addition to BMPR2, BMPs can bind and signal through ActR2A and ActR2B, there is a possibility that inhibins contribute to the regulation of the BMP-cascades as well as the activin cascades. BMP and BMP-R1 binding with ActR2A/ActR2B induces Smad1/5/8 activation, whereas activin-A or -B and activin type 1 receptor (ALK4 or ALK7) will induce activation of Smad2/3. This emphasizes the diversity of the system and, that the type I receptor specifies the Smad signal [130].

The receptor binding and activities of the BMPs are regulated by numerous extracellular regulators [123]. These binding factors include noggin, chordin and twisted gastrulation (TSG) as well as DAN (differential screening selected gene aberrative in neuroblastoma) family members NBL1 (Dan), cerbus 1 and gremlin-1 and -2.

1.7.5.1 BMPs in pathological conditions

In agreement with the drastic developmental defects, caused by BMP knockout, abnormal BMP signaling activity has been associated with several pathological conditions. Aberrant BMP signaling activity can result from overproduction and/or activity of BMP antagonists, or from mutation of the components in the BMP signaling pathway. In agreement with its role in bone development, BMP-2 has also been implicated in osteoporosis and in osteoarthritis [215].

Mutations in the *BMPR2* gene are frequently found in patients with familiar pulmonary hypertension [221]. Mutations in *BMPR1A* and *SMAD4* genes are linked to hereditary juvenile polyposis syndrome which increases the risk of colon cancer [222].

BMP cascades are strongly implicated in fibrotic diseases. Upregulation of TGF-β and downregulation of BMP expression and signaling is strongly implicated in chronic renal diseases, including fibrosis [223] and in liver fibrosis [224]. BMP-4 signaling is severely impaired in the lungs of IPF patients due to the overexpression of BMP antagonist gremlin [225]. In a mouse model, asbestos induced lung fibrosis is reduced by BMP-7 treatment [226]. Considering this evidence, a drug that could restore the balance between TGF-β and BMP signaling pathways would have a therapeutic potential [227].

BMP-7 and BMP-4 are frequently overexpressed in human cancer samples [228, 229]. *In vitro* data suggests that, for instance in breast cancer cells, BMPs have a complex role in the regulation of proliferation, migration and invasion [228, 230]. It has been reported that BMP-2 serum levels are

elevated in non-small-cell lung cancer (NSCLC) patients, and BMP-2 levels are more elevated in the patients with more progressed disease and correlated with poor prognosis [231]. Whereas BMP-2 is only moderately expressed in normal lung, it is strongly overexpressed in NSCLC patient tumor samples and localizes specifically in the cancer cells [232]. *In vitro* data and mouse experiments have suggested that BMP-2 functions in a cancer promoting manner in NSCLC. Clearly, different BMPs have distinct functions in different cancer types. The role of the BMPs in cancer is likely complicated and ligand and context dependent. In pathological context, BMPs have been linked to both EMT and MET [56]. Not surprisingly, increased cancer risk is one of the reported serious side effects of clinically approved and applied human recombinant BMPs-2 and -7 [149].

1.7.5.2 BMPs in mesothelioma

The data on BMPs in malignant mesothelioma are very restricted. The genes *BMP6* and *BMP3b* have been found to be silenced by promoter methylation in mesothelioma tumor samples [233]. The BMP inhibitor gremlin-1 is overexpressed in mesothelioma [234].

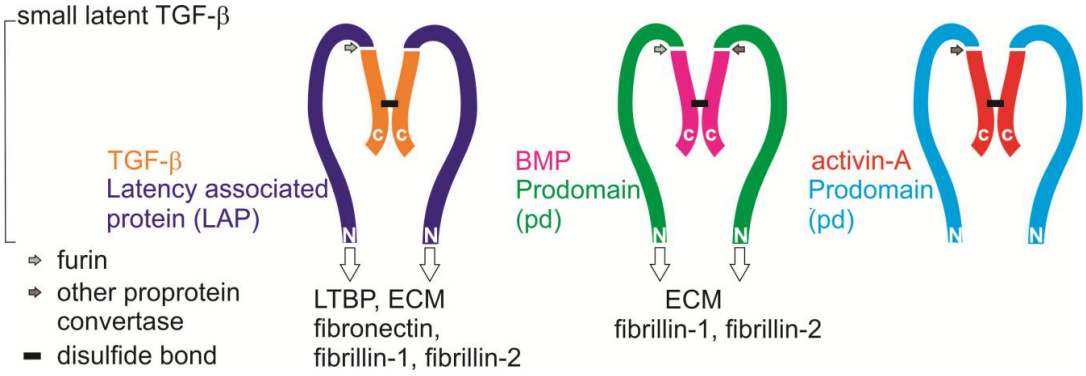

Figure 3. Schematic presentation of the structure of the TGF-β superfamily members. TGF-βs, BMPs and activins are synthetized as precursor proteins with a N-terminal prodomain and a C-terminal mature active disulfide bond linked ligand dimer. The propepide is cleaved by furin or other proprotein convertase (PC) endopeptidases. After this, LAP in TGF-β and prodomains (pds) in BMPs and activin-A remain non-covalently associated with the active peptide. LAP renders latency in small latent complex of TGF-β. This is likely not the case in BMPs and activin-A. TGF- β is targeted to ECM fibronectin and fibrillin microfibrils via association with latent TGF- β binding proteins (LTBPs). BMPs are targeted to microfibrills through their prodomains, whereas activins remain soluble. Adapted from [92, 94, 126, 127, 157, 158, 185, 235, 236].

1.8 Inhibitors of bone morphogenetic proteins

Of the plethora of BMP binding regulators, many share the cysteine–knots of the TGF-β superfamily [123]. These extracellular regulators bind and sequester ligands and have an indispensable role in the control of BMP signals by restricting their access to the receptors.

1.8.1 Introduction to the BMP antagonists

Although the BMP expression levels are strictly regulated, the bioavailability is the integral way of controlling BMP action [150]. The bioavailability is controlled by targeting the mature BMPs to the ECM structures, as discussed earlier (1.7.5) and by extracellular regulators that bind distinct BMPs with different affinities. Over 15 BMP antagonists are currently known, and they are classified into three subgroups according to the size of the cysteine-knot. The DAN family has an eight-membered ring in the knot, and it includes Dan (NO3/Nbl1, neuroblastoma suppression of tumorigenesity1), gremlin-1 (DRM, downregulated by *v-mos* / IHG-2, induced in high glucose-2), gremlin-2 (PRDC, protein related to Dan and cerberus), cerberus (Cer1), coco (Dan5), USAG-1 (uterine sensitization-associated gene-1/ Sostdc1, sclerostin domain containing 1), sclerostin and some others. Twisted gastrulation (Tsg) has a nine-membered ring, and the chordin family, noggin, FST and FSTL3 ten-membered rings. These antagonists are a disparate group. They vary in size, sequence and the way they interact with the BMPs. FST and FSTL3 were discussed above. Only Gremlin-1 from the DAN-family will be discussed here in more detail.

1.8.2 Gremlin-1

Gremlin-1 (DRM) was initially found as a novel gene downregulated in *mos*-transformed cells and suggested to play a role in cell growth control or viability, and tissue specific differentiation [237]. Gremlin gene *GREM1* is located in chromosome 15 in human (http://www.ncbi.nlm.nih.gov/gene, accessed on 1.9.2014). Gremlin-1 was predicted to have a molecular weight of 20.682, potential nuclear localization signals near the C-terminus, potential N-linked glycosylation sites, and multiple potential sites for phosphorylation [237]. Gremlin is a secreted glycosylated and phosphorylated protein [238].

Gremlin-1 acts as a homodimer and binds and inhibits BMPs-2, -4 and -7 [238, 239], which are all osteogenic BMPs, meaning they can all initiate bone formation [149]. Gremlin-1 exerts its most important functions during development; gremlin-1 mediated BMP antagonism regulates limb, kidney and lung development [221, 240, 241]. Gremlin-1 null mice often die before birth due to lung septation defects and lack of kidneys [240]. In addition to lung, kidney and limb development, gremlin-1 is also central in skeletal development, as well as in postnatal skeletal homeostasis [242].

Gremlin-1 expression in majority of adult tissues is low, but moderate expression levels have been reported in some healthy adult tissues such as kidneys, skin and bone marrow suggesting a specific function also in adult tissues [243]. Analysis of human samples and *in vitro* data suggests that gremlin-1 can support the stem cell niche in human intestinal epithelial cells and in human hepatocellular carcinoma [244, 245]. TGF-β can induce gremlin-1 expression *in vitro* [225, 246], and in serial sections of biopsies in patients with chronic allograft nephropathy gremlin-1 and TGF-β mRNAs have been found co-expressed, suggesting that this is also the case *in vivo* [247].

1.8.3 Gremlin-1 in pathological conditions

Emerging evidence links gremlin-1 to fibrosis and more specifically to fibrosis related EMT. Gremlin-1 has been reported to be downstream mediator of TGF-β1 induced EMT in human tubular epithelial cells [248, 249] and gremlin-1 has been suggested to function in a similar manner in patients with chronic allograft nephropathy [247]. In this study, gremlin-1 expression localized in the areas of interstitial fibrosis and expression correlated with tubulointerstitial fibrosis. *In vitro* data by Rodrigues-Diez (2014) [249] suggests positive feedback-loop: gremlin-1 was reported to act as a downstream mediator of TGF-β1 but, intriguingly, silencing gremlin-1 was reported to inhibit TGF-β1-mediated matrix production and EMT in cultured human tubular epithelial cells. Furthermore, gremlin-1 was reported to activate Smad3 and increase nuclear localization of both Smad3 and Smad2 together with Smad4 directly and independently of TGF-β [249]. Gremlin-1 induced EMT also in retinal pigment epithelial cells [250]. In addition, gremlin-1 overexpressing lung carcinoma (A549) cells downregulate E-cadherin and exhibit increased migration and invasion [251].

Gremlin-1 is highly expressed in the IPF lungs, upregulated in mouse hypoxic lungs and plays a central role in lung fibrosis as well as in the pathophysiology of pulmonary hypertension [221, 225, 226]. In non-ischemic heart failure, gremlin-1 expression correlates with the degree of myocardial fibrosis and is a predictor of adverse outcome [252].

Gremlin-1 is frequently found expressed by the stromal cells in the microenvironment of human carcinomas [253]. However, in sarcoma and in lung, colon, cervical and pancreatic cancer, as well as in carcinomas of ovary, kidney and breast, gremlin-1 has been found highly expressed and localized into the tumor tissue [254]. Gremlin-1 has been reported to co-operate with other BMP inhibitors, including FST, in human colorectal cancer and to promote cancer progression in invasive fronts [255]. It is likely that gremlin-1 has an oncogenic role in thoracic malignancies as it is overexpressed in lung adenocarcinoma and in malignant mesothelioma [234, 256]. In contrast, in pancreatic neuroendocrine tumors gremlin-1 has been suggested to have a tumor suppressive role [257]. In report from Chen (2002)[258], gremlin-1 inhibited neoplastic transformation through transcriptional activation of the cell cycle inhibitor $p21^{Cip1}$ and by reducing activated levels of MAPK/ERK1/2.

Although gremlin-1 was originally suggested to have a tumor suppressive role [237], it is nowadays more frequently reported to be tumor promoting. It appears that the function of gremlin-1 in carcinogenesis is complex and context dependent; it differs between the tissue, cell and cancer type. Gremlin-1 interacts with the YWHAH (14-3-3η) protein [254]. YWHAH belongs to the family of conserved 14-3-3 proteins with a multitude of binding properties and which are crucial in variety of cellular processes such as cell cycle progression, the control of the DNA damage check point and apoptosis [254, 259]. However, no report on the function of the interaction of YWHAH with gremlin-1 is yet available. Gremlin-1 may contribute to cancer progression also through BMP independent mechanisms [251, 256]. Gremlin-1 can bind to VEGFR2 (vascular endothelial growth factor receptor 2) in a BMP independent manner and induce angiogenesis *in vivo* [260]. Gremlin-1 may also modulate inflammatory cell responses by inhibiting monocyte migration through interaction with cell surface slit proteins [261].

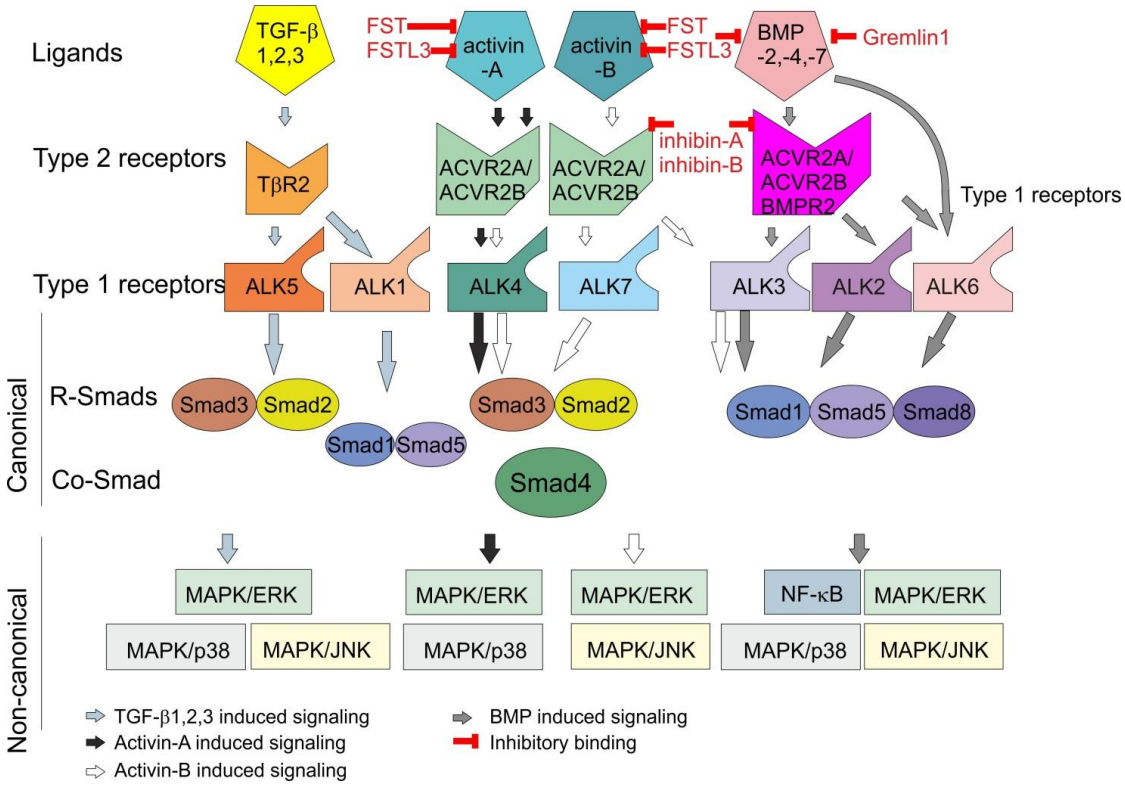

Figure 4. Signaling cascades of some of the TGF-β superfamily members. Ligand binding recruits type 2 and type 1 receptors. Type 1 receptor specifies the receptor-Smad (R-Smad) identity. All receptor Smads share the same common-partner Smad (co-Smad, Smad4). The canonical Smad- signaling pathways as well as non-canonical non-Smad pathways induced by TGF-βs are presented with light gray arrows. In addition to ALK5 mediated Smad2/3 and ALK1 mediated Smad1/5 responses, TGF-βs can activate MAPkinases ERK, JNK and p38. The canonical as well as non-canonical pathways induced by activin-A are represented with black arrows. In addition to ALK4 mediated Smad2/3 activation, activin-A can activate MAPkinases ERK and p38. Activin-B induced pathways are shown with white arrows. Activin-B can induce the same ALK4 mediated Smad2/3 cascade as activin-A but, in addition, activin-B can induce Smad2/3 through ALK7 and Smad1/5/8 through ALK3. Activin-B can also activate MAPkinases ERK and JNK. BMPs-2, -4 and -7 induced pathways are shown with dark grey arrows. BMPs can recruit first the type 1 receptors. The BMPs activate Smad1/5/8 through ALK3, ALK2 and ALK6. In addition, BMPs can activate MAPkinases ERK, JNK and p38 and NF-κB pathways. Inhibitory binding is shown with red bars. Follistatin (FST) binds and inhibits activin-A and –B and BMPs. Follistatin like 3 (FSTL3) binds and inhibits activin-A and –B and BMP-2. Gremlin-1 binds and inhibits BMPs-2, -4 and -7. Inhibin-A and inhibin-B bind activin type 2 receptors (ACVRA and ACVR2B) and prevent activins and BMPs from recruiting them to active receptor complexes. Adapted and modified from [139, 150, 193].

2. Aims of the study

The main aim of this study was to extend the understanding of molecular mechanisms of asbestos exposure related diseases. In the first study, we set out to find out pathways and mechanisms through which asbestos induces cancer and fibrosis in lung epithelial cells. Because EMT is implicated in both fibrosis and cancer, we tested whether asbestos fibers were able to induce EMT *in vitro*. In the next two studies we focused on mesothelioma. Mesothelioma is characterized by resistance to chemotherapy and local invasion, and it lacks efficient treatment. In these last two studies, we aimed to specify novel potential therapeutic target molecules and pathways from the TGF-β superfamily members and their extracellular regulators. In more detail, we aimed to characterize the role of these molecules as well as implicated intracellular signaling cascades in mesothelioma cell chemoresistance, migration and invasion. The specific aims of this study were:

1. To investigate the ability of asbestos to induce EMT
2. To find novel gremlin-1 interacting proteins and to characterize the function of gremlin-1 in mesothelioma tumors
3. To characterize how gremlin-1 contributes to mesothelioma progression
4. To investigate the expression and function of activin-A and activin-B in mesothelioma

3. Materials and methods

3.1 Cell lines and human primary cells

Human primary mesothelioma cells were harvested from pleural effusion samples of mesothelioma patients. Cells were centrifuged, washed and seeded on plastic culture dishes. At the early stages of primary mesothelioma (JP) cell cultures serum level was 20%. BEAS-2B cells were maintained in LHC-9 medium (Invitrogen). Primary human lung bronchial epithelial cells (NHBE) were maintained in BEGM (Bronchial Epithelial Cell Growth Medium) and small airway epithelial cells (SAEC) in SAGM (Small Airway Epithelial Cell Growth Medium) according to the manufactures (Lonza) instructions. The other cells and cell lines were maintained as follows: A549 in minimum essential medium (MEM), Met5A, H2052, 211H, H28, H2452 cells and primary mesothelioma cells in Roswell Park Memorial Institute medium (RPMI) supplemented with 10% (v/v) fetal bovine serum and 100 units/ml penicillin, 100 µg/ml Streptomycin and 2mM L-glutamine (Gibco).

Table 1. Primary cells

Primary cells	Description	Source	Used in study
SAEC	human small airway epithelial cells	Lonza	I
NHBE	human bronchial epithelial cells	Lonza	I
JP1	human mesothelioma cells	pleural effusion	II, III
JP3	human mesothelioma cells	pleural effusion	II, III
JP4	human mesothelioma cells	pleural effusion	II, III
JP5	human mesothelioma cells	pleural effusion	II, III

Table 2. Immortalized cells or cancer cell lines

Cell line	Description	Reference	Used in study
A549	human lung carcinoma cells	ATCC, CCL-185	I
BEAS-2B	immortalized human bronchial epithelial cells	ATCC, CRL-9609	I
Met5A	immortalized human mesothelial cells	Ke (1989) [272]	II, III
211H	biphasic human mesothelioma cell line	ATCC, CRL-2081	II, III
H2452	human mesothelioma cell line	ATCC, CRL-5946	II, III
H2052	human mesothelioma cell line	ATCC, CRL-5915	II, III
H28	human mesothelioma cell line	ATCC, CRL-5820	II, III

3.2 Three dimensional cultures

3.2.1 Lung epithelial cells (I)

Three dimensional (3D) cultures of lung epithelial cells (A549 and SAEC) were generated using Matrigel basement membrane matrix (BD Bioscience). Ice cold Matrigel was laid to chambered cover glasses (Nunc) on ice and allowed to solidify at 37°C. The cells were seeded on top of the Matrigel. Normal complete culture medium was used on the 3D cultures to produce the polarized structures. New medium was added every 2-3 days. Asbestos and TGF-β1 treatments were started on 3-7 days old cultures and continued for one week. 3D cultures in Matrigel were fixed with 4% paraformaldehyde/PBS for overnight at room temperature. After fixation the paraformaldehyde/PBS was removed and the gels were embedded in paraffin and cut into 4 µm sections.

3.2.2 Mesothelioma cells (III)

In the invasive growth assay, two layers of Matrigel gel were used. The lower layer on 96-well plate was allowed to solidify at 37˚C for 45 minutes. Next, cells were seeded. The cells were allowed to attach for 1 hour after which the media was carefully removed and replaced with the top gel. The cells were pre-treated with sActR2B-Fc, sAMHR2-Fc, DMSO or PD98059 for 15 minutes before seeding where indicated. The top gel was added and allowed to solidify for 30 minutes after which media was added on top of the culture. Inhibitors were also added to the both layers of Matrigel and to the cell culture media on top of the gel. The cells were imaged 36 hours after seeding, and sprouting from the cell clusters indicated invasive growth.

3.3 Reagents

Table 3. Reagents and growth factors

Name	**Description**	**Used concentration**	**Reference**	**Used in study**
TNF-α	tumor necrosis factor-α, human recombinant	5 ng/ml	R&D Systems	I
TGF-β	transforming growth factor-β, human recombinant	0.5 and 2 ng/ml	R&D Systems	I
crocidolite asbestos	amphibole asbestos fibers in PBS	0.5, 1 and 5 µg/ cm²	Finnish Institute of Occupational Health	I
SB431542	inhibitor of ALK5, 4 and 7	6 µM	Sigma	I
PD98059	inhibitor of MEK	30 µM	Calbiochem	I, III
SP600125	inhibitor of JNK	10 µM	Calbiochem	I
JSH-23	inhibitor of nuclear localization of NF-κB	20 µM	Calbiochem	I
activin-A	human recombinant	25 ng/ml	R&D Systems	III
activin-B	human recombinant	25 ng/ml	R&D Systems	III
sActR2B-Fc	recombinant Fc-fusion protein containing the ectodomain of human ActR2B. Sequesters ligands and inhibits their binding to cell surface receptors	200 or 650 ng/ml (2D) or 10 µg/ml (3D)	Hulmi (2013) [262]	III
sAMHR2-Fc	recombinant fusion protein containing the ectodomain of human AMHR2	200 or 650 ng/ml (2D) or 10 µg/ml (3D)	Hulmi (2013) [262]	III

Table 4. Antibodies

List of the antibodies used in the study. IF, immunofluorescence; IHC, immunohistochemistry; IB, immunoblotting; PLA, in situ proximity ligation assay.

Name	Source	Application	Reference	Used in study
E-cadherin	mouse	IB, IF	BD Transduction Laboratories	I
α-SMA	mouse monoclonal	IB	NeoMarkers	I
α-SMA	mouse/1A4	IB	Sigma	II
NF-κB (p65,RelA)	rabbit polyclonal	IF	Calbiochem	I
phospho-Smad2	rabbit polyclonal	IB	Professor Peter ten Dijke	I
Smad2/3	mouse	IB	BD Transduction Laboratories	I
phospho-ERK1/2	rabbit monoclonal /D1314.4E	IB	Cell Signaling	I, II, III
total ERK	mouse (3A7)	IB	Cell Signaling	I, II, III
ZO-1	rabbit polyclonal	IF	BD Transduction Laboratories	I
SP-D	rabbit polyclonal	IHC	Santa Cruz	I
β-tubulin	rabbit polyclonal	IB	Santa Cruz	I, II, III
calretinin	mouse/DAK-Calret1	IF, IHC	DAKO	II
cytokeratin-7	rabbit /EP16204	IF	Novus Biological	II
vimentin	mouse/V9	IF, IB	Santa Cruz	II
N-cadherin	mouse/32	IB	BD Biosciences	II
HA	mouse/16B12	IB	Covance	II
fibrillin-1	mouse/2499	IF	Millipore	II
fibrillin-1	rabbit/ pAb9543	IHC, IF	Professor Lynn Sakai	II
fibrillin-2	mouse/48	IHC, PLA	Millipore	II
gremlin-1	rabbit pAb	IHC	Abcam	II
gremlin-1	goat pAb	IHC, PLA	Santa Cruz	II
gremlin-1	rabbit pAb	IF	Santa Cruz	II
Slug	rabbit pAb	IB, IHC	Sigma	II
WT1	mouse/WT49	IHC	Novocastra	II
phospho-AKT (S473)	rabbit polyclonal	IB	Cell Signaling	II
phospho-AKT (T308)	rabbit polyclonal	IB	Cell Signaling	II
total AKT	rabbit polyclonal	IB	Cell Signaling	II
V5	mouse monoclonal	IB	Invitrogen	II
activin-A	mouse monoclonal (18/26A)	IHC, IB	AnshLabs LLC	III

activin-B	mouse monoclonal (12/9A)	IHC	AnshLabs LLC	III
activin-B	mouse monoclonal (46A/F)	IB	AnshLabs LLC	III
FST	mouse monoclonal 4/73C	IHC	AnshLabs LLC	III
FST	mouse monoclonal 4/208	IB	AnshLabs LLC	III

3.4 Generation of IκB 32/36A expressing stable cell line (I)

Retroviruses containing the vector pBabePuro (Addgene) and the construct pBabePuro IκB32/36A that express a dominant-negative mutant of IκB (kindly provided by Juha Klefström, University of Helsinki) were produced in 293GPG packaging cell line [263]. The dominant negative function is described in Traenckner (1995) [102]. The producer cells were transfected overnight using Fugene transfection reagent (Roche), followed by collection of cell conditioned medium, which was then used to transduce A549 cells. Puromycin (5 μg/ml) selection was started two days after transduction.

3.5 Transient transfection and reporter assay (I, II, III)

Table 5. Promoter and expression constructs

Name	**Description**	**Reference**	**Used in study**
$(CAGA)_{12}$-luc	Smad3 responsive	Prof. Peter ten Dijke	I, III
ARE-luc	Smad2 responsive	Prof. Peter ten Dijke	I, III
FAST-1	Smad2 required transcription factor	Prof. Peter ten Dijke	I, III
$(Bre)_2$-luc	Smad1/5 responsive	Prof. Peter ten Dijke	II, III
pRL-TK	Renilla luciferase control	Promega	I, II, III

3.5.1 Smad responsive promoters (I, II, III)

The cells to be transfected were seeded in 6-well or 96-well plates. The next day the cells were co-transfected with a total of 2 μg of promoter constructs (1 well on 6 well plate or 40 wells on 96 well plate) $(CAGA)_{12}$-luc (Smad3 responsive) or ARE-luc (Smad2 responsive) and Fast-1 or $(Bre)_2$-luc (Smad1/5 responsive) together with pRL-TK plasmid using Fugene HD transfection reagent (Roche). The pRL-TK plasmid contains the Renilla luciferase gene under control of the constitutively expressed thymidine kinase promoter, and it was used in dual luciferase assays to normalize the transfection efficiency. The next day the stimulation by asbestos, TGF-β1 or activins was started in serum free media. After overnight stimulation the cells were lysed and subjected to luciferase activity measurements by Dual Luciferase Reporter Assay (Promega) and DCR-1 luminometer (MGM Instruments Digene Diagnostics Inc.).

3.5.2 10-pathway Cancer reporter array (I)

Dual luciferase based Cignal Finder 10-Pathway Cancer Reporter Array (SABioscience) was used according to manufacturer's instructions. Briefly, the cells were transfected during plating on 24-well plate using Fugene transfection reagent (Roche). The cells were allowed to recover overnight. The cells were lysed and subjected to luciferase activity measurements by Dual Luciferase Reporter Assay and DCR-1 luminometer. Unspesific reporter responses to TGF-β1 or asbestos were tested but none was observed.

3.6 Analysis of the mesothelioma tumor tissue

Table 6. Mesothelioma tumor tissues

Patient	Type	Location	Age at diagnosis	Gender	Smoker	Exposure	Used in study
JP1	epithelioid	pleura	53	male	yes	yes	II, III
JP2	biphasic	pleura	71	male	no	no	II, III
JP3	epithelioid	pleura	63	male	yes	yes	II, III
JP4	biphasic	peritoneum	72	female	?	?	II, III
JP5	epithelioid	pleura	69	female	yes	no	II, III
JP6	biphasic	pleura	71	female	no	no	II, III
JP7	epithelioid	pleura	62	male	yes	yes	II, III
JP8	epithelioid	pleura	63	male	yes	?	III
JP9	epithelioid	pleura	54	male	yes	yes	III
JP10	epithelioid	pleura	75	male	no	yes	III
JP11	epithelioid	pleura	65	male	no	yes	III
JP12	epithelioid	pleura	60	male	yes	yes	III
NP1	normal pleura	pleura	32	male	yes	no	II
NP2	normal pleura	pleura	34	male	yes	?	II

3.6.1 Immunohistochemical analysis (II, III)

Paraffin-embedded tissues from mesothelioma tumor samples were cut into 2.5 µm sections, which were then deparaffinized in xylene and rehydrated in graded alcohol. Antigens were retrieved by heating in 10 mM citrate buffer (pH 6.0). For immunostaining, the Novolink Polymer Detection System (Novocastra, Leica Biosystems Newcastle Ltd.), Histostain Plus Broad Spectrum Kit (Zymed), or ImmPRESS reagent kit (Vector Laboratories,) was used according to the respective manufacturer's protocol. The sections were incubated with the primary antibody at 4°C overnight. The bound antibodies were visualized by using peroxidase substrates 9-ethyl-3-aminocarbozole (AEC; Zymed) or 3-,3-diaminobenzidine (DAB; Leica). The sections were counterstained with Mayer's hematoxylin and mounted on glass slides. Control sections were treated with isotype controls for mouse (Zymed), rabbit (Invitrogen), or goat (Jackson Immunoresearch Laboratories) to determine the specificity of the staining. For follistatin staining, the formalin-fixed, paraffin embedded specimens were stained according to the manufacturer's staining protocol [with the Leica Bond Polymer Refine Detection-kit, Bond Epitope Retrievel Solution 2 for 20 mins, R.T.U. Normal

Horse serum 2,5% (Vector Laboratories) blocking] on Leica BOND-MAX fully automated staining system. The sections were incubated with the primary antibodies at room temperature for 1 h. The bound antibodies were visualized by DAB (Vector Laboratories). The sections were counterstained with Mayer's hematoxylin and mounted on glass slides. Images were captured with Nikon DS-Fi1 or with Axio Imager with ApoTome (Zeiss, Göttingen, Germany) by using Axio Vison 4.8 software (Zeiss). From H&E and SP-D stained sections, images were captured with Olympus BX51 and Artray Artcam 300 MI.

3.6.2 In situ proximity ligation assay (II)

Gremlin-1 and fibrillin protein interactions were studied by proximity ligation assay (Olink Bioscience) [264]. First, acetone-fixed frozen sections of mesothelioma tumor samples were incubated overnight with primary antibodies: anti-gremlin-1 antibody together with anti-fibrillin-2 antibody. Secondary antibodies (α-goat and α-mouse) conjugated with DNA probes which, when in close proximity, formed a closed circle with the added oligonucleotides and ligase enzyme. This closed circle was amplified by rolling-circle amplification reaction. Fluorescently labeled oligonucleotides complementary to the circle were hybridized in the reaction, resulting in spot-like positive signals indicating that the two primary antibodies are bound in close proximity. Cell nuclei were visualized with 2,4-diamidino-2-phenylindole (DAPI). Images were captured with Axioplan 2 epifluorescence microscope (Zeiss) and AxioCam HRm 14-bit grayscale CCD camera Axiovision 4.6 software (Zeiss).

3.7 RNA analysis

3.7.1 RNA isolation and cDNA synthesis (I, II, III)

Total cellular RNA was isolated using RNeasy Mini kit (Qiagen) and reverse transcribed to cDNA using Random hexamer primers (Invitrogen) and Superscript III reverse transcriptase (I) (Life Technologies) or iScript cDNA synthesis Kit (Bio-Rad) (II, III) according to manufacturer's instructions.

3.7.2 Quantitative RT-PCR (I, II, III)

The cDNAs were amplified using TaqMan Assays-on-Demand gene expression products (Applied Biosystems) and CFX96 real-time PCR detection system (BioRad). The levels of gene expression were determined using the ΔΔCt method, and the results have been expressed as mRNA expression levels normalized to the levels of a gene with a constant expression (TBP, TATA binding protein).

3.7.3 siRNA transfection (II)

The cells were seeded on a 6-well plate. The next day the cells were transfected with either gremlin-1 siRNAs (gremlin-1 siRNA1, siRNA2 and siRNA3 (Ambion) or control siRNA (Ambion), for 6 hours in the absence of antibiotics by using Lipofectamine 2000 transfection reagent (Invitrogen). The cells were collected from the 6-well plates three days after transfection and the RNA was extracted.

3.8 Protein analysis

3.8.1 Immunofluorescence analysis (I, II)

The cells were grown on glass coverslips and cultured for the indicated times. The cells were fixed with 4% paraformaldehyde/PBS at room temperature for 10-20 minutes or with methanol at -20°C for 15 minutes or overnight. Nonspecific binding of the antibodies was prevented by blocking with 5% BSA/PBS for 30 minutes. During blocking, 0.3% Triton X-100 was added when permeabilization of cells was needed. All antibody dilutions and washing steps were made in Dulbecco's PBS containing 0.5% BSA. The cells on coverslips were incubated with the primary antibodies for 1-2 hours at room temperature and then washed. The bound primary antibodies were detected using AlexaFluor secondary antibodies (Molecular Probes). TRITC-conjugated phalloidin (Sigma) was used for the detection of F-actin (I). Finally, the coverslips were washed with water and mounted on glass slides with Vectashield mounting medium containing DAPI (Vector laboratories). Images were captured with Axioplan 2 epifluorescence microscope and Axio Cam HR camera using Axiovision 4.5 software (Zeiss) at the Biomedicum Imaging Unit of the University of Helsinki.

Fixed 3D cultures in Matrigel were embedded in paraffin and cut into 4 µm sections. These sections were then deparaffinized in xylene and rehydrated in graded alcohol. Antigens were retrieved by heating in 10 mM citrate buffer (pH 6.0). The sections were blocked with 5% non-fat dry milk/PBS, which contained normal goat serum (Jackson Immuno Reseach) at room temperature for 30 minutes followed by incubation with primary antibodies diluted in blocking buffer at 4°C overnight. The sections were then incubated with AlexaFluor secondary antibodies at room temperature for 1 h, washed several times and mounted using Vectashield Hard Set mounting medium. The nuclei were visualized with DAPI. The images were captured as described above. Digital morphometry was conducted using Image Pro Plus 7.0 program.

3.8.2 Cell conditioned media (III)

Conditioned media from mesothelioma cell cultures were collected for two days, concentrated using Amicon Ultra 10K centrifugal filters (Millipore) and analyzed with SDS-PAGE and immunoblotting.

3.8.3 SDS-PAGE and immunoblotting (Western blotting) (I, II, III)

The cells were lysed in RIPA buffer (50 mM Tris-HCl, pH 7.4, 150 mM NaCl, 1mM EDTA, 1% NP-40, 0.2% Na deoxycholate) containing protease and phosphatase inhibitors (Roche Diagnostics) for 15 minutes on ice. Protein concentrations were measured using a BCA Protein Assay Kit (Pierce). Equal amounts of protein were separated by SDS-PAGE using 4-20% gradient Tris-glycine gels (Bio-Rad). Proteins were transferred to Protran nitrocellulose membranes (Whatman**)** by using a semi-dry blotting system (Bio-Rad). Membranes were first blocked with 5% non-fat dry milk in TBS/0.05% Tween-20 to prevent non-specific binding of the antibodies and incubated with the primary antibodies diluted in 5% BSA in TBS/0.05% Tween-20 at 4˚C overnight and then with biotin-conjugated secondary antibodies (DAKO) at room temperature for 1 h. After several washing steps, the final detection was performed using HRP-conjugated streptavidin and an enhanced

chemiluminescence Western blotting detection system (Amersham). Immunoblot band intensities were analyzed by the Scion Image (Scion Corporation) (I, II) and by ImageJ (III) software.

3.8.4 Human phospho-kinase array (II)

Control and gremlin-1 siRNA treated cells were lysed and alterations in phospho-kinase levels were analyzed using a Proteome profiler array (ARY003b, R&D Systems) according to manufacturer's instructions. Quantity One version 4.6 (BioRad) was used for quantification. The kinase array was performed twice.

3.9 Gremlin-1 interaction studies (II)

3.9.1 Expression constructs and stable transfection

C-terminally tagged whole length gremlin-1 construct was generated by Gateway-cloning the gremlin-1 construct from the Human Orfeome Collection (Thermo Scientific) to a pTO-SHc-GW-FRT plasmid with c-terminal Strep-tag III and human influenza hemagglutinin (HA)-tag [265]. Flip-In human embryonic kidney (HEK) 293 cells (Life Technologies) were grown as recommended. Stable transfection of cells was carried out as described by Glatter (2009) [266]. After two weeks of culture, hygromycin B resistant clones were tested for tetracycline (Sigma) inducible gremlin-1 expression

3.9.2 Affinity purification

Transfected Flip-In HEK293 cells were stimulated with tetracycline (25 ng/ml) to induce gremlin-1 expression. After a 24-hour stimulation, cells were lysed in HNN-lysis buffer [50 mM HEPES pH 8, 150 mM NaCl, 50 mM NaF, 1 mM PMSF, 1.5 mM Na-vanadate, 0.5% NP-40 and protease inhibitors (Sigma)] followed by double affinity purification [266]. Briefly, cell lysates were passed through Strep-Tactin columns (IBA GmbH) followed by elution of bound proteins with 2.5 mM biotin. Next, the eluate was immunoprecipitated using anti-HA agarose (Sigma). Proteins were finally eluted using 0.2 M glycine and neutralized.

3.9.3 Protein digestion

Protein amount from the elution fractions was precipitated using trichloroacetic acid (TCA). First, TCA was added to the elution fractions to a final concentration of 25%, followed by incubation for 30 minutes on ice. The precipitates were centrifuged, washed once with ice cold 0.1M HCl in acetone and once with acetone. The pellets were then allowed to dry. For trypsin digestion the precipitated proteins were dissolved in 50 mM ammonium bicarbonate, pH 8.9, containing 0.1% Rapigest detergent (Waters). Proteins were reduced using DTT for 30 minutes at 60ºC followed by alkylation using iodoacetamide for 30 minutes at room temperature in the dark. Proteins were digested with trypsin (Promega, Madison, WI) for 18 hours at 37°C and then the Rapigest detergent was hydrolyzed with HCl for 45 minutes at 37°C. Peptides were purified with PepClean C18 Spin Columns (Thermo Fisher) according to the manufacturer's protocol. Finally the purified peptides were dissolved in 0.1% formic acid for mass spectrometric analysis.

3.9.4 LS-MS/MS analysis

Mass spectrometric analysis was performed using nanoAcquity UPLC – liquid chromatography system on-line with Waters Synapt G2 mass spectrometer (Waters). Waters nanoAcquity UPLC Trap Column (Symmetry C18, 180µm x 20mm, 5µm) was used as trapping and Waters nanoAcquity UPLC Column (BEH130 C18, 75µm x 150mm, 1.7µm) as analytical column. Four µl of sample was injected and run using 90 minutes gradient from 3% to 40% mobile phase B (0.1% formic acid in acetonitrile). As mobile phase A 0.1% formic acid in water was used.

Data was collected in a data dependent acquisition manner by collecting eight fragmentation spectra simultaneously. Switch limit from MS to MS/MS was set to peak intensity of 200. Fragmentation data for detected peaks was collected for 5 seconds and then excluded from fragmentation for 120 seconds. Scan time for both MS and MS/MS was one second. No lockmass correction was used.

The raw data was processed with Mascot Distiller software (version 2.3.1.0, Matrix Science), and a database search was performed using the Mascot search engine (version 2.2.04) against Swiss-Prot human database (dated 16.6.2010). MudPIT scoring and Ion score cut-off limit of 20 were used to identify peptides. Require bold red-specification was used to limit the results to those proteins which have at least one unique peptide. Carbamidomethylated cysteine was set as fixed modification and oxidation of methionine as variable modification. Peptide mass tolerance for search was 0.2 Daltons and 0.1Da for fragment ion search. A maximum of two missed trypsin cleavages was allowed. The Mascot Distiller processed data was also searched using GPM X!Tandem search engine51 using same the parameters.

3.9.5 Expression and purification of recombinant gremlin-1

The expression construct pGremlin-1_V5/HIS in pEF-IRES-P contains cDNA encoding human gremlin-1 with C-terminal tags (V5 and 6HIS). H2052 and H28 cells were transiently transfected with this construct or the expression vector using Fugene HD transfection reagent (Promega). CHO cells were stably transfected, and gremlin-containing cell culture supernatants produced as described by Hulmi (2013) [262]. The media was then dialyzed against 50 mM sodium phosphate buffer, pH 7.2, and 1 M NaCl (buffer A) and loaded on a 1 ml HiTrap column (GE Health Care, Waukesha, WI) previously charged with $CoCl_2$ and equilibrated with buffer A. The loaded column was washed with 40 column volumes of buffer A, and subjected to a fast protein liquid chromatography (GEHC) gradient run starting with buffer A containing 0-100% buffer B (buffer A with 250mM imidazole). Fractions were analyzed by SDS-PAGE for their purity and molecular mass, and imidazole in these fractions was removed by dialysis against buffer A. For further concentration and purification, gremlin-1 containing fractions were dialyzed against TBS and subjected to affinity chromatography using a 1 ml HiTrap heparin column (GEHC). Bound gremlin-1 was eluted in a 0 to 1 M NaCl gradient.

3.9.6 Surface plasmon resonance

Binding analyses were performed using a BIAcore2000 (GEHC). First, 2000 RUs of gremlin-1 were covalently coupled to carboxymethyldextran hydrogel 500M sensor chips (XanTec) using the amine coupling kit following the manufacturer's instructions (GEHC). Binding assays with N-

terminal fibrillin-1 (rF11) and -2 peptides (rF86) as analytes were performed as described by Sengle (2008a)[99]. Kinetic constants were calculated by nonlinear fitting of association and dissociation curves (BIAevaluation 4.1 software).

3.10 Measurement of cell viability and apoptosis (II)

Cell viability was assessed by MTT assay (R&D Systems). Briefly, cells were seeded on 96-well plates (10,000/well), and the next day the cells were treated with different concentrations of paclitaxel (Hospira). The metabolic activity of the cells was measured after 48 hours according to the manufacturer's instructions. Apoptosis was assayed with TUNEL technology using In Situ cell death detection kit (Roche). Cells were seeded on glass coverslips, cultured overnight and transfected with siRNAs as described above. Cells were then fixed and stained according to the manufacturer's instructions three days after transfection.

3.11 Measurement of cell proliferation (II)

To a measure cell proliferation, the cells were seeded on 12-well plates and counted 1, 2 and 3 days after transfection using TC10 automated cell counter (BioRad).

3.12 Measurement of cell migration (III)

3.12.1 Live cell imaging

Incucyte ZOOM 2013A kinetic live cell imaging system (Essen Bioscience) was used according to the manufacturer's instructions to monitor the cell migration. Briefly, the cells were plated on 96-well plates, and the next day a wound was applied on confluent monolayer using a woundmaker (Essen Bioscience). The media was replaced with serum-free media supplemented with the activin blocker (sActR2B-Fc) when indicated. Two distinct pictures were captured of each well every 2 hours for 48 hours. Data was analyzed with Incucyte ZOOM 2013A software, and the relative wound density was used as a measure of the wound closure.

3.12.2 Scratch wound assay

For conventional scratch wound assay, the cells were seeded on 12-well plates, and the wounds were made on confluent monolayers using a P200 pipette tip. The media was replaced with serum-free media supplemented with DMSO, PD98059 or sActR2B-Fc where indicated. Two pictures were captured of each well after 0, 6, 24 and 48 hours using Nikon Eclipse TS 100 and Digital Sight DS-L2. The quantification of the wound density was done using Image ProPlus 7.0 software. The percentage of area occupied by the cells relative to percentage of wound area was defined, and that area was normalized to wound density data at 0 hour time point. The control treated wound density was set to one.

3.13 A statement for the use of patients samples (II,III)

A statement for the use of human mesothelioma tissue and pleural effusion materials was received from the Ethics Committee of the Helsinki University Hospital, Helsinki, Finland (number 308/13/0301/2010). All patients gave informed consent to participate in the study. Tissue biopsies and pleural effusion samples were obtained from patients undergoing diagnostic procedures and had

a clinical and/or radiological suspicion of malignant mesothelioma. All patients included in the study were later diagnosed to have mesothelioma. Control pleural samples were obtained from two male smokers who were operated for pneumothorax.

3.14 Statistical analysis (I, II, III)

Data were analyzed using PASW Statistics 18 (I, II) and 21 (III) programs for Windows (SPSS). Statistical difference between two independent groups was evaluated using nonparametric Mann-Whitney U-test. Statistical difference between more than two independent groups was evaluated using nonparametric Kruskal-Wallis test. A p-value of less than 0.05 was considered statistically significant.

4. Results and discussion

4.1 The ability of crocidolite asbestos to induce EMT *in vitro* (I)

Asbestosis and IPF are both fibrotic diseases of the lung. Although in asbestosis the initiating component is known, whereas in IPF it remains unknown, these diseases share many features including histopathology of usual interstitial pneumonia (UIP). EMT is implicated in IPF and other fibrotic diseases (see 1.3.5). EMT is also implicated in lung cancer [267], both asbestos related and no-asbestos related, and mesenchymal characteristics are associated with worse patient prognosis. EMT is associated with local invasion and distal metastasis, and contributes to drug resistance and anti-apoptotic phenotypes of cancer cells [61]. In addition, asbestos exposure can induce signaling pathways linked to EMT (see review of the literature). Therefore, we set out to investigate the ability of crocidolite asbestos to induce EMT in lung epithelial cells *in vitro*.

4.1.1 Exposure to crocidolite asbestos leads to loss of epithelial characteristics in lung epithelial cells

The loss of cell junctions is a hallmark of EMT [58]. We found that in 3D cultures of both A549 carcinoma cells and small airway epithelial cells (SAEC) asbestos exposure led to downregulation of E-cadherin protein levels. This indicates the loss of epithelial phenotype. In 2D environment, A549 cells were the only cell type in which asbestos exposure downregulated E-cadherin and tight junction protein ZO-1 (I; Figures 1 and 2). A549 cells are widely used because they retain many characteristics of the type II lung epithelial cells. Primary human small airway (SAECs) or bronchial (NHBE) epithelial cells, as well as immortalized bronchial epithelial cells (BEAS-2B), most likely lose their type II characteristics in 2D cultures. These cells did not show signs of EMT in 2D even when stimulated with TGF-β1, which is a known inducer of EMT. When SAECs were placed in 3D environment, they retained type II characteristics, indicated by the production of surfactant protein –D (SP-D), and the cells downregulated E-cadherin in response to asbestos and TGF-β1 exposure (I; Figure 8). This suggests that only the type II lung epithelial cell phenotype has enough plasticity to initiate EMT processes. This seems logical, since the alveolar type II epithelial cells do exhibit more plasticity. They are the proliferative lung epithelial cell population and progenitor cells for the type I cells [18, 19]. As majority of the alveolar surface area is composed of type I cells [6], it is plausible that the cells that are exposed to an oxidative stress would not be susceptible to EMT. However, considering the fundamental role that the small type II cell population has, EMT in this population would have detrimental impact.

Transcriptional downregulation of E-cadherin has been reported to be a late event in EMT [56, 57]. However, we saw TGF-β1 induced downregulation of E-cadherin mRNA in A549 cells already after three days, and it persisted after six days (I; Figure 1). Even after six days, asbestos exposure did not lead to downregulation of E-cadherin mRNA in A549 cells. Transcriptional changes, such as upregulation of snail and slug, can also occur at a later state of EMT [57]. We found that TGF-β1 induced snail and especially slug expression already after one hour stimulation, and the levels were further elevated up to three and six days. Asbestos was able to induce snail and slug expression in A549 cells after six days, and late upregulation of these transcription factors could later lead to transcriptional repression of E-cadherin to establish the loss of epithelial junctions and complete

EMT. TGF-β1 is a potent biological inducer of EMT (see 1.3). In contrast, asbestos induced EMT may not have all the same characteristics as a growth factor induced EMT. For instance, the time scale of EMT events, the expression profile of the mesenchymal markers and the effector pathways were different to what has been reported for TGF-β1 induced EMT in A549 cells [268].

4.1.2 Pathway activities differ between normal and cancer cells

TGF-β1 induced EMT in A549 cells has been suggested to be Smad2 mediated [268]. Initially, we hypothesized that asbestos exposure could stimulate endogenous TGF-β activity, possibly by ROS mediated activation of latent TGF-βs, and this would induce Smad mediated EMT. However, whereas TGF-β1 induced robust Smad2 and Smad3 activation in A549 cells, asbestos failed to do so (I; Figure 5). Consistent with this, blocking TGF-β type 1 receptors with SB431542 could not prevent decrease in E-cadherin in asbestos exposed cells, whereas it did so in TGF-β1 exposed cells. In order to characterize the underlying pathway(s) of asbestos induced loss of epithelial phenotype, cancer associated pathway array was used to compare the basal activity of different pathways in SAECs and A549 cells grown in 2D (I; Figure 6). This array indicated three pathways, MAPK/JNK, NF-κB and MAPK/ERK, which all have been implicated in EMT (see 1.3). MAPKs ERK and JNK are also non-canonical pathways for TGF-β (1.7.3 and Figure 4 in thesis).

4.1.3 MAPK/ERK pathway contributes to asbestos induced epithelial plasticity

We found that asbestos induced ERK activation in A549 cells (I; Figure 7). Furthermore, the loss of epithelial phenotype and reorganization of the actin cytoskeleton induced by asbestos in 2D could be prevented by the inhibition of MAPK/ERK phosphorylating kinase MEK by PD98059. Asbestos has been reported to induce ERK activation [26]. MAPK/ERK pathway has been linked to EMT (see 1.3) and is implicated in fibrotic and malignant diseases (see 1.6.3). Interestingly, also radiation induced EMT in A549 and in rat alveolar type II epithelial cells (RLE-6TN) has been reported to be ERK mediated [269]. Our findings are in concord with the literature and emphasize targeting MAPK/ERK pathway in the treatment of asbestos induced lung cancer and asbestosis. However, much more research is needed, and the future treatments are likely to target multiple pathways. The inhibition of MAPK/ERK (PD98059), MAPK/JNK (SP600125) or NF-κB (dominant negative mutant IκB32/36A) pathways had no effect on asbestos induced α-SMA induction. Consistent with the recognized role of NF-κB in cell survival and in stress responses (see 1.5) inhibition of the NF-κB pathway in A549 cancer cell line led to significantly decreased cell survival, particularly when exposed to asbestos.

Cytoplasmic protein β-catenin interacts with E-cadherin in adherens junctions [56]. When E-cadherin is cleaved or removed from the membrane, β-catenin is released and either degraded or it can enter the nucleus and regulate transcription. Nuclear localization of β-catenin is implicated in EMT and has been reported to contribute to the activation of the α-SMA promoter (reviewed in [270]). This would be interesting to study in more detail in the future.

4.2 Localization and function of gremlin-1 in mesothelioma ECM *in vitro* and in tumor tissue (II)

Gremlin-1 was originally suggested to have a tumor suppressive role [237], but nowadays it is more frequently reported to be tumor promoting [254]. Gremlin-1 is overexpressed in lung adenocarcinoma and in malignant mesothelioma [234, 256]. We set out to analyze whether gremlin-1 overexpression contributed to mesothelioma development and progression. We started by searching for new gremlin-1 interacting proteins *in vitro* after which the results were validated in mesothelioma tumor samples. We also confirmed the key findings of the *in vitro* functional studies in the mesothelioma patient samples.

4.2.1 Characterization of primary mesothelioma cells

In order to best recapitulate the phenotypic characteristics of mesothelioma tumors *in vitro*, primary mesothelioma cells from the clinical pleural effusion samples of mesothelioma patients were collected. Majority of the harvested cells (JP-cells) were found to be able to proliferate on a cell culture dish and were positive for mesothelial markers calretinin and cytokeratin-7 (CK-7) as well as for vimentin, which is frequently expressed in cancer cells. Calretinin and CK-7 expression confirmed the mesothelial origin of the cells, whereas May-Grünwald-Giemsa (MGG) and Papanicolaou (PAPA) stainings (unpublished observation) of the cytospin samples, together with the characteristic vacuolated cytoplasm [271] (see Figure 4 in II) and vimentin expression, confirmed their malignant characteristics. These primary cells, especially at early passages, represent mesothelioma much better than established cell lines, which during passaging and culturing may have lost or altered the gene expression of phenotypic proteins, sometimes even the expression of calretinin or CK-7, or both (unpublished observation). This loss of initial phenotype will also happen to JP cells during prolonged culturing (unpublished observation, thesis Figure 5). Therefore, for mechanistic studies it is critical to choose cell lines that faithfully recapitulate the investigated characteristics of primary tumor cells, as has been done in II and III. Representative cell lines are a necessity because primary cells will eventually lose their original characteristics, after which they alter their primary gene expression profile and phenotype. During studies II and III, we have found H2052 cells to resemble primary mesothelioma cells closely in respect of the proteins and characteristics analyzed in these studies.

We used non-malignant Met5A cells as a control cell line. These cells are normal human mesothelial cells immortalized with SV (simian virus) 40 early region DNA [272]. These cells are widely used, and alternative control cells are limited. SV40 virus is frequently found in MM and also in other malignancies, but its contribution to the development of the malignancy has remained controversial [30, 273].

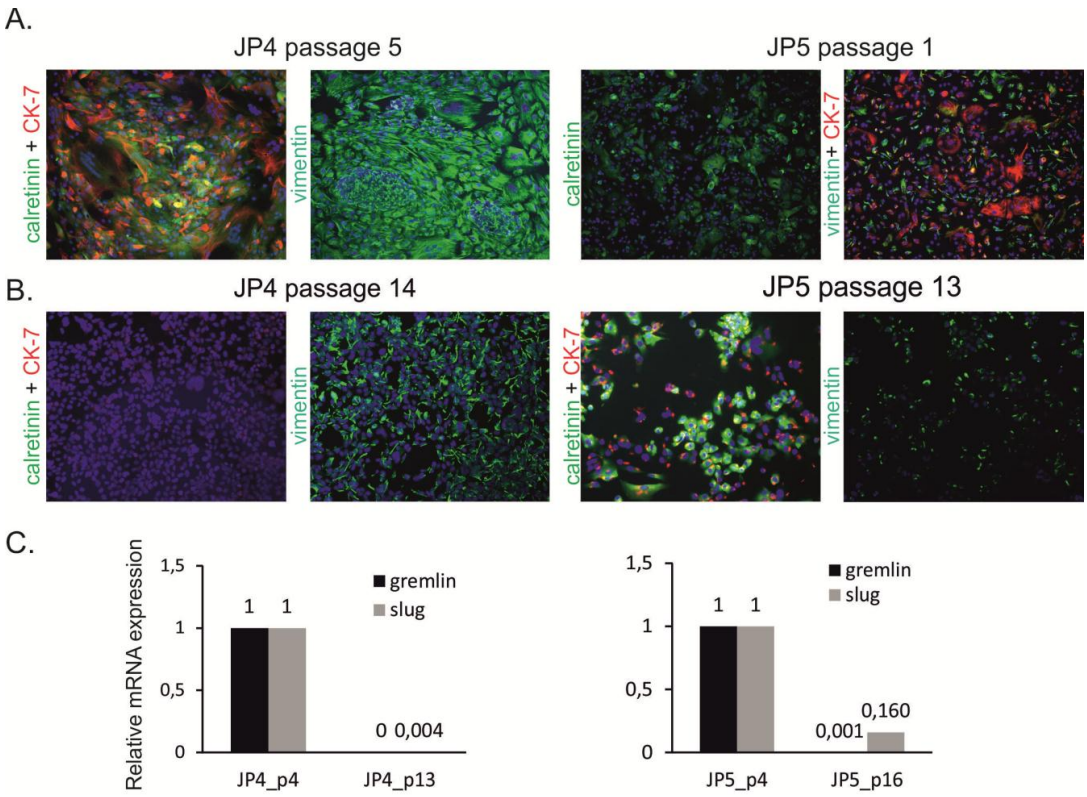

Figure 5. Primary mesothelioma cells lose phenotypic gene expression during prolonged culture. (A) Early passages of the primary mesothelioma cells (JP4 and JP5) recapitulate tumor characteristics and express calretinin and CK-7, diagnostic marker proteins for mesothelioma. (B) JP4 cells lose the expression of these markers at later passages. JP5 cells retain mesothelial marker expression. (C) Irrespective of the marker expression, both JP cells lose the expression of gremlin-1 and transcription factor slug, key molecules of the second study, during passaging. Gremlin-1 and slug were highly expressed in early passages of primary cells as well as in the mesothelioma tumors. The characteristics that are beneficial in tumor progression *in vivo* are not necessary beneficial in adaption to cell culture *in vitro* and are therefore not maintained. Instead, cell culture selects for fast proliferating cells.

4.2.2 Fibrillin-1 and -2 are novel gremlin-1 interacting proteins

The search for new gremlin-1 interacting proteins was done using systematic affinity purification coupled with mass spectrometry identification (AP-MS). Fibrillin-2 was identified in all three replicate experiments. This interaction was further confirmed by testing for direct interactions between purified gremlin-1 and recombinant N-terminal fragments of fibrillin-2 and fibrillin-1 using surface plasmon resonance technology. High affinity interaction between gremlin-1 and the N-terminal peptides were observed (II; Figure 1, Table 1). Interestingly, also BMPs-2, -4, -7 and -10 bind to the N-terminal end of both fibrillin-1 and fibrillin-2 [99](and 1.7.5).

4.2.3 Gremlin-1 and fibrillin-2 and/or fibrillin-1 are concomitantly overexpressed and co-localize in mesothelioma tumor tissue and *in vitro*

Validation of the *in vitro* interactions was done by immunohistochemical staining and by in situ proximity ligation assay (PLA) in mesothelioma tumor samples. In immunohistochemical staining gremlin-1 and fibrillin-2 expression was low and fibrillin-1 absent in normal mesothelium (II; Figure 2). In reactive mesothelium, both gremlin-1 and fibrillin-2 expression were moderately elevated whereas in mesothelioma tumor samples both gremlin-1 and fibrillin-2 were highly expressed. Fibrillin-1 was detected only in the stroma of one tumor sample. Gremlin-1 and fibrillin-2 exhibited strikingly similar staining patterns, which was not surprising considering that the two had been found to interact *in vitro*. The interaction in the mesothelioma tumors was further validated with proximity ligation assay, which showed clear co-localization of gremlin-1 and fibrillin-2 in mesothelioma tumors with intermolecular distance being less than 40 nm, which is the theoretical maximum distance achieved by this method. Unlike the tumors, primary mesothelioma cells expressed both fibrillin-1 and -2, and gremlin-1 was found to co-localize with fibrillin-1 (II; Figure 5) in culture. As mentioned earlier, gremlin-1 interacted *in vitro* with both fibrillin-1 and -2, but fibrillin-1 was mainly absent from the tumors.

Previously, Seddon et al. (2006) [253] reported gremlin-1 expression in the stromal cells in carcinomas, whereas we found gremlin-1 expression in mesothelioma tumor cells. Carcinomas are highly complex tumors and likely differ in organization from mesotheliomas, which are reasonably unique tumors in nature.

The cells remodel the ECM and the ECM interacts with the cells and influences cell adhesion, proliferation, migration and survival [80]. Furthermore, altered ECM can initiate and support EMT [61] and promote the progression of fibrosis and cancer. We showed that mesothelioma cells remodel the surrounding ECM by producing excess fibrillin-2. Fibrillin-2 is normally expressed during development, and the expression in healthy adult pleura is low (1.4.2 and II; Figure 2). Re-expression of developmental programs is associated with cancer progression [274]. Consistently, also gremlin-1 is a developmental protein (1.8.2). Efficient deposition of gremlin-1 into fibrillin-2 containing fibers in mesothelioma ECM may enable production of larger amounts of gremlin-1. This could also partially explain the concomitant overexpression of fibrillin-2 and gremlin-1. This resembles what has been reported for TGF-βs and LTBP-1 in mesothelioma. TGF-β expression and activity are high in mesothelioma tumors [164, 165, 174]. LTBPs are required for targeting TGF-β into ECM (see 1.7.3). Interestingly, LTBP-1 is found abundantly expressed in the stroma of mesothelioma patient samples [164], suggesting that it might function as a reservoir for increased TGF-β levels. It is important to note, that those BMPs which gremlin antagonizes, BMPs -2, -4 and -7 are also targeted to microfibrills [94, 99]. Thus, gremlin-1 appears to be deposited close to its biological targets, and this might have functional importance. However, experiments on mice and on cultured mouse osteoblasts suggest that although both fibrillins-1 and -2 bind and store both TGF-βs and BMPs, the distinct fibrillins may modulate the bioavailability of TGF-βs and BMPs differentially [93]. Depletion of fibrillin-2 led to increased activation of TGF-β, whereas both TGF-β and BMP signaling were elevated in fibrillin-1 depleted cells.

4.2.4 Intracellular signaling is affected by gremlin-1

In mechanistic studies, we found that silencing gremlin-1 severely impaired H2052 cell proliferation and led to significant alterations in cell signaling pathways (II; Figures 6 and 7). Parts of the observed alterations were clearly attributable to increased BMP activity. Silencing gremlin-1 with siRNA interference lead to significant increase in the MAPK/ERK phosphorylation levels. This could also be due to increased BMP activity because MAPK/ERK is one of the non-canonical pathways for BMPs (see 1.7.5 and thesis Figure 4). H2052 and primary mesothelioma cells do express endogenous BMPs, especially high levels of BMP-2. BMP-2 has also been reported to promote cancer cell migration and invasiveness via Smad1 and via MAPK/ERK pathways [275, 276]. As expected, when gremlin-1 was silenced, BMP activity in H2052 cells increased, demonstrated by increased activity of Smad1/5 pathway and increased expression of Id1.

High MAPK/ERK activity can also lead to growth arrest by elevating the levels of p21[108]. Our finding that silencing gremlin-1 led to severe reduction in cell proliferation (II; Figure 6) with concomitant upregulation of ERK activity and p21 expression (II; Figure 7) is in agreement with proposed model that both too low as well as too high MAPK/ERK activity levels promote cell cycle arrest via p21 [108].

In H2052 mesothelioma cells, the AKT phosphorylation levels (S473) were high (II; Figure 7). AKT, and particularly this phosphosite, is frequently phosphorylated in MM and contributes to chemoresistance [46, 121]. Our data supports this. Although after silencing gremlin-1 we saw no change in the AKT (S473) phosphorylation levels, the phosphorylation of AKT target and regulator of mTOR, PRAS40, was increased in gremlin silenced cells. Furthermore, gremlin-1 binds directly to the 14-3-3 protein [254], which also binds and regulates PRAS40 and other PI3-K/AKT/mTor pathway proteins [122].

As mentioned, the majority of mesotheliomas (see 1.2) have wild type functional p53. We found that silencing gremlin-1 in H2052 mesothelioma cells increased phosphorylation of p53 (S46 and S392) and the expression of p53 target gene p21(Cip1/Waf1) (II; Figure 7), which promotes cell cycle arrest in G1 [277]. Accordingly, forced gremlin-1 overexpression in H2052 and H28 cells (of which the latter has minor endogenous expression levels, see Figure 4 in II) reduced the p21 mRNA levels. These results propose gremlin-1 a role in cell proliferation and survival. This is also supported by our finding that silencing gremlin-1 severely impaired cell proliferation in H2052 mesothelioma cells (II; Figure 6). Clearly, gremlin-1 is involved in a more complex network of pathways than solely BMP inhibition, and the distinction between BMP-dependent and BMP-independent mechanisms may prove challenging.

4.2.5 Gremlin-1 sustains chemoresistant EMT phenotype through slug

Slug functions as a potent EMT inducer, regulating the expression of many genes repressing the epithelial and promoting the mesenchymal state [58]. We found high gremlin-1 and high slug expression strongly associated (II; Figure 8). They were co-expressed in the MM tumor samples and in the cells and cell lines exhibiting high gremlin-1 expression (JP cells and H2052). Instead, cell lines exhibiting low gremlin-1expression exhibited also low slug expression levels but, when forced to overexpress gremlin-1, increased also slug expression levels (II; Figure 8). Furthermore,

when gremlin-1 expression was silenced, slug expression levels decreased. Concomitant downregulation was also observed in primary mesothelioma cells during prolonged culture (thesis Figure 5). Simultaneously with slug expression levels in H2052 cells, expression levels of mesenchymal markers N-cadherin, vimentin, α-SMA and fibronectin decreased and epithelial marker E-cadherin increased (II; Figure 8). We have also observed similar upregulation of E-cadherin in late passages of JP-cells (our unpublished observation, not shown) suggesting that the mesenchymal phenotype of the JP-cells is at least partially lost together with gremlin-1 and slug expression. Our results suggest that gremlin-1 supports mesenchymal phenotype in mesothelioma cells through transcription factor slug. Snail expression levels in primary mesothelioma cells did not differ from the expression levels in Met5A cells. This is in agreement with the suggested hierarchy in snail and slug expression. In this hypothesis, snail is expressed at the onset of the transition, whereas slug and other transcription factors are subsequently induced to maintain the mesenchymal phenotype [65]. Mesothelioma invades surrounding tissues aggressively. During EMT, a switch from E- to N-cadherin leads to the loosening of intercellular contacts and facilitates migration [56].

Gremlin-1 induces and supports EMT, and EMT is associated with elevated expression of matrix metalloproteinases (MMPs), which degrade the extracellular matrix (ECM) (see 1.3.5). ECM degradation can release more fibrillin bound gremlin-1 and TGF-β bound to fibrillin and fibronectin and they can further promote cancer progression.

A recent report by de Reynies (2014) [41] identified two subgroups in mesothelioma, which associated with better (C1) or worse (C2) prognosis irrespective of the histological subtype. Interestingly, the C2 subgroup exhibited mesenchymal (EMT) phenotype. In agreement with what is known of the prognosis of the sarcomatoid mesothelioma, all sarcomatoid mesotheliomas fell into the C2 subgroup. Importantly, this subgrouping was able to differentiate mesotheliomas to better (C1) and worse (C2) prognosis subgroups within the epithelioid histological subtype. In the C2 subgroup also slug and gremlin-1, in addition to other mesenchymal markers, were upregulated and E-cadherin was downregulated compared to the C1 group whereas in the C1 group gremlin-1 and slug were expressed less and E-cadherin more compared to the C2 group. This is in agreement with our findings and suggests that gremlin-1 could be the key factor promoting the mesenchymal phenotype and it might hold potential not just as therapeutic target but also as prognostic marker in mesothelioma.

EMT phenotype is implicated in chemoresistance (1.3.5). Chemoresistance is a major problem in the management of MM (see 1.2.5.). We found that the mesothelioma cells expressing high gremlin-1 tolerated chemotherapeutic drug paclitaxel better compared to the cells with low gremlin-1 expression. Furthermore, silencing gremlin-1 expression led to sensitization to the cytotoxic effects of the chemotherapeutic drugs paclitaxel and pemetrexed. This together, with what was discussed of the potential role of gremlin-1 in the regulation of PI3-K/AKT cascades and its contribution to chemoresistance on MM, strongly proposes a central role for gremlin-1 in mesothelioma chemoresistance and possibly a way to overcome this problem. Targeting EMT in cancer is challenging [61]. The cells can switch between epithelial and mesenchymal states or retain characteristics of both phenotypes. Therefore specific targets such as gremlin-1 are needed. No chemical inhibitor for gremlin-1 is yet available, but a small interfering RNA targeting human gremlin-1 has been patented (http://www.lens.org/lens/patent/US_7741470_B2, accessed on

1.9.2014). Gene expression can efficiently be silenced with siRNAs in mouse models using cationic liposome-siRNA complex or other vehicles in infusion [278, 279]. Intriguingly, encouraging results in mesothelioma have been reported using fully humanized monoclonal antibodies for targeting T-cell receptor protein cytotoxic T-lymphocyte-associated protein 4 (CTLA4) [280]. Studying efficacy of a specific antibody targeting gremlin-1 could be worthwhile in mesothelioma. Due to its specific and consistent overexpression in mesothelioma [234] (and II) and low expression in most normal adult tissues [243], gremlin-1 would make potential therapeutic target.

4.3 Role of activins in mesothelioma cell migration and invasion *in vitro* (III)

Activins function as multifaceted regulators of inflammation, immunity and angiogenesis [180, 186]. They regulate differentiation and proliferation of various cell types and are central in wound healing [188]. Activins can be tumor suppressive or tumor promoting depending on the tumor and tissue type [181]. Activin-A has been reported to be overexpressed and to promote growth in mesothelioma [212]. This study was conducted to characterize the expression and signaling pathways of activin-A and -B in mesothelioma and the contribution of activin- dependent signaling cascades in mesothelioma progression.

4.3.1 Activin-A and activin-B are overexpressed in mesothelioma tumors and in cultured mesothelioma cells

We found activin-A and activin-B highly expressed in mesothelioma tumors and in primary mesothelioma cells (III; Figure 1). Predominant expression of activin-A in biphasic mesothelioma cells (JP4 and 211H) was an interesting finding. The mesothelioma cell lines were very variable in their activin expression, and the cell lines used in the mechanistic studies were selected based on their high activin expression resembling primary cells (H2052 and 211H). Also FST was found abundantly expressed in the tumors and in the representative cell lines. The primary mesothelioma cells, however, expressed high levels of FSTL-3 instead of FST.

FSTL-3 resembles FST and binds and inhibits activins and BMP-2 [203]. Interestingly, in primary mesothelioma cells BMP inhibitor gremlin-1 and BMP-2 (II) as well as FSTL3 and activins-A and -B (III) were upregulated compared to the Met5A control cells. Gremlin-1, FST and activin expressions were abundant also in the tumor tissues. These observations emphasize the role of the TGF-β superfamily members and their extracellular regulators in mesothelioma. In study II, we found that BMP-2 is highly expressed in mesothelioma cell lines and especially in primary mesothelioma cells. The high FST/FSTL3 expression in mesothelioma cells may therefore not only counteract high activin levels but also BMP-2 activity. Co-operation of BMP inhibitors, including gremlin-1 and FST, in cancer progression has been reported previously in colorectal cancer desmoplastic invasion fronts [255]. We found high activin-A and FST expression in mesothelioma tumor samples, as well as in H2052 and 211H cell lines. In cell culture of rodent pituitary and granulosa cells, activin-A induces FST expression [281, 282]. Furthermore, recombinant BMP-2 can induce activin-A and FST expression in mouse prechondroblastic cell line [283]. Together with our findings, this suggests a complex network of regulation.

We also found ACVR2A and ALK7 overexpression in mesothelioma cells (III; Figure 2). The contribution of ALK7 overexpression remains to be elucidated, as well as its predominant ligand in mesothelioma. In addition to activin-B, also Nodal, a developmental morphogen implicated in cancer progression [284, 285], is a ligand for ALK7. Intriguingly activin-A has been reported to induce Nodal and maintain self-renewal and pluripotency in human embryonic stem cells *in vitro* [286]. In this setting, activin-A was also reported to suppress BMP expression and signals.

Interestingly, the attenuation of the canonical Smad2/3 response and switch to non-canonical MAPK/ERK signaling (see 4.3.2) was also associated with a switch of the predominant type 2 receptor from ACVR2B to ACVR2A. The ACVR2A overexpression possibly serves to enhance activin induced MAPK/ERK signals, which promote cell migration and invasion (see 4.3.3). Type 1 receptor specifies the R-Smad response [130], but it would be interesting to investigate whether type 2 receptors could contribute to the specification of the non-canonical signals or selection between canonical and non-canonical signals.

4.3.2 Attenuation of canonical Smad3 response to activins associates with migratory and invasive phenotype

We found that majority of the mesothelioma cells had attenuated Smad3 response to activins, and this was associated with a migratory and invasive phenotype (III; Figures 3, 4 and 5). Interestingly, the mesothelioma cell lines with attenuated Smad3 response to activins (211H and H2052) did activate Smad3 in response to TGF-β1 stimulation (unpublished observation, thesis Figure 6) suggesting that the attenuation of the Smad3 response was activin specific. Smad2 response was attenuated in H2052 and in JP5 cells expressing both activin-A and -B but activated in 211H cells, expressing practically only activin-A (III; Figure 1 and 3). Furthermore, JP5 and H2052 activated MAPK/ERK also in response to exogenous human recombinant activin-A and –B (III; Figure 6). Smad2 and Smad3 differ in their ability to bind DNA as well as their cellular targets [145]. Whereas the MH1 domain of Smad3 and Smad4 can directly bind DNA, MH1 domain of Smad2 cannot. Smad2 and Smad3 activation can also have distinct effects on cell migration [287]. In this study, however, attenuation of the Smad3 response to activins was consistently associated with a migratory and invasive phenotype.

We found invasive and migratory characteristics to depend on activin mediated signals. Migration and invasion could be abolished by inhibiting activin signaling by sequestering extracellular activins by soluble type 2 receptor (sActR2B-Fc) (III; Figure 4 and 5). For therapeutic point of view this is interesting. In mouse model, soluble type 2 activin receptor has been used [288]. In this model, inhibition of activin-A by soluble receptor was shown to inhibit cancer associated muscle wasting and cachexia efficiently and to prolong survival of the tumor bearing animals.

It has been suggested that TGF-β induced transcriptional responses would be primarily mediated by Smad3/Smad4 complexes, whereas activin responses would be mainly mediated by Smad2/Smad4 complexes [139]. This, however, is likely not the case in mesothelioma cells. In H2052 and JP5 cells also Smad2 response to activins was attenuated (III; Figure 3). Furthermore, in control Met5A and in H28 mesothelioma cells activins did induce robust Smad3 activation.

FST and FSTL3 bind soluble activins and prevent their binding to the receptors [202, 203]. In the cells exhibiting high FST/FSTL-3 expression and attenuation of the Smad3 response, activins did, however, elicit responses, explicitly the MAPK/ERK cascade. If high FST/FSTL3 levels would explain attenuation of the Smad3 response, no alternative signaling cascades in response to activins should be detected as activins could not bind their cell surface receptors. Thus, high expression of FST/FSTL-3 cannot account for the attenuation of the Smad3 response in mesothelioma cells.

4.3.3 Activin stimulated MAPK/ERK phosphorylation supports mesothelioma cell migration and invasion

We found MAPK/ERK pathway to be the major pathway mediating the activin stimulated migration and invasion in mesothelioma cells. Consistently in all cells (H2052, JP5 and in 211H), sequestering of extracellular activins by soluble type 2 receptor (sActR2B-Fc) led to significant reduction in ERK phosphorylation levels (III; Figure 6) concurrently with the impairment of migration and invasion (III; Figure 4 and 5). Furthermore, inhibiting ERK phosphorylating kinase MEK caused similar impairment of cell migration and invasion (III; Figure 6) as observed with sActR2B-Fc.

The MAPK/ERK pathway is known to promote EMT (see 1.3.2). Migration and invasion are characteristics of cells of the mesenchymal phenotype. It is therefore possible, that like many other members of the TGF-β superfamily, also activin-A, and possibly also activin-B, could be able to support mesenchymal phenotype. We found a switch of activin signaling from the Smad3 pathway to the MAPK/ERK pathway and this switch promoted migration and invasion. This agrees with the concept that pathological EMT is an important mechanism in the progression of mesothelioma and agrees with reported importance of MAPK/ERK pathway in mesothelioma (1.2.6 and 1.6.3).

We did not clearly differentiate which activin, –A or –B, was the major factor in the MAPK/ERK mediated cell migration and invasion. However, the migratory and invasive 211H cells expressed almost exclusively activin-A, and this speaks for the major role for activin-A. Likely *in vivo* mesothelioma cell invasion requires co-operation of both activins-A and –B mediated ERK and other cascades, as well as numerous other factors and pathways.

The well-studied growth factor of the same family, TFG-β, has a dual function during carcinogenesis. At first TFG-β acts as a tumor suppressor but eventually it switches to a tumor promoting role [140, 145], and this has been suggest to occur by suppressing the Smad2/3 activity with concomitant increase in ERK activation [151] (see also 1.7.3.1). Our results suggest that activins could act in a similar manner. Another proposed mechanism to explain how TGF-β induced growth inhibitory signals could be overcome suggests increased inhibitory phosphorylation of Smad2/3 in the linker region by elevated ERK activity [147]. Our results are consistent also with this mechanism. Interestingly, *in vitro* data suggest that in also prostate cancer cells, a loss of sensitivity to activin-A mediated growth inhibitory and apoptotic signals takes place during cancer progression [209].

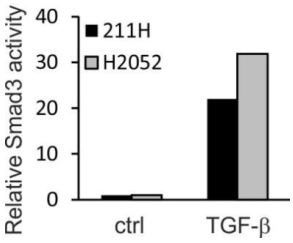

Figure 6. TGF-β induced Smad3 response in 211H and H2052 cells. The mesothelioma cell lines exhibiting attenuated Smad3 response to activins do activate Smad3 in response to TGF-β (2 ng/ml) stimulation.

The key findings of this thesis are gathered in Figure 7.

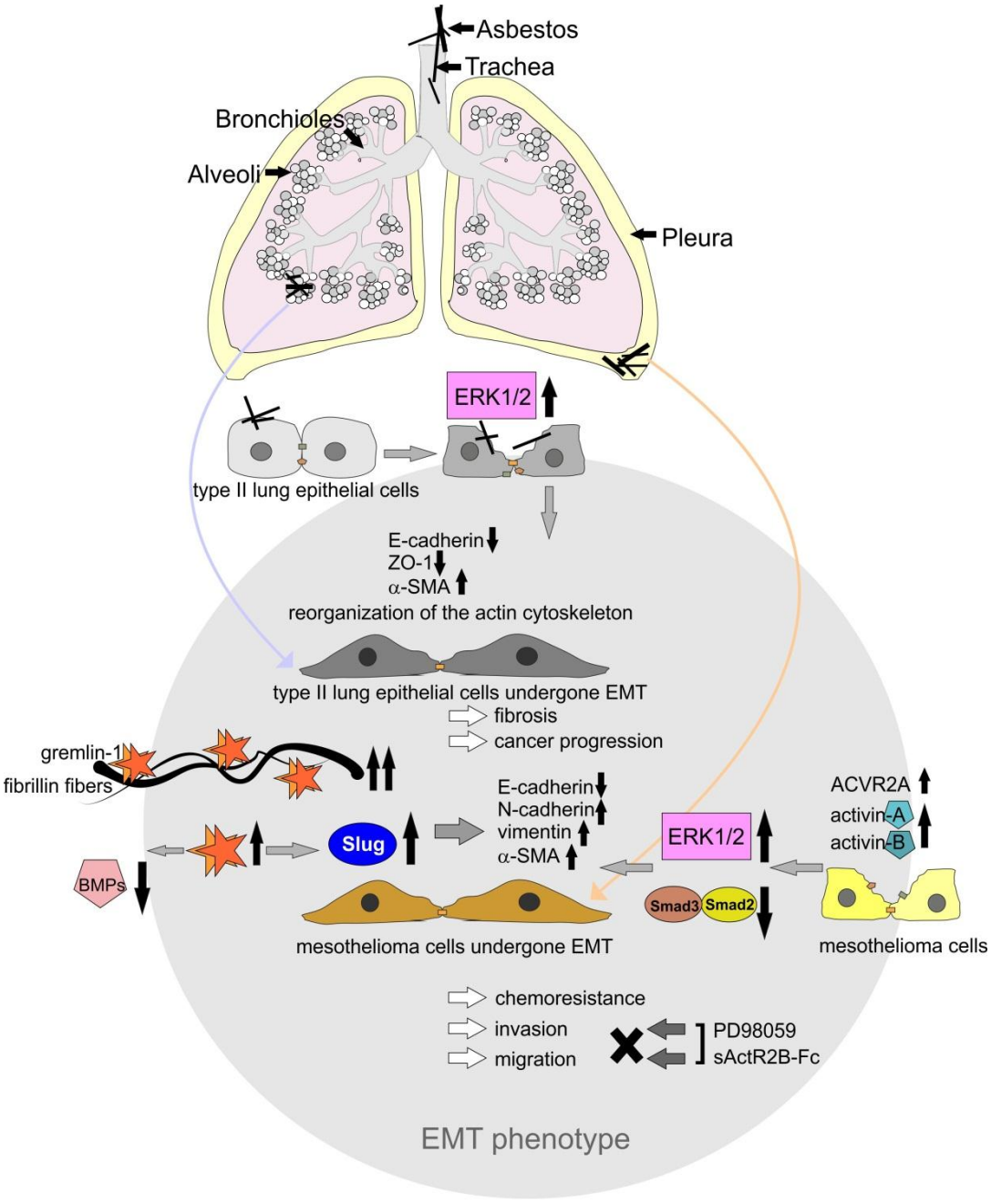

Figure 7. Synthesis of the work. Asbestos exposure of lung epithelial cells can induce EMT like processes which promote fibrosis and cancer progression. Asbestos fibers can induce MAPK/ERK activation. MAPK/ERK pathway initiated epithelial plasticity in type II lung epithelial cells leads to downregulation of E-cadherin and ZO-1 and to dissolution of epithelial junctions and reorganization of cortical actin to stress fibers. EMT in the lung type II epithelial cells likely results from co-operation of various signaling pathways and transcription factors, which induce mesenchymal markers (such as α-SMA) and complete EMT. In mesothelioma, BMP inhibitor gremlin-1 and ECM protein fibrillin-2 are highly overexpressed. Concomitant upregulation of gremlin-1 and fibrillin-2 enables gremlin-1 deposition into mesothelioma ECM. Gremlin-1 supports chemoresistant EMT phenotype through transcription factor slug. Slug downregulates epithelial E-cadherin and upregulates mesenchymal proteins N-cadherin, vimentin and α-SMA. EMT phenotype can also promote invasion. Activin-A and activin–B are overexpressed in mesothelioma. Attenuation of the canonical Smad2/3 response and switch to non-canonical MAPK/ERK signaling promotes mesothelioma cell migration and invasion. Simultaneous switch of the predominant type 2 receptor from ACVR2B to ACVR2A with concomitant upregulation of ACVR2A may further enhance the invasion promoting signaling. Inhibiting activin activity by sequestering extracellular activins by soluble activin receptor (sActR2B-Fc) or inhibiting ERK phosphorylating kinase (PD98059) impairs mesothelioma cell migration and invasion.

5. Conclusions and future perspectives

The understanding of the molecular mechanisms of EMT as well as asbestos elicited physiological and cellular responses has increased tremendously in the past years. The work presented in this thesis supports the concept of pathological EMT as one key mechanism not only in the pathogenesis of fibrosis (asbestosis) and asbestos induced lung cancer, but also in the progression and chemoresistance of mesothelioma. Due to the extensive latency preceding the diseases, eventually understanding the molecular mechanisms of pathogenesis and progression of asbestosis, lung cancer and mesothelioma will, possibly provide an opportunity to prevent the outbreak of disease in the exposed individuals, or at least slow down the process.

Whether gremlin-1 and activin-A play a cancer promoting or cancer suppressing role in carcinogenesis is currently under debate and appear to depend on the tissue and cancer type. However, we and others [212, 234] have shown that in mesothelioma they have properties that are likely to promote tumor development. The situation is, however, complicated by the tight interplay between gremlin-1, the other regulators and the other members and of the TGF-β superfamily, not to mention the diversity and overlap of the signaling cascades. Nonetheless, gremlin-1 and activin-A, and possibly also activin-B, have presented themselves as putative candidates for targeted therapy in mesothelioma and should be investigated further.

The finding that gremlin-1 localized into fibrillin-2 containing microfibrills in mesothelioma tumor ECM was completely new. Concomitant overexpression of fibrillin-2 and gremlin-1 possibly enables the expression and deposition of larger amounts of gremlin-1 compared to if no efficient extra cellular deposition was available. We found that high gremlin-1 expression supports the EMT phenotype and our results and the literature suggest that EMT is an important process in chemoresistance. In mesothelioma, chemoresistance is an enormous problem. Our results suggest that gremlin-1 holds potential as a way to target chemoresistance in mesothelioma and should be thoroughly investigated. Gremlin-1 overexpression in mesothelioma appears to be consistent and high [234](and II). This together with low expression in normal lung and weak or moderate expression in majority of tissues in healthy adults [243] suggests that gremlin-1 would also be a very specific therapeutic target. No chemical inhibitor for gremlin-1 is available currently. Possible means by which gremlin-1 could be targeted in mesothelioma include specific siRNAs and specific antibodies.

Our results of the involvement of the MAPK/ERK pathway in asbestos induced epithelial plasticity and in mesothelioma cell migration and invasion are in agreement with the current view on molecular pathogenesis of asbestos exposure related diseases. The evidence that implicates MAPK/ERK pathway in mesothelioma pathogenesis is strong. However, small molecule EGFR tyrosine kinase inhibitors have failed to show clinical efficacy in MM patients [28]. Our *in vitro* data suggests an alternative way of ERK activation in MM - through activin receptors. This is an important finding since the MEK inhibitor trametinib has proven rather toxic for normal tissues, which limits therapeutic use [289]and the efficiency of another MEK inhibitor, selumetinib appears to be limited to patients with BRAF mutations [290]. Targeting Raf/MEK/ERK pathway is complicated because it is able to promote cell proliferation but also cell cycle arrest[108].

We showed that by sequestering activins or by inhibiting ERK activation cell migration and invasion were impaired. Mesothelioma progresses predominantly through local invasion. Therefore, activins as therapeutic target in mesothelioma invasion *in vivo* would be important to investigate in the future. In mouse model soluble activin receptors have already been found to be efficient in inhibiting activin-A activity [288].

Although mesothelioma has a certain unique characteristics it does share many common features of other solid tumors. The understanding of mesothelioma pathogenesis can also benefit the research of other cancers. Our finding that gremlin-1 supported chemoresistant EMT phenotype could be a mechanism not limited to mesothelioma and should be investigated in other cancer types, particularly in those overexpressing gremlin-1.

How do cancer cells escape from the normal regulatory activin signals and how do activins become cancer promoting? Our work suggest that this happened by switching from the canonical Smad pathway to the non-canonical MAPK/ERK pathway. This could be a more general mechanisms in thoracic cancers, where activin-A is frequently overexpressed and associated with worse outcome [210, 211].

Cysteine knot proteins gremlin-1, activin-A, TGF-β and the BMPs likely co-operate through a complex network to regulate cell plasticity and proliferation in asbestos exposure related diseases, and this is shown in Figure 8.

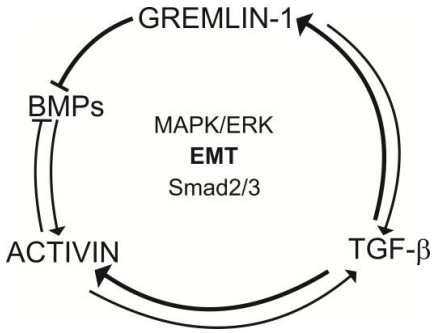

Figure 8. Gremlin-1 and TGF-β superfamily members in cell plasticity in lung and pleural diseases. Gremlin-1, activin-A and TGF-β are all highly expressed in malignant mesothelioma. Aberrant TGF-β activity, activin-A and gremlin-1 overexpression are also implicated in other fibrotic and malignant diseases of the lung (see review of the literature). TGF-β can induce the expression of gremlin-1 and activin-A [169, 225, 248, 249]. Literature implies, that activin-A and gremlin-1 could also induce TGF-β expression [169, 249]. Gremlin-1 antagonizes BMPs -2, -4 and -7. BMP-2 has been reported to induce activin-A expression [283] and respectively, activin-A has been reported to suppress BMP expression and signals [286]. Through activation of Smad2/3 and MAPK/ERK as well as other signaling pathways these bioactive molecules may induce EMT and sustain the mesenchymal phenotype, which promote fibrosis, cancer invasion and chemoresistance.

In future we need to thoroughly investigate the specific contributions of gremlin-1 and activins in mesothelioma development, progression and chemoresistance as well as the intermolecular signaling networks of gremlin-1 and activins with the other members of the TGF-β superfamily. Gremlin-1 and activins can become true therapeutic targets in mesothelioma only after full characterization of their specific roles, interactions and the mechanisms through which these molecules promote EMT, invasion and chemoresistance.

5. Acknowledgements

This study was carried out in the research group of Katri Koli in Translational Cancer Biology Research Program (former Molecular and Cancer Biology Research Program) and in the Transplantation Laboratory of Haartman Institute in the University of Helsinki during years 2008-2014. Current and former directors of the Research Program Professors Kari Alitalo and Jorma Keski-Oja, as well as former and current heads of the Biomedicum Helsinki, Professors Olli Jänne and Sampsa Hautaniemi, are acknowledge for providing excellent facilities for conducting research.

I wish to express my appreciation to my supervisor Katri Koli for introducing me to the world of science and for her patience with me throughout these years. Thank you for the guidance and for teaching me various technical things in the lab as well as numerous things related to scientific writing and scientific world. I also want to thank Kati for memorable moments with Singapore Sling in Raffles Hotel and Samuel Adams in Boston.

I warmly thank all former and current members of the Koli Lab; Anna Kantola, Liisa Murray, Emma Paasikivi and Mira Tissari, for a great working atmosphere. Liisa Murray is especially acknowledged for the co-authorship of the second paper, Miao Yin for significant contribution in and co-authorship of the third paper and Emma Paasikivi for excellent technical assistance in the third paper.

This study was carried out in close collaboration with Myllärniemi Lab. I am grateful to Marjukka Myllärniemi for her co-authorship and especially for her view as a physician and help with statistical and quantification issues. Eva Sutinen is acknowledged for her excellent technical assistance throughout the project and for co-authorship in the third paper.

I wish to express my gratitude to docents Terttu Harju and Hannu Koistinen for careful review of this thesis and for constructive comments.

This thesis would not have been possible without the contribution of the co-authors in the manuscripts into which this thesis is based on. Thank you Ville Parviainen and Risto Renkonen, Alexander P. Wohl and Gerhard Sengle, Sakari Joenväärä, Markku Varjosalo, Mikko Rönty, Olli Ritvos and Arja Pasternack for the productive and successful collaboration.

The research group of Jorma Keski-Oja has been our helpful neighbor throughout these years. I want to thank all former and current members of the Keski-Oja Lab; Marko Hyytiäinen, Yizhou Hu, Huini Li, Pipsa Meller, Lotta Sankkila, Nami Sugiyama, Olga Tatti, Piia Vehviläinen and Irene Ylivinkka for always benign helpful and for creating a pleasant working environment. Anne Remes and Sami Starast have provided indispensable technical help during the years.

Merja Koivulahti I thank for her help in secretarial issues but more importantly for entertaining us with stories and pictures of the goings-on of her dogs.

Tiia Pelkonen is thanked for revising the language of this thesis.

All the mesothelioma patients who willingly participated in the study of this devastating disease are warmly acknowledged.

Biomedicum Imaging Unit (BIU) is acknowledged for providing excellent equipment and help in the imaging field.

I thank Outi Leppäranta for her co-authorship in the second paper and also for superb peer support and good company especially during the end of this project. Also my other biochemist friends Maria Pulkkinen, Emilia Carlsson and Martin Hermansson are acknowledged for good company, discussions and most of all for staying my friends all these years. Päivi Telenius, an oddity among my friends no being a biochemist, I thank for regular irregular meetings and great company and discussions not involving science.

I am grateful for my parents, Heikki and Marjatta Tamminen for enabling me to educate myself and for my twin sister Emmi and little brother Herman for generating a unique atmosphere to grow up in. Mummi, my hero, I want to thank for always bringing things to right perspective and demonstrating what a great power positive attitude can have.

Importantly, I want to thank Pasi for the support throughout these years. You understand me better than anyone. Thank you for your patience and support and thank you for sharing the passion for travelling and speed and taking care that I've had a life during this thesis project.

This work was financed by Sigrid Jusélius Foundation, Academy of Finland, Jalmari and Rauha Ahokas Foundation, Jane and Aatos Erkko Foundation, Magnus Ehrnrooth Foundation, the Finnish Anti-Tuberculosis Association and University of Helsinki as well as personal grants from Helsinki University, HES-foundation, Biomedicum Helsinki Foundation and travel grants from Helsinki University (Chancellors travel grand) and from The Finnish Respiratory Society.

7. References

1. Mossman BT, Lippmann M, Hesterberg TW, Kelsey KT, Barchowsky A, Bonner JC. Pulmonary endpoints (lung carcinomas and asbestosis) following inhalation exposure to asbestos. *J Toxicol Environ Health B Crit Rev*. **14:** 76-121. 2011

2. Shukla A, Ramos-Nino M, Mossman B. Cell signaling and transcription factor activation by asbestos in lung injury and disease. *Int J Biochem Cell Biol*. **35:** 1198-1209. 2003

3. Stayner L, Welch LS, Lemen R. The worldwide pandemic of asbestos-related diseases. *Annu Rev Public Health*. **34:** 205-216. 2013

4. Huuskonen MS, Rantanen J. Finnish Institute of Occupational Health (FIOH): prevention and detection of asbestos-related diseases, 1987-2005. *Am J Ind Med*. **49:** 215-220. 2006

5. Sekido Y. Molecular pathogenesis of malignant mesothelioma. *Carcinogenesis*. **34:** 1413-1419. 2013

6. Liu G, Cheresh P, Kamp DW. Molecular basis of asbestos-induced lung disease. *Annu Rev Pathol*. **8:** 161-187. 2013

7. Lynch JP, 3rd, Fishbein MC, Saggar R, Zisman DA, Belperio JA. Idiopathic pulmonary fibrosis. *Expert Rev Respir Med*. **1:** 377-389. 2007

8. Clarke DL, Carruthers AM, Mustelin T, Murray LA. Matrix regulation of idiopathic pulmonary fibrosis: the role of enzymes. *Fibrogenesis Tissue Repair*. **6:** 20. 2013

9. Schneider F, Sporn TA, Roggli VL. Asbestos fiber content of lungs with diffuse interstitial fibrosis: An analytical scanning electron microscopic analysis of 249 cases. *Arch Pathol Lab Med*. **134:** 457-461. 2010

10. Warnock ML, Wolery G. Asbestos bodies or fibers and the diagnosis of asbestosis. *Environ Res*. **44:** 29-44. 1987

11. Nielsen LS, Baelum J, Rasmussen J, Dahl S, Olsen KE, Albin M, Hansen NC, Sherson D. Occupational asbestos exposure and lung cancer--a systematic review of the literature. *Arch Environ Occup Health*. **69:** 191-206. 2014

12. Weiss W. Asbestosis: a marker for the increased risk of lung cancer among workers exposed to asbestos. *Chest*. **115:** 536-549. 1999

13. Le Jeune I, Gribbin J, West J, Smith C, Cullinan P, Hubbard R. The incidence of cancer in patients with idiopathic pulmonary fibrosis and sarcoidosis in the UK. *Respir Med*. **101:** 2534-2540. 2007

14. Noble PW, Albera C, Bradford WZ, Costabel U, Glassberg MK, Kardatzke D, King TE, Jr., Lancaster L, Sahn SA, Szwarcberg J, Valeyre D, du Bois RM. Pirfenidone in patients with idiopathic pulmonary fibrosis (CAPACITY): two randomised trials. *Lancet*. **377:** 1760-1769. 2011

15. Franko A, Dolzan V, Arneric N, Dodic-Fikfak M. The influence of gene-gene and gene-environment interactions on the risk of asbestosis. *Biomed Res Int*. **2013:** 405743. 2013

16. Hirvonen A, Saarikoski ST, Linnainmaa K, Koskinen K, Husgafvel-Pursiainen K, Mattson K, Vainio H. Glutathione S-transferase and N-acetyltransferase genotypes and asbestos-associated pulmonary disorders. *J Natl Cancer Inst*. **88:** 1853-1856. 1996

17. Kamp DW. Asbestos-induced lung diseases: an update. *Transl Res*. **153:** 143-152. 2009

18. Miller BE, Hook GE. Hypertrophy and hyperplasia of alveolar type II cells in response to silica and other pulmonary toxicants. *Environ Health Perspect*. **85:** 15-23. 1990

19. Ward HE, Nicholas TE. Alveolar type I and type II cells. *Aust N Z J Med*. **14:** 731-734. 1984

20. Bonner JC. Regulation of PDGF and its receptors in fibrotic diseases. *Cytokine Growth Factor Rev*. **15:** 255-273. 2004

21. Shukla A, Gulumian M, Hei TK, Kamp D, Rahman Q, Mossman BT. Multiple roles of oxidants in the pathogenesis of asbestos-induced diseases. *Free Radic Biol Med*. **34:** 1117-1129. 2003

22. Heintz NH, Janssen YM, Mossman BT. Persistent induction of c-fos and c-jun expression by asbestos. *Proc Natl Acad Sci U S A*. **90:** 3299-3303. 1993

23. Heintz NH, Janssen-Heininger YM, Mossman BT. Asbestos, lung cancers, and mesotheliomas: from molecular approaches to targeting tumor survival pathways. *Am J Respir Cell Mol Biol*. **42:** 133-139. 2010

24. Haegens A, Barrett TF, Gell J, Shukla A, Macpherson M, Vacek P, Poynter ME, Butnor KJ, Janssen-Heininger YM, Steele C, Mossman BT. Airway epithelial NF-κB activation modulates asbestos-induced inflammation and mucin production in vivo. *J Immunol*. **178:** 1800-1808. 2007

25. Janssen YM, Barchowsky A, Treadwell M, Driscoll KE, Mossman BT. Asbestos induces nuclear factor κ B (NF-κB) DNA-binding activity and NF-κB-dependent gene expression in tracheal epithelial cells. *Proc Natl Acad Sci U S A*. **92:** 8458-8462. 1995

26. Zanella CL, Posada J, Tritton TR, Mossman BT. Asbestos causes stimulation of the extracellular signal-regulated kinase 1 mitogen-activated protein kinase cascade after phosphorylation of the epidermal growth factor receptor. *Cancer Res*. **56:** 5334-5338. 1996

27. Cox LS. Multiple pathways control cell growth and transformation: overlapping and independent activities of p53 and p21Cip1/WAF1/Sdi1. *J Pathol*. **183:** 134-140. 1997

28. Mossman BT, Shukla A, Heintz NH, Verschraegen CF, Thomas A, Hassan R. New insights into understanding the mechanisms, pathogenesis, and management of malignant mesotheliomas. *Am J Pathol*. **182:** 1065-1077. 2013

29. Husain AN, Colby T, Ordonez N, Krausz T, Attanoos R, Beasley MB, Borczuk AC, Butnor K, Cagle PT, Chirieac LR, Churg A, Dacic S, Fraire A, Galateau-Salle F, Gibbs A, Gown A, Hammar S, Litzky L, Marchevsky AM, Nicholson AG, Roggli V, Travis WD, Wick M. Guidelines for pathologic diagnosis of malignant mesothelioma: 2012 update of the consensus statement from the International Mesothelioma Interest Group. *Arch Pathol Lab Med*. **137:** 647-667. 2013

30. Carbone M, Ly BH, Dodson RF, Pagano I, Morris PT, Dogan UA, Gazdar AF, Pass HI, Yang H. Malignant mesothelioma: facts, myths, and hypotheses. *J Cell Physiol*. **227:** 44-58. 2012

31. Baker PM, Clement PB, Young RH. Malignant peritoneal mesothelioma in women: a study of 75 cases with emphasis on their morphologic spectrum and differential diagnosis. *Am J Clin Pathol*. **123:** 724-737. 2005

32. Kannerstein M, Churg J. Peritoneal mesothelioma. *Hum Pathol*. **8:** 83-94. 1977

33. Garland LL, Rankin C, Gandara DR, Rivkin SE, Scott KM, Nagle RB, Klein-Szanto AJ, Testa JR, Altomare DA, Borden EC. Phase II study of erlotinib in patients with malignant pleural mesothelioma: a Southwest Oncology Group Study. *J Clin Oncol*. **25:** 2406-2413. 2007

34. Govindan R, Kratzke RA, Herndon JE, 2nd, Niehans GA, Vollmer R, Watson D, Green MR, Kindler HL. Gefitinib in patients with malignant mesothelioma: a phase II study by the Cancer and Leukemia Group B. *Clin Cancer Res*. **11:** 2300-2304. 2005

35. Hegmans JP, Veltman JD, Lambers ME, de Vries IJ, Figdor CG, Hendriks RW, Hoogsteden HC, Lambrecht BN, Aerts JG. Consolidative dendritic cell-based immunotherapy elicits cytotoxicity against malignant mesothelioma. *Am J Respir Crit Care Med*. **181:** 1383-1390. 2010

36. Krug LM, Dao T, Brown AB, Maslak P, Travis W, Bekele S, Korontsvit T, Zakhaleva V, Wolchok J, Yuan J, Li H, Tyson L, Scheinberg DA. WT1 peptide vaccinations induce CD4 and CD8 T cell immune responses in patients with mesothelioma and non-small cell lung cancer. *Cancer Immunol Immunother*. **59:** 1467-1479. 2010

37. Hassan R, Cohen SJ, Phillips M, Pastan I, Sharon E, Kelly RJ, Schweizer C, Weil S, Laheru D. Phase I clinical trial of the chimeric anti-mesothelin monoclonal antibody MORAb-009 in patients with mesothelin-expressing cancers. *Clin Cancer Res*. **16:** 6132-6138. 2010

38. Yang H, Rivera Z, Jube S, Nasu M, Bertino P, Goparaju C, Franzoso G, Lotze MT, Krausz T, Pass HI, Bianchi ME, Carbone M. Programmed necrosis induced by asbestos in human mesothelial cells causes high-mobility group box 1 protein release and resultant inflammation. *Proc Natl Acad Sci U S A*. **107:** 12611-12616. 2010

39. Tabata C, Shibata E, Tabata R, Kanemura S, Mikami K, Nogi Y, Masachika E, Nishizaki T, Nakano T. Serum HMGB1 as a prognostic marker for malignant pleural mesothelioma. *BMC Cancer*. **13:** 205. 2013

40. Jube S, Rivera ZS, Bianchi ME, Powers A, Wang E, Pagano I, Pass HI, Gaudino G, Carbone M, Yang H. Cancer cell secretion of the DAMP protein HMGB1 supports progression in malignant mesothelioma. *Cancer Res*. **72:** 3290-3301. 2012

41. de Reynies A, Jaurand MC, Renier A, Couchy G, Hysi I, Elarouci N, Galateau-Salle F, Copin MC, Hofman P, Cazes A, Andujar P, Imbeaud S, Petel F, Pairon JC, Le Pimpec-Barthes F, Zucman-Rossi J, Jean D. Molecular classification of malignant pleural mesothelioma: identification of a poor prognosis subgroup linked to the epithelial-to-mesenchymal transition. *Clin Cancer Res*. **20:** 1323-1334. 2014

42. Musti M, Kettunen E, Dragonieri S, Lindholm P, Cavone D, Serio G, Knuutila S. Cytogenetic and molecular genetic changes in malignant mesothelioma. *Cancer Genet Cytogenet*. **170:** 9-15. 2006

43. Testa JR, Cheung M, Pei J, Below JE, Tan Y, Sementino E, Cox NJ, Dogan AU, Pass HI, Trusa S, Hesdorffer M, Nasu M, Powers A, Rivera Z, Comertpay S, Tanji M, Gaudino G, Yang H, Carbone M. Germline BAP1 mutations predispose to malignant mesothelioma. *Nat Genet*. **43:** 1022-1025. 2011

44. Xu J, Kadariya Y, Cheung M, Pei J, Talarchek J, Sementino E, Tan Y, Menges CW, Cai KQ, Litwin S, Peng H, Karar J, Rauscher FJ, Testa JR. Germline Mutation of Bap1 Accelerates Development of Asbestos-Induced Malignant Mesothelioma. *Cancer Res*. 2014

45. Ni Z, Liu Y, Keshava N, Zhou G, Whong W, Ong T. Analysis of K-ras and p53 mutations in mesotheliomas from humans and rats exposed to asbestos. *Mutat Res*. **468:** 87-92. 2000

46. Altomare DA, You H, Xiao GH, Ramos-Nino ME, Skele KL, De Rienzo A, Jhanwar SC, Mossman BT, Kane AB, Testa JR. Human and mouse mesotheliomas exhibit elevated AKT/PKB activity, which can be targeted pharmacologically to inhibit tumor cell growth. *Oncogene*. **24:** 6080-6089. 2005

47. de Melo M, Gerbase MW, Curran J, Pache JC. Phosphorylated extracellular signal-regulated kinases are significantly increased in malignant mesothelioma. *J Histochem Cytochem*. **54:** 855-861. 2006

48. Shukla A, Hillegass JM, MacPherson MB, Beuschel SL, Vacek PM, Butnor KJ, Pass HI, Carbone M, Testa JR, Heintz NH, Mossman BT. ERK2 is essential for the growth of human epithelioid malignant mesotheliomas. *Int J Cancer*. **129:** 1075-1086. 2011

49. Berman DW, Crump KS. A meta-analysis of asbestos-related cancer risk that addresses fiber size and mineral type. *Crit Rev Toxicol*. **38 Suppl 1:** 49-73. 2008

50. Kielkowski D, Nelson G, Rees D. Risk of mesothelioma from exposure to crocidolite asbestos: a 1995 update of a South African mortality study. *Occup Environ Med*. **57:** 563-567. 2000

51. Antao VC, Larson TC, Horton DK. Libby vermiculite exposure and risk of developing asbestos-related lung and pleural diseases. *Curr Opin Pulm Med*. **18:** 161-167. 2012

52. Sahin AA, Coplu L, Selcuk ZT, Eryilmaz M, Emri S, Akhan O, Baris YI. Malignant pleural mesothelioma caused by environmental exposure to asbestos or erionite in rural Turkey: CT findings in 84 patients. *AJR Am J Roentgenol*. **161:** 533-537. 1993

53. Burgers JA, Damhuis RA. Prognostic factors in malignant mesothelioma. *Lung Cancer*. **45 Suppl 1:** S49-54. 2004

54. Muscat JE, Wynder EL. Cigarette smoking, asbestos exposure, and malignant mesothelioma. *Cancer Res*. **51:** 2263-2267. 1991

55. Ciardiello F, Tortora G. EGFR antagonists in cancer treatment. *N Engl J Med*. **358:** 1160-1174. 2008

56. Lamouille S, Xu J, Derynck R. Molecular mechanisms of epithelial-mesenchymal transition. *Nat Rev Mol Cell Biol*. **15:** 178-196. 2014

57. Huang RY, Guilford P, Thiery JP. Early events in cell adhesion and polarity during epithelial-mesenchymal transition. *J Cell Sci*. **125:** 4417-4422. 2012

58. Thiery JP, Acloque H, Huang RY, Nieto MA. Epithelial-mesenchymal transitions in development and disease. *Cell*. **139:** 871-890. 2009

59. Hay ED. The mesenchymal cell, its role in the embryo, and the remarkable signaling mechanisms that create it. *Dev Dyn*. **233:** 706-720. 2005

60. Thiery JP, Sleeman JP. Complex networks orchestrate epithelial-mesenchymal transitions. *Nat Rev Mol Cell Biol*. **7:** 131-142. 2006

61. Davis FM, Stewart TA, Thompson EW, Monteith GR. Targeting EMT in cancer: opportunities for pharmacological intervention. *Trends Pharmacol Sci*. 2014

62. Moustakas A, Heldin P. TGFβ and matrix-regulated epithelial to mesenchymal transition. *Biochim Biophys Acta*. **1840:** 2621-2634. 2014

63. Barrallo-Gimeno A, Nieto MA. The Snail genes as inducers of cell movement and survival: implications in development and cancer. *Development*. **132:** 3151-3161. 2005

64. Kataoka H, Murayama T, Yokode M, Mori S, Sano H, Ozaki H, Yokota Y, Nishikawa S, Kita T. A novel snail-related transcription factor Smuc regulates basic helix-loop-helix transcription factor activities via specific E-box motifs. *Nucleic Acids Res*. **28:** 626-633. 2000

65. Peinado H, Olmeda D, Cano A. Snail, Zeb and bHLH factors in tumour progression: an alliance against the epithelial phenotype? *Nat Rev Cancer*. **7:** 415-428. 2007

66. De Craene B, van Roy F, Berx G. Unraveling signalling cascades for the Snail family of transcription factors. *Cell Signal*. **17:** 535-547. 2005

67. Strippoli R, Benedicto I, Perez Lozano ML, Cerezo A, Lopez-Cabrera M, del Pozo MA. Epithelial-to-mesenchymal transition of peritoneal mesothelial cells is regulated by an ERK/NF-κB/Snail1 pathway. *Dis Model Mech*. **1:** 264-274. 2008

68. Duffield JS, Lupher M, Thannickal VJ, Wynn TA. Host responses in tissue repair and fibrosis. *Annu Rev Pathol*. **8:** 241-276. 2013

69. Iwano M, Plieth D, Danoff TM, Xue C, Okada H, Neilson EG. Evidence that fibroblasts derive from epithelium during tissue fibrosis. *J Clin Invest*. **110:** 341-350. 2002

70. Brabletz T, Jung A, Reu S, Porzner M, Hlubek F, Kunz-Schughart LA, Knuechel R, Kirchner T. Variable β-catenin expression in colorectal cancers indicates tumor progression driven by the tumor environment. *Proc Natl Acad Sci U S A*. **98:** 10356-10361. 2001

71. Prall F. Tumour budding in colorectal carcinoma. *Histopathology*. **50:** 151-162. 2007

72. Fassina A, Cappellesso R, Guzzardo V, Dalla Via L, Piccolo S, Ventura L, Fassan M. Epithelial-mesenchymal transition in malignant mesothelioma. *Mod Pathol*. **25:** 86-99. 2012

73. Shih JY, Yang PC. The EMT regulator slug and lung carcinogenesis. *Carcinogenesis*. **32:** 1299-1304. 2011

74. Strutz F, Zeisberg M, Ziyadeh FN, Yang CQ, Kalluri R, Muller GA, Neilson EG. Role of basic fibroblast growth factor-2 in epithelial-mesenchymal transformation. *Kidney Int*. **61:** 1714-1728. 2002

75. Orlichenko LS, Radisky DC. Matrix metalloproteinases stimulate epithelial-mesenchymal transition during tumor development. *Clin Exp Metastasis*. **25:** 593-600. 2008

76. Feldman GJ, Mullin JM, Ryan MP. Occludin: structure, function and regulation. *Adv Drug Deliv Rev*. **57:** 883-917. 2005

77. Gout S, Huot J. Role of cancer microenvironment in metastasis: focus on colon cancer. *Cancer Microenviron*. **1:** 69-83. 2008

78. Tsang KY, Cheung MC, Chan D, Cheah KS. The developmental roles of the extracellular matrix: beyond structure to regulation. *Cell Tissue Res*. **339:** 93-110. 2010

79. Clause KC, Barker TH. Extracellular matrix signaling in morphogenesis and repair. *Curr Opin Biotechnol*. **24:** 830-833. 2013

80. Wight TN, Potter-Perigo S. The extracellular matrix: an active or passive player in fibrosis? *Am J Physiol Gastrointest Liver Physiol*. **301:** G950-955. 2011

81. Rozario T, DeSimone DW. The extracellular matrix in development and morphogenesis: a dynamic view. *Dev Biol*. **341:** 126-140. 2010

82. Kleinman HK, Philp D, Hoffman MP. Role of the extracellular matrix in morphogenesis. *Curr Opin Biotechnol*. **14:** 526-532. 2003

83. Cukierman E, Bassi DE. Physico-mechanical aspects of extracellular matrix influences on tumorigenic behaviors. *Semin Cancer Biol*. **20:** 139-145. 2010

84. Clark RA. Fibronectin matrix deposition and fibronectin receptor expression in healing and normal skin. *J Invest Dermatol*. **94:** 128S-134S. 1990

85. Shimbori C, Gauldie J, Kolb M. Extracellular matrix microenvironment contributes actively to pulmonary fibrosis. *Curr Opin Pulm Med*. **19:** 446-452. 2013

86. Kharaishvili G, Simkova D, Bouchalova K, Gachechiladze M, Narsia N, Bouchal J. The role of cancer-associated fibroblasts, solid stress and other microenvironmental factors in tumor progression and therapy resistance. *Cancer Cell Int*. **14:** 41. 2014

87. Hohenester E, Yurchenco PD. Laminins in basement membrane assembly. *Cell Adh Migr*. **7:** 56-63. 2013

88. Sakai LY, Keene DR, Engvall E. Fibrillin, a new 350-kD glycoprotein, is a component of extracellular microfibrils. *J Cell Biol*. **103:** 2499-2509. 1986

89. Zhang H, Apfelroth SD, Hu W, Davis EC, Sanguineti C, Bonadio J, Mecham RP, Ramirez F. Structure and expression of fibrillin-2, a novel microfibrillar component preferentially located in elastic matrices. *J Cell Biol*. **124:** 855-863. 1994

90. Ramirez F, Sakai LY. Biogenesis and function of fibrillin assemblies. *Cell Tissue Res*. **339:** 71-82. 2010

91. Saharinen J, Hyytiäinen M, Taipale J, Keski-Oja J. Latent transforming growth factor-β binding proteins (LTBPs)--structural extracellular matrix proteins for targeting TGF-β action. *Cytokine Growth Factor Rev*. **10:** 99-117. 1999

92. Koli K, Saharinen J, Hyytiäinen M, Penttinen C, Keski-Oja J. Latency, activation, and binding proteins of TGF-β. *Microsc Res Tech*. **52:** 354-362. 2001

93. Nistala H, Lee-Arteaga S, Smaldone S, Siciliano G, Carta L, Ono RN, Sengle G, Arteaga-Solis E, Levasseur R, Ducy P, Sakai LY, Karsenty G, Ramirez F. Fibrillin-1 and -2 differentially modulate endogenous TGF-β and BMP bioavailability during bone formation. *J Cell Biol*. **190:** 1107-1121. 2010

94. Sengle G, Ono RN, Lyons KM, Bachinger HP, Sakai LY. A new model for growth factor activation: type II receptors compete with the prodomain for BMP-7. *J Mol Biol*. **381:** 1025-1039. 2008

95. Robinson PN, Godfrey M. The molecular genetics of Marfan syndrome and related microfibrillopathies. *J Med Genet*. **37:** 9-25. 2000

96. Dietz HC, Cutting GR, Pyeritz RE, Maslen CL, Sakai LY, Corson GM, Puffenberger EG, Hamosh A, Nanthakumar EJ, Curristin SM, et al. Marfan syndrome caused by a recurrent de novo missense mutation in the fibrillin gene. *Nature*. **352:** 337-339. 1991

97. Lee B, Godfrey M, Vitale E, Hori H, Mattei MG, Sarfarazi M, Tsipouras P, Ramirez F, Hollister DW. Linkage of Marfan syndrome and a phenotypically related disorder to two different fibrillin genes. *Nature*. **352:** 330-334. 1991

98. Benke K, Agg B, Szilveszter B, Tarr F, Nagy ZB, Polos M, Daroczi L, Merkely B, Szabolcs Z. The role of transforming growth factor-β in Marfan syndrome. *Cardiol J*. **20:** 227-234. 2013

99. Sengle G, Charbonneau NL, Ono RN, Sasaki T, Alvarez J, Keene DR, Bachinger HP, Sakai LY. Targeting of bone morphogenetic protein growth factor complexes to fibrillin. *J Biol Chem*. **283:** 13874-13888. 2008

100. Gasparini C, Celeghini C, Monasta L, Zauli G. NF-κB pathways in hematological malignancies. *Cell Mol Life Sci*. **71:** 2083-2102. 2014

101. Hoesel B, Schmid JA. The complexity of NF-κB signaling in inflammation and cancer. *Mol Cancer*. **12:** 86. 2013

102. Traenckner EB, Pahl HL, Henkel T, Schmidt KN, Wilk S, Baeuerle PA. Phosphorylation of human IκB-α on serines 32 and 36 controls IκB-α proteolysis and NF-κB activation in response to diverse stimuli. *EMBO J*. **14:** 2876-2883. 1995

103. Munshi A, Ramesh R. Mitogen-activated protein kinases and their role in radiation response. *Genes Cancer*. **4:** 401-408. 2013

104. Kyriakis JM, Avruch J. Mammalian MAPK signal transduction pathways activated by stress and inflammation: a 10-year update. *Physiol Rev*. **92:** 689-737. 2012

105. Pearson G, Robinson F, Beers Gibson T, Xu BE, Karandikar M, Berman K, Cobb MH. Mitogen-activated protein (MAP) kinase pathways: regulation and physiological functions. *Endocr Rev*. **22:** 153-183. 2001

106. Lopez-Otin C, Hunter T. The regulatory crosstalk between kinases and proteases in cancer. *Nat Rev Cancer*. **10:** 278-292. 2010

107. Cseh B, Doma E, Baccarini M. "RAF" neighborhood: Protein-protein interaction in the Raf/Mek/Erk pathway. *FEBS Lett*. **588:** 2398-2406. 2014

108. Park JI. Growth arrest signaling of the Raf/MEK/ERK pathway in cancer. *Front Biol (Beijing)*. **9:** 95-103. 2014

109. Hong SK, Yoon S, Moelling C, Arthan D, Park JI. Noncatalytic function of ERK1/2 can promote Raf/MEK/ERK-mediated growth arrest signaling. *J Biol Chem*. **284:** 33006-33018. 2009

110. Klein EA, Assoian RK. Transcriptional regulation of the cyclin D1 gene at a glance. *J Cell Sci*. **121:** 3853-3857. 2008

111. Mercer K, Chiloeches A, Huser M, Kiernan M, Marais R, Pritchard C. ERK signalling and oncogene transformation are not impaired in cells lacking A-Raf. *Oncogene*. **21:** 347-355. 2002

112. Mikula M, Schreiber M, Husak Z, Kucerova L, Ruth J, Wieser R, Zatloukal K, Beug H, Wagner EF, Baccarini M. Embryonic lethality and fetal liver apoptosis in mice lacking the c-raf-1 gene. *EMBO J*. **20:** 1952-1962. 2001

113. Wojnowski L, Stancato LF, Larner AC, Rapp UR, Zimmer A. Overlapping and specific functions of Braf and Craf-1 proto-oncogenes during mouse embryogenesis. *Mech Dev*. **91:** 97-104. 2000

114. Garnett MJ, Marais R. Guilty as charged: B-RAF is a human oncogene. *Cancer Cell*. **6:** 313-319. 2004

115. Wan PT, Garnett MJ, Roe SM, Lee S, Niculescu-Duvaz D, Good VM, Jones CM, Marshall CJ, Springer CJ, Barford D, Marais R. Mechanism of activation of the RAF-ERK signaling pathway by oncogenic mutations of B-RAF. *Cell*. **116:** 855-867. 2004

116. Shukla A, Hillegass JM, MacPherson MB, Beuschel SL, Vacek PM, Pass HI, Carbone M, Testa JR, Mossman BT. Blocking of ERK1 and ERK2 sensitizes human mesothelioma cells to doxorubicin. *Mol Cancer*. **9:** 314. 2010

117. Sun S, Ning X, Zhai Y, Du R, Lu Y, He L, Li R, Wu W, Sun W, Wang H. Egr-1 mediates chronic hypoxia-induced renal interstitial fibrosis via the PKC/ERK pathway. *Am J Nephrol*. **39:** 436-448. 2014

118. Madala SK, Schmidt S, Davidson C, Ikegami M, Wert S, Hardie WD. MEK-ERK pathway modulation ameliorates pulmonary fibrosis associated with epidermal growth factor receptor activation. *Am J Respir Cell Mol Biol*. **46:** 380-388. 2012

119. Baughman RP, Lower EE, Miller MA, Bejarano PA, Heffelfinger SC. Overexpression of transforming growth factor-α and epidermal growth factor-receptor in idiopathic pulmonary fibrosis. *Sarcoidosis Vasc Diffuse Lung Dis*. **16:** 57-61. 1999

120. Hardie WD, Hagood JS, Dave V, Perl AK, Whitsett JA, Korfhagen TR, Glasser S. Signaling pathways in the epithelial origins of pulmonary fibrosis. *Cell Cycle*. **9:** 2769-2776. 2010

121. Ramos-Nino ME, Vianale G, Sabo-Attwood T, Mutti L, Porta C, Heintz N, Mossman BT. Human mesothelioma cells exhibit tumor cell-specific differences in phosphatidylinositol 3-kinase/AKT activity that predict the efficacy of Onconase. *Mol Cancer Ther*. **4:** 835-842. 2005

122. Dunlop EA, Tee AR. Mammalian target of rapamycin complex 1: signalling inputs, substrates and feedback mechanisms. *Cell Signal*. **21:** 827-835. 2009

123. Weiss A, Attisano L. The TGFβ superfamily signaling pathway. *Wiley Interdiscip Rev Dev Biol*. **2:** 47-63. 2013

124. Daopin S, Piez KA, Ogawa Y, Davies DR. Crystal structure of transforming growth factor-β 2: an unusual fold for the superfamily. *Science*. **257:** 369-373. 1992

125. Harrison CA, Al-Musawi SL, Walton KL. Prodomains regulate the synthesis, extracellular localisation and activity of TGF-β superfamily ligands. *Growth Factors*. **29:** 174-186. 2011

126. Gray AM, Mason AJ. Requirement for activin A and transforming growth factor--β 1 pro-regions in homodimer assembly. *Science*. **247:** 1328-1330. 1990

127. Gregory KE, Ono RN, Charbonneau NL, Kuo CL, Keene DR, Bachinger HP, Sakai LY. The prodomain of BMP-7 targets the BMP-7 complex to the extracellular matrix. *J Biol Chem*. **280:** 27970-27980. 2005

128. McDonald NQ, Hendrickson WA. A structural superfamily of growth factors containing a cystine knot motif. *Cell*. **73:** 421-424. 1993

129. Boyd FT, Cheifetz S, Andres J, Laiho M, Massague J. Transforming growth factor-β receptors and binding proteoglycans. *J Cell Sci Suppl*. **13:** 131-138. 1990

130. Itoh S, Itoh F, Goumans MJ, Ten Dijke P. Signaling of transforming growth factor-β family members through Smad proteins. *Eur J Biochem*. **267:** 6954-6967. 2000

131. Kondo S, Hashimoto M, Etoh Y, Murata M, Shibai H, Muramatsu M. Identification of the two types of specific receptor for activin/EDF expressed on Friend leukemia and embryonal carcinoma cells. *Biochem Biophys Res Commun*. **161:** 1267-1272. 1989

132. Paralkar VM, Hammonds RG, Reddi AH. Identification and characterization of cellular binding proteins (receptors) for recombinant human bone morphogenetic protein 2B, an initiator of bone differentiation cascade. *Proc Natl Acad Sci U S A*. **88:** 3397-3401. 1991

133. Attisano L, Wrana JL. Signal transduction by members of the transforming growth factor-β superfamily. *Cytokine Growth Factor Rev*. **7:** 327-339. 1996

134. Shibanuma M, Kuroki T, Nose K. Release of H2O2 and phosphorylation of 30 kilodalton proteins as early responses of cell cycle-dependent inhibition of DNA synthesis by transforming growth factor β 1. *Cell Growth Differ*. **2:** 583-591. 1991

135. Zhang Y, Feng X, We R, Derynck R. Receptor-associated Mad homologues synergize as effectors of the TGF-β response. *Nature*. **383:** 168-172. 1996

136. ten Dijke P, Korchynskyi O, Valdimarsdottir G, Goumans MJ. Controlling cell fate by bone morphogenetic protein receptors. *Mol Cell Endocrinol*. **211:** 105-113. 2003

137. Liu F, Ventura F, Doody J, Massague J. Human type II receptor for bone morphogenic proteins (BMPs): extension of the two-kinase receptor model to the BMPs. *Mol Cell Biol*. **15:** 3479-3486. 1995

138. Nohno T, Ishikawa T, Saito T, Hosokawa K, Noji S, Wolsing DH, Rosenbaum JS. Identification of a human type II receptor for bone morphogenetic protein-4 that forms differential heteromeric complexes with bone morphogenetic protein type I receptors. *J Biol Chem*. **270:** 22522-22526. 1995

139. Derynck R, Zhang YE. Smad-dependent and Smad-independent pathways in TGF-β family signalling. *Nature*. **425:** 577-584. 2003

140. Drabsch Y, ten Dijke P. TGF-β signalling and its role in cancer progression and metastasis. *Cancer Metastasis Rev*. **31:** 553-568. 2012

141. Inman GJ, Hill CS. Stoichiometry of active smad-transcription factor complexes on DNA. *J Biol Chem*. **277:** 51008-51016. 2002

142. Heldin CH, Landstrom M, Moustakas A. Mechanism of TGF-β signaling to growth arrest, apoptosis, and epithelial-mesenchymal transition. *Curr Opin Cell Biol*. **21:** 166-176. 2009

143. Afrakhte M, Moren A, Jossan S, Itoh S, Sampath K, Westermark B, Heldin CH, Heldin NE, ten Dijke P. Induction of inhibitory Smad6 and Smad7 mRNA by TGF-β family members. *Biochem Biophys Res Commun*. **249:** 505-511. 1998

144. Mu Y, Gudey SK, Landström M. Non-Smad signaling pathways. *Cell Tissue Res*. **347:** 11-20. 2012

145. de Caestecker MP, Piek E, Roberts AB. Role of transforming growth factor-β signaling in cancer. *J Natl Cancer Inst*. **92:** 1388-1402. 2000

146. Wrighton KH, Feng XH. To (TGF)β or not to (TGF)β: fine-tuning of Smad signaling via post-translational modifications. *Cell Signal*. **20:** 1579-1591. 2008

147. Kretzschmar M, Doody J, Timokhina I, Massague J. A mechanism of repression of TGFβ/ Smad signaling by oncogenic Ras. *Genes Dev*. **13:** 804-816. 1999

148. Funaba M, Zimmerman CM, Mathews LS. Modulation of Smad2-mediated signaling by extracellular signal-regulated kinase. *J Biol Chem*. **277:** 41361-41368. 2002

149. Carreira AC, Lojudice FH, Halcsik E, Navarro RD, Sogayar MC, Granjeiro JM. Bone morphogenetic proteins: facts, challenges, and future perspectives. *J Dent Res*. **93:** 335-345. 2014

150. Bragdon B, Moseychuk O, Saldanha S, King D, Julian J, Nohe A. Bone morphogenetic proteins: a critical review. *Cell Signal*. **23:** 609-620. 2011

151. Zhang Q, Yu N, Lee C. Mysteries of TGF-β Paradox in Benign and Malignant Cells. *Front Oncol*. **4:** 94. 2014

152. Isogai Z, Ono RN, Ushiro S, Keene DR, Chen Y, Mazzieri R, Charbonneau NL, Reinhardt DP, Rifkin DB, Sakai LY. Latent transforming growth factor β-binding protein 1 interacts with fibrillin and is a microfibril-associated protein. *J Biol Chem*. **278:** 2750-2757. 2003

153. Saharinen J, Keski-Oja J. Specific sequence motif of 8-Cys repeats of TGF-βbinding proteins, LTBPs, creates a hydrophobic interaction surface for binding of small latent TGF-β. *Mol Biol Cell*. **11:** 2691-2704. 2000

154. Miyazono K, Hellman U, Wernstedt C, Heldin CH. Latent high molecular weight complex of transforming growth factor β 1. Purification from human platelets and structural characterization. *J Biol Chem*. **263:** 6407-6415. 1988

155. Munger JS, Huang X, Kawakatsu H, Griffiths MJ, Dalton SL, Wu J, Pittet JF, Kaminski N, Garat C, Matthay MA, Rifkin DB, Sheppard D. The integrin αvβ6 binds and activates latent TGFβ1: a mechanism for regulating pulmonary inflammation and fibrosis. *Cell*. **96:** 319-328. 1999

156. Kulkarni AB, Huh CG, Becker D, Geiser A, Lyght M, Flanders KC, Roberts AB, Sporn MB, Ward JM, Karlsson S. Transforming growth factor β 1 null mutation in mice causes excessive inflammatory response and early death. *Proc Natl Acad Sci U S A*. **90:** 770-774. 1993

157. Dubois CM, Blanchette F, Laprise MH, Leduc R, Grondin F, Seidah NG. Evidence that furin is an authentic transforming growth factor-β1-converting enzyme. *Am J Pathol*. **158:** 305-316. 2001

158. Dubois CM, Laprise MH, Blanchette F, Gentry LE, Leduc R. Processing of transforming growth factor β1 precursor by human furin convertase. *J Biol Chem*. **270:** 10618-10624. 1995

159. Barcellos-Hoff MH, Dix TA. Redox-mediated activation of latent transforming growth factor-β 1. *Mol Endocrinol*. **10:** 1077-1083. 1996

160. Sato Y, Tsuboi R, Lyons R, Moses H, Rifkin DB. Characterization of the activation of latent TGF-β by co-cultures of endothelial cells and pericytes or smooth muscle cells: a self-regulating system. *J Cell Biol*. **111:** 757-763. 1990

161. Crawford SE, Stellmach V, Murphy-Ullrich JE, Ribeiro SM, Lawler J, Hynes RO, Boivin GP, Bouck N. Thrombospondin-1 is a major activator of TGF-β1 in vivo. *Cell*. **93:** 1159-1170. 1998

162. Munger JS, Harpel JG, Giancotti FG, Rifkin DB. Interactions between growth factors and integrins: latent forms of transforming growth factor-β are ligands for the integrin αvβ1. *Mol Biol Cell*. **9:** 2627-2638. 1998

163. Mu D, Cambier S, Fjellbirkeland L, Baron JL, Munger JS, Kawakatsu H, Sheppard D, Broaddus VC, Nishimura SL. The integrin αvβ8 mediates epithelial homeostasis through MT1-MMP-dependent activation of TGF-β1. *J Cell Biol*. **157:** 493-507. 2002

164. Vehviläinen P, Koli K, Myllärniemi M, Lindholm P, Soini Y, Salmenkivi K, Kinnula VL, Keski-Oja J. Latent TGF-β binding proteins (LTBPs) 1 and 3 differentially regulate transforming growth factor-β activity in malignant mesothelioma. *Hum Pathol*. **42:** 269-278. 2011

165. Jagirdar J, Lee TC, Reibman J, Gold LI, Aston C, Begin R, Rom WN. Immunohistochemical localization of transforming growth factor β isoforms in asbestos-related diseases. *Environ Health Perspect*. **105 Suppl 5:** 1197-1203. 1997

166. Khalil N, O'Connor RN, Unruh HW, Warren PW, Flanders KC, Kemp A, Bereznay OH, Greenberg AH. Increased production and immunohistochemical localization of transforming growth factor-β in idiopathic pulmonary fibrosis. *Am J Respir Cell Mol Biol*. **5:** 155-162. 1991

167. Leppäranta O, Sens C, Salmenkivi K, Kinnula VL, Keski-Oja J, Myllärniemi M, Koli K. Regulation of TGF-β storage and activation in the human idiopathic pulmonary fibrosis lung. *Cell Tissue Res*. **348:** 491-503. 2012

168. Helmig S, Belwe A, Schneider J. Association of transforming growth factor β1 gene polymorphisms and asbestos-induced fibrosis and tumors. *J Investig Med*. **57:** 655-661. 2009

169. Karagiannidis C, Hense G, Martin C, Epstein M, Ruckert B, Mantel PY, Menz G, Uhlig S, Blaser K, Schmidt-Weber CB. Activin A is an acute allergen-responsive cytokine and provides a link to TGF-β-mediated airway remodeling in asthma. *J Allergy Clin Immunol*. **117:** 111-118. 2006

170. Edlund S, Bu S, Schuster N, Aspenstrom P, Heuchel R, Heldin NE, ten Dijke P, Heldin CH, Landström M. Transforming growth factor-β1 (TGF-β)-induced apoptosis of prostate cancer cells involves Smad7-dependent activation of p38 by TGF-β-activated kinase 1 and mitogen-activated protein kinase kinase 3. *Mol Biol Cell*. **14:** 529-544. 2003

171. Edlund S, Lee SY, Grimsby S, Zhang S, Aspenstrom P, Heldin CH, Landström M. Interaction between Smad7 and β-catenin: importance for transforming growth factor β-induced apoptosis. *Mol Cell Biol*. **25:** 1475-1488. 2005

172. Zhang S, Ekman M, Thakur N, Bu S, Davoodpour P, Grimsby S, Tagami S, Heldin CH, Landström M. TGFβ1-induced activation of ATM and p53 mediates apoptosis in a Smad7-dependent manner. *Cell Cycle*. **5:** 2787-2795. 2006

173. Wang J, Zhao J, Chu ES, Mok MT, Go MY, Man K, Heuchel R, Lan HY, Chang Z, Sung JJ, Yu J. Inhibitory role of Smad7 in hepatocarcinogenesis in mice and in vitro. *J Pathol*. **230:** 441-452. 2013

174. DeLong P, Carroll RG, Henry AC, Tanaka T, Ahmad S, Leibowitz MS, Sterman DH, June CH, Albelda SM, Vonderheide RH. Regulatory T cells and cytokines in malignant pleural effusions secondary to mesothelioma and carcinoma. *Cancer Biol Ther*. **4:** 342-346. 2005

175. Kissick HT, Ireland DJ, Krishnan S, Madondo M, Beilharz MW. Tumour eradication and induction of memory against murine mesothelioma by combined immunotherapy. *Immunol Cell Biol*. **90:** 822-826. 2012

176. Suzuki E, Kim S, Cheung HK, Corbley MJ, Zhang X, Sun L, Shan F, Singh J, Lee WC, Albelda SM, Ling LE. A novel small-molecule inhibitor of transforming growth factor β type I receptor kinase (SM16) inhibits murine mesothelioma tumor growth in vivo and prevents tumor recurrence after surgical resection. *Cancer Res*. **67:** 2351-2359. 2007

177. Stevenson JP, Kindler HL, Papasavvas E, Sun J, Jacobs-Small M, Hull J, Schwed D, Ranganathan A, Newick K, Heitjan DF, Langer CJ, McPherson JM, Montaner LJ, Albelda SM. Immunological effects of the TGFβ-blocking antibody GC1008 in malignant pleural mesothelioma patients. *Oncoimmunology*. **2:** e26218. 2013

178. Vale W, Rivier J, Vaughan J, McClintock R, Corrigan A, Woo W, Karr D, Spiess J. Purification and characterization of an FSH releasing protein from porcine ovarian follicular fluid. *Nature*. **321:** 776-779. 1986

179. Mason AJ, Niall HD, Seeburg PH. Structure of two human ovarian inhibins. *Biochem Biophys Res Commun*. **135:** 957-964. 1986

180. Hedger MP, de Kretser DM. The activins and their binding protein, follistatin-Diagnostic and therapeutic targets in inflammatory disease and fibrosis. *Cytokine Growth Factor Rev*. **24:** 285-295. 2013

181. Risbridger GP, Schmitt JF, Robertson DM. Activins and inhibins in endocrine and other tumors. *Endocr Rev*. **22:** 836-858. 2001

182. Mellor SL, Cranfield M, Ries R, Pedersen J, Cancilla B, de Kretser D, Groome NP, Mason AJ, Risbridger GP. Localization of activin β(A)-, β(B)-, and β(C)-subunits in humanprostate and evidence for formation of new activin heterodimers of β(C)-subunit. *J Clin Endocrinol Metab*. **85:** 4851-4858. 2000

183. Deli A, Kreidl E, Santifaller S, Trotter B, Seir K, Berger W, Schulte-Hermann R, Rodgarkia-Dara C, Grusch M. Activins and activin antagonists in hepatocellular carcinoma. *World J Gastroenterol*. **14:** 1699-1709. 2008

184. Huylebroeck D, Van Nimmen K, Waheed A, von Figura K, Marmenout A, Fransen L, De Waele P, Jaspar JM, Franchimont P, Stunnenberg H, et al. Expression and processing of the activin-A/erythroid differentiation factor precursor: a member of the transforming growth factor-β superfamily. *Mol Endocrinol*. **4:** 1153-1165. 1990

185. Walton KL, Makanji Y, Wilce MC, Chan KL, Robertson DM, Harrison CA. A common biosynthetic pathway governs the dimerization and secretion of inhibin and related transforming growth factor β (TGFβ) ligands. *J Biol Chem*. **284:** 9311-9320. 2009

186. Vale W, Wiater E, Gray P, Harrison C, Bilezikjian L, Choe S. Activins and inhibins and their signaling. *Ann N Y Acad Sci*. **1038:** 142-147. 2004

187. Ling N, Ying SY, Ueno N, Shimasaki S, Esch F, Hotta M, Guillemin R. Pituitary FSH is released by a heterodimer of the β-subunits from the two forms of inhibin. *Nature*. **321:** 779-782. 1986

188. Antsiferova M, Werner S. The bright and the dark sides of activin in wound healing and cancer. *J Cell Sci*. **125:** 3929-3937. 2012

189. Thompson TB, Cook RW, Chapman SC, Jardetzky TS, Woodruff TK. Beta A versus beta B: is it merely a matter of expression? *Mol Cell Endocrinol*. **225:** 9-17. 2004

190. Takahashi S, Uchimaru K, Harigaya K, Asano S, Yamashita T. Tumor necrosis factor and interleukin-1 induce activin A gene expression in a human bone marrow stromal cell line. *Biochem Biophys Res Commun*. **188:** 310-317. 1992

191. Tanimoto K, Yoshida E, Mita S, Nibu Y, Murakami K, Fukamizu A. Human activin βA gene. Identification of novel 5' exon, functional promoter, and enhancers. *J Biol Chem*. **271:** 32760-32769. 1996

192. Thompson DA, Cronin CN, Martin F. Genomic cloning and sequence analyses of the bovine α-, β A- and β B-inhibin/activin genes. Identification of transcription factor AP-2-binding sites in the 5'-flanking regions by DNase I footprinting. *Eur J Biochem*. **226:** 751-764. 1994

193. Waite KA, Eng C. From developmental disorder to heritable cancer: it's all in the BMP/TGF-β family. *Nat Rev Genet*. **4:** 763-773. 2003

194. Willis SA, Zimmerman CM, Li LI, Mathews LS. Formation and activation by phosphorylation of activin receptor complexes. *Mol Endocrinol*. **10:** 367-379. 1996

195. Bernard DJ, Lee KB, Santos MM. Activin B can signal through both ALK4 and ALK7 in gonadotrope cells. *Reprod Biol Endocrinol*. **4:** 52. 2006

196. Tsuchida K, Nakatani M, Yamakawa N, Hashimoto O, Hasegawa Y, Sugino H. Activin isoforms signal through type I receptor serine/threonine kinase ALK7. *Mol Cell Endocrinol*. **220:** 59-65. 2004

197. Besson-Fournier C, Latour C, Kautz L, Bertrand J, Ganz T, Roth MP, Coppin H. Induction of activin B by inflammatory stimuli up-regulates expression of the iron-regulatory peptide hepcidin through Smad1/5/8 signaling. *Blood*. **120:** 431-439. 2012

198. Huang HM, Chang TW, Liu JC. Basic fibroblast growth factor antagonizes activin A-mediated growth inhibition and hemoglobin synthesis in K562 cells by activating ERK1/2 and deactivating p38 MAP kinase. *Biochem Biophys Res Commun*. **320:** 1247-1252. 2004

199. Zhang L, Deng M, Parthasarathy R, Wang L, Mongan M, Molkentin JD, Zheng Y, Xia Y. MEKK1 transduces activin signals in keratinocytes to induce actin stress fiber formation and migration. *Mol Cell Biol*. **25:** 60-65. 2005

200. Zhang M, Liu NY, Wang XE, Chen YH, Li QL, Lu KR, Sun L, Jia Q, Zhang L. Activin B promotes epithelial wound healing in vivo through RhoA-JNK signaling pathway. *PLoS One*. **6:** e25143. 2011

201. Zhang M, Sun L, Wang X, Chen S, Jia Q, Liu N, Chen Y, Kong Y, Zhang L, Zhang AL. Activin B promotes BM-MSC-mediated cutaneous wound healing by regulating cell migration via the JNK-ERK signaling pathway. *Cell Transplant*. 2013

202. Harrington AE, Morris-Triggs SA, Ruotolo BT, Robinson CV, Ohnuma S, Hyvönen M. Structural basis for the inhibition of activin signalling by follistatin. *EMBO J*. **25:** 1035-1045. 2006

203. Tsuchida K, Arai KY, Kuramoto Y, Yamakawa N, Hasegawa Y, Sugino H. Identification and characterization of a novel follistatin-like protein as a binding protein for the TGF-β family. *J Biol Chem*. **275:** 40788-40796. 2000

204. Matsuse T, Ikegami A, Ohga E, Hosoi T, Oka T, Kida K, Fukayama M, Inoue S, Nagase T, Ouchi Y, Fukuchi Y. Expression of immunoreactive activin A protein in remodeling lesions associated with interstitial pulmonary fibrosis. *Am J Pathol*. **148:** 707-713. 1996

205. Hedger MP, Drummond AE, Robertson DM, Risbridger GP, de Kretser DM. Inhibin and activin regulate [3H]thymidine uptake by rat thymocytes and 3T3 cells in vitro. *Mol Cell Endocrinol*. **61:** 133-138. 1989

206. Ohga E, Matsuse T, Teramoto S, Katayama H, Nagase T, Fukuchi Y, Ouchi Y. Effects of activin A on proliferation and differentiation of human lung fibroblasts. *Biochem Biophys Res Commun*. **228:** 391-396. 1996

207. Yamashita S, Maeshima A, Kojima I, Nojima Y. Activin A is a potent activator of renal interstitial fibroblasts. *J Am Soc Nephrol*. **15:** 91-101. 2004

208. Dunphy KA, Schneyer AL, Hagen MJ, Jerry DJ. The role of activin in mammary gland development and oncogenesis. *J Mammary Gland Biol Neoplasia*. **16:** 117-126. 2011

209. Ottley E, Gold E. Insensitivity to the growth inhibitory effects of activin A: an acquired capability in prostate cancer progression. *Cytokine Growth Factor Rev*. **23:** 119-125. 2012

210. Seder CW, Hartojo W, Lin L, Silvers AL, Wang Z, Thomas DG, Giordano TJ, Chen G, Chang AC, Orringer MB, Beer DG. Upregulated INHBA expression may promote cell proliferation and is associated with poor survival in lung adenocarcinoma. *Neoplasia*. **11:** 388-396. 2009

211. Seder CW, Hartojo W, Lin L, Silvers AL, Wang Z, Thomas DG, Giordano TJ, Chen G, Chang AC, Orringer MB, Beer DG. INHBA overexpression promotes cell proliferation and may be epigenetically regulated in esophageal adenocarcinoma. *J Thorac Oncol*. **4:** 455-462. 2009

212. Hoda MA, Munzker J, Ghanim B, Schelch K, Klikovits T, Laszlo V, Sahin E, Bedeir A, Lackner A, Dome B, Setinek U, Filipits M, Eisenbauer M, Kenessey I, Torok S, Garay T, Hegedus B, Catania A, Taghavi S, Klepetko W, Berger W, Grusch M. Suppression of activin A signals inhibits growth of malignant pleural mesothelioma cells. *Br J Cancer*. **107:** 1978-1986. 2012

213. Mueller TD, Nickel J. Promiscuity and specificity in BMP receptor activation. *FEBS Lett*. **586:** 1846-1859. 2012

214. Chen D, Zhao M, Mundy GR. Bone morphogenetic proteins. *Growth Factors*. **22:** 233-241. 2004

215. Bandyopadhyay A, Yadav PS, Prashar P. BMP signaling in development and diseases: a pharmacological perspective. *Biochem Pharmacol*. **85:** 857-864. 2013

216. Lee-Hoeflich ST, Causing CG, Podkowa M, Zhao X, Wrana JL, Attisano L. Activation of LIMK1 by binding to the BMP receptor, BMPRII, regulates BMP-dependent dendritogenesis. *EMBO J*. **23:** 4792-4801. 2004

217. Podkowa M, Zhao X, Chow CW, Coffey ET, Davis RJ, Attisano L. Microtubule stabilization by bone morphogenetic protein receptor-mediated scaffolding of c-Jun N-terminal kinase promotes dendrite formation. *Mol Cell Biol*. **30:** 2241-2250. 2010

218. Yamaguchi K, Nagai S, Ninomiya-Tsuji J, Nishita M, Tamai K, Irie K, Ueno N, Nishida E, Shibuya H, Matsumoto K. XIAP, a cellular member of the inhibitor of apoptosis protein family, links the receptors to TAB1-TAK1 in the BMP signaling pathway. *EMBO J*. **18:** 179-187. 1999

219. Sorrentino A, Thakur N, Grimsby S, Marcusson A, von Bulow V, Schuster N, Zhang S, Heldin CH, Landström M. The type I TGF-β receptor engages TRAF6 to activate TAK1 in a receptor kinase-independent manner. *Nat Cell Biol*. **10:** 1199-1207. 2008

220. Yamashita M, Fatyol K, Jin C, Wang X, Liu Z, Zhang YE. TRAF6 mediates Smad-independent activation of JNK and p38 by TGF-β. *Mol Cell*. **31:** 918-924. 2008

221. Costello CM, Cahill E, Martin F, Gaine S, McLoughlin P. Role of gremlin in the lung: development and disease. *Am J Respir Cell Mol Biol*. **42:** 517-523. 2010

222. Hardwick JC, Kodach LL, Offerhaus GJ, van den Brink GR. Bone morphogenetic protein signalling in colorectal cancer. *Nat Rev Cancer*. **8:** 806-812. 2008

223. Meng XM, Chung AC, Lan HY. Role of the TGF-β/BMP-7/Smad pathways in renal diseases. *Clin Sci (Lond)*. **124:** 243-254. 2013

224. Gressner OA, Rizk MS, Kovalenko E, Weiskirchen R, Gressner AM. Changing the pathogenetic roadmap of liver fibrosis? Where did it start; where will it go? *J Gastroenterol Hepatol*. **23:** 1024-1035. 2008

225. Koli K, Myllärniemi M, Vuorinen K, Salmenkivi K, Ryynänen MJ, Kinnula VL, Keski-Oja J. Bone morphogenetic protein-4 inhibitor gremlin is overexpressed in idiopathic pulmonary fibrosis. *Am J Pathol*. **169:** 61-71. 2006

226. Myllärniemi M, Lindholm P, Ryynänen MJ, Kliment CR, Salmenkivi K, Keski-Oja J, Kinnula VL, Oury TD, Koli K. Gremlin-mediated decrease in bone morphogenetic protein signaling promotes pulmonary fibrosis. *Am J Respir Crit Care Med*. **177:** 321-329. 2008

227. Leppäranta O, Tikkanen JM, Bespalov MM, Koli K, Myllärniemi M. Bone morphogenetic protein-inducer tilorone identified by high-throughput screening is antifibrotic in vivo. *Am J Respir Cell Mol Biol*. **48:** 448-455. 2013

228. Alarmo EL, Pärssinen J, Ketolainen JM, Savinainen K, Karhu R, Kallioniemi A. BMP7 influences proliferation, migration, and invasion of breast cancer cells. *Cancer Lett*. **275:** 35-43. 2009

229. Alarmo EL, Rauta J, Kauraniemi P, Karhu R, Kuukasjärvi T, Kallioniemi A. Bone morphogenetic protein 7 is widely overexpressed in primary breast cancer. *Genes Chromosomes Cancer*. **45:** 411-419. 2006

230. Ampuja M, Jokimäki R, Juuti-Uusitalo K, Rodriguez-Martinez A, Alarmo EL, Kallioniemi A. BMP4 inhibits the proliferation of breast cancer cells and induces an MMP-dependent migratory phenotype in MDA-MB-231 cells in 3D environment. *BMC Cancer*. **13:** 429. 2013

231. Choi YJ, Kim ST, Park KH, Oh SC, Seo JH, Shin SW, Kim JS, Kim YH. The serum bone morphogenetic protein-2 level in non-small-cell lung cancer patients. *Med Oncol*. **29:** 582-588. 2012

232. Langenfeld EM, Calvano SE, Abou-Nukta F, Lowry SF, Amenta P, Langenfeld J. The mature bone morphogenetic protein-2 is aberrantly expressed in non-small cell lung carcinomas and stimulates tumor growth of A549 cells. *Carcinogenesis*. **24:** 1445-1454. 2003

233. Kimura K, Toyooka S, Tsukuda K, Yamamoto H, Suehisa H, Soh J, Otani H, Kubo T, Aoe K, Fujimoto N, Kishimoto T, Sano Y, Pass HI, Date H. The aberrant promoter methylation of BMP3b and BMP6 in malignant pleural mesotheliomas. *Oncol Rep*. **20:** 1265-1268. 2008

234. Wang DJ, Zhi XY, Zhang SC, Jiang M, Liu P, Han XP, Li J, Chen Z, Wang CL. The bone morphogenetic protein antagonist Gremlin is overexpressed in human malignant mesothelioma. *Oncol Rep*. **27:** 58-64. 2012

235. Constam DB, Robertson EJ. Regulation of bone morphogenetic protein activity by pro domains and proprotein convertases. *J Cell Biol*. **144:** 139-149. 1999

236. Cui Y, Jean F, Thomas G, Christian JL. BMP-4 is proteolytically activated by furin and/or PC6 during vertebrate embryonic development. *EMBO J*. **17:** 4735-4743. 1998

237. Topol LZ, Marx M, Laugier D, Bogdanova NN, Boubnov NV, Clausen PA, Calothy G, Blair DG. Identification of drm, a novel gene whose expression is suppressed in transformed cells and which can inhibit growth of normal but not transformed cells in culture. *Mol Cell Biol*. **17:** 4801-4810. 1997

238. Topol LZ, Bardot B, Zhang Q, Resau J, Huillard E, Marx M, Calothy G, Blair DG. Biosynthesis, post-translation modification, and functional characterization of Drm/Gremlin. *J Biol Chem*. **275:** 8785-8793. 2000

239. Hsu DR, Economides AN, Wang X, Eimon PM, Harland RM. The Xenopus dorsalizing factor Gremlin identifies a novel family of secreted proteins that antagonize BMP activities. *Mol Cell*. **1:** 673-683. 1998

240. Michos O, Panman L, Vintersten K, Beier K, Zeller R, Zuniga A. Gremlin-mediated BMP antagonism induces the epithelial-mesenchymal feedback signaling controlling metanephric kidney and limb organogenesis. *Development*. **131:** 3401-3410. 2004

241. Zuniga A, Haramis AP, McMahon AP, Zeller R. Signal relay by BMP antagonism controls the SHH/FGF4 feedback loop in vertebrate limb buds. *Nature*. **401:** 598-602. 1999

242. Canalis E, Parker K, Zanotti S. Gremlin1 is required for skeletal development and postnatal skeletal homeostasis. *J Cell Physiol*. **227:** 269-277. 2012

243. Laurila R, Parkkila S, Isola J, Kallioniemi A, Alarmo EL. The expression patterns of gremlin 1 and noggin in normal adult and tumor tissues. *Int J Clin Exp Pathol*. **6:** 1400-1408. 2013

244. Guimei M, Baddour N, Elkaffash D, Abdou L, Taher Y. Gremlin in the pathogenesis of hepatocellular carcinoma complicating chronic hepatitis C: an immunohistochemical and PCR study of human liver biopsies. *BMC Res Notes*. **5:** 390. 2012

245. Kosinski C, Li VS, Chan AS, Zhang J, Ho C, Tsui WY, Chan TL, Mifflin RC, Powell DW, Yuen ST, Leung SY, Chen X. Gene expression patterns of human colon tops and basal crypts and BMP antagonists as intestinal stem cell niche factors. *Proc Natl Acad Sci U S A*. **104:** 15418-15423. 2007

246. McMahon R, Murphy M, Clarkson M, Taal M, Mackenzie HS, Godson C, Martin F, Brady HR. IHG-2, a mesangial cell gene induced by high glucose, is human gremlin. Regulation by extracellular glucose concentration, cyclic mechanical strain, and transforming growth factor-β1. *J Biol Chem*. **275:** 9901-9904. 2000

247. Carvajal G, Droguett A, Burgos ME, Aros C, Ardiles L, Flores C, Carpio D, Ruiz-Ortega M, Egido J, Mezzano S. Gremlin: a novel mediator of epithelial mesenchymal transition and fibrosis in chronic allograft nephropathy. *Transplant Proc*. **40:** 734-739. 2008

248. Rodrigues-Diez R, Lavoz C, Carvajal G, Rayego-Mateos S, Rodrigues Diez RR, Ortiz A, Egido J, Mezzano S, Ruiz-Ortega M. Gremlin is a downstream profibrotic mediator of transforming growth factor-β in cultured renal cells. *Nephron Exp Nephrol*. **122:** 62-74. 2012

249. Rodrigues-Diez R, Rodrigues-Diez RR, Lavoz C, Carvajal G, Droguett A, Garcia-Redondo AB, Rodriguez I, Ortiz A, Egido J, Mezzano S, Ruiz-Ortega M. Gremlin activates the Smad pathway linked to epithelial mesenchymal transdifferentiation in cultured tubular epithelial cells. *Biomed Res Int*. **2014:** 802841. 2014

250. Lee H, O'Meara SJ, O'Brien C, Kane R. The role of gremlin, a BMP antagonist, and epithelial-to-mesenchymal transition in proliferative vitreoretinopathy. *Invest Ophthalmol Vis Sci*. **48:** 4291-4299. 2007

251. Kim M, Yoon S, Lee S, Ha SA, Kim HK, Kim JW, Chung J. Gremlin-1 induces BMP-independent tumor cell proliferation, migration, and invasion. *PLoS One*. **7:** e35100. 2012

252. Mueller KA, Tavlaki E, Schneider M, Jorbenadze R, Geisler T, Kandolf R, Gawaz M, Mueller, II, Zuern CS. Gremlin-1 identifies fibrosis and predicts adverse outcome in patients with heart failure undergoing endomyocardial biopsy. *J Card Fail*. **19:** 678-684. 2013

253. Sneddon JB, Zhen HH, Montgomery K, van de Rijn M, Tward AD, West R, Gladstone H, Chang HY, Morganroth GS, Oro AE, Brown PO. Bone morphogenetic protein antagonist gremlin 1 is widely expressed by cancer-associated stromal cells and can promote tumor cell proliferation. *Proc Natl Acad Sci U S A*. **103:** 14842-14847. 2006

254. Namkoong H, Shin SM, Kim HK, Ha SA, Cho GW, Hur SY, Kim TE, Kim JW. The bone morphogenetic protein antagonist gremlin 1 is overexpressed in human cancers and interacts with YWHAH protein. *BMC Cancer*. **6:** 74. 2006

255. Karagiannis GS, Treacy A, Messenger D, Grin A, Kirsch R, Riddell RH, Diamandis EP. Expression patterns of bone morphogenetic protein antagonists in colorectal cancer desmoplastic invasion fronts. *Mol Oncol*. 2014

256. Mulvihill MS, Kwon YW, Lee S, Fang LT, Choi H, Ray R, Kang HC, Mao JH, Jablons D, Kim IJ. Gremlin is overexpressed in lung adenocarcinoma and increases cell growth and proliferation in normal lung cells. *PLoS One*. **7:** e42264. 2012

257. Chen MH, Yeh YC, Shyr YM, Jan YH, Chao Y, Li CP, Wang SE, Tzeng CH, Chang PM, Liu CY, Hsiao M, Huang CY. Expression of gremlin 1 correlates with increased angiogenesis and progression-free survival in patients with pancreatic neuroendocrine tumors. *J Gastroenterol*. **48:** 101-108. 2013

258. Chen B, Athanasiou M, Gu Q, Blair DG. Drm/Gremlin transcriptionally activates p21(Cip1) via a novel mechanism and inhibits neoplastic transformation. *Biochem Biophys Res Commun*. **295:** 1135-1141. 2002

259. Lee CG, Park GY, Han YK, Lee JH, Chun SH, Park HY, Lim KH, Kim EG, Choi YJ, Yang K, Lee CW. Roles of 14-3-3η in mitotic progression and its potential use as a therapeutic target for cancers. *Oncogene*. **32:** 1560-1569. 2013

260. Mitola S, Ravelli C, Moroni E, Salvi V, Leali D, Ballmer-Hofer K, Zammataro L, Presta M. Gremlin is a novel agonist of the major proangiogenic receptor VEGFR2. *Blood*. **116:** 3677-3680. 2010

261. Chen B, Blair DG, Plisov S, Vasiliev G, Perantoni AO, Chen Q, Athanasiou M, Wu JY, Oppenheim JJ, Yang D. Cutting edge: bone morphogenetic protein antagonists Drm/Gremlin and Dan interact with Slits and act as negative regulators of monocyte chemotaxis. *J Immunol*. **173:** 5914-5917. 2004

262. Hulmi JJ, Oliveira BM, Silvennoinen M, Hoogaars WM, Ma H, Pierre P, Pasternack A, Kainulainen H, Ritvos O. Muscle protein synthesis, mTORC1/MAPK/Hippo signaling, and capillary density are altered by blocking of myostatin and activins. *Am J Physiol Endocrinol Metab*. **304:** E41-50. 2013

263. Ory DS, Neugeboren BA, Mulligan RC. A stable human-derived packaging cell line for production of high titer retrovirus/vesicular stomatitis virus G pseudotypes. *Proc Natl Acad Sci U S A*. **93:** 11400-11406. 1996

264. Soderberg O, Gullberg M, Jarvius M, Ridderstrale K, Leuchowius KJ, Jarvius J, Wester K, Hydbring P, Bahram F, Larsson LG, Landegren U. Direct observation of individual endogenous protein complexes in situ by proximity ligation. *Nat Methods*. **3:** 995-1000. 2006

265. Varjosalo M, Sacco R, Stukalov A, van Drogen A, Planyavsky M, Hauri S, Aebersold R, Bennett KL, Colinge J, Gstaiger M, Superti-Furga G. Interlaboratory reproducibility of large-scale human protein-complex analysis by standardized AP-MS. *Nat Methods*. **10:** 307-314. 2013

266. Glatter T, Wepf A, Aebersold R, Gstaiger M. An integrated workflow for charting the human interaction proteome: insights into the PP2A system. *Mol Syst Biol*. **5:** 237. 2009

267. Sato M, Shames DS, Hasegawa Y. Emerging evidence of epithelial-to-mesenchymal transition in lung carcinogenesis. *Respirology*. **17:** 1048-1059. 2012

268. Kasai H, Allen JT, Mason RM, Kamimura T, Zhang Z. TGF-β1 induces human alveolar epithelial to mesenchymal cell transition (EMT). *Respir Res*. **6:** 56. 2005

269. Nagarajan D, Melo T, Deng Z, Almeida C, Zhao W. ERK/GSK3β/Snail signaling mediates radiation-induced alveolar epithelial-to-mesenchymal transition. *Free Radic Biol Med*. **52:** 983-992. 2012

270. Kage H, Borok Z. EMT and interstitial lung disease: a mysterious relationship. *Curr Opin Pulm Med*. **18:** 517-523. 2012

271. Henderson DW, Reid G, Kao SC, van Zandwijk N, Klebe S. Challenges and controversies in the diagnosis of mesothelioma: Part 1. Cytology-only diagnosis, biopsies, immunohistochemistry, discrimination between mesothelioma and reactive mesothelial hyperplasia, and biomarkers. *J Clin Pathol*. **66:** 847-853. 2013

272. Ke Y, Reddel RR, Gerwin BI, Reddel HK, Somers AN, McMenamin MG, LaVeck MA, Stahel RA, Lechner JF, Harris CC. Establishment of a human in vitro mesothelial cell model system for investigating mechanisms of asbestos-induced mesothelioma. *Am J Pathol*. **134:** 979-991. 1989

273. Rivera Z, Strianese O, Bertino P, Yang H, Pass H, Carbone M. The relationship between simian virus 40 and mesothelioma. *Curr Opin Pulm Med*. **14:** 316-321. 2008

274. Dormoy V, Jacqmin D, Lang H, Massfelder T. From development to cancer: lessons from the kidney to uncover new therapeutic targets. *Anticancer Res*. **32:** 3609-3617. 2012

275. Gordon KJ, Kirkbride KC, How T, Blobe GC. Bone morphogenetic proteins induce pancreatic cancer cell invasiveness through a Smad1-dependent mechanism that involves matrix metalloproteinase-2. *Carcinogenesis*. **30:** 238-248. 2009

276. Kang MH, Oh SC, Lee HJ, Kang HN, Kim JL, Kim JS, Yoo YA. Metastatic function of BMP-2 in gastric cancer cells: the role of PI3K/AKT, MAPK, the NF-κB pathway, and MMP-9 expression. *Exp Cell Res*. **317:** 1746-1762. 2011

277. Dulic V, Kaufmann WK, Wilson SJ, Tlsty TD, Lees E, Harper JW, Elledge SJ, Reed SI. p53-dependent inhibition of cyclin-dependent kinase activities in human fibroblasts during radiation-induced G1 arrest. *Cell*. **76:** 1013-1023. 1994

278. Miyawaki-Shimizu K, Predescu D, Shimizu J, Broman M, Predescu S, Malik AB. siRNA-induced caveolin-1 knockdown in mice increases lung vascular permeability via the junctional pathway. *Am J Physiol Lung Cell Mol Physiol*. **290:** L405-413. 2006

279. Thakker DR, Natt F, Husken D, Maier R, Muller M, van der Putten H, Hoyer D, Cryan JF. Neurochemical and behavioral consequences of widespread gene knockdown in the adult mouse brain by using nonviral RNA interference. *Proc Natl Acad Sci U S A*. **101:** 17270-17275. 2004

280. Calabro L, Morra A, Fonsatti E, Cutaia O, Amato G, Giannarelli D, Di Giacomo AM, Danielli R, Altomonte M, Mutti L, Maio M. Tremelimumab for patients with chemotherapy-resistant advanced malignant mesothelioma: an open-label, single-arm, phase 2 trial. *Lancet Oncol*. **14:** 1104-1111. 2013

281. Bilezikjian LM, Corrigan AZ, Blount AL, Vale WW. Pituitary follistatin and inhibin subunit messenger ribonucleic acid levels are differentially regulated by local and hormonal factors. *Endocrinology*. **137:** 4277-4284. 1996

282. Shintani Y, Dyson M, Drummond AE, Findlay JK. Regulation of follistatin production by rat granulosa cells in vitro. *Endocrinology*. **138:** 2544-2551. 1997

283. Kearns AE, Demay MB. BMP-2 induces the expression of activin βA and follistatin in vitro. *J Cell Biochem*. **79:** 80-88. 2000

284. Quail DF, Siegers GM, Jewer M, Postovit LM. Nodal signalling in embryogenesis and tumourigenesis. *Int J Biochem Cell Biol*. **45:** 885-898. 2013

285. Tsuchida K, Nakatani M, Uezumi A, Murakami T, Cui X. Signal transduction pathway through activin receptors as a therapeutic target of musculoskeletal diseases and cancer. *Endocr J*. **55:** 11-21. 2008

286. Xiao L, Yuan X, Sharkis SJ. Activin A maintains self-renewal and regulates fibroblast growth factor, Wnt, and bone morphogenic protein pathways in human embryonic stem cells. *Stem Cells*. **24:** 1476-1486. 2006

287. Ungefroren H, Groth S, Sebens S, Lehnert H, Gieseler F, Fandrich F. Differential roles of Smad2 and Smad3 in the regulation of TGF-β1-mediated growth inhibition and cell migration in pancreatic ductal adenocarcinoma cells: control by Rac1. *Mol Cancer*. **10:** 67. 2011

288. Zhou X, Wang JL, Lu J, Song Y, Kwak KS, Jiao Q, Rosenfeld R, Chen Q, Boone T, Simonet WS, Lacey DL, Goldberg AL, Han HQ. Reversal of cancer cachexia and muscle wasting by ActRIIB antagonism leads to prolonged survival. *Cell*. **142:** 531-543. 2010

289. Infante JR, Fecher LA, Falchook GS, Nallapareddy S, Gordon MS, Becerra C, DeMarini DJ, Cox DS, Xu Y, Morris SR, Peddareddigari VG, Le NT, Hart L, Bendell JC, Eckhardt G, Kurzrock R, Flaherty K, Burris HA, 3rd, Messersmith WA. Safety, pharmacokinetic, pharmacodynamic, and efficacy data for the oral MEK inhibitor trametinib: a phase 1 dose-escalation trial. *Lancet Oncol*. **13:** 773-781. 2012

290. Patel SP, Lazar AJ, Papadopoulos NE, Liu P, Infante JR, Glass MR, Vaughn CS, LoRusso PM, Cohen RB, Davies MA, Kim KB. Clinical responses to selumetinib (AZD6244; ARRY-142886)-based combination therapy stratified by gene mutations in patients with metastatic melanoma. *Cancer*. **119:** 799-805. 2013

I

ARTICLE
Journal of Cellular Biochemistry 113:2234–2247 (2012)

Journal of Cellular Biochemistry

Asbestos Exposure Induces Alveolar Epithelial Cell Plasticity Through MAPK/Erk Signaling

Jenni A. Tamminen,[1] Marjukka Myllärniemi,[2,3,4] Marko Hyytiäinen,[4,5] Jorma Keski-Oja,[4,5] and Katri Koli[1*]

[1] *Research Programs Unit, Molecular and Cancer Biology and Transplantation Laboratory, Haartman Institute, University of Helsinki, Helsinki, Finland*

[2] *Department of Clinical and Clinicotheoretical Medicine, University of Helsinki, Helsinki, Finland*

[3] *Department of Pulmonary Medicine, Helsinki University Central Hospital, Helsinki, Finland*

[4] *HUSLAB, Helsinki University Hospital, Helsinki, Finland*

[5] *Research Programs Unit, Molecular and Cancer Biology and Departments of Virology and Pathology, Haartman Institute, University of Helsinki, Helsinki, Finland*

ABSTRACT

The inhalation of asbestos fibers is considered to be highly harmful, and lead to fibrotic and/or malignant disease. Epithelial-to-mesenchymal transition (EMT) is a common pathogenic mechanism in asbestos associated fibrotic (asbestosis) and malignant lung diseases. The characterization of molecular pathways contributing to EMT may provide new possibilities for prognostic and therapeutic applications. The role of asbestos as an inducer of EMT has not been previously characterized. We exposed cultured human lung epithelial cells to crocidolite asbestos and analyzed alterations in the expression of epithelial and mesenchymal marker proteins and cell morphology. Asbestos was found to induce downregulation of E-cadherin protein levels in A549 lung carcinoma cells in 2-dimensional (2D) and 3D cultures. Similar findings were made in primary small airway epithelial cells cultured in 3D conditions where the cells retained alveolar type II cell phenotype. A549 cells also exhibited loss of cell–cell contacts, actin reorganization and expression of α-smooth muscle actin (α-SMA) in 2D cultures. These phenotypic changes were not associated with increased transforming growth factor (TGF)-β signaling activity. MAPK/Erk signaling pathway was found to mediate asbestos-induced downregulation of E-cadherin and alterations in cell morphology. Our results suggest that asbestos can induce epithelial plasticity, which can be interfered by blocking the MAPK/Erk kinase activity. J. Cell. Biochem. 113: 2234–2247, 2012.

KEY WORDS: EMT; ASBESTOS EXPOSURE ASSOCIATED DISEASES; FIBROSIS; CANCER

Asbestos is a common name for a group of naturally occurring hydrated silica fibers. Because of their tensile strength and resilient structural and chemical properties asbestos fibers have been used in various construction and insulating purposes. Asbestos exposure raises the risk for non-malignant inflammatory conditions such as pleural effusions, pleural plaques, and asbestosis (asbestos-induced lung fibrosis) [Kamp, 2009]. It is a severe condition in which loss of lung function can lead to death [Frank, 1980]. Malignant conditions associated with asbestos exposure include pleural and peritoneal mesothelioma and lung cancer. Diffuse malignant mesothelioma is a fatal tumor arising from mesothelial cells or underlying mesenchymal cells in the

The authors declare no conflict of interests.

Additional supporting information may be found in the online version of this article.

Grant sponsor: Academy of Finland; Grant sponsor: Finnish Cancer Foundation; Grant sponsor: Sigrid Jusélius Foundation; Grant sponsor: Yrjö Jahnsson Foundation; Grant sponsor: Magnus Ehrnrooth Foundation; Grant sponsor: Biocentrum Helsinki; Grant sponsor: Helsinki University Hospital Fund; Grant sponsor: University of Helsinki; Grant sponsor: Jalmari and Rauha Ahokas Foundation; Grant sponsor: Foundation of the Finnish Anti-Tuberculosis Association; Grant sponsor: Finnish Cultural Foundation.

*Correspondence to: Dr. Katri Koli, University of Helsinki, Biomedicum/B502a1, P.O. Box 63, Haartmaninkatu 8, 00014 Helsinki, Finland. E-mail: katri.koli@helsinki.fi

Manuscript Received: 1 February 2012; Manuscript Accepted: 2 February 2012

Accepted manuscript online in Wiley Online Library (wileyonlinelibrary.com): 14 February 2012

DOI 10.1002/jcb.24094 • © 2012 Wiley Periodicals, Inc.

pleura, pericardium, and peritoneum [Mossman et al., 1990]. Asbestos-induced lung cancer is indistinguishable from that caused by tobacco smoke [Roggli and Sanders, 2000]. Although asbestos has been banned, the long latency preceding diseases together with the remaining risk for exposure during renovation and demolition works are expected to lead to increased incidence of asbestos exposure-related diseases worldwide [Huuskonen and Rantanen, 2006].

Epithelial-to-mesenchymal transition (EMT), a series of alterations occurring in cell architecture and behavior, is implicated in fibrotic diseases and in cancer progression. In EMT epithelial cells lose their epithelial characteristics and gain properties of mesenchymal cell [Thiery and Sleeman, 2006]. Cells undergoing EMT lose epithelial marker proteins such as the adherens junction protein E-cadherin and tight junction protein zonula occludens (ZO)-1 and begin to express mesenchymal proteins such as smooth muscle actin (SMA), collagen, vimentin, and fibronectin. Loss of epithelial markers and expression of mesenchymal marker proteins correlate with tumor progression and poor prognosis [Thiery, 2002; Peinado et al., 2004; Barrallo-Gimeno and Nieto, 2005; Moody et al., 2005; Thiery and Sleeman, 2006]. Loss of E-cadherin-dependent intercellular adhesion contributes to increased tumor cell motility and invasion into surrounding tissues [Brabletz et al., 2001; Guarino, 2007]. EMT can give rise to metastasizing cells from the primary tumors and contribute to metastasis development [Thiery, 2002; Huber et al., 2005].

After epithelial injury, EMT is likely to have a role in repair and scar formation [Willis and Borok, 2007]. In organ fibrosis including lung, kidney, eye, and liver, EMT may contribute to fibroblast accumulation and parenchyma destruction in advanced fibrosis [Guarino et al., 2009]. Markers of EMT have been identified from epithelial cells of idiopathic pulmonary fibrosis (IPF) patients [Willis and Borok, 2007]. Asbestosis and IPF exhibit many similarities including histopathology of usual interstitial pneumonia (UIP). These diseases may share common pathogenic mechanisms.

Despite active research, understanding of molecular mechanisms underlying the pathogenesis of asbestos-associated malignancies, and of fibrotic lung diseases has remained insufficient for the development of efficient treatments. Increasing evidence has recognized reactive oxygen species (ROS) and reactive nitrogen species (RNS) as important mediators of asbestos-induced toxicity [Mossman and Churg, 1998; Shukla et al., 2003; Kamp, 2009]. These reactive species oxidate and/or nitrolysate proteins and DNA [Shukla et al., 2003] and alter cell signal transduction pathways. Increased levels of ROS as well as endoplasmic reticulum stress have been implicated in alveolar epithelial cell EMT [Zhong et al., 2011]. In addition, asbestos exposure can lead to increased production and activation of various growth factors and cytokines [Robledo and Mossman, 1999; Yin et al., 2007].

Because asbestos exposure can induce signaling pathways previously linked to epithelial cell plasticity, we hypothesized that asbestos may initiate EMT processes which contribute to the pathogenesis of fibrotic and malignant lung diseases. Here, we found that asbestos-induced EMT-like alterations in human A549 lung carcinoma cells. Primary human lung epithelial cells did not show similar alterations, which was likely due to loss of alveolar type II cell phenotype in 2D cultures. However, primary cells cultured in 3D exhibited abundant cell surface E-cadherin expression, surfactant protein production and were sensitive to asbestos-induced loss of E-cadherin protein expression. To identify possible sites of therapeutic interference, we analyzed in detail the mechanism of asbestos-induced phenotypic changes in A549 epithelial cells.

MATERIALS AND METHODS

GROWTH FACTORS, ANTIBODIES, AND INHIBITORS

Transforming growth factor (TGF)-β1 and tumor necrosis factor (TNF)-α were from R&D Systems. Mouse monoclonal anti-E-cadherin, mouse monoclonal Smad2/3, and rabbit polyclonal anti-ZO-1 antibodies were from BD Transduction Laboratories and Invitrogen, respectively. Rabbit polyclonal anti-phospho-42/44 MAP kinase (Thr202/Tyr 204) and mouse monoclonal anti-44/42 MAPK (Erk1/2) (3A7) antibodies were from Cell Signaling Technology, rabbit polyclonal antibody against NF-κB (p65, RelA) from Calbiochem. Rabbit polyclonal anti-β-tubulin and rabbit polyclonal anti-SP-D antibodies were from Santa Cruz Biotechnology. Rabbit polyclonal anti phospho-Smad2 was provided by Peter ten Dijke (The Netherlands Cancer Institute, Amsterdam). Mouse monoclonal α-smooth muscle actin antibody was from NeoMarkers. The inhibitor of TGF-β superfamily type I activin receptor-like kinase (ALK) receptors, SB431542, was from Sigma and used at 6 μM concentration. PD98059 [inhibitor of MAP kinase kinase (MEK), used at 30 μM], SP600125 [inhibitor of c-Jun N-terminal kinase (JNK), used at 10 μM], JSH-23 (inhibitor of the nuclear translocation of NF-kB p65, used at 20 μM) were from Calbiochem.

TWO DIMENSIONAL CELL CULTURES

Primary human bronchial epithelial cells (NHBE) and small airway epithelial cells (SAEC) were from Lonza and cultured according to manufacturer's instructions. One batch of NHBE cells and several independent batches of SAECs were used in the experiments. Cells were used between passages 4 and 8. BEAS-2B cells are non-malignant immortalized human bronchial epithelial cells (ATCC). They were grown in LHC-9 medium according to manufacturer's instructions (Invitrogen). Human A549 lung epithelial cells (ATCC) originate from carcinoma tissue, but have retained some characteristics of alveolar type II epithelial cells. These cells were grown in minimal essential medium (MEM) supplemented with 10% fetal bovine serum (Gibco) and antibiotics.

For experiments the cells were seeded on six-well plates and treated with increasing concentrations of crocidolite asbestos (obtained from the Finnish Institute of Occupational Health) or TGF-β1 for the indicated times. For longer incubations fresh culture medium was changed every 2–3 days. The experiments were performed under standard culture conditions. Only short stimulations for the analysis of Smad2 phosphorylation were performed under serum-free conditions. The inhibitors were added to the medium 1 h prior to stimulation where indicated. Images of cells were captured using Axiovert 200 inverted epifluorescence

microscope and Axio-Cam HR camera (Zeiss) at the Biomedicum Imaging Unit of the University of Helsinki.

THREE DIMENSIONAL CELL CULTURES

Three dimensional (3D) cultures were generated using Matrigel basement membrane matrix (Beckton-Dickinson). Ice cold Matrigel was added to chambered coverglasses (Nunc) on ice and allowed to solidify at 37°C for 2 h. Subconfluent A549 or SAEC cells were trypsinized and seeded on top of Matrigel (5×10^4 cells/chamber). Normal complete culture medium was used to produce the polarized 3D structures. New medium was added every 2–3 days. Asbestos and TGF-β1 treatments were started on 3- to 7-day-old cultures and continued for 1 week.

GENERATION OF IκB 32/36A EXPRESSING STABLE CELL LINES

Retroviral vector pBabePuro was from Addgene and the construct pBabePuro IκB32/36A expressing a dominant-negative mutant of IκB was kindly provided by Juha Klefström (University of Helsinki), dominant negative function described in [Traenckner et al., 1995]. Retroviruses were produced in 293GPG packaging cell line [Ory et al., 1996]. Briefly, the producer cells were transfected overnight using Fugene transfection reagent (Roche) followed by collection of cell-conditioned medium, which was then used to transduce A549 cells. Puromycin selection was started 2 days after transduction.

TRANSIENT TRANSFECTION AND LUCIFERASE ASSAY

Cells to be transfected were seeded in six-well plates. The next day the cells were co-transfected with a total of 2 μg of promoter constructs (CAGA)12-luc (Smad3 responsive) or ARE-luc (Smad2 responsive) and Fast-1 provided by Peter ten Dijke (The Netherlands Cancer Institute, Amsterdam) together with pRL-TK (Renilla Luciferase control, Promega) plasmid using Fugene HD transfection reagent (Roche). The pRL-TK plasmid contains the *Renilla* luciferase gene under the control of a constitutively expressed thymidine kinase promoter, and was used in dual luciferase assays to normalize the transfection efficiency. Dual luciferase based Cignal Finder 10-Pathway Cancer Reporter Array (SABioscience) was used according to manufacturer's instructions. Cells were lysed and subjected to luciferase activity measurements by Dual Luciferase Reporter Assay (Promega) and DCR-1 luminometer (MGM Instruments Digene Diacnostics Inc.). Treatment with TGF-β or asbestos was not found to unspecifically alter luciferase activity of the promoter constructs.

RNA ISOLATION AND QUANTITATIVE RT-PCR

Total cellular RNA was isolated using RNeasy Mini kit (Qiagen) and reverse transcribed to cDNA using Random hexamer primers (Invitrogen) and Superscript III reverse transcriptase (Life Technologies) according to manufacturer's instructions. The cDNAs were amplified using TaqMan Assays-on-Demand gene expression products (Applied Biosystems) and CFX96 Real-time PCR detection system (BioRad). Control amplifications directly from RNA were performed in order to rule out DNA contamination. The levels of gene expression were determined using the C_t method, and the results have been expressed as mRNA expression levels normalized to the levels of a gene with a constant expression (TBP, TATA-binding protein).

SDS–PAGE AND IMMUNOBLOTTING

Cells were lysed in RIPA buffer (50 mM Tris–HCl, pH 7.4, 150 mM NaCl, 1 mM EDTA, 1% NP-40, 0.2% Na-deoxycholate) containing protease inhibitors (Roche Diagnostics) on ice for 15 min. For the analysis of Smad2 phosphorylation cells were lysed in lysis buffer (20 mM Tris–HCl, pH 8, 120 mM NaCl, 0.5% NP-40, 1 mM Na_3VO_4) containing protease inhibitors (Roche Diagnostics) on ice for 15 min. Protein concentrations were measured using a BCA Protein Assay Kit (Pierce). Equal amounts of protein were separated by SDS–PAGE using 10% or 4–20% gradient Tris–glycine gels (Lonza) and transferred to Protran nitrocellulose membranes (Whatman) using a semi-dry blotting system (Bio-Rad). Membranes were first blocked with 5% non-fat milk in TBS/0.05% Tween-20 to prevent non-specific binding of the antibodies and then incubated with the primary or biotin-conjugated secondary antibodies (DAKO) in TBS/5% BSA-0.05% Tween-20 at room temperature for 1 h. After several washing steps, the final detection was performed using HRP-conjugated streptavidin and an enhanced chemiluminescence Western blotting detection system (Amersham). Three independent experiments were included for the analyses of protein band intensities with the Scion Image analysis program (Scion Corporation).

IMMUNOFLUORESCENCE ANALYSIS AND MICROSCOPY

Cells were seeded on glass coverslips and cultured for the indicated times. For the detection of E-cadherin, NF-κB (p65), or F-actin cells were fixed with 4% paraformaldehyde/PBS at room temperature for 10 min. For the detection of ZO-1, the cells were fixed with methanol at −20°C for 15 min. Nonspecific binding of the antibodies was prevented by blocking with 5% BSA/PBS for 30 min. During blocking 0.3% Tx-100 was added when permeabilization of cells was needed. All antibody dilutions and washing steps were made in Dulbecco's PBS containing 0.5% BSA. The cells on coverslips were incubated with the primary antibodies for 1 h at room temperature and washed. The bound primary antibodies were detected using AlexaFluor secondary antibodies (Molecular Probes). TRITC-conjugated phalloidin (Sigma) was used for the detection of F-actin. Finally, the coverslips were washed with water and mounted on glass slides with Vectashield mounting medium containing DAPI (Vector Laboratories). Images were captured with Axioplan 2 epifluorescence microscope and Axio-Cam HR camera using Axiovision 4.5 software (Zeiss) at the Biomedicum Imaging Unit of the University of Helsinki.

3D cultures in Matrigel were fixed with 4% paraformaldehyde/PBS for overnight at room temperature. Fixed gels were embedded in paraffin and cut into 4 μm sections, which were then deparaffinized in xylene and rehydrated in graded alcohol. Antigens were retrieved by heating in 10 mM citrate buffer (pH 6.0). The sections were blocked with 5% non-fat milk/PBS containing normal goat serum (Jackson Immuno Reseach) at room temperature for 30 min followed by incubation with primary antibodies diluted in blocking buffer at +4°C overnight. The sections were then incubated with AlexaFluor secondary antibodies at room temperature for 1 h,

washed several times and mounted using Vectashield Hard Set mounting medium. The nuclei were visualized with DAPI. The images were captured as described above. Digital morphometry was conducted using Image Pro Plus 7.0 (Media Cybernetics) program. A representative picture from the control group was used to generate a filter for the detection of E-cadherin fluorescence intensity relative to unstained area in the 3D structure. Six to 10 independent pictures of each group were analyzed using this filter. Images were captured from H&E and SP-D stained sections with Olympus BX51 and Artray Artcam 300 MI.

STATISTICAL ANALYSIS

Data were analyzed using PASW Statistics 18 program for Windows. Statistical differences in E-cadherin levels in 3D cultures were evaluated using the nonparametric Kruskal–Wallis test (A549 cultures, all groups) or Mann–Whitney *U*-test (SAEC cultures, asbestos-exposed group vs. control group). Differences in mRNA expression levels (asbestos-exposed group vs. control group) and E-cadherin immunoblot band intensities (asbestos-exposed group vs. control group and DMSO treated vs. PD98059 treated group) were analyzed with Mann–Whitney *U*-test. A *P*-value of ≤ 0.05 was considered statistically significant.

RESULTS

ASBESTOS EXPOSURE INDUCES DOWNREGULATION OF EPITHELIAL PROTEINS IN TRANSFORMED LUNG EPITHELIAL CELLS

To test whether asbestos can induce EMT and downregulation of epithelial proteins we exposed cultured lung epithelial cells to crocidolite asbestos (0.5–5 $\mu g/cm^2$) under standard culture conditions for 3 days followed by analyses of E-cadherin protein levels by immunoblotting. TGF-β1, a known inducer of EMT, was used as a control. In primary human bronchial epithelial cells (NHBE) and small airway epithelial cells (SAEC) as well as in immortalized but non-malignant human bronchial epithelial cells (BEAS-2B) neither asbestos nor TGF-β1 treatment was able to alter E-cadherin protein levels (Fig. 1A). In contrast, in human lung carcinoma cells (A549) E-cadherin levels were clearly decreased when treated with asbestos or TGF-β1. Interestingly, TGF-β1 induced E-cadherin downregulation already after 1 day, while asbestos-induced downregulation was not detected until after 3 days (Fig. 1B).

Loss of E-cadherin is considered to be a universal marker for the loss of the epithelial phenotype. In monolayer cultures only in A549 carcinoma derived cells asbestos seemed to induce alterations consistent with the initiation of EMT. We addressed the effects of asbestos on the cell surface localization of epithelial junction proteins in A549 cells next. Cells grown on glass coverslips were exposed to asbestos (5 $\mu g/cm^2$) or TGF-β1 (2 ng/ml) for 3 days after which the cells were fixed and stained with antibodies specific for E-cadherin or the tight junction protein ZO-1. Asbestos exposure induced a significant downregulation of cell surface E-cadherin consistent with the immunoblotting result (Fig. 2). ZO-1 staining was also decreased or lost from cell contacts in asbestos-treated cells. As expected, TGF-β1 induced similar alterations in these epithelial junctional proteins [Kasai et al., 2005].

E-cadherin mRNA levels were examined by quantitative RT-PCR using specific primers (Materials and Methods section). Unexpectedly, A549 cells exposed to asbestos for 3 or 6 days showed no downregulation of E-cadherin mRNA levels (Fig. 1C). In contrast, TGF-β1 treated cells expressed clearly lower levels of E-cadherin mRNA, suggesting that TGF-β1 and asbestos mediate their effects via different mechanisms. Transcription factors Snail and Slug have been implicated in EMT associated downregulation of E-cadherin transcription, and their mRNA levels were analyzed next. As expected, TGF-β1 induced dramatically the expression of Snail and especially of Slug by 3 days (Fig. 1D). The expression was further increased by 6 days. Unlike TGF-β1, asbestos at 3 days had no effect and at 6 days induced only a very modest increase in the expression of these transcription factors, which is consistent with E-cadherin mRNA expression levels. Further analysis of early time points revealed induction of both transcription factors by TGF-β1 already after 1 h stimulation, but no alterations during asbestos exposure (Supplementary Fig. 1).

The BMP inhibitor gremlin is a TGF-β target gene involved in the induction of EMT processes [Koli et al., 2006; Lee et al., 2007]. To analyze whether asbestos exposure can increase gremlin expression in A549 cells we analyzed gremlin mRNA levels by quantitative RT-PCR. Gremlin mRNA levels in asbestos exposed A549 cells were found to be comparable to control levels (Supplementary Fig. 2). In contrast, TGF-β1 increased gremlin mRNA levels nearly fivefold at 3 days and over 10-fold at 6 days.

EPITHELIAL PHENOTYPE IS ALTERED BY ASBESTOS ALSO IN THREE DIMENSIONAL A549 CULTURES

In three-dimensional cultures cells adopt a morphology, which mimics better in vivo situations. The structural organization of cells can be protective against exogenous signals [Schmeichel and Bissell, 2003], which prompted us to study asbestos-induced alterations in A549 cells cultured on Matrigel (Materials and Methods section). Cells cultured for 2 weeks without stimulatory factors formed well-organized structures with polarized cells displaying abundant E-cadherin staining around a central lumen (Fig. 3A). Asbestos or TGF-β1 treatments were initiated on 1-week-old cultures and continued for another week. TGF-β1 was found to alter the appearance of the 3D structures, making them more scattered and less well organized. In control cultures, cells disappeared from the centre of the structure, which was less pronounced in the TGF-β-exposed cultures (Fig. 3A). In addition, the cell surface E-cadherin levels were significantly decreased in asbestos-treated cultures (from ~60% of a total area in the structures to ~35%, Materials and Methods section) and even more in TGF-β1 treated cultures (from ~60% to ~15%; Fig. 3B). These results suggest that the epithelial marker E-cadherin is significantly decreased by asbestos exposure also in three-dimensional cultures consistent with the initiation of EMT.

INDUCTION OF MESENCHYMAL CHARACTERISTICS IN A549 CELLS BY ASBESTOS EXPOSURE

We investigated next whether asbestos exposed cells gained mesenchymal characteristics typical for cells undergoing EMT. Alterations in cell morphology were first analyzed in monolayer

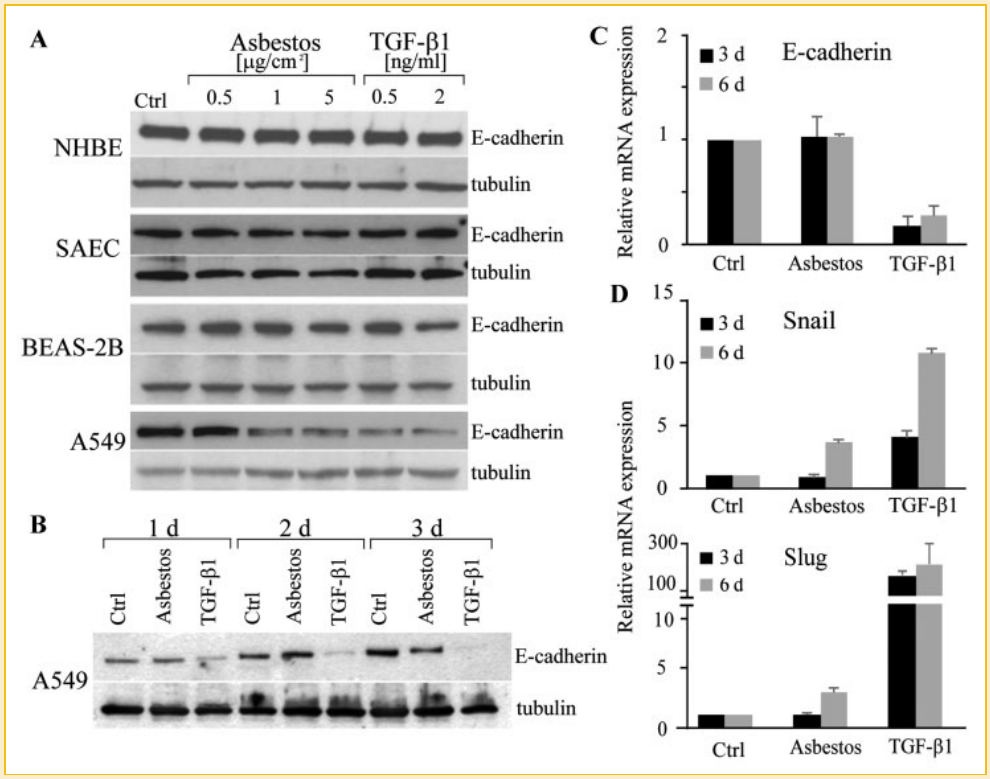

Fig. 1. Asbestos exposure leads to downregulation of E-cadherin protein levels in A549 lung carcinoma cells. A: Primary human bronchial epithelial cells (NHBE), small airway epithelial cells (SAEC), immortalized non-malignant bronchial epithelial cells (BEAS-2B), and lung carcinoma cells (A549) were exposed to asbestos or TGF-β1 for 3 days followed by analyses of E-cadherin protein levels by immunoblotting. Tubulin was used as a loading control. B: A549 cells were exposed to asbestos or TGF-β1 for the indicated times followed by analyses of E-cadherin protein levels. C,D: A549 cells were exposed to asbestos as indicated. Total cellular RNA was isolated followed by quantitative RT-PCR analyses of E-cadherin (C) or Snail and Slug (D) mRNA expression levels. Expression levels were normalized to the expression levels of TBP and are expressed relative to control. Error bars represent standard deviation of the means ($n = 2$).

cultures exposed to asbestos for 3 days. Asbestos exposure was found to induce the loss of the typical cobblestone-like appearance of A549 cells, which became scattered and more elongated (Fig. 4A). Asbestos exposed cells also frequently exhibited larger intercellular space and less cell–cell contacts. Alterations in actin organization were visualized by phalloidin staining, which showed re-organization of actin into longitudinal stress fibers (Fig. 4A).

The expression of mesenchymal genes associated with EMT was analyzed next. A549 cells were exposed to asbestos for 3 days, total cellular RNA was extracted and the expression levels of vimentin, fibronectin (FN), N-cadherin, collagen 1 (Col1A1), and α-smooth muscle actin (α-SMA) were measured by quantitative RT-PCR. Asbestos exposure-induced fourfold increase in α-SMA and threefold increase in collagen 1 mRNA levels (Fig. 4B). However, only the induction of α-SMA expression reached statistical significance. Vimentin, FN, and N-cadherin mRNA levels were not altered significantly. To analyze alterations in α-SMA protein levels, cells were exposed to asbestos for 3 or 6 days followed by immunoblotting analyses. Consistent with mRNA expression results, asbestos exposure increased α-SMA protein levels (Fig. 4C). The results suggest that in addition to downregulation of epithelial proteins, asbestos is able to alter epithelial cell morphology and induce the expression of certain profibrotic genes as well as proteins associated with the progression of EMT.

ASBESTOS-INDUCED DOWNREGULATION OF E-CADHERIN IN A549 CELLS IS NOT ASSOCIATED WITH INCREASED TGF-β ACTIVATION

Asbestos has been reported to induce gene transcription of TGF-β and other cytokines [Yin et al., 2007]. In addition, ROS are generated during asbestos exposure [Mossman and Marsh, 1989] and asbestos generated ROS may activate latent forms of TGF-β [Pociask et al., 2004]. TGF-β signals mainly through Smad2 and Smad3 transcription factors, which are phosphorylated and transported into the nucleus upon ligand binding [Nakao et al., 1997]. To test whether asbestos increases TGF-β signaling activity in our model, A549 cells were transiently transfected with constructs containing luciferase gene under the control of TGF-β responsive promoters (Smad3

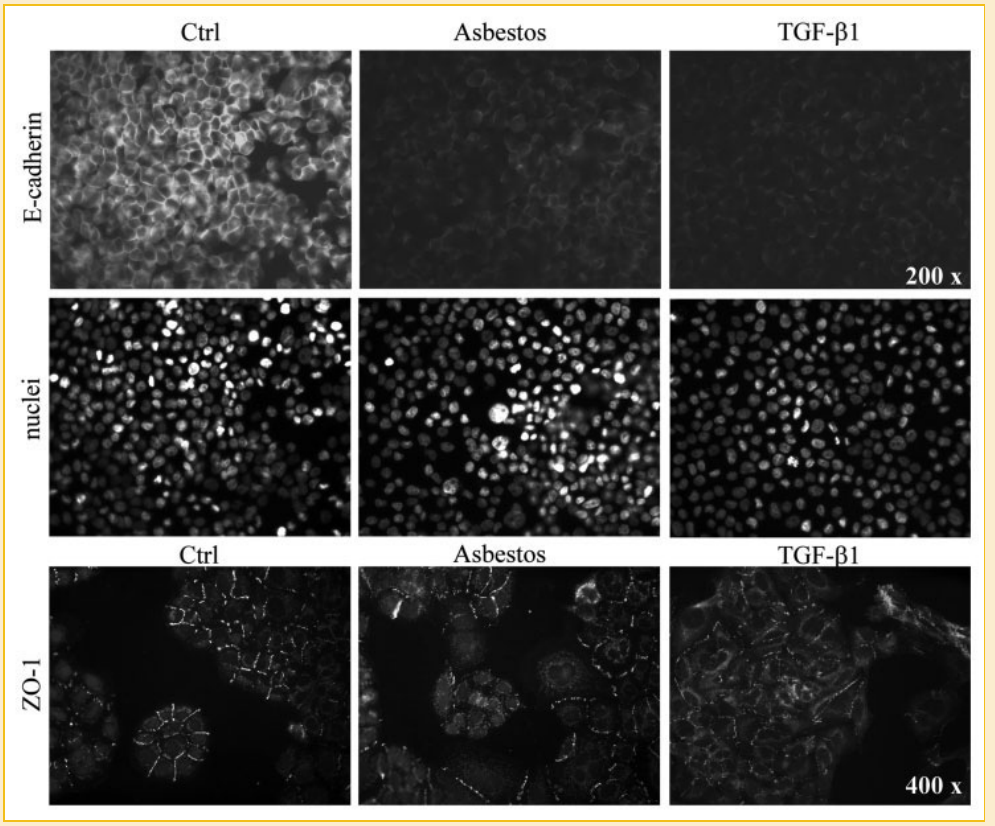

Fig. 2. Epithelial marker proteins decrease from cell junctions of A549 cells after asbestos exposure. A549 cells were seeded on glass coverslips, exposed to asbestos (5 μg/cm^2) or TGF-β1 (2 ng/ml) for 3 days, fixed and stained with antibodies specific for E-cadherin or ZO-1. DAPI staining was used to visualize nuclei. Original magnifications are indicated on the right.

responsive $CAGA_{12}$-luc or Smad2 responsive ARE-luc, Materials and Methods section) followed by exposure to asbestos and measurement of luciferase activity. Exposure to asbestos for 3 days was not able to induce $CAGA_{12}$-luc (Fig. 5A) or ARE-luc (not shown) activity in A549 cells, while TGF-β1 induced signaling activity as expected. To validate these results we analyzed Smad2 phosphorylation, that is, activation at early time points (1, 5, and 24 h) after asbestos or TGF-β1 stimulation. A549 cells were exposed to asbestos or TGF-β1 for the indicated times followed by immunoblotting analyses of P-Smad2. TGF-β1 induced phosphorylation of Smad2 peaked at 1 h and decreased thereafter (Fig. 5B). Asbestos, however, did not induce Smad2 phosphorylation at any time point.

TGF-β can also signal via Smad-independent pathways, which may contribute to cell plasticity. To further assess the possible role of TGF-β in asbestos-induced downregulation of E-cadherin, A549 cells were exposed to asbestos in the presence of SB431542, an inhibitor of TGF-β type I receptors. Interestingly, SB431542 had only a moderate effect on asbestos-induced downregulation of E-cadherin (Fig. 5C). In the presence of SB431542 asbestos was still able to induce significant downregulation of E-cadherin levels, while TGF-β1-induced downregulation was completely blocked as expected (Fig. 5D). The result suggests that asbestos-induced EMT-like phenotype in A549 cells does not depend on Smad2/3 signaling and is not fully explained by induction of TGF-β-mediated pathways.

MAPK/JNK, MAPK/Erk, AND NF-κB SIGNALING ACTIVITY DIFFER BETWEEN NORMAL AND TRANSFORMED CELLS

Cancer cells have typically high activity of cellular signaling pathways, which are silent or active at low levels in non-malignant cells. To screen for differences that make A549 cells more susceptible to asbestos-induced EMT-like alterations than primary cells (Fig. 1A), we compared the basal activity levels of selected cancer-associated signaling pathways in A549 cells and those of normal SAECs using a commercial Cancer Reporter promoter array (Materials and Methods section). Cells were transiently transfected with the promoter constructs and cultured for 2 days under standard culture conditions before the activity measurements. In addition to the p53 pathway, the signaling activities of

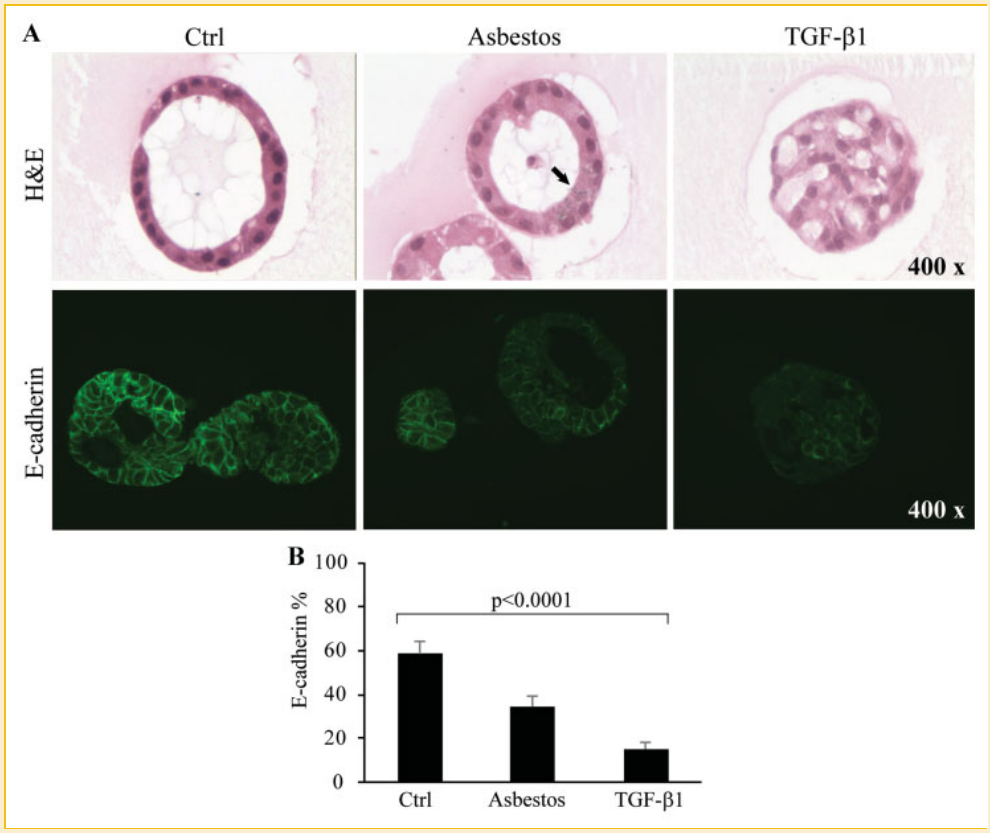

Fig. 3. Epithelial phenotype of A549 cells is altered by asbestos and TGF-β in three dimensional cultures. Cells were grown on Matrigel basement membrane matrix for 1 week followed by exposure to asbestos (5.0 μg/cm^2) or TGF-β1 (2.0 ng/ml) for another week. A: The structures were stained with H&E or antibodies specific for E-cadherin. Asbestos fibers detectable within the cells are indicated with an arrow. Magnifications are indicated on the right. B: Digital image analysis of the staining intensity of E-cadherin relative to non-stained cellular area in the structures. The amount of E-cadherin is expressed as percentage relative to non-stained cellular area. Error bars represent SEM of the samples ($n = 10$). E-cadherin positive area differ significantly between the groups (Ctrl, asbestos, TGF-β), $P < 0.0001$.

mitogen activated protein kinase/c-jun N-terminal kinase (MAPK/JNK), MAPK/extracellular signal-regulated kinase (Erk), and Nuclear factor kappa B (NF-κB) pathways were significantly elevated in A549 cells (Fig. 6A). These three pathways have been previously implicated in EMT and were selected for further analyses.

BLOCKADE OF NF-κB PATHWAY DOES NOT ALTER CELLULAR RESPONSES TO ASBESTOS

The role of NF-κB signaling in asbestos-induced responses in A549 cells was analyzed by blocking this pathway using a dominant negative inhibitor of nuclear factor kappa B (IκB) 32/36A expression construct. Mutated serines in IκB32/36A render it unsusceptible to phosphorylation, and therefore prevent its removal from its inhibitory association with NF-κB [Traenckner et al., 1995]. Stable A549 cell lines expressing IκB32/36A were generated by retroviral transduction (Materials and Methods section). Immunofluorescence analyses of the NF-κB subunit p65 showed that IκB32/36A expression inhibited TNF-α induced nuclear localization of p65 (Fig. 6B) suggesting efficient blockade of NF-κB pathway activity. A549 cells stably transduced with the dominant negative IκB exhibited severely decreased cell proliferation/survival (not shown). The use of JSH-23, a chemical inhibitor of the NF-κB pathway, also resulted in reduced number of cells with altered morphology (not shown) suggesting a role for NF-κB signaling in A549 cell survival. This may have an effect also on cellular responses to asbestos treatment. However, expression of IκB32/36A did not alter asbestos-induced E-cadherin downregulation (Fig. 6C) or α-SMA mRNA induction (Fig. 6D) in A549 cells.

MAPK/Erk PATHWAY CONTRIBUTES TO ASBESTOS-INDUCED EMT-LIKE TRANSITION IN A549 CELLS

The role of MAPK/Erk and MAPK/JNK pathways in asbestos-induced downregulation of E-cadherin was analyzed using chemical inhibitors of MAP kinase kinase MEK (PD98059, 30 μM) and c-Jun

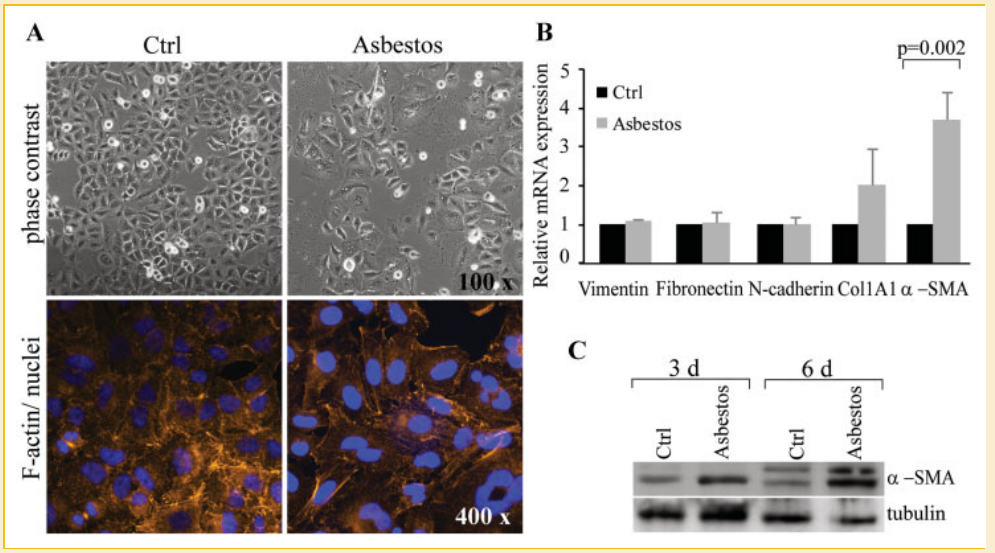

Fig. 4. Asbestos exposed cells gain mesenchymal characteristics. A: A549 cells seeded on culture plates or on glass coverslips, were exposed to asbestos (5 μg/cm^2) for 3 days. Live cells were imaged or the cells were fixed and stained with phalloidin to visualize F-actin. DAPI stain was used to visualize the nuclei. Original magnifications are indicated on the right. B: A549 cells were exposed to asbestos for 3 days. Total cellular RNA was isolated followed by quantitative RT-PCR analyses using specific primers for vimentin, fibronectin, N-cadherin, collagen 1A1 or α-smooth muscle actin (α-SMA). Expression levels were normalized to the expression levels of TBP and are expressed relative to control. Error bars represent standard deviation of the means ($n \geq 2$). C: A549 cells were exposed to asbestos (5 μg/cm^2) as indicated followed by analyses of α-SMA protein levels by immunoblotting. Tubulin was used as a loading control.

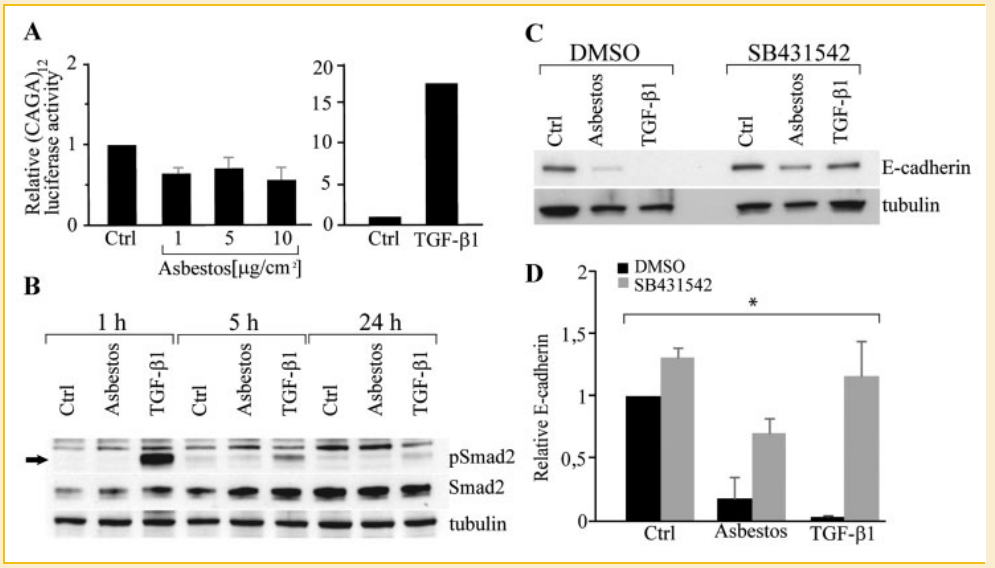

Fig. 5. Asbestos-induced downregulation of E-cadherin is not associated with increased TGF-β activity. A: A549 cells transiently transfected with Smad3 responsive (CAGA)12-luciferase promoter construct were exposed to asbestos (1–10 μg/cm^2) or TGF-β1 (100 pg/ml) for 3 days and subjected to luciferase activity measurement. The luciferase activities were normalized to constitutively expressed *Renilla* luciferase activities, and the results are expressed relative to control. The error bars represent standard deviation of the means ($n = 2$). A representative experiment of TGF-β induced luciferase activity is shown on the right. B: A549 cells were exposed to asbestos (5 μg/cm^2) or TGF-β1 (2 ng/ml) for the indicated times and analyzed for Smad2 phosphorylation (P-Smad2) or total Smad2 by immunoblotting. Tubulin was used as a loading control. C: A549 cells were exposed to asbestos (5 μg/cm^2) or TGF-β1 (2 ng/ml) for 3 days in the presence of an inhibitor of TGF-β type I receptors (SB431542, 6 μM) or DMSO used as a control followed by analyses of E-cadherin protein levels by immunoblotting. Tubulin was used as a loading control. D: E-cadherin band intensities were quantified and normalized to tubulin. The results are expressed relative to control. Error bars represent standard deviation of the means ($n = 3$). Normalized E-cadherin band intensities differ significantly between the groups (Kruskal–Wallis test), $^*P = 0.035$.

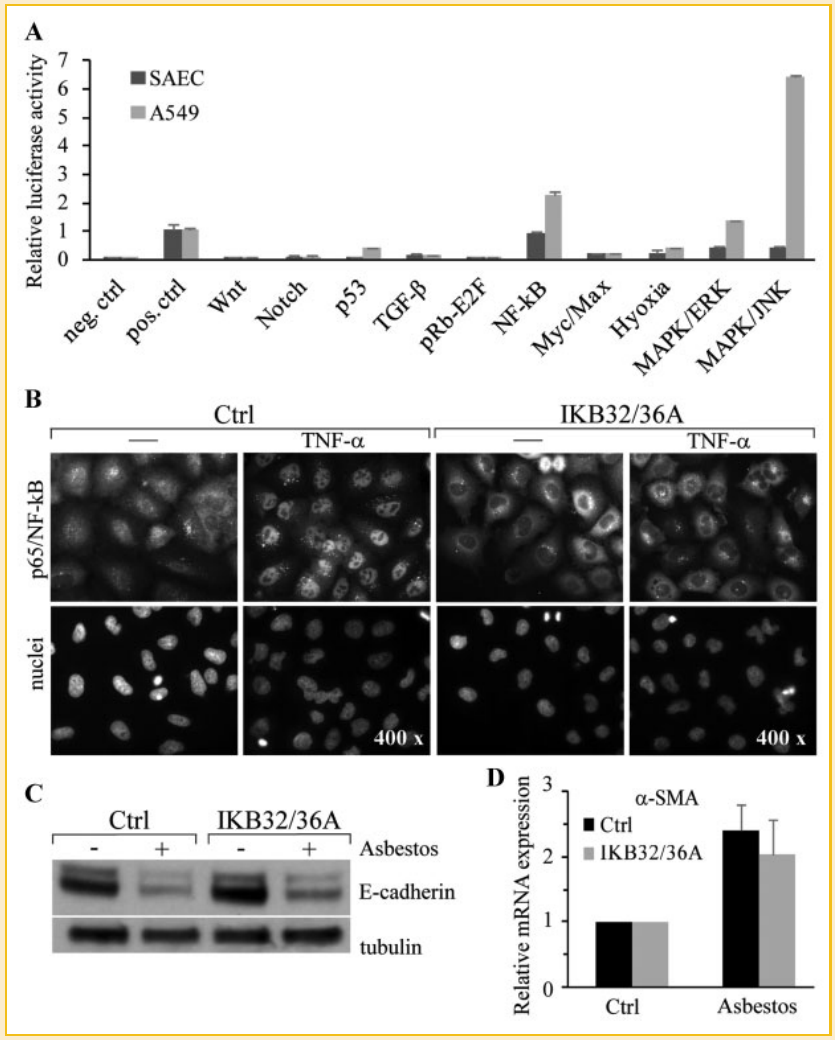

Fig. 6. The activity of MAP-kinases and NF-κB differ between SAECs and A549 cells but blockade of NF-κB pathway in A549 cells does not interfere with E-cadherin downregulation or α-SMA induction by asbestos. A: Basal activities of selected pathways were compared between A549 cells and primary human SAECs using a pathway reporter array. The results are expressed as relative activities and the values are normalized to the positive control. The error bars represent standard deviation of the means (n = 2). B: A549 cells transduced with either control virus or virus containing a dominant negative mutant of IκB (IκB32/36A) were seeded on glass coverslips, exposed to TNF-α (5 ng/ml) for 2 h, fixed and stained with p65 specific antibody to analyze NF-κB nuclear localization. Original magnification is indicated on the right. C: Stably virus transduced A549 cells were exposed to asbestos (5 μg/cm^2) for 3 days and analyzed for E-cadherin protein levels. Tubulin was used as a loading control. D: Stably virus transduced A549 cells were exposed to asbestos for 3 days, total cellular RNA was isolated followed by quantitative RT-PCR analyses using specific primer for α-smooth muscle actin (α-SMA). Expression levels were normalized to the expression levels of TBP and are expressed relative to control. Error bars represent standard deviation of the means (n = 2).

N-terminal kinase/stress-activated protein kinase JNK (SP600125, 10 μM). A549 cells were pre-treated with the inhibitors for 1 h before exposure to asbestos (5 μg/cm^2) under standard culture conditions for 3 days. Immunoblotting analyses suggested that inhibition of MAPK/Erk pathway during the exposure significantly reversed E-cadherin downregulation, while inhibition of MAPK/JNK pathway had no effect (Fig. 7A). Quantification of band intensities (E-cadherin/tubulin) showed statistically significant E-cadherin downregulation by asbestos in control (DMSO)-treated cells, which was reversed by PD98059 (Fig. 7B). Interestingly, PD98059 also

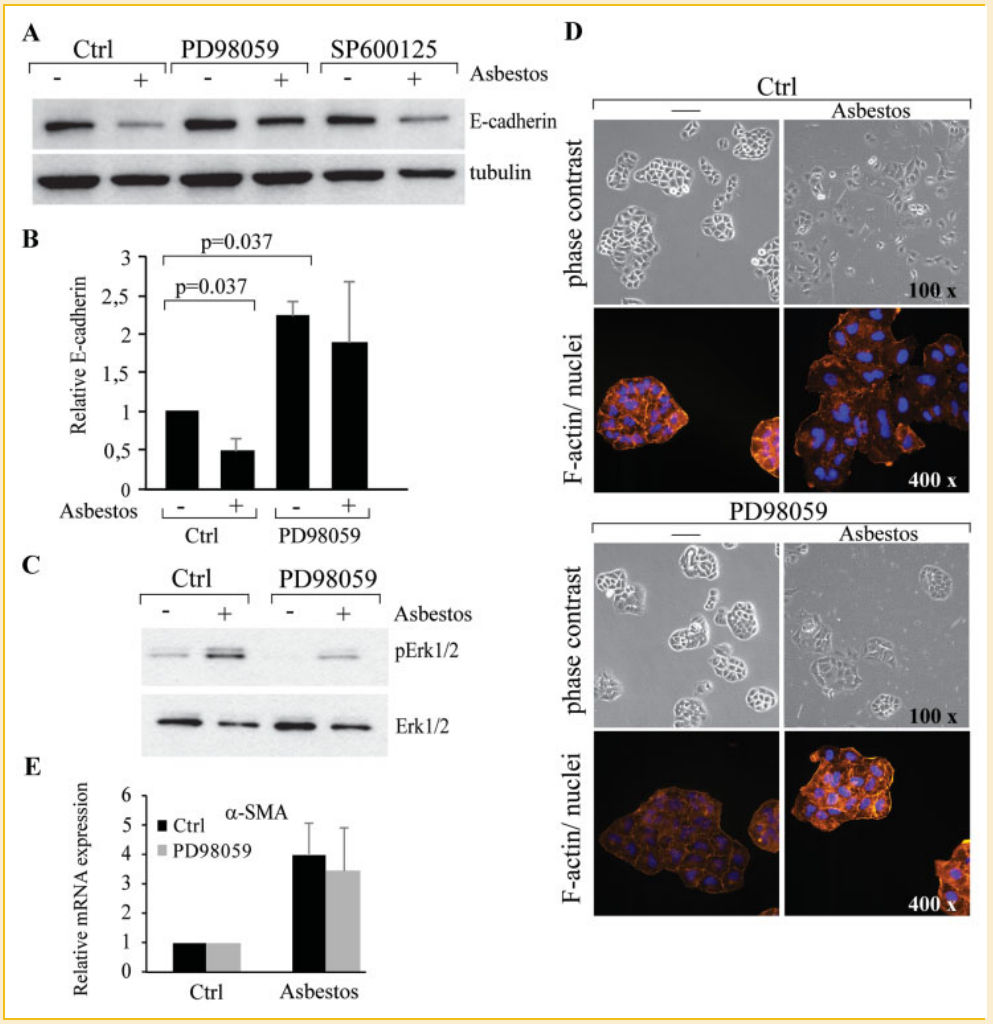

Fig. 7. MAPK/Erk1/2 pathway contributes to asbestos induced loss of epithelial phenotype in A549 cells. A: A549 cells were pre-treated with inhibitors of MAP kinase kinase MEK (PD98059, 30 μM) or JNK (SP600125, 10 μM) or treated with DMSO only (Ctrl) and exposed to asbestos (5 μg/cm^2) for 3 days followed by analyses of E-cadherin protein levels by immunoblotting. Tubulin was used as a loading control. B: E-cadherin band intensities were quantified and normalized to tubulin. The results are expressed relative to control. Error bars represent standard deviation of the means (n = 3). Normalized E-cadherin band intensities differ significantly between the groups (unexposed, asbestos), $P = 0.037$ and (unexposed Ctrl treated, unexposed PD98059 treated), $P = 0.037$. C: A549 cells were pre-treated with PD98059 or DMSO (Ctrl) and exposed to asbestos for 3 days followed by analyses of ERK1/2 phosphorylation, that is, activation or total ERK1/2 levels by immunoblotting. D: A549 cells were seeded on culture plates or on glass coverslips, pre-treated and stimulated as above. Live cells were imaged or the cells were fixed and stained with phalloidin to visualize F-actin. DAPI stain was used to visualize the nuclei. Original magnifications are indicated on the right. E: A549 cells were pre-treated and stimulated as above. Total cellular RNA was isolated followed by quantitative RT-PCR analyses using specific primer for α-smooth muscle actin (α-SMA). Expression levels were normalized to the expression levels of TBP and are expressed relative to control. Error bars represent standard deviation of the means (n = 3).

significantly increased the basal levels of E-cadherin (Fig. 7B) further pointing to a role for MAPK/Erk pathway in the regulation of E-cadherin levels. In agreement, asbestos exposure further enhanced Erk1/2 phosphorylation, which could be reduced to basal levels by the addition of PD98059 (Fig. 7C).

We analyzed next whether the inhibition of MAPK/Erk pathway could also inhibit asbestos-induced morphological alterations in A549 cells. PD98059 pre-treated cells were exposed to asbestos under standard culture conditions for 3 days, fixed and stained with phalloidin to visualize F-actin. Scattering of cells and loss

of cell–cell contacts induced by asbestos were almost completely blocked by the addition of PD98059 (Fig. 7D). However, α-SMA mRNA induction by asbestos exposure was not altered by inhibition of MAPK/Erk activity, suggesting that asbestos-induced mesenchymal gene expression is regulated by other signaling pathways (Fig. 7E).

PRIMARY SMALL AIRWAY EPITHELIAL CELLS RETAIN TYPE II CELL PHENOTYPE IN 3D CULTURES AND DOWNREGULATE E-CADHERIN IN RESPONSE TO ASBESTOS EXPOSURE

Bronchial epithelial cells have been suggested to be less susceptible to EMT than alveolar epithelial cells [Buckley et al., 2010], which may explain our results with monolayer cultures of NHBE and BEAS-2B cells. Furthermore, SAECs in monolayer cultures may spontaneously differentiate and lose alveolar type II cell phenotype, which can influence the sensitivity to EMT. Different interactions between the cells and with the environment in two and in three dimensional cultures are also likely to promote different responses [Schmeichel and Bissell, 2003]. Therefore, we cultured SAEC cells in 3D cultures on Matrigel to investigate the effects of asbestos in 3D environment. Cells seeded on top of Matrigel formed cell aggregates, which in 10 days re-organized into saccular-like structures. Cells facing the lumen were shown to produce surfactant protein D (Fig. 8A) suggesting that in 3D the alveolar type II cell phenotype is retained. These saccular-like structures exhibited abundant E-cadherin staining around the cells (Fig. 8B). Asbestos exposure was initiated on 3-day-old cultures and continued for 1 week. Cell surface E-cadherin levels were significantly decreased in asbestos-treated structures (from ~25% of a total area in saccular structure to ~7,5%; Fig. 8B,C). These results suggest that also normal primary SAEC cells are susceptible to asbestos-induced cell plasticity when cultured in an environment supporting alveolar type II cell phenotype.

DISCUSSION

The development of asbestosis is directly associated with the extent and length of asbestos exposure, but cancer can develop even at low pulmonary concentrations of asbestos fibers [Kamp, 2009]. Asbestos-related or other forms of pulmonary fibrosis, especially IPF, significantly elevate the risk for lung cancer [Kamp, 2009]. Interestingly, Vancheri et al. [2010] have recently suggested that IPF could be considered as a neoproliferative disorder of the lung since there are many similarities between the pathogenic hallmarks of IPF and cancer. Recapitulation of developmental programs such as EMT is one common feature which may play an important role in disease progression [Selman et al., 2008] and the characterization of molecular mechanisms contributing to EMT may provide new

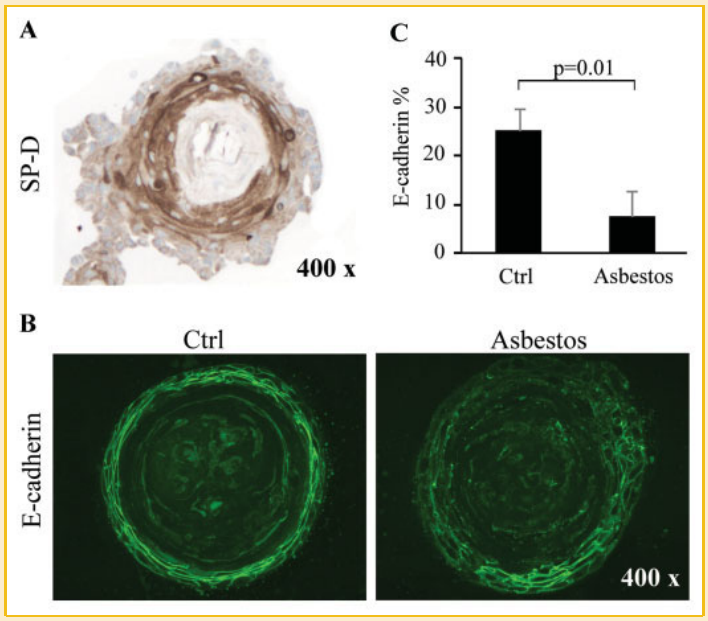

Fig. 8. SAECs retain alveolar type II cell phenotype in three dimensional cultures and downregulate E-cadherin in response to asbestos exposure. Cells were grown on Matrigel basement membrane matrix for 3 days followed by exposure to asbestos (5.0 μg/cm^2) for 1 week. A: Saccular structures were stained with antibodies specific for SP-D. B: Saccular structures were stained with antibodies specific for E-cadherin. Original magnifications are indicated on the right. C: Digital image analysis of the staining intensity of E-cadherin relative to non-stained cellular area in saccular structures. The amount of E-cadherin is expressed as percentage relative to non-stained cellular area. Error bars represent SEM of the samples ($n \geq 6$). E-cadherin positive area differ significantly between the groups (Ctrl, asbestos), $P = 0.01$.

possibilities for prognostic and therapeutic applications. We found here that asbestos exposure can lead to downregulation of epithelial proteins, changes in cell morphology and induction of certain profibrotic genes consistent with the induction of EMT. These molecular alterations may contribute to the progression of asbestos-associated fibrotic and malignant lung diseases.

In the current study, A549 adenocarcinoma cells but not cultured primary small airway or bronchial epithelial cells were induced to undergo EMT by exposure to asbestos or TGF-β under normal 2D culture conditions suggesting that normal cells are not very sensitive to epithelial transitions. This is in agreement with a previous report suggesting that normal mammary epithelial cells are not sensitive to TGF-β mediated EMT unless sensitized by ionizing radiation [Andarawewa et al., 2007]. However, recent studies have described TGF-β induced EMT also in primary human cells [Doerner and Zuraw, 2009; Camara and Jarai, 2010]. Different origin of the cells and differences in culture conditions may explain some of the differences between studies [Buckley et al., 2010]. Intracellular signaling pathways responsible for cell polarity are regulated in significantly different manner in cells depending on whether the cells are cultured in 2D or 3D environment [Schmeichel and Bissell, 2003]. A549 cells cultured on 2D display some features of type II epithelial cells and show cobblestone morphology with cell surface expression of E-cadherin. Primary SAECs, which have not been adapted to monolayer culture, showed abundant levels of E-cadherin but it was mainly localized intracellularly. Furthermore, primary cells rapidly lose the alveolar type II cell phenotype in 2D monolayer cultures. We found that under 3D culture conditions, SAEC cells displayed abundant cell surface E-cadherin, produced surfactant proteins characteristic to type II epithelial cells and were sensitive to asbestos-induced dowregulation of E-cadherin. In conclusion, our results suggest that asbestos can induce epithelial plasticity in both primary cells and A549 cell line displaying type II cell features.

A549 cells provide a tool for the characterization of molecular mechanisms contributing to asbestos pathogenicity in epithelial cells. In the current report, we illustrate a clear asbestos-induced downregulation of epithelial proteins E-cadherin and ZO-1, which is associated with a decrease in cell–cell contacts and a morphological change towards more elongated phenotype characterized by actin reorganization. Asbestos was able to efficiently induce E-cadherin downregulation both in two- and three-dimensional cell culture models. Interestingly, downregulation of E-cadherin protein level was not associated with downregulation of E-cadherin transcription. In agreement with this, only a small and late induction of transcription factors Snail and Slug was detected in asbestos exposed cells. The delayed time and modest nature of Snail and Slug induction by asbestos could be one reason why it was not associated with transcriptional repression of E-cadherin at 6 days. Asbestos-induced late induction of Snail and Slug may, however, become significant during later times and lead to transcriptional repression of E-cadherin. Time points beyond 6 days were, however, not investigated in this study. Transcriptional downregulation of E-cadherin has been suggested to be a late event in EMT [Janda et al., 2002]. However, TGF-β stimulation did result in down-regulation of E-cadherin mRNA levels pointing to different mechanisms of action. Possible mechanisms for asbestos-induced downregulation of E-cadherin are post-translational regulation or proteolytic processing and degradation.

Asbestos containing iron can induce ROS generation, which in turn has been suggested to activate latent forms of TGF-β [Pociask et al., 2004]. Sullivan et al. [2008] propose a model where asbestos elicits TNF-α expression, which leads to increased TGF-β expression by activating MAPK/Erk pathway and that these increased amounts of latent TGF-β are activated by asbestos-induced ROS. We have also previously found that high concentrations of asbestos can induce TGF-β signaling activity in primary human bronchial epithelial cells [Myllärniemi et al., 2008]. Therefore, it was unexpected to find that in A549 cells asbestos did not induce TGF-β signaling activity nor was the downregulation of E-cadherin fully reversed by blocking TGF-β receptor-mediated signaling. Relatively small and late induction of Snail and Slug transcription factors and the profile of mesenchymal gene induction reinforced the notion that asbestos and TGF-β are not likely to share a common mechanism of action at least in A549 lung carcinoma cells. However, it is likely that there exists co-operation between asbestos-induced pathways and TGF-β in in vivo lung.

Analyses of differences in signaling pathway activities between A549 cells and primary SAECs in monolayer cultures highlighted MAPK/JNK, MAPK/Erk, and NF-κB pathway activities. All these pathways have been linked to various EMT-processes, mostly induced by TGF-β [Min et al., 2008; Kalluri and Weinberg, 2009]. Inhibition of MAPK/Erk [Li and Mattingly, 2008] or NF-κB [Huber et al., 2004] prevents EMT in Ras-transformed mammary epithelial cells. A549 cells have homozygous G12S K-Ras, but these cells likely do not depend on Ras for survival [Singh et al., 2009]. As reported earlier [Jiang et al., 2001] blocking NF-κB activity severely impaired the proliferation/survival of A549 cells, but did not appear to interfere with asbestos mediated downregulation of E-cadherin or induction of α-SMA expression. Asbestos can induce NF-κB activity [Nymark et al., 2007], which is likely to play a role in cell survival [Sartore-Bianchi et al., 2007]. However, NF-κB activity did not contribute to asbestos induced EMT-like transition in cell systems used here.

Asbestos is known to induce EGFR activation by direct interaction leading to activation of the MAPK/Erk pathway [Zanella et al., 1996]. In agreement with previous studies, we observed asbestos-mediated induction or Erk1/2 phosphorylation in A549 cells. Inhibition of MAPK/Erk activity clearly prevented asbestos-mediated downregulation of E-cadherin protein levels and restored cell–cell contacts. These results suggest that MAPK/Erk activation plays an important role in asbestos-induced loss of the epithelial phenotype and is in agreement with a previous study showing that MAPK inhibitors were effective in restoring E-cadherin localization to cell–cell junctions in breast epithelial cells with moderate Ras activity without significant effect on E-cadherin expression levels [Li and Mattingly, 2008]. Furthermore, in normal mammary epithelial cells MAPK/Erk activation by ionizing radiation co-operates with TGF-β1 to induce EMT [Andarawewa et al., 2007]. However, a recent article by Ramos et al. [2010] reports reversal of TGF-β1 induced E-cadherin downregulation by co-expression of FGF-1. Particularly, MAPK/Erk activity was shown to contribute

to this FGF-1-mediated inhibitory activity suggesting context-dependent regulation of E-cadherin.

Induction of α-SMA expression by asbestos was not blocked by the inhibition of MAPK/Erk activity. In kidney tubular cells disruption of cell contacts or forced actin polymerization can activate the α-SMA promoter [Fan et al., 2007]. However, in A549 cells restoration of cell–cell contacts by inhibition of MAPK/Erk activity was not able to block α-SMA expression suggesting other mechanism for asbestos-mediated α-SMA expression. We have recently identified GATA-6 transcription factor as an important mediator of TGF-β induced α-SMA expression [Leppäranta et al., 2010]. Although asbestos was not able to induce TGF-β signaling activity in A549 cells, activation of GATA-6 by asbestos through other mechanisms is an interesting possibility.

Induction of EMT is a shared pathogenic mechanism in fibrotic and malignant lung diseases. Here, we reveal the role of asbestos fibers in the initiation of EMT and the importance of the MAPK/Erk pathway in reduced E-cadherin levels and altered cell morphology leading to reduced cell–cell contacts characteristic to a motile phenotype. However, in A549 cells asbestos induced the expression of certain profibrotic genes, but not fibronectin or N-cadherin and induced only slightly the expression of the transcription factors Snail and Slug associated with the transcriptional shift during the progression of EMT. Thus, it is possible that asbestos induces a transitional EMT and/or likely co-operates with other factors activated in diseased lung, such as inflammatory cytokines and growth factors. Our results support the concept of blocking MAPK/Erk signaling as one strategy to develop anti-fibrotic and anti-cancer therapies [Leivonen et al., 2005; Roberts and Der, 2007].

ACKNOWLEDGMENTS

We thank Kaisa Lehti (Research Programs Unit, Genome-Scale Biology, University of Helsinki) for the help with three dimensional cultures as well as Eva Sutinen, Anne Remes and Sami Starast for excellent technical assistance. This work was supported by the Academy of Finland (KK, JK-O, MM), Finnish Cancer Foundation (JK-O), Sigrid Jusélius Foundation (KK, JK-O, MM), Yrjö Jahnsson Foundation (KK), Magnus Ehrnrooth Foundation (KK), Biocentrum Helsinki (JK-O), Helsinki University Hospital Fund (JK-O), University of Helsinki (JK-O), Jalmari and Rauha Ahokas Foundation (KK, MM), Foundation of the Finnish Anti-Tuberculosis Association (KK, MM), and Finnish Cultural Foundation (KK, MH).

REFERENCES

Andarawewa KL, Erickson AC, Chou WS, Costes SV, Gascard P, Mott JD, Bissell MJ, Barcellos-Hoff MH. 2007. Ionizing radiation predisposes nonmalignant human mammary epithelial cells to undergo transforming growth factor β induced epithelial to mesenchymal transition. Cancer Res 67:8662–8670.

Barrallo-Gimeno A, Nieto MA. 2005. The Snail genes as inducers of cell movement and survival: Implications in development and cancer. Development 132:3151–3161.

Brabletz T, Jung A, Reu S, Porzner M, Hlubek F, Kunz-Schughart LA, Knuechel R, Kirchner T. 2001. Variable β-catenin expression in colorectal cancers indicates tumor progression driven by the tumor environment. Proc Natl Acad Sci USA 98:10356–10361.

Buckley ST, Medina C, Ehrhardt C. 2010. Differential susceptibility to epithelial-mesenchymal transition (EMT) of alveolar, bronchial and intestinal epithelial cells in vitro and the effect of angiotensin II receptor inhibition. Cell Tissue Res 342:39–51.

Camara J, Jarai G. 2010. Epithelial-mesenchymal transition in primary human bronchial epithelial cells is Smad-dependent and enhanced by fibronectin and TNF-α. Fibrogenesis Tissue Repair 3:2.

Doerner AM, Zuraw BL. 2009. TGF-β1 induced epithelial to mesenchymal transition (EMT) in human bronchial epithelial cells is enhanced by IL-1β but not abrogated by corticosteroids. Respir Res 10:100.

Fan L, Sebe A, Peterfi Z, Masszi A, Thirone AC, Rotstein OD, Nakano H, McCulloch CA, Szaszi K, Mucsi I, Kapus A. 2007. Cell contact-dependent regulation of epithelial-myofibroblast transition via the rho-rho kinase-phospho-myosin pathway. Mol Biol Cell 18:1083–1097.

Frank AL. 1980. Clinical observations following asbestos exposure. Environ Health Perspect 34:27–30.

Guarino M. 2007. Epithelial-mesenchymal transition and tumour invasion. Int J Biochem Cell Biol 39:2153–2160.

Guarino M, Tosoni A, Nebuloni M. 2009. Direct contribution of epithelium to organ fibrosis: Epithelial-mesenchymal transition. Hum Pathol 40:1365–1376.

Huber MA, Azoitei N, Baumann B, Grunert S, Sommer A, Pehamberger H, Kraut N, Beug H, Wirth T. 2004. NF-κB is essential for epithelial-mesenchymal transition and metastasis in a model of breast cancer progression. J Clin Invest 114:569–581.

Huber MA, Kraut N, Beug H. 2005. Molecular requirements for epithelial-mesenchymal transition during tumor progression. Curr Opin Cell Biol 17:548–558.

Huuskonen MS, Rantanen J. 2006. Finnish Institute of Occupational Health (FIOH): Prevention and detection of asbestos-related diseases, 1987–2005. Am J Ind Med 49:215–220.

Janda E, Lehmann K, Killisch I, Jechlinger M, Herzig M, Downward J, Beug H, Grunert S. 2002. Ras and TGFβ cooperatively regulate epithelial cell plasticity and metastasis: Dissection of Ras signaling pathways. J Cell Biol 156:299–313.

Jiang Y, Cui L, Yie TA, Rom WN, Cheng H, Tchou-Wong KM. 2001. Inhibition of anchorage-independent growth and lung metastasis of A549 lung carcinoma cells by IκBβ. Oncogene 20:2254–2263.

Kalluri R, Weinberg RA. 2009. The basics of epithelial-mesenchymal transition. J Clin Invest 119:1420–1428.

Kamp DW. 2009. Asbestos-induced lung diseases: An update. Transl Res 153:143–152.

Kasai H, Allen JT, Mason RM, Kamimura T, Zhang Z. 2005. TGF-β1 induces human alveolar epithelial to mesenchymal cell transition (EMT). Respir Res 6:56.

Koli K, Myllärniemi M, Vuorinen K, Salmenkivi K, Ryynänen MJ, Kinnula VL, Keski-Oja J. 2006. Bone morphogenetic protein-4 inhibitor gremlin is overexpressed in idiopathic pulmonary fibrosis. Am J Pathol 169:61–71.

Lee H, O'Meara SJ, O'Brien C, Kane R. 2007. The role of gremlin, a BMP antagonist, and epithelial-to-mesenchymal transition in proliferative vitreoretinopathy. Invest Ophthalmol Vis Sci 48:4291–4299.

Leivonen SK, Häkkinen L, Liu D, Kähäri VM. 2005. Smad3 and extracellular signal-regulated kinase 1/2 coordinately mediate transforming growth factor-β-induced expression of connective tissue growth factor in human fibroblasts. J Invest Dermatol 124:1162–1169.

Leppäranta O, Pulkkinen V, Koli K, Vähatalo R, Salmenkivi K, Kinnula VL, Heikinheimo M, Myllärniemi M. 2010. Transcription factor GATA-6 is expressed in quiescent myofibroblasts in idiopathic pulmonary fibrosis. Am J Respir Cell Mol Biol 42:626–632.

Li Q, Mattingly RR. 2008. Restoration of E-cadherin cell-cell junctions requires both expression of E-cadherin and suppression of ERK MAP kinase activation in Ras-transformed breast epithelial cells. Neoplasia 10:1444–1458.

Min C, Eddy SF, Sherr DH, Sonenshein GE. 2008. NF-κB and epithelial to mesenchymal transition of cancer. J Cell Biochem 104:733–744.

Moody SE, Perez D, Pan TC, Sarkisian CJ, Portocarrero CP, Sterner CJ, Notorfrancesco KL, Cardiff RD, Chodosh LA. 2005. The transcriptional repressor Snail promotes mammary tumor recurrence. Cancer Cell 8:197–209.

Mossman BT, Churg A. 1998. Mechanisms in the pathogenesis of asbestosis and silicosis. Am J Respir Crit Care Med 157:1666–1680.

Mossman BT, Marsh JP. 1989. Evidence supporting a role for active oxygen species in asbestos-induced toxicity and lung disease. Environ Health Perspect 81:91–94.

Mossman BT, Bignon J, Corn M, Seaton A, Gee JB. 1990. Asbestos: Scientific developments and implications for public policy. Science 247:294–301.

Myllärniemi M, Lindholm P, Ryynänen MJ, Kliment CR, Salmenkivi K, Keski-Oja J, Kinnula VL, Oury TD, Koli K. 2008. Gremlin-mediated decrease in bone morphogenetic protein signaling promotes pulmonary fibrosis. Am J Respir Crit Care Med 177:321–329.

Nakao A, Imamura T, Souchelnytskyi S, Kawabata M, Ishisaki A, Oeda E, Tamaki K, Hanai J, Heldin CH, Miyazono K, ten Dijke P. 1997. TGF-β receptor-mediated signalling through Smad2, Smad3 and Smad4. EMBO J 16:5353–5362.

Nymark P, Lindholm PM, Korpela MV, Lahti L, Ruosaari S, Kaski S, Hollmen J, Anttila S, Kinnula VL, Knuutila S. 2007. Gene expression profiles in asbestos-exposed epithelial and mesothelial lung cell lines. BMC Genomics 8:62.

Ory DS, Neugeboren BA, Mulligan RC. 1996. A stable human-derived packaging cell line for production of high titer retrovirus/vesicular stomatitis virus G pseudotypes. Proc Natl Acad Sci USA 93:11400–11416.

Peinado H, Portillo F, Cano A. 2004. Transcriptional regulation of cadherins during development and carcinogenesis. Int J Dev Biol 48:365–375.

Pociask DA, Sime PJ, Brody AR. 2004. Asbestos-derived reactive oxygen species activate TGF-β1. Lab Invest 84:1013–1023.

Ramos C, Becerril C, Montano M, Garcia-De-Alba C, Ramirez R, Checa M, Pardo A, Selman M. 2010. FGF-1 reverts epithelial-mesenchymal transition induced by TGF-β1 through MAPK/ERK kinase pathway. Am J Physiol Lung Cell Mol Physiol 299:L222–L231.

Roberts PJ, Der CJ. 2007. Targeting the Raf-MEK-ERK mitogen-activated protein kinase cascade for the treatment of cancer. Oncogene 26:3291–3310.

Robledo R, Mossman B. 1999. Cellular and molecular mechanisms of asbestos-induced fibrosis. J Cell Physiol 180:158–166.

Roggli VL, Sanders LL. 2000. Asbestos content of lung tissue and carcinoma of the lung: A clinicopathologic correlation and mineral fiber analysis of 234 cases. Ann Occup Hyg 44:109–117.

Sartore-Bianchi A, Gasparri F, Galvani A, Nici L, Darnowski JW, Barbone D, Fennell DA, Gaudino G, Porta C, Mutti L. 2007. Bortezomib inhibits nuclear factor-κB dependent survival and has potent in vivo activity in mesothelioma. Clin Cancer Res 13:5942–5951.

Schmeichel KL, Bissell MJ. 2003. Modeling tissue-specific signaling and organ function in three dimensions. J Cell Sci 116:2377–2388.

Selman M, Pardo A, Kaminski N. 2008. Idiopathic pulmonary fibrosis: Aberrant recapitulation of developmental programs? PLoS Med 5:e62.

Shukla A, Gulumian M, Hei TK, Kamp D, Rahman Q, Mossman BT. 2003. Multiple roles of oxidants in the pathogenesis of asbestos-induced diseases. Free Radic Biol Med 34:1117–1129.

Singh A, Greninger P, Rhodes D, Koopman L, Violette S, Bardeesy N, Settleman J. 2009. A gene expression signature associated with "K-Ras addiction" reveals regulators of EMT and tumor cell survival. Cancer Cell 15:489–500.

Sullivan DE, Ferris M, Pociask D, Brody AR. 2008. The latent form of TGFβ(1) is induced by TNFα through an ERK specific pathway and is activated by asbestos-derived reactive oxygen species in vitro and in vivo. J Immunotoxicol 5:145–149.

Thiery JP. 2002. Epithelial-mesenchymal transitions in tumour progression. Nat Rev Cancer 2:442–454.

Thiery JP, Sleeman JP. 2006. Complex networks orchestrate epithelial-mesenchymal transitions. Nat Rev Mol Cell Biol 7:131–142.

Traenckner EB, Pahl HL, Henkel T, Schmidt KN, Wilk S, Baeuerle PA. 1995. Phosphorylation of human IκB-α on serines 32 and 36 controls Iκ B-α proteolysis and NF-κ B activation in response to diverse stimuli. EMBO J 14:2876–2883.

Vancheri C, Failla M, Crimi N, Raghu G. 2010. Idiopathic pulmonary fibrosis: A disease with similarities and links to cancer biology. Eur Respir J 35:496–504.

Willis BC, Borok Z. 2007. TGF-β-induced EMT: Mechanisms and implications for fibrotic lung disease. Am J Physiol Lung Cell Mol Physiol 293:L525–L534.

Yin Q, Brody AR, Sullivan DE. 2007. Laser capture microdissection reveals dose-response of gene expression in situ consequent to asbestos exposure. Int J Exp Pathol 88:415–425.

Zanella CL, Posada J, Tritton TR, Mossman BT. 1996. Asbestos causes stimulation of the extracellular signal-regulated kinase 1 mitogen-activated protein kinase cascade after phosphorylation of the epidermal growth factor receptor. Cancer Res 56:5334–5338.

Zhong Q, Zhou B, Ann DK, Minoo P, Liu Y, Banfalvi A, Krishnaveni MS, Dubourd M, Demaio L, Willis BC, Kim KJ, duBois RM, Crandall ED, Beers MF, Borok Z. 2011. Role of endoplasmic reticulum stress in epithelial-mesenchymal transition of alveolar epithelial cells: Effects of misfolded surfactant protein. Am J Respir Cell Mol Biol 45:498–509.

SUPPLEMENTARY DATA

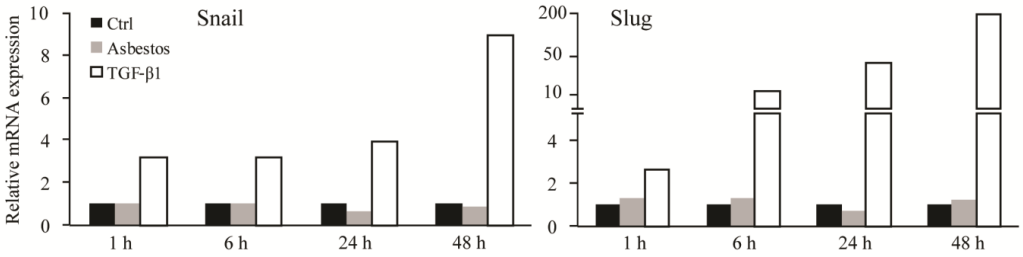

Figure 1. Asbestos fails to induce Snail or Slug expression during early exposure times. Total cellular RNA was isolated at the indicated time points after asbestos (5 µg/cm²) or TGF-β1 (2 ng/ml) exposure followed by quantitative RT-PCR analyses using specific primers for Snail and Slug. The mRNA expression levels were normalized to the expression levels of TBP and are expressed relative to control.

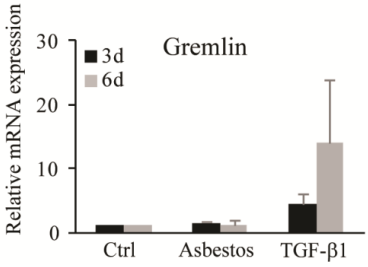

Figure 2. Asbestos fails to induce gremlin expression. Total cellular RNA was isolated at the indicated time points after asbestos (5 µg/cm²) or TGF-β1 (2 ng/ml) exposure followed by quantitative RT-PCR analyses using specific primer for gremlin 1. The mRNA expression levels were normalized to the expression levels of TBP and are expressed relative to control (n=2).

II

OPEN

Citation: Oncogenesis (2013) **2**, e66; doi:10.1038/oncsis.2013.29

www.nature.com/oncsis

ORIGINAL ARTICLE

Gremlin-1 associates with fibrillin microfibrils *in vivo* and regulates mesothelioma cell survival through transcription factor slug

JA Tamminen[1,2], V Parviainen[2], M Rönty[3,4], AP Wohl[5], L Murray[1,2], S Joenväärä[2], M Varjosalo[6], O Leppäranta[7], O Ritvos[3,8], G Sengle[5], R Renkonen[2,3], M Myllärniemi[7] and K Koli[1,2]

Malignant mesothelioma is a form of cancer that is highly resistant to conventional cancer therapy for which no major therapeutic advances have been introduced. Here, we identify gremlin-1, a known bone morphogenetic protein inhibitor crucial for embryonic development, as a potential therapeutic target for mesothelioma. We found high expression levels of gremlin-1 in the mesothelioma tumor tissue, as well as in primary mesothelioma cells cultured from pleural effusion samples. Downregulation of gremlin-1 expression by siRNA-mediated silencing in a mesothelioma cell line inhibited cell proliferation. This was associated with downregulation of the transcription factor slug as well as mesenchymal proteins linked to cancer epithelial-to-mesenchymal transition. Further, resistance to paclitaxel-induced cell death was associated with high gremlin-1 and slug expression. Treatment of gremlin-1-silenced mesothelioma cells with paclitaxel or pemetrexed resulted in efficient loss of cell survival. Finally, our data suggest that concomitant upregulation of fibrillin-2 in mesothelioma provides a mechanism for extracellular localization of gremlin-1 to the tumor microenvironment. This was supported by the demonstration of interactions between gremlin-1, and fibrillin-1 and -2 peptides as well as by colocalization of gremlin-1 to fibrillin microfibrils in cells and tumor tissue samples. Our data suggest that gremlin-1 is also a potential target for overcoming drug resistance in mesothelioma.

Oncogenesis (2013) **2,** e66; doi:10.1038/oncsis.2013.29; published online 26 August 2013

Subject Categories: Molecular oncology

Keywords: gremlin; fibrillin; mesothelioma; EMT; slug

INTRODUCTION

Malignant mesothelioma is an aggressive tumor, which originates from the mesothelial surface cells lining the serous body cavities such as the pleura, peritoneum or pericardium.[1] Mesothelioma is strongly linked to asbestos exposure, and it may take several decades to develop after initial exposure.[2] Because of the long latency, the incidence of mesothelioma will increase in the near future worldwide.[3,4] Mesothelioma is resistant to chemo- and radiotherapy, leading to poor prognosis for patients suffering from this malignancy.[4] New markers for screening and monitoring the disease and in particular new drug targets are needed.

Cancer progression is associated with a re-expression of developmental programs, which contribute to the proliferative and invasive properties of tumor cells.[5,6] Gremlin-1 is a cysteine knot protein, which belongs to the DAN family of bone morphogenetic protein (BMP) antagonists. Gremlin-1 can bind to and inhibit the functions of BMP-2, -4 and -7.[7,8] These three BMP isoforms are targeted to fibrillin microfibrils, suggesting extracellular regulation of bioavailability.[9] Gremlin-1-mediated BMP antagonism is crucial for mouse lung and kidney development.[10] In adult mouse and human tissues gremlin-1 expression is low. Originally, gremlin-1 was identified as a gene downregulated in *v-mos*-transformed fibroblasts and therefore called Drm.[11] However, recent studies suggest the overexpression of gremlin-1 in epithelial cancers including lung carcinomas.[12,13]

The role of gremlin-1 in cancer has remained largely unclear. As our preliminary results suggested an upregulation of gremlin in mesothelioma tissue, we set out to find molecular interactions of gremlin and study the biological function of gremlin in mesothelioma.

RESULTS

Gremlin-1 interacts with fibrillin-1 and -2

A search for new gremlin interacting proteins was carried out using systematic affinity purification coupled with mass spectrometry identification (AP-MS). We used the well-characterized Flip-In-HEK293 cell system to produce C-terminally tagged gremlin-1 and a standardized workflow for the purification of protein complexes from cell lysates[14] (Figure 1a). A low tetracycline concentration (25 ng/ml) was selected for gremlin-1 induction (Figure 1b). Immunoblotting analyses after different affinity purification steps suggested that gremlin was well recovered (Figure 1c).

In order to characterize the interactome of gremlin-1, immunopurified proteins were identified using mass spectrometry. Proteins

[1]Research Programs Unit, Translational Cancer Biology, University of Helsinki, Helsinki, Finland; [2]Transplantation Laboratory, Haartman Institute, University of Helsinki, Helsinki, Finland; [3]Helsinki University Central Hospital and Hospital Laboratory, Helsinki, Finland; [4]Department of Pathology, University of Helsinki, Helsinki, Finland; [5]Center for Biochemistry, Medical Faculty, University of Cologne, Cologne, Germany; [6]Institute of Biotechnology, University of Helsinki, Helsinki, Finland; [7]Division of Pulmonary Medicine, Department of Medicine, University of Helsinki, Helsinki, Finland and [8]Department of Bacteriology and Immunology, University of Helsinki, Helsinki, Finland. Correspondence: Dr K Koli, University of Helsinki, Biomedicum/B502a1, PO Box 63, Haartmaninkatu 8, Helsinki 00014, Finland.
E-mail: katri.koli@helsinki.fi
Received 10 July 2013; accepted 16 July 2013

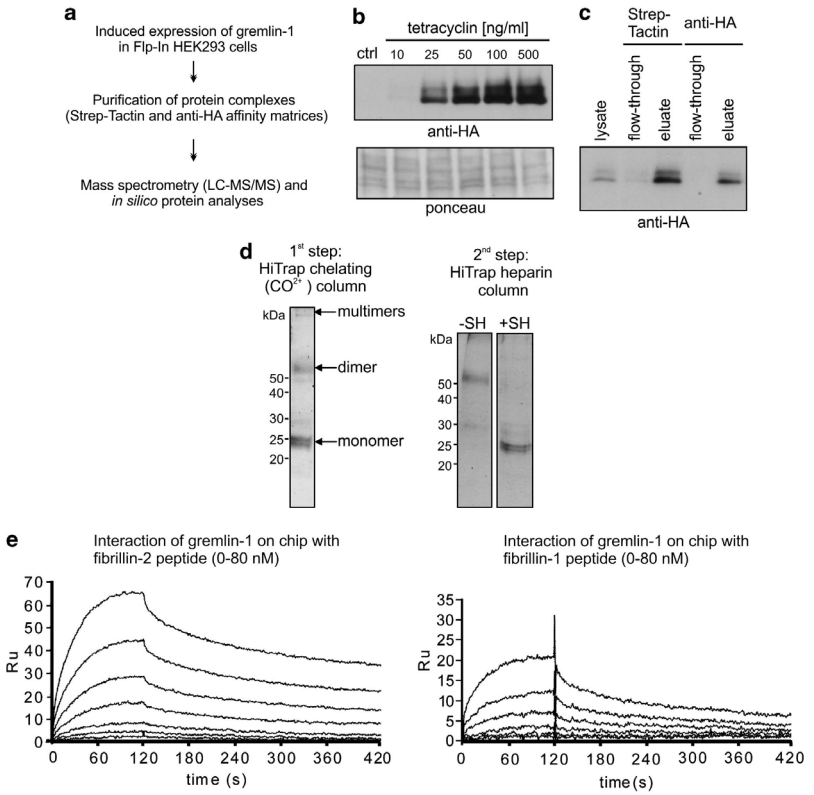

Figure 1. Gremlin-1 interacts with fibrillin-1 and -2. (**a**) Gremlin-1 protein interaction screen outline. (**b**) Flip-In HEK293/gremlin-1 cells were treated with increasing concentrations of tetracycline for 24 h followed by immunoblotting analyses using anti-HA antibodies. Ponceau staining of proteins indicates equal loading. (**c**) Immunoblotting analyses of gremlin-1, using anti-HA antibodies, after Strep-tactin and anti-HA affinity purification steps. (**d**) Purification of gremlin-1 from conditioned media of stably transfected HEK293 cells. After elution from a $CoCl_2$-loaded HiTrap column using a C-terminally placed His_6-affinity-tag protein, bands corresponding to monomeric, dimeric and multimeric gremlin-1 were detected via SDS–PAGE followed by Coomassie staining. A subsequent second purification step via a HiTrap heparin column yielded mostly dimeric gremlin-1, which shifted to the position of monomeric gremlin under reducing conditions (+SH). (**e**) Interaction studies between gremlin-1 and N-terminal peptides of fibrillin-1 and -2 using a surface plasmon resonance technology. Gremlin-1 was immobilized on a sensor chip and fibrillin-1 and -2 peptides in a concentration range from 80 to 0 nM were flown over as analytes. Affinity constants (K_d) for both interactions were about 10 nM (Table 1), indicating a high affinity interaction between gremlin-1 and the main building blocks of fibrillin microfibrils.

were first digested using trypsin and then fractionated with reverse-phase chromatography online using a mass spectrometer. The resulting peptide spectra were identified with two different search engines. A total of 12 proteins were identified to interact with gremlin-1 in three replicate experiments and with both search engines. The interaction data were filtered using a protein list (data not shown) of 377 unspecific binding proteins acquired using Flip-In-HEK293 cell line transfected with the affinity tag containing plasmid. The final filtered list contained four proteins: cytokeratin-9 (Swiss-Prot: P35527), fibrillin-2 (Swiss-Prot: P35556), cytokeratin-2a (Swiss-Prot: P35908) and APOBEC1-binding protein 2 (Swiss-Prot: Q9UBS4). Fibrillin-2 was identified in all three replicate experiments and with both search engines, which improves the confidence of the identification. In addition, fibrillin-2 was identified with up to three distinct and good scoring peptides in two of the replicates further validating the interaction of fibrillin-2 and gremlin-1. Fibrillins are constituents of extracellular microfibrils and have a role in elastin assembly.[15] They also sequester and regulate the bioavailability of growth factors such as BMP isoforms.[9]

Table 1. Surface plasmon resonance affinity data for tested interactions between gremlin-1 and fibrillin-1 and -2 N-terminal peptides

Interaction (ligand/analyte)	k_{on} *(1/M*s)/*k_{off} *(1/s)*	K_d *(nM)*
gremlin-1 dimer/ fibrillin-2 (rF86)	2.41×10^5/ 2.18×10^{-3}	9.05
gremlin-1 dimer/ fibrillin-1 (rF11)	1.92×10^5/ 1.45×10^{-3}	7.55

In order to confirm our findings, we tested direct interactions between purified gremlin-1 and recombinant N-terminal peptides of fibrillin-1 and -2 in protein–protein interaction assays using surface plasmon resonance technology. When purified gremlin-1 (Figure 1d) was used as a ligand immobilized on the sensor chip surface and N-terminal fibrillin were flown over as analytes direct interactions with molecular affinities in the low nanomolar range (Table 1) could be measured (Figure 1e). This suggests a high

molecular interaction between gremlin-1 and the two main building blocks of fibrillin microfibrils.

Gremlin-1 and fibrillin-2 are overexpressed in the mesothelioma tumor tissue and colocalize *in vivo*

To analyze whether gremlin-1 and fibrillins are coexpressed *in vivo*, tissue biopsies from mesothelioma patients included in this study were stained with specific antibodies. We had previously shown low levels of gremlin expression in the normal lung.[16] Here, we detected low expression of gremlin in normal mesothelial cells (Figure 2a). Gremlin-1 staining was, however, detected in non-malignant, reactive mesothelial cells in control samples (pneumothorax). Intense gremlin-1 immunoreactivity was observed in all mesothelioma samples ($n = 6$). Fibrillin-2 immunoreactivity was shown in a strikingly similar staining pattern as observed for gremlin-1 in these tumor samples, suggesting concomitant upregulation of these developmental genes in mesothelioma. Some fibrillin-2 staining was detectable also in non-malignant reactive mesothelium. Calretinin and WT1 (Wilm's tumor 1) are diagnostic markers for mesothelioma and were used here to identify the tumor tissue. Analyses of serial tissue sections suggested that gremlin-1 and fibrillin-2 staining localizes to calretinin-positive and -negative tumor areas (Figure 2b). Some WT-1 positivity, however, was observed in calretinin-negative areas, which represent sarcomatoid part of the tumor with more diffuse growth properties. Fibrillin-1 staining was negative in 5/6 mesothelioma and in control pleura samples. Only one mesothelioma sample showed fibrillin-1 immunoreactivity, which was specifically detected in stromal-like areas (not shown).

We analyzed colocalization of gremlin-1 with fibrillin-2 in tumor tissue using the proximity ligation assay. Intensive colocalization signals were observed for gremlin-1 and fibrillin-2 throughout the tumor tissues, suggesting that they localize to similar structures *in vivo* (Figure 3).

Primary human mesothelioma cells express high levels of gremlin-1 and fibrillin-2

Primary cells were cultured from mesothelioma patients' pleural effusion samples (JP1-5). Cells were characterized by immunofluorescence staining using mesothelial markers calretinin and cytokeratin (CK)-7 as well as vimentin, which is commonly expressed by tumor cells. Majority of the cells were calretinin- and/or CK-7 positive and stained also for vimentin (Figure 4a). This suggests that the cells, which were able to proliferate, were mainly primary tumor cells. Gremlin-1 mRNA expression levels were high in these primary cells compared with Met5A cells, which are immortalized but non-tumorigenic mesothelial cells (Figure 4b). Further, the mRNA expression levels of fibrillin-1 and -2 were high in these cells (Figure 4b). The results show that primary mesothelioma cells can be cultured from pleural effusion samples and that the cells retain the phenotypic expression of these developmental genes.

Gremlin-1 is known to inhibit the functions of BMP-2, -4 and to some extent also BMP-7.[7,8] Therefore, the expression levels of these BMP isoforms were analyzed in primary mesothelioma cells.

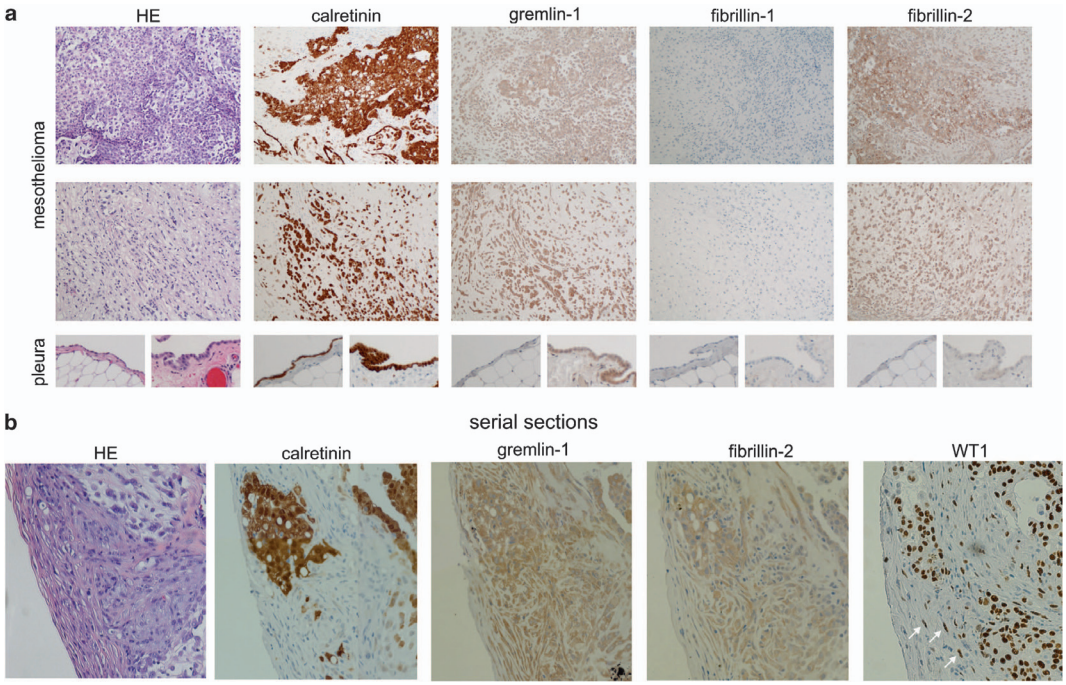

Figure 2. Overexpression of gremlin-1 and fibrillin-2 in mesothelioma. (**a**) Immunohistochemical staining of mesothelioma and control pleura samples using calretinin, gremlin-1, fibrillin-1 and fibrillin-2 antibodies. Hematoxylin and eosin (HE) staining is shown on the left. Abundant gremlin-1 and fibrillin-2 immunoreactivity is observed in both calretinin-negative and -positive tumor areas. Normal mesothelium (pleura, left panel) shows very low levels of staining, whereas reactive normal mesothelium (pleura, right panel) shows faint fibrillin-2 and moderate gremlin-1 staining. (**b**) Immunohistochemical staining of serial mesothelioma sections suggests similar staining patterns for gremlin-1 and fibrillin-2. Staining was observed also in calretinin-negative stromal-like areas, which contained isolated Wilms' tumor protein (WT1)-positive tumor cells (white arrows).

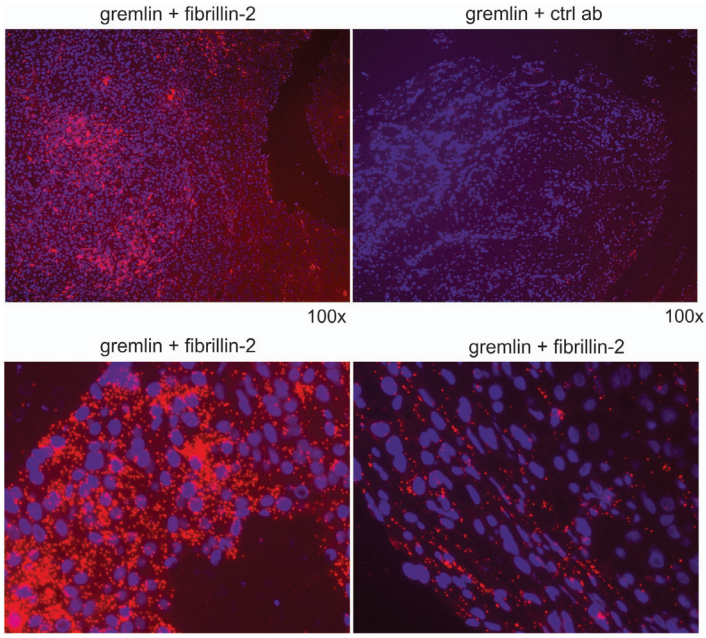

Figure 3. Colocalization analyses of gremlin-1 with fibrillin-2 in mesothelioma tumor tissue. Proximity ligation assay was used to detect colocalization of gremlin-1 with fibrillin-2 in mesothelioma tumor tissue. Positive colocalization signals (red dots) were abundant throughout the tumor tissue. Negative control with gremlin antibody plus mouse isotype control is shown on the upper right panel.

Interestingly, abundant expression of BMP-2 was observed (Figure 4b), whereas BMP-4 levels were comparable and BMP-7 levels only slightly higher compared with Met5A cells (not shown).

The expression patterns of gremlin-1, fibrillins and BMP-2 were also analyzed in four established mesothelioma cell lines (211H, H28, H2452 and H2052). Only one of these cell lines, H2052, resembled primary mesothelioma cells and expressed high levels of gremlin-1, fibrillin-2 and BMP-2 (Figure 4c). Therefore, this cell line was chosen for further mechanistic studies.

Gremlin-1 associates with fibrillin-1 in cultured mesothelioma cells

Mesothelioma cells were cultured for 1 week and then analyzed by immunofluorescence staining using antibodies specific for gremlin-1 or fibrillins. Although expressed at the mRNA level, fibrillin-2 protein was not detected in any of the cultured mesothelioma cells analyzed at this time point (not shown), which may reflect late extracellular matrix (ECM) deposition *in vitro*. Primary mesothelioma cells and H2052 cells *in vitro* also expressed fibrillin-1 mRNA, and this was reflected in the staining pattern showing fibrillar staining for fibrillin-1 and gremlin-1 (Figure 5a). No staining was observed in H2452 cells. Double immunofluorescence labeling suggested colocalization and targeting of gremlin-1 into fibrillin-1 containing microfibrils *in vitro*. H2052 cells transfected with fibrillin-1-specific siRNA showed reduced mRNA expression levels (Figure 5b) and significantly reduced fibrillin-1 staining, indicating efficient silencing of protein expression (Figure 5c). This led to reduced deposition of gremlin into fibrillar structures suggesting that extracellular targeting of gremlin is dependent on fibrillins.

Gremlin-1 silencing severely impairs mesothelioma cell growth and survival

To investigate the role of gremlin-1 in mesothelioma cell growth, H2052 cells were transfected with gremlin-specific siRNAs. Efficient silencing of gremlin-1 expression was observed at mRNA and protein levels (Figures 6a and b). Cell proliferation was assayed by counting cells 1–5 days after transfection. Two independent siRNAs targeted against gremlin-1 were observed to significantly decrease the number of cells at all time points (Figure 6c). This suggests that H2052 cell proliferation is dependent on gremlin expression.

To determine whether lack of gremlin induces apoptosis, H2052 cells were cultured on coverslips, transfected with siRNAs and analyzed with TUNEL assay 3 days after transfection (Figure 6d). Hardly any TUNEL-positive cells were detected in control or gremlin siRNA-transfected cells. DAPI staining also showed intact nuclei in both groups. These results suggest that although lack of gremlin impaired cell proliferation, it did not induce apoptosis.

Cellular signaling pathway activities are altered in gremlin-1-silenced cells

Changes in BMP signaling activity were analyzed. Gremlin-1 silencing increased BMP-dependent reporter activity in H2052 cells (Figure 7a) as well as the expression of a BMP target gene *Id1* (inhibitor of differentiation/DNA binding 1, Figure 7b), suggesting that endogenous gremlin-1 regulates BMP activity negatively. Further, Id1 expression was found significantly reduced in primary mesothelioma cells compared with Met5A cells (Figure 7c).

To further investigate cellular signaling pathways regulated by gremlin, we analyzed alteration in phospho-kinase levels using a commercial array (see Materials and methods). H2052 cells were found to have high basal level of phospho-Akt (S473), which was not altered in gremlin-1-silenced cells (Figures 7d–f). However, phosphorylation of the Akt substrate and regulator of mTOR signaling, PRAS40 (T246), was increased. Erk1/2 phosphorylation was also significantly increased in gremlin-1-silenced cells (g). Further, increased levels of p53 phosphorylation (S46 and S392)

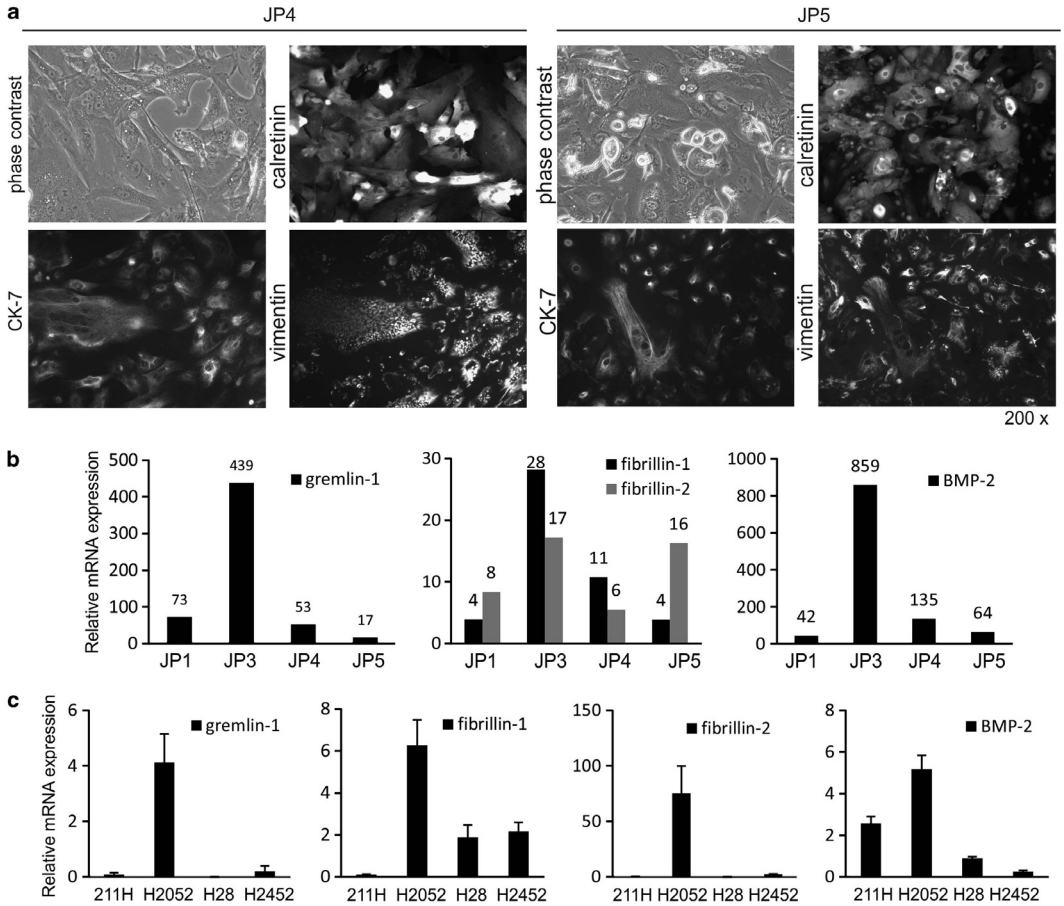

Figure 4. Primary mesothelioma cells express high levels of gremlin-1. Primary mesothelioma cells (JP cells) were isolated from pleural effusion samples. (**a**) Immunofluorescence staining suggests that the cells were positive for the mesothelial marker calretinin. Co-staining with cytokeratine (CK)-7 and vimentin antibodies suggests that the tumor cells co-express these marker proteins. (**b**) Primary mesothelioma cells were analyzed for gremlin-1, fibrillin-1 and -2 and BMP-2 mRNA expression by quantitative RT–PCR. The levels were normalized to the expression levels of TATA-binding protein and are expressed relative to the expression levels in Met5A cells (immortalized, non-tumorigenic mesothelial cells), which were set to 1. (**c**) Established mesothelioma cell lines were analyzed for gremlin-1, fibrillin-1 and -2 and BMP-2 mRNA expression by quantitative RT–PCR. The error bars represent s.d. ($n = 2$).

were reflected in increased mRNA expression levels of p21 (Cip1/Waf1) in H2052 cells (Figure 7h). In agreement, overexpression of gremlin-1 in H2052 and H28 cells decreased p21 expression levels (Figure 7i).

Gremlin-1 expression is associated with EMT phenotype and chemoresistance

Gremlin-1 expression has been linked to EMT processes. Therefore, we determined whether mesothelioma cells with high gremlin levels express transcription factors snail and slug, which are transcriptional repressors of E-cadherin and induce EMT.[17] Whereas the mRNA expression levels of snail were comparable in mesothelioma cells and Met5A cells, slug expression levels were high in primary mesothelioma cells (Figure 8a). Slug expression in mesothelioma tumor samples was analyzed using immunohistochemical staining (Figures 8b and c). All of the analyzed tumor samples ($n = 6$) were positive for slug. Mesothelioma tumors exhibited mostly diffuse and granular cytoplasmic staining, but also nuclear staining was detected in certain tumor areas. Slug staining localized to gremlin-positive areas and was detected also in calretinin-negative areas.

Similar to primary mesothelioma cells H2052 cells, which express high levels of gremlin-1, exhibited high slug expression (Figure 8d). Conversely, Met5A and H2452 cells showed very low levels of slug mRNA expression consistent with low gremlin-1 expression levels. Slug protein levels also showed a dramatic difference between H2052 and H2452 cells (Figure 8d). Silencing of gremlin-1 by siRNA transfection significantly reduced slug mRNA and protein expressions in H2052 cells (Figure 8e and i). Similar results were also obtained with primary mesothelioma cells (Figure 8f). Further, overexpression of gremlin-1 in H28 cells led to increased slug mRNA expression (Figure 8g). The mRNA and especially protein expression levels of mesenchymal proteins, N-cadherin, vimentin and α-smooth muscle actin were significantly downregulated in gremlin-1-silenced H2052 cells (Figures

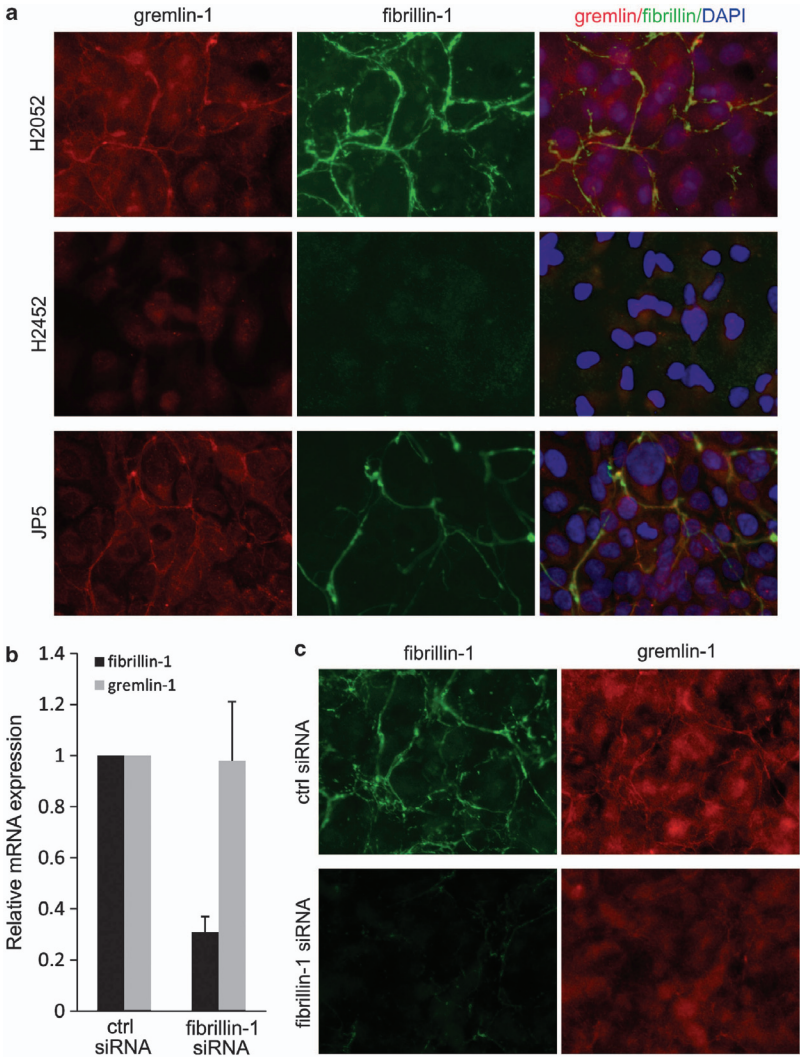

Figure 5. Gremlin-1 and fibrillin-1 co-localize in mesothelioma cell ECM *in vitro*. (**a**) Mesothelioma cell lines (H2052 and H2452) and primary mesothelioma cells (JP5) were co-stained for gremlin-1 and fibrillin-1 and analyzed using immunofluorescence microscopy. A fibrillar staining pattern was observed in H2052 and JP5 cells. (**b**) In control (ctrl) and fibrillin-1 siRNA-transfected H2052 cells, the mRNA expression levels of gremlin-1 and fibrillin-1 were analyzed by quantitative RT-PCR. The levels were normalized to the expression levels of TATA-binding protein and are expressed relative to each control, which was set to 1. The error bars represent s.d. ($n = 2$). (**c**) Double-immunofluorescence staining of siRNA-treated H2052 cells with gremlin-1 and fibrillin-1 antibodies. Note the lack of fibrillar gremlin-1 staining in fibrillin-1-silenced cells.

8h and i). Fibrillin-1 and -2 mRNA expression levels were also significantly reduced (Figure 8h), suggesting that gremlin-1 maintains the expression of microfibrillar genes. Further, fibronectin expression was downregulated (Figure 8h), and the epithelial marker E-cadherin was upregulated (Figure 8j). These results suggest that EMT-related alterations are reversed in gremlin-1-silenced cells.

Slug expression and EMT-phenotype are also associated with tumor chemoresistance.[18–21] The importance of high gremlin and slug expression to sensitivity to paclitaxel-mediated mesothelioma cell death was analyzed using the MTT proliferation/viability assay. H2052 cells, which express high levels of gremlin-1 and slug, were found more resistant to paclitaxel than H2452 cells (Figure 8k). Next, control and gremlin-1 siRNA-transfected H2052 cells were treated with paclitaxel or pemetrexed, and cell numbers were quantified 3 days after transfection. Treatment with paclitaxel or pemetrexed in combination with gremlin-1 siRNA led to efficient cell death (Figure 8l).

DISCUSSION

Gremlin-1-mediated inhibition of BMP-signaling is important for normal development. Mice lacking gremlin-1 die before birth because of severe defects in kidney and lung development.[10] In

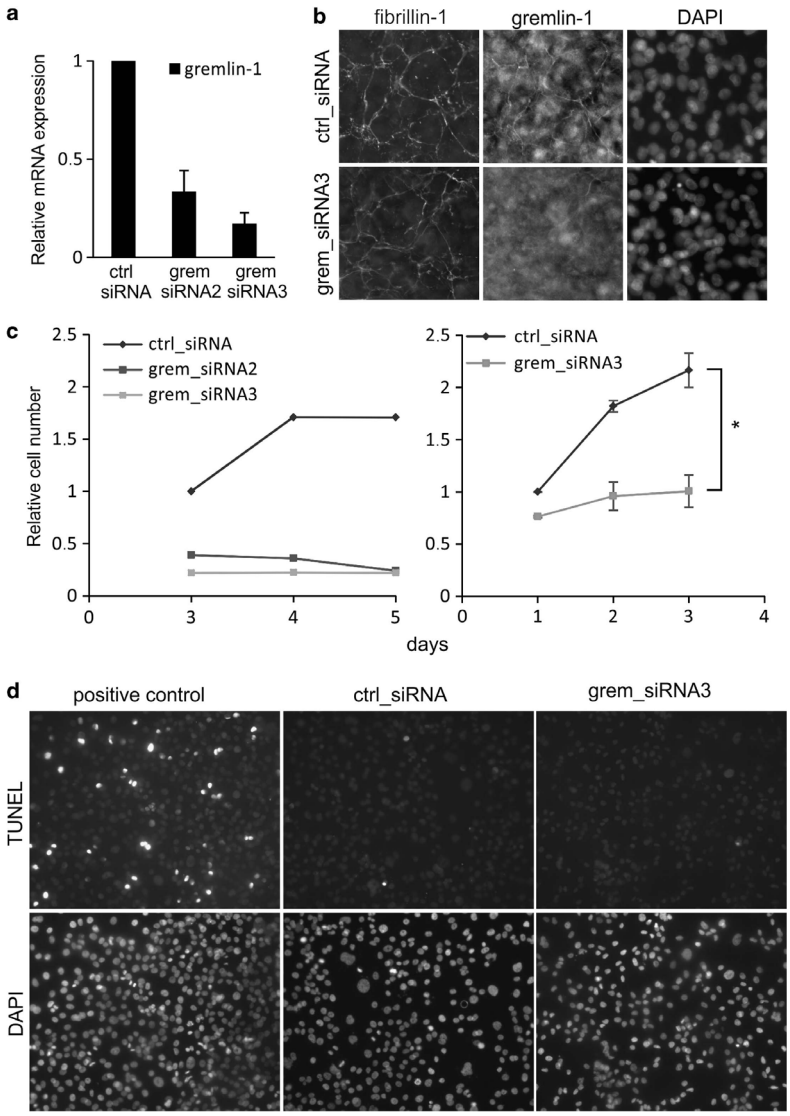

Figure 6. Gremlin-1 silencing impairs H2052 mesothelioma cell proliferation. (**a**) The efficiency of gremlin-1 siRNA silencing was analyzed with quantitative RT-PCR as in figure 5. The error bars represent s.d. ($n = 4$). (**b**) Double immunofluorescence staining of siRNA-treated H2052 cells with gremlin-1 and fibrillin-1 antibodies. Note the lack of fibrillar gremlin-1 staining, which is suggestive of efficient silencing using gremlin siRNA3. (**c**) H2052 cell proliferation was analyzed by counting cells 1–5 days after siRNA transfection. Both gremlin siRNAs reduced dramatically the number of cells 3–5 days after transfection (left panel, a representative experiment is shown). Same effect was seen also at earlier time points (right panel). The error bars represent s.d. ($n = 3$, $^*P = 0.05$). (**d**) Silencing gremlin-1 by siRNA3 did not induce apoptosis as measured using TUNEL staining. DNase I-treated cells (control) show positive staining. Nuclei are stained with DAPI.

adult tissues including lung gremlin-1 expression is low. In idiopathic pulmonary fibrosis , gremlin-1 is highly upregulated in the lung parenchyma, where it contributes to idiopathic pulmonary fibrosis pathogenesis by blocking BMP-mediated signals.[16] Gremlin-1 has been found to be upregulated also in many carcinoma tissues as well as in mesothelioma.[12,13,22] The role of gremlin-1 in malignant tissue appears complex and is likely mediated both by BMP-dependent and -independent functions. There are reports suggesting tumor-specific gremlin-1 expression,[12] while other reports suggest expression in cancer-associated stromal cells.[13] Here, we find high gremlin immunoreactivity in the mesothelioma tumor tissue. Analyses of serial mesothelioma tissue sections suggested that gremlin-1 can localize to calretinin-positive, epithelial-appearing tumor areas and also to aberrant looking and stromal-like calretinin-negative areas. These tissue areas contained some WT1-positive tumor cells.

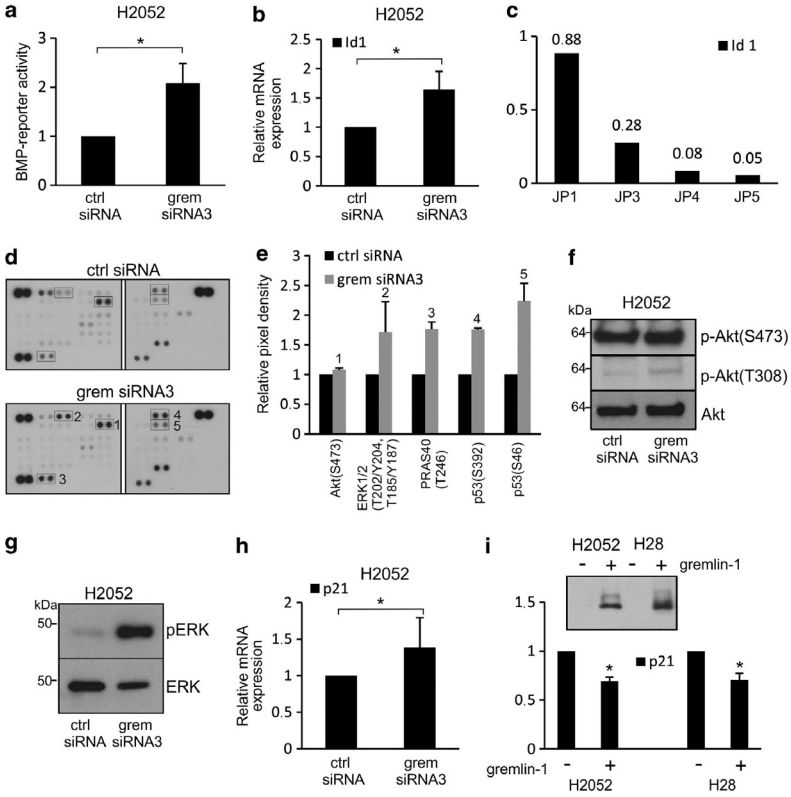

Figure 7. Cellular signaling in gremlin-1-silenced cells. (**a**) BMP-dependent reporter activity was analyzed in control and gremlin-1 siRNA-treated H2052 cells. The levels are expressed relative to control, which was set to 1. The error bars represent s.d. ($n = 4$, $^*P < 0.01$). (**b**) Id1 mRNA expression levels were analyzed by quantitative RT–PCR. The levels are expressed relative to control. $n = 3$, $^*P < 0.05$. (**c**) Id1 mRNA expression levels in primary mesothelioma cells. The levels are expressed relative to the expression levels in Met5A cells. (**d**) Cell lysates from control and gremlin-1 siRNA-treated H2052 cells were analyzed using a commercial phospho-protein array. (**e**) Quantification of alterations in the amounts of phospho-proteins ($n = 2$). Changes were also verified by immunoblotting analyses of Akt (**f**) and ERK (**g**) pathway proteins. Molecular weight markers are indicated on the left. Expression levels of p21 (Cip1/Waf1), a p53 target gene, were analyzed in gremlin-1 siRNA-treated (**h**) and gremlin-1-transfected cells (**i**) by quantitative RT-PCR. The levels are expressed relative to control, which was set to 1. $n = 3$, $^*P < 0.05$. I, inset. Gremlin-1 overexpression in H2052 and H28 cells was verified by immunoblotting using an antibody against the V5 tag.

Our results suggest that gremlin-1 localizes mainly in and around mesothelioma tumor cells.

Using a sophisticated large-scale protein interaction screen, we were able to identify fibrillin-2 as a novel gremlin-1 interacting protein. The interaction was also verified using a cell surface plasmon resonance technology. *Fibrillin-2* is a developmental gene, which is found in adult vasculature and is upregulated in idiopathic pulmonary fibrosis, scleroderma and during skin wound healing.[23,24] Idiopathic pulmonary fibrosis and cancer pathogenesis have common features including aberrant activation of mediators of tissue repair processes.[25] Our discovery that high fibrillin-2 immunoreactivity is associated with mesothelioma tumor tissue is a novel finding and supports this idea. Fibrillins (fibrillin-1 and -2) are large extracellular glycoproteins, which form heteromeric fibrillar structures, the so called fibrillin microfibrils, which are essential for elastin assembly.[26] Fibrillins also regulate growth factor signaling by sequestering TGF-β complexes as well as BMP-isoforms into extracellular matrix structures.[27] Gremlin-1 can bind to and inhibit the functions of BMP-2, -4 and -7, all of which have been shown to associate with fibrillins.[9] Here, we find that gremlin-1 can bind to fibrillin-1 and -2 *in vitro* and colocalizes with fibrillin-2 in mesothelioma tumor tissue *in vivo*. Conceptually this is a new finding, spatially localizing a BMP inhibitor molecule with its target proteins through fibrillin microfibrils. High levels of fibrillin-2 are likely to contribute to tumor cell behavior through aberrant extracellular matrix structure and regulation of gremlin-1 function.

Primary mesothelioma cells were cultured from patients' pleural effusion samples and analyzed after few passages of culture. Immunofluorescence microscopy analyses indicated that the cells, which were able to grow, represented mostly tumor cells. Gremlin-1 was expressed at mRNA and protein levels and fibrillin-2 at mRNA level by these primary cells, suggesting that they retain the pathological expression pattern of these genes. Interestingly, fibrillin-1 but not fibrillin-2 protein was detected in the matrix structures after 1 week culture of the primary cells. This likely reflects the temporal production of ECM proteins and remodeling of matrix structures during *in vitro* cell cultures.[28,29] Fibrillin-2 is likely assembled late during this process. In agreement with the protein interaction studies, gremlin-1 localized to fibrillin-1-

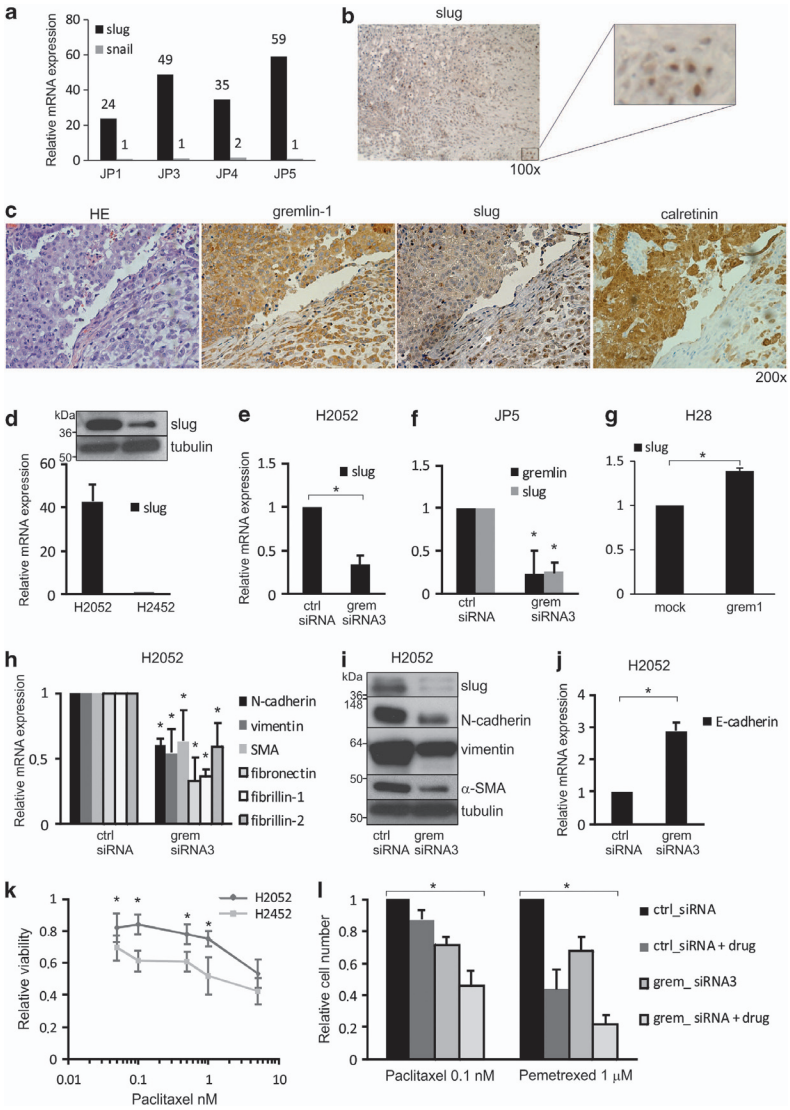

Figure 8. Gremlin-1 regulates slug expression and EMT phenotype. (**a**) Primary human mesothelioma cells (JP) were analyzed for snail and slug mRNA expression by quantitative RT-PCR. The levels were normalized to the expression levels of TATA-binding protein and are expressed relative to the expression levels in Met5A cells, which were set to 1. (**b**, **c**) Immunohistochemical staining of a mesothelioma section using slug antibodies shows mostly diffuse and granular cytoplasmic staining in the tumor tissue. Nuclear staining was also observed in certain tumor areas (**b**, right panel). (**c**) Analyses of serial mesothelioma tissue sections suggested that slug and gremlin staining colocalized in the same tumor areas. (**d**) Slug mRNA expression levels in H2052 and H2452 cells were analyzed by quantitative RT–PCR. The levels are expressed relative to H2452 expression levels, which were set to 1. The error bars represent s.d. ($n = 5$). INSET: immunoblotting analyses of slug. Tubulin is used as a loading control. Molecular weight markers are indicated on the left. (**e**–**g**) Slug mRNA expression levels were analyzed in control and gremlin-1 siRNA-treated H2052 and JP5 cells or H28 cells transfected with gremlin-1 (grem1) or control vector (mock). The levels are expressed relative to control, which was set to 1. The error bars represent s.d. (JP5, $n = 3$, $^*P < 0.05$; H2052, $n = 4$, $^*P < 0.01$; H28, $n = 3$, $^*P = < 0.05$). (**h**) N-cadherin, vimentin, α-SMA, fibronectin and fibrillin mRNA expression levels were analyzed in control and gremlin siRNA-treated H2052 cells by quantitative RT-PCR. The error bars represent s.d. ($n \geqslant 3$, $^*P < 0.05$). (**i**) Immunoblotting analyses of slug, N-cadherin, vimentin and α-SMA in control and gremlin-1 siRNA-treated H2052 cells. Tubulin is used as a loading control. (**j**) E-cadherin mRNA expression levels were analyzed in control and gremlin siRNA-treated H2052 cells by quantitative RT–PCR. Error bars represent s.d. ($n = 3$, $^*P < 0.05$). (**k**) H2052 and H2452 cells were treated with the indicated concentrations of paclitaxel after which cell proliferation/viability was analyzed with MTT assay ($n = 4$, $^*P < 0.05$). (**l**) Quantification of cell numbers after combined treatment with control or gremlin-1 siRNA and paclitaxel (0.1 nM, 24 h) or pemetrexed (1 μM, 48 h). Cell numbers were counted 3 days after transfection ($n \geqslant 4$, $^*P = 0.002$).

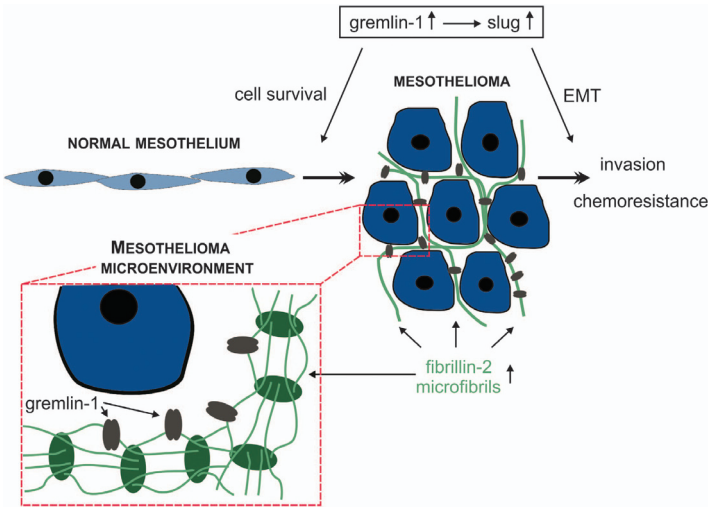

Figure 9. A model for the functions of gremlin-1 and fibrillin-2 in mesothelioma. Gremlin-1 induces proliferation and epithelial-to-mesenchymal transition (EMT) in mesothelioma cells. EMT is mediated by induction of the transcription factor slug and leads to chemoresistance and acquisition of invasive properties. Gremlin-1 is targeted to the tumor microenvironment through binding to fibrillin-2 microfibrils.

containing structures in mesothelioma cell ECM. Gene expression analyses suggested that compared with immortalized but non-tumorigenic mesothelial cells (Met5A), primary mesothelioma cells also expressed significantly higher levels of BMP-2. This is an interesting finding as BMP-2 has been linked to tumor invasion and metastasis.[30–32] Future studies will reveal whether BMP-2 is functional in the presence of high levels of its inhibitor protein.

We used the knowledge of gene expression patterns of primary mesothelioma cells to find a representative established mesothelioma cell line for mechanistic studies. H2052 cells expressed high levels of gremlin-1, fibrillin-2 and BMP-2 similar to all of the primary cells. Gremlin-1 silencing in these cells reduced cell proliferation dramatically. This is in agreement with previous studies suggesting that gremlin-1 can induce proliferation of cancer cells.[33–35] Interestingly, we observed gremlin-1 immunoreactivity also in reactive mesothelium, which associates gremlin-1 expression to a proliferative phenotype even in non-malignant mesothelial cells. Gremlin-1 expression has been linked to mesenchymal cells surrounding stem cell niches, which support proliferation of epithelial cells through blocking BMP activities.[13,36] Mesenchymal stem cells also express high levels of gremlin-1 (GeneSapiens database[37]). Our data suggest a model in which cancer cells can acquire the ability to produce high levels of gremlin-1, which is targeted to the tumor microenvironment through fibrillin binding (see Figure 9).

Signaling pathways linked to the regulation of cell survival, apoptosis and autophagy were altered in gremlin-1-silenced H2052 cells. Similar to our findings, negative regulation of Erk1/2 phosphorylation by gremlin-1 has been previously found in osteosarcoma cells;[38] however, gremlin overexpression in Saos-2 cell was found to reduce proliferation. We observed increased p53 phosphorylation and expression of its target gene, *p21*, in gremlin-1-silenced cells, suggesting a link to reduced cell survival. Further, the phosphorylation of the Akt substrate PRAS40 was significantly increased. Although PRAS40 has been linked to diabetes and cancer, its pathological functions are not well understood.[39] Interestingly, gremlin-1 has been shown to bind directly to a 14-3-3 protein,[12] which in turn binds and regulates the PRAS40 and other Akt/mTOR pathway proteins. Future studies will reveal the mechanistic details how cellular and secreted gremlin-1 regulates these pathways.

We and others have previously linked gremlin-1 expression to EMT processes.[16,40,41] In cancer cells, markers of EMT often suggest more advanced disease, invasive capacity and chemoresistance.[21,42] We found that the transcription factor slug, a master regulator of EMT, was upregulated in mesothelioma cells concurrently with gremlin-1. Silencing of gremlin-1 expression led to reduced slug mRNA and protein levels. Further, mesenchymal markers of EMT, vimentin, α-smooth muscle actin, fibronectin and N-cadherin were downregulated in gremlin-1-silenced cells, whereas epithelial marker E-cadherin was upregulated. These results are in agreement with previous studies linking the expression of EMT-related transcription factors to mesothelioma[43,44] and provide evidence that gremlin functions as a regulator of these transitional processes. EMT and slug expression have also been suggested to be involved in regulating cancer stemness as well as chemoresistance.[18,20,42] In agreement, we observed that high gremlin-1 and slug expressions in mesothelioma cells were associated with reduced sensitivity to paclitaxel-mediated cell death. Combined treatment with paclitaxel and gremlin-1 siRNA led to efficient cell death *in vitro*. Similar results were obtained with pemetrexed, which is a relatively new cancer drug used in the treatment of mesothelioma in combination with platinum compounds.[45] This indicates that blocking gremlin-1 function may be beneficial in mesothelioma especially when combined with chemotherapy.

Mesothelioma is an aggressive tumor with limited treatment options. Further, an increase is expected in the incidence of mesothelioma,[3,4] which sets an urgent need for new drug target molecules. Although the number of patient tissues analyzed in our study was relatively small ($n = 6$), the pathological expression of gremlin-1 was a clear concept. It is also reinforced by other studies suggesting a role for gremlin-1 in cancer cell proliferation.[12,13,33,34] Gremlin-1 has also BMP-independent angiogenic functions,[46] which may well contribute to tumor progression. Blocking gremlin-1 function in mesothelioma might offer means to fight the chemoresistance of this tumor.

MATERIALS AND METHODS

Antibodies

Antibodies used in the study are summarized in Table 2.

Patients and tissues specimen

A statement for the use of human tissue and pleural effusion materials was received from the Ethics Committee of the Helsinki University Hospital, Helsinki, Finland (number 308/13/0301/2010). All patients gave informed consent to participate in the study. Tissue biopsies and pleural effusion samples were obtained from patients undergoing diagnostic procedures and had a clinical and/or radiological suspicion of malignant mesothelioma. All patients included in the study ($n = 7$) were later diagnosed to have mesothelioma (Table 3). Control pleural samples were obtained from two male smokers who were operated for pneumothorax.

Cell culture and transient transfection

Immortalized normal mesothelial cells (Met5A),[47] and mesothelioma cell lines (211H, H28, H2452 and H2052) were from ATCC. Primary mesothelioma cells (named JP cells) were acquired from pleural effusion samples from patients suffering from malignant mesothelioma. Cells were centrifuged, washed and seeded on plastic culture dishes in RPMI-1640 medium (Sigma, St Louis, MO, USA) supplemented with 10% fetal bovine serum (Sigma) and antibiotics. The medium was changed every 3–4 days. Cells were passaged 2–3 times before immunofluorescence analysis of mesothelioma marker proteins was performed. Cells were also cultured for 6–7 days for RNA isolation and gene expression analyses. For further experiments JP5 cells were cultured and used between passages 3–7. Transfection of cells was carried out using siRNAs for gremlin, fibrillin-1 or a negative control (Life Technologies, Paisley, UK) as described.[48] The BMP reporter construct (Bre2-luc, kindly provided by Dr Peter ten Dijke, Leiden University Medical Center, the Netherlands) was transfected into H2052 cells to assess BMP-dependent signaling activity as described.[49]

Expression constructs and stable transfection

C-terminal gremlin-1 construct was generated by Gateway-cloning, the gremlin-1 construct from the Human Orfeome Collection (Thermo Scientific, FL, USA) to a pTO-SHc-GW-FRT plasmid with c-terminal Strep-tag III and human influenza hemagglutinin (HA)-tag.[14] Flip-In human embryonic kidney (HEK) 293 cells (Life Technologies) were grown as recommended. Stable transfection of cells was carried out as described.[50] After 2 weeks of culture, hygromycin B-resistant clones were tested for tetracycline (Sigma)-inducible gremlin-1 expression (see Figure 1b).

Affinity purification

Transfected Flip-In HEK293 cells were stimulated with tetracycline (25 ng/ml) to induce gremlin-1 expression. After a 24-h stimulation, cells were lysed in HNN-lysis buffer (50 mM HEPES pH 8, 150 mM NaCl, 50 mM NaF, 1 mM PMSF, 1.5 mM Na-vanadate, 0.5% NP-40 and protease inhibitors (Sigma)) followed by double affinity purification as described.[50] Briefly, cell lysates were passed through Strep-Tactin columns (IBA GmbH) followed by elution of bound proteins with 2.5 mM biotin. Next, the eluate was immunoprecipitated using anti-HA agarose (Sigma). Proteins were finally eluted using 0.2 M glycine and neutralized.

Protein digestion

The total protein amount from the elution fractions was precipitated using trichloroacetic acid (TCA). First, TCA was added to the elution fractions to final concentration of 25% followed by incubation for 30 min on ice. The precipitates were centrifuged, washed once with ice cold 0.1 M HCl in acetone and once with acetone. The pellets were then allowed to dry. For trypsin digestion the precipitated proteins were dissolved in 50 mM ammonium bicarbonate, pH 8.9, containing 0.1% Rapigest detergent (Waters, Milford, MA, USA). Proteins were reduced using DTT for 30 min at 60 °C followed by alkylation using iodoacetamide for 30 min at room temperature in dark. Proteins were digested with trypsin (Promega, Madison, WI, USA) for 18 h at 37 °C, and then the Rapigest detergent was hydrolyzed with HCl for 45 min at 37 °C. Peptides were purified with PepClean C18 Spin Columns (Thermo Fisher, Rockford, IL, USA) according to the manufacturer's protocol. Finally, the purified peptides were dissolved in 0.1% formic acid for MS analysis.

Table 3. Mesothelioma patient characteristics

Patient	*Type*	*Location*	*Age*	*Gender*	*IHC*	*Cells*
JP1	Epithelial	Pleura	53	Male	+	+
JP2	Biphasic	Pleura	71	Male	+	−
JP3	Epithelial	Pleura	63	Male	+	+
JP4	Biphasic	Peritoneum	72	Female	−	+
JP5	Epithelial	Pleura	69	Female	+	+
JP6	Biphasic	Pleura	71	Female	+	−
JP7	Epithelial	Pleura	61	Male	+	−

Tissues analyzed by immunohistochemistry (IHC) and pleural effusion samples obtained for cell culture (cells) are indicated.

Table 2. List of antibodies used in the study

Name	*Source*	*Application*	*Supplier*
calretinin	mouse/DAK-Calret1	IF, IHC	DAKO, Glostrup, Denmark, Germany
cytokeratin-7	rabbit /EP16204	IF	Novus Biologicals, Littleton, CO, USA
vimentin	mouse/V9	IF, IB	Santa Cruz, Santa Cruz, CA, USA
N-cadherin	mouse/32	IB	BD Biosciences, Franklin Lakes, NJ, USA
α-SMA	mouse/1A4	IB	Sigma, St Louis, MO, USA
HA	mouse/16B12	IB	Covance, Princeton, NJ, USA
fibrillin-1	mouse/2499	IF	Millipore, Billerica, MA, USA
fibrillin-1	rabbit/ pAb9543	IHC, IF	Professor Lynn Sakai
fibrillin-2	mouse/48	IHC, PLA	Millipore
gremlin-1	rabbit pAb	IHC	Abcam, Cambridge, UK
gremlin-1	goat pAb	IHC, PLA	Santa Cruz
gremlin-1	rabbit pAb	IF	Santa Cruz
Slug	rabbit pAb	IB, IHC	Sigma
WT1	mouse/WT49	IHC	Novocastra, Newcastle, UK
p-Akt (S473)	rabbit pAb	IB	Cell Signaling, Danvers, MA, USA
p-Akt (T308)	rabbit pAb	IB	Cell Signaling
Akt	rabbit pAb	IB	Cell Signaling
p-Erk1/2	rabbit mAb/D13.14.4E	IB	Cell Signaling
Erk1	mouse/3A7	IB	Cell Signaling
V5	Mouse mAb	IB	Invitrogen

Abbreviations: IB, immunoblotting; IF, immunofluorescence; IHC, immunohistochemistry; PLA, proximity ligation assay.

LC-MS/MS analysis

Mass spectrometric analysis was performed using nanoAcquity UPLC – liquid chromatography system on-line with a Waters Synapt G2 mass spectrometer (Waters S.A.S., Saint-Quentin, France). Waters nanoAcquity UPLC Trap Column (Symmetry C18, 180 μm × 20 mm, 5 μm) was used as trapping and Waters nanoAcquity UPLC Column (BEH130 C18, 75 μm × 150 mm, 1.7 μm) as analytical column. Four microliters of sample was injected and run using 90 min gradient from 3 to 40% mobile phase B (0.1% formic acid in acetonitrile). 0.1% formic acid in water was used as mobile phase A.

Data were collected with data dependent acquisition manner collecting eight fragmentation spectra simultaneously. Switch limit from MS to MS/MS was set to peak intensity of 200. Fragmentation data for detected peaks were collected for 5 s and then excluded from fragmentation for 120 s. Scan time for both MS and MS/MS was one second. No lockmass correction was used.

The raw data were processed with Mascot Distiller software (version 2.3.1.0, Matrix Science, London, UK), and database search was performed using Mascot search engine (version 2.2.04) against Swiss-Prot human database (dated 16.6.2010). MudPIT scoring and Ion score cutoff limit of 20 were used to identify peptides. Require bold red- specification was used to limit the results to those proteins that have at least one unique peptide. Carbamidomethylated cysteine was set as fixed modification and oxidation of methionine as variable modification. Peptide mass tolerance for search was 0.2 Da and 0.1 Da for fragment ion search. A maximum of two missed trypsin cleavages was allowed. The Mascot Distiller processed data were also searched using GPM X!Tandem search engine[51] using same parameters.

Expression and purification of recombinant gremlin-1

The expression construct pGremlin-1_V5/HIS in pEF-IRES-P contains cDNA encoding human gremlin-1 with C-terminal tags (V5 and 6HIS). H2052 and H28 cells were transiently transfected with this construct or the expression vector using Fugene HD transfection reagent (Promega). CHO cells were stably transfected, and gremlin-containing cell culture supernatants were produced as described.[52] The media was then dialyzed against 50 mM sodium phosphate buffer, pH 7.2 and 1 M NaCl (buffer A) and loaded on a 1-ml HiTrap column (GE Health Care, Waukesha, WI, USA) previously charged with $CoCl_2$ and equilibrated with buffer A. The loaded column was washed with 40 column volumes of buffer A and subjected to a fast protein liquid chromatography (GEHC) gradient run starting with buffer A containing 0–100% buffer B (buffer A with 250 mM imidazole). Fractions were analyzed using SDS–PAGE for their purity and molecular mass, and imidazole in these fractions was removed by dialysis against buffer A. For further concentration and purification, gremlin-1-containing fractions were dialyzed against TBS and subjected to affinity chromatography using a 1-ml HiTrap heparin column (GEHC). Bound gremlin-1 was eluted in a 0–1 M NaCl gradient.

Surface plasmon resonance

Binding analyses were performed using a BIAcore2000 (GEHC). 2000 Rus of gremlin-1 were covalently coupled to carboxymethyldextran hydrogel 500 M sensor chips (XanTec, Düsseldorf, Germany) using the amine coupling kit following the manufacturer's instructions (GEHC). Binding assays with N-terminal fibrillin-1 (rF11) and -2 peptides (rF86) as analytes were performed as previously described.[9] Kinetic constants were calculated by nonlinear fitting of association and dissociation curves (BIAevaluation 4.1 software).

Immunohistochemical staining and proximity ligation assay

Immunohistochemical staining of tumor tissues and proximity ligation assay were performed as described.[24] Images were captured with Nikon DS-Fi1 or with Axio Imager with ApoTome (Zeiss, Göttingen, Germany) or with using Axio Vison 4.8 software (Zeiss).

SDS–PAGE and immunoblotting

Cells were lysed in RIPA lysis buffer (50 mM Tris-HCl, pH 7.4, 150 mM NaCl, 1 mM EDTA, 1% NP-40, 0.2% sodium deoxycholate) containing protease inhibitors (Roche, Mannheim, Germany) for 15 min on ice. Protein concentrations were measured using a BCA protein assay Kit (Pierce, Rockfors, IL, USA). SDS–PAGE and immunoblotting were performed as described.[53]

RNA isolation and gene expression analyses

Isolation of total cellular RNA, reverse transcription and quantitative real-time PCR were carried out as described.[53] The relative gene expression differences were calculated with the comparative delta delta cycle threshold (ΔΔCT) method, and the results have been expressed as mRNA expression levels normalized to the levels of a gene with a constant expression (TATA-binding protein).

Immunofluorescence analyses and microscopy

Cells were grown on glass coverslips for the indicated times and fixed with 4% paraformaldehyde in PBS at room temperature for 10 min or with ice cold methanol at $-20\,^{\circ}C$ for 20 min. Immunofluorescence staining was carried out as described.[53] Images were captured with a Axioplan 2 epifluorescence microscope (Zeiss) and AxioCam HRm 14-bit grayscale CCD camera Axiovision 4.6 software (Zeiss).

Human phospho-kinase array

Control and gremlin-1 siRNA-treated cells were lysed, and alterations in phospho-kinase levels were analyzed using a Proteome profiler array (ARY003b, R&D Systems, Gaitherburg, MD, USA) according to the manufacturer's instructions. Quantity One version 4.6 (BioRad, Hercules, CA, USA) was used for quantification. The kinase array was performed twice, and the results are expressed as average of the two experiments.

Measurements of cell viability and apoptosis

Cell proliferation/viability was assessed using MTT assay (R&D Systems). Briefly, cells were seeded on 96-well plates (10 000/well) and were treated the next day with different concentrations of paclitaxel (Hospira, Lake Forest, IL, USA). The metabolic activity of cells was measured after 48 h according to the manufacturer's instructions. Apoptosis was assayed using a TUNEL technology using *In Situ* cell death detection kit (Roche). Cells were seeded on glass coverslips, cultured overnight and transfected with siRNAs. Cells were then fixed and stained, according to the manufacturer's instructions, 3 days after transfection.

Statistical analyses

Data were analyzed using PASW Statistics 18 program for Windows (SPSS, Chicago, IL, USA). Statistical difference between two independent groups was evaluated using nonparametric Mann–Whitney *U*-test. Statistical difference between more than two independent groups was evaluated using nonparametric Kruskal–Wallis test. A *P*-value of <0.05 was considered statistically significant.

CONFLICT OF INTEREST

The authors declare no conflict of interest.

ACKNOWLEDGEMENTS

We thank Eva Sutinen for coordinating patient sample collection and performing immunohistochemical staining experiments, Arja Pasternack for CHO cell transfection and production of conditioned media, Sami Starast for technical assistance, Professor Jorma Keski-Oja for discussions, Professor Lynn Sakai (Oregon Health and Science University, Portland, OR) for the fibrillin-1 antibody and fibrillin-1 and -2 peptides, and Biomedicum Imaging Unit for imaging support. This work was supported by Academy of Finland, Sigrid Jusélius Foundation, Jalmari and Rauha Ahokas Foundation, Magnus Ehrnrooth Foundation, Finnish Cultural Foundation, Foundation of the Finnish Anti-Tuberculosis Association, Deutsche Forschungsgemeinschaft (SFB829, project B12 to GS).

REFERENCES

1 Mossman BT, Bignon J, Corn M, Seaton A, Gee JB. Asbestos: scientific developments and implications for public policy. *Science* 1990; **247**: 294–301.
2 Lanphear BP, Buncher CR. Latent period for malignant mesothelioma of occupational origin. *J Occup Med* 1992; **34**: 718–721.
3 Huuskonen MS, Rantanen J. Finnish Institute of Occupational Health (FIOH): prevention and detection of asbestos-related diseases, 1987-2005. *Am J Ind Med* 2006; **49**: 215–220.
4 Vorobiof DA, Mafafo K. Malignant pleural mesothelioma: medical treatment update. *Clin Lung Cancer* 2009; **10**: 112–117.

5 Dormoy V, Jacqmin D, Lang H, Massfelder T. From development to cancer: lessons from the kidney to uncover new therapeutic targets. *Anticancer Res* 2012; **32**: 3609–3617.
6 Micalizzi DS, Farabaugh SM, Ford HL. Epithelial-mesenchymal transition in cancer: parallels between normal development and tumor progression. *J Mammary Gland Biol Neoplasia* 2010; **15**: 117–134.
7 Hsu DR, Economides AN, Wang X, Eimon PM, Harland RM. The Xenopus dorsalizing factor Gremlin identifies a novel family of secreted proteins that antagonize BMP activities. *Mol Cell* 1998; **1**: 673–683.
8 Topol LZ, Bardot B, Zhang Q, Resau J, Huillard E, Marx M *et al.* Biosynthesis, post-translation modification, and functional characterization of Drm/Gremlin. *J Biol Chem* 2000; **275**: 8785–8793.
9 Sengle G, Charbonneau NL, Ono RN, Sasaki T, Alvarez J, Keene DR *et al.* Targeting of bone morphogenetic protein growth factor complexes to fibrillin. *J Biol Chem* 2008; **283**: 13874–13888.
10 Michos O, Panman L, Vintersten K, Beier K, Zeller R, Zuniga A *et al.* antagonism induces the epithelial-mesenchymal feedback signaling controlling metanephric kidney and limb organogenesis. *Development* 2004; **131**: 3401–3410.
11 Topol LZ, Marx M, Laugier D, Bogdanova NN, Boubnov NV, Clausen PA *et al.* Identification of drm, a novel gene whose expression is suppressed in transformed cells and which can inhibit growth of normal but not transformed cells in culture. *Mol Cell Biol* 1997; **17**: 4801–4810.
12 Namkoong H, Shin SM, Kim HK, Ha SA, Cho GW, Hur SY *et al.* The bone morphogenetic protein antagonist gremlin 1 is overexpressed in human cancers and interacts with YWHAH protein. *BMC Cancer* 2006; **6**: 74.
13 Sneddon JB, Zhen HH, Montgomery K, van de Rijn M, Tward AD, West R *et al.* Bone morphogenetic protein antagonist gremlin 1 is widely expressed by cancer-associated stromal cells and can promote tumor cell proliferation. *Proc Natl Acad Sci USA* 2006; **103**: 14842–14847.
14 Varjosalo M, Sacco R, Stukalov A, van Drogen A, Planyavsky M, Hauri S *et al.* Interlaboratory reproducibility of large-scale human protein-complex analysis by standardized AP-MS. *Nat Methods* 2013; **10**: 307–314.
15 Ramirez F, Sakai LY. Biogenesis and function of fibrillin assemblies. *Cell Tissue Res* 2010; **339**: 71–82.
16 Koli K, Myllärniemi M, Vuorinen K, Salmenkivi K, Ryynänen MJ, Kinnula VL *et al.* Bone morphogenetic protein-4 inhibitor gremlin is overexpressed in idiopathic pulmonary fibrosis. *Am J Pathol* 2006; **169**: 61–71.
17 Thiery JP, Acloque H, Huang RY, Nieto MA. Epithelial-mesenchymal transitions in development and disease. *Cell* 2009; **139**: 871–890.
18 Catalano A, Rodilossi S, Rippo MR, Caprari P, Procopio A. Induction of stem cell factor/c-Kit/slug signal transduction in multidrug-resistant malignant mesothelioma cells. *J Biol Chem* 2004; **279**: 46706–46714.
19 Haslehurst AM, Koti M, Dharsee M, Nuin P, Evans K, Geraci J *et al.* EMT transcription factors snail and slug directly contribute to cisplatin resistance in ovarian cancer. *BMC Cancer* 2012; **12**: 91.
20 Mani SA, Guo W, Liao MJ, Eaton EN, Ayyanan A, Zhou AY *et al.* The epithelial-mesenchymal transition generates cells with properties of stem cells. *Cell* 2008; **133**: 704–715.
21 Polyak K, Weinberg RA. Transitions between epithelial and mesenchymal states: acquisition of malignant and stem cell traits. *Nat Rev Cancer* 2009; **9**: 265–273.
22 Wang DJ, Zhi XY, Zhang SC, Jiang M, Liu P, Han XP *et al.* The bone morphogenetic protein antagonist Gremlin is overexpressed in human malignant mesothelioma. *Oncol Rep* 2012; **27**: 58–64.
23 Brinckmann J, Hunzelmann N, Kahle B, Rohwedel J, Kramer J, Gibson MA *et al.* Enhanced fibrillin-2 expression is a general feature of wound healing and sclerosis: potential alteration of cell attachment and storage of TGF-β. *Lab Invest* 2010; **90**: 739–752.
24 Leppäranta O, Sens C, Salmenkivi K, Kinnula VL, Keski-Oja J, Myllärniemi M *et al.* Regulation of TGF-β storage and activation in the human idiopathic pulmonary fibrosis lung. *Cell Tissue Res* 2012; **348**: 491–503.
25 Vancheri C, Failla M, Crimi N, Raghu G. Idiopathic pulmonary fibrosis: a disease with similarities and links to cancer biology. *Eur Respir J* 2010; **35**: 496–504.
26 Lin G, Tiedemann K, Vollbrandt T, Peters H, Batge B, Brinckmann J *et al.* Homo- and heterotypic fibrillin-1 and -2 interactions constitute the basis for the assembly of microfibrils. *J Biol Chem* 2002; **277**: 50795–50804.
27 Ramirez F, Rifkin DB. Extracellular microfibrils: contextual platforms for TGFβ and BMP signaling. *Curr Opin Cell Biol* 2009; **21**: 616–622.
28 Dallas SL, Chen Q, Sivakumar P. Dynamics of assembly and reorganization of extracellular matrix proteins. *Curr Top Dev Biol* 2006; **75**: 1–24.
29 Koli K, Hyytiäinen M, Ryynänen MJ, Keski-Oja J. Sequential deposition of latent TGF-β binding proteins (LTBPs) during formation of the extracellular matrix in human lung fibroblasts. *Exp Cell Res* 2005; **310**: 370–382.
30 Gordon KJ, Kirkbride KC, How T, Blobe GC. Bone morphogenetic proteins induce pancreatic cancer cell invasiveness through a Smad1-dependent mechanism that involves matrix metalloproteinase-2. *Carcinogenesis* 2009; **30**: 238–248.
31 Kang MH, Oh SC, Lee HJ, Kang HN, Kim JL, Kim JS *et al.* Metastatic function of BMP-2 in gastric cancer cells: the role of PI3K/AKT, MAPK, the NF-κB pathway, and MMP-9 expression. *Exp Cell Res* 2011; **317**: 1746–1762.
32 Katsuno Y, Hanyu A, Kanda H, Ishikawa Y, Akiyama F, Iwase T *et al.* Bone morphogenetic protein signaling enhances invasion and bone metastasis of breast cancer cells through Smad pathway. *Oncogene* 2008; **27**: 6322–6333.
33 Kim M, Yoon S, Lee S, Ha SA, Kim HK, Kim JW *et al.* Gremlin-1 induces BMP-independent tumor cell proliferation, migration, and invasion. *PLoS One* 2012; **7**: e35100.
34 Mulvihill MS, Kwon YW, Lee S, Fang LT, Choi H, Ray R *et al.* Gremlin is over-expressed in lung adenocarcinoma and increases cell growth and proliferation in normal lung cells. *PLoS One* 2012; **7**: e42264.
35 Sneddon JB, Werb Z. Location, location, location: the cancer stem cell niche. *Cell Stem Cell* 2007; **1**: 607–611.
36 Kosinski C, Li VS, Chan AS, Zhang J, Ho C, Tsui WY *et al.* Gene expression patterns of human colon tops and basal crypts and BMP antagonists as intestinal stem cell niche factors. *Proc Natl Acad Sci USA* 2007; **104**: 15418–15423.
37 Kilpinen S, Autio R, Ojala K, Iljin K, Bucher E, Sara H *et al.* Systematic bioinformatic analysis of expression levels of 17,330 human genes across 9,783 samples from 175 types of healthy and pathological tissues. *Genome Biol* 2008; **9**: R139.
38 Chen B, Athanasiou M, Gu Q, Blair DG. Drm/Gremlin transcriptionally activates p21(Cip1) via a novel mechanism and inhibits neoplastic transformation. *Biochem Biophys Res Commun* 2002; **295**: 1135–1141.
39 Wang H, Zhang Q, Wen Q, Zheng Y, Lazarovici P, Jiang H *et al.* Proline-rich Akt substrate of 40kDa (PRAS40): a novel downstream target of PI3k/Akt signaling pathway. *Cell Signal* 2012; **24**: 17–24.
40 Carvajal G, Droguett A, Burgos ME, Aros C, Ardiles L, Flores C *et al.* Gremlin: a novel mediator of epithelial mesenchymal transition and fibrosis in chronic allograft nephropathy. *Transplant Proc* 2008; **40**: 734–739.
41 Lee H, O'Meara SJ, O'Brien C, Kane R. The role of gremlin, a BMP antagonist, and epithelial-to-mesenchymal transition in proliferative vitreoretinopathy. *Invest Ophthalmol Vis Sci* 2007; **48**: 4291–4299.
42 Shih JY, Yang PC. The EMT regulator slug and lung carcinogenesis. *Carcinogenesis* 2011; **32**: 1299–1304.
43 Fassina A, Cappellesso R, Guzzardo V, Dalla Via L, Piccolo S, Ventura L *et al.* Epithelial-mesenchymal transition in malignant mesothelioma. *Mod Pathol* 2012; **25**: 86–99.
44 Merikallio H, Pääkko P, Salmenkivi K, Kinnula V, Harju T, Soini Y. Expression of snail, twist, and Zeb1 in malignant mesothelioma. *APMIS* 2012; **121**: 1–10.
45 Pasello G, Ceresoli GL, Favaretto A. An overview of neoadjuvant chemotherapy in the multimodality treatment of malignant pleural mesothelioma. *Cancer Treat Rev* 2013; **39**: 10–17.
46 Mitola S, Ravelli C, Moroni E, Salvi V, Leali D, Ballmer-Hofer K *et al.* Gremlin is a novel agonist of the major proangiogenic receptor VEGFR2. *Blood* 2010; **116**: 3677–3680.
47 Ke Y, Reddel RR, Gerwin BI, Reddel HK, Somers AN, McMenamin MG *et al.* Establishment of a human in vitro mesothelial cell model system for investigating mechanisms of asbestos-induced mesothelioma. *Am J Pathol* 1989; **134**: 979–991.
48 Koli K, Ryynänen MJ, Keski-Oja J. Latent TGF-β binding proteins (LTBPs)-1 and -3 coordinate proliferation and osteogenic differentiation of human mesenchymal stem cells. *Bone* 2008; **43**: 679–688.
49 Myllärniemi M, Lindholm P, Ryynänen MJ, Kliment CR, Salmenkivi K, Keski-Oja J *et al.* Gremlin-mediated decrease in bone morphogenetic protein signaling promotes pulmonary fibrosis. *Am J Respir Crit Care Med* 2008; **177**: 321–329.
50 Glatter T, Wepf A, Aebersold R, Gstaiger M. An integrated workflow for charting the human interaction proteome: insights into the PP2A system. *Mol Syst Biol* 2009; **5**: 237.
51 Fenyo D, Eriksson J, Beavis R. Mass spectrometric protein identification using the global proteome machine. *Methods Mol Biol* 2010; **673**: 189–202.
52 Hulmi JJ, Oliveira BM, Silvennoinen M, Hoogaars WM, Ma H, Pierre P *et al.* Muscle protein synthesis, mTORC1/MAPK/Hippo signaling, and capillary density are altered by blocking of myostatin and activins. *Am J Physiol Endocrinol Metab* 2013; **304**: E41–E50.
53 Tamminen JA, Myllärniemi M, Hyytiäinen M, Keski-Oja J, Koli K. Asbestos exposure induces alveolar epithelial cell plasticity through MAPK/Erk signaling. *J Cell Biochem* 2012; **113**: 2234–2247.

III

Overexpression of activin-A and -B in malignant mesothelioma – attenuated Smad3 signaling responses and ERK activation promote cell migration and invasive growth

[1,2]Jenni A. Tamminen, [1,2]Miao Yin, [3,4]Mikko Rönty, [3,5]Eva Sutinen, [3,6] Arja Pasternack [3,6] Olli Ritvos, [2,3,5]Marjukka Myllärniemi and [1,2,]Katri Koli

[1]Research Programs Unit, Translational Cancer Biology, University of Helsinki, Finland; [2]Transplantation Laboratory, Haartman Institute, University of Helsinki, Finland; [3]Helsinki University Central Hospital and Hospital Laboratory, Helsinki, Finland; [4]Department of Pathology, University of Helsinki, Finland; [5]Department of Medicine, Division of Pulmonary Medicine, University of Helsinki, Finland; [6] Department of Bacteriology and Immunology, University of Helsinki, Finland

Short title: Activins in mesothelioma invasive growth

Correspondence: Katri Koli, University of Helsinki, Biomedicum/B502a1, P.O.Box 63, Haartmaninkatu 8, 00014 Helsinki, Finland. E-mail: katri.koli@helsinki.fi, Tel. +358 2 941 25035

ABSTRACT
Activin-A and activin-B, members of the TGF-β superfamily, are regulators of reproductive functions, inflammation and wound healing. These dimeric molecules regulate various cellular activities such as proliferation, migration and suvival. Malignant mesothelioma is an asbestos exposure related tumor affecting mainly pleura and it usually has a dismal prognosis. Here, we demonstrate that both activin-A and -B are abundantly expressed in mesothelioma tumor tissue as well as in cultured primary and established mesothelioma cells. Migratory and invasive mesothelioma cells were also found to have attenuated activation of the Smad2/3 pathway in response to activins. Migration and invasive growth of the cells in three-dimentional matrix was prevented by inhibition of activin activity using a soluble activin receptor 2B (sActR2B-Fc). This was associated with decreased ERK activity. Furthermore, migration and invasive growth was significantly inhibited by blocking ERK phosphorylation. Mesothelioma tumors are locally invasive and our results clearly suggest that acivins have a tumor-promoting function in mesothelioma through increasing expression and switching from canonical Smad3 pathway to non-canonical ERK pathway signaling. Blocking activin activity offers a new therapeutic approach for inhibition of mesothelioma invasive growth.

Key words: mesothelioma, activin, invasive growth

Abbreviations: ACVR2, type 2 activin receptor; ALK, activin receptor-like kinase; ERK, extracellular signal-regulated kinase; FST, follistatin; FSTL3, follistatin like 3; JNK, c-Jun N-terminal kinase; TGF-β, transforming growth factor- β

INTRODUCTION

Malignant mesothelioma is a rare but very aggressive tumor originating from mesothelial cells lining body cavities. Most commonly mesothelioma affects pleura, sometimes peritoneum and very rarely pericardium. Mesothelioma is usually related to previous asbestos exposure and develops during a latency of 20-40 years [1]. The incidence of mesothelioma is expected to increase worldwide in the near future [2,3]. Late stage of the disease at the time of diagnosis as well as only moderate effectiveness of current therapies lead to negligible survival time of the patients after diagnosis. Novel potential diagnostic markers for early detection and drug targets are needed for mesothelioma.

Activins, members of the TGF-β superfamily of growth factors, are known regulators of development and reproductive functions [4]. Currently, activins, especially activin-A, are also recognised as important regulators of immune responses, wound healing and cancer [5]. Activins enhance cell proliferation and migration as well as scar formation during wound healing [5]. Increased cell proliferation and migration are also characteristics of cancer cells. In addition, activins may also promote tumor progression indirectly by altering the tumor microenvironment through regulation of immune functions and angiogenesis. Whether activins promote or inhibit carcinogenesis depends on the cell, tissue and cancer type [5-7]. A recent study reports that activin-A promotes mesothelioma cell growth and migration through regulation of cyclin D [8].

The genes *INHBA* and *INHBB* code for the activin β-subunits, which form disulfide-linked functional dimers. Homodimerization of the β_A-subunits generates activin-A and β_B-subunits form activin-B [9]. The β-subunits can also heterodimerizise and form activin-AB. The β-subunits heterodimerisize also with α- subunits and form inhibins, which inhibit activin action by competing for activin receptors. Activin signaling is also regulated by soluble inhibitors follistatin (FST) and follistatin like-3 (FSTL3) [10], which inhibit activin action by binding to activins and blocking association with cell surface receptors [11].

Activins signal through activin type 1 and type 2 transmembrane serine/threonine kinase receptors. Activin action is initiated when activin binds to a type 2 activin receptor (ACVR2A or ACVR2B). This binding leads to recruitment, phosphorylation and activation of type 1 activin receptor followed by phosphorylation and activation of Smad proteins. Both activins-A and -B can activate the Smad2/3 pathway through type 2 receptors and common type 1 receptor ActR1B (activin like kinase-4, ALK-4) [12]. Activin-B can also activate Smad2/3 via ActR1C (ALK7) [13,14]. Furthermore, activin-B has been reported to activate Smad1/5/8 through BMPR1A (ALK3)[15]. The receptors that bind TGF-β-family members can also activate non-Smad proteins [16]. Activin-A can induce ERK and p38 MAP kinase phosphorylation [17], and activin-B has been reported to be able to phosphorylate SAPK/JNK and to induce keratinocyte migration [18] and wound healing [19]. Furthermore, activation of both JNK and ERK is required for activin-B induced migration in bone marrow-derived mesenchymal stem cells [20]. Activin-A and activin-B have partially overlapping expression patterns but are functionally distinct [21].

In this study, we characterized activin-A and -B expression and their receptors in mesothelioma tissue and in cultured primary and established mesothelioma cells. We aimed to clarify the role of

Smad mediated and non-canonical activin signaling in mesothelioma cell migration and invasion. We report here that activins are abundantly expressed in mesothelioma cells and that by blocking activin activity the migration and invasive growth of mesothelioma cells can be significantly reduced. Furthermore, our results suggest a new mechanism through which mesothelioma cells promote migration and invasive growth: switching activin signaling from canonical Smad3 pathway to non-canonical ERK pathway signaling.

MATERIALS AND METHODS

Antibodies and growth factors

Mouse monoclonal antibodies against human activin-A (mAb 18/26A) and activin-B (mAb 12/9A for IHC, 46A/F for Western blotting) subunits and follistatin (mAb 4/73C for IHC, 4/208 for Western blotting) were generated by AnshLabs LLC (Webster, TX). Rabbit monoclonal p-ERK1/2 and mouse monoclonal ERK1 were from Cell Signaling (Danvers, MA). Human recombinant activins were from R&D Systems (Gaithersburg, MD) and used at 25 ng/ml. The recombinant fusion protein contaning the ectodomain of human ActR2B (sActR2B-Fc) or anti-Müllerian hormone receptor (sAMHR2-Fc) fused to the Fc domain of human IgG1 was produced as described previously [22] and used at 650 ng/ml (2D) or 10 µg/ml (3D). Soluble receptors sequester ligands and inhibit their binding to cell surface receptors. MAP kinase kinase (MEK) inhibitor PD98059 was from Calbiochem (Merck, Darmstadt, Germany) and used at 30 µM.

Patients and tissues specimen

A statement for the use of human tissue and pleural effusion materials was approved by the Ethics Committee of the Helsinki University Hospital, Helsinki, Finland (permit number 308/13/0301/2010). All patients gave written informed consent to participate in the study. Tissue biopsies and pleural effusion samples were obtained from patients who were undergoing diagnostic procedures and who had a clinical and/or radiological suspicion of malignant mesothelioma. All patients included in the study (n=12) were later diagnosed to have mesothelioma confirmed by a biopsy from the tumor tissue (Table 1).

Immunohistochemical staining

Paraffin-embedded tissue from mesothelioma tumor samples were processed and stained using the Novolink Polymer Detection System (Novocastra, Leica Biosystems, Newcastle upon Tyne, UK) and visualized by diaminobenzidine (DAB, Vector Laboratories) has been reported previously [23]. For follistatin staining, the formalin-fixed paraffin embedded specimens were stained on Leica BOND-MAX fully automated staining system as defined in the manufacturer's staining protocol [with the Leica Bond Polymer Refine Detection-kit, Bond Epitope Retrievel Solution 2, 20 mins, R.T.U. Normal Horse serum 2,5% (Vector Laboratories, Burlingame, CA) blocking]. Images of IHC sections were captured with Nikon DS-Fi1 (Nikon, Amsterdam, Netherlands).

Cell culture

Immortalized normal mesothelial cells (Met5A) [24] and mesothelioma cell lines (211H, H28, H2452, H2052) were from ATCC. Primary mesothelioma cells (JP cells) were obtained from pleural effusion samples from malignant mesothelioma patients as described in Tamminen et al. 2013[25]. Cells were cultured in RPMI-1640 media (Sigma, St Luis, MO) supplemented with 10% fetal bovine serum (Gibco, Paisley, UK) and antibiotics (Gibco, Grand Island NY). Cells were stimulated with activin-A (25 ng/ml), activin-B (25 ng/ml) or sActR2B-Fc (650 ng/ml) for 90 minutes under serum-free conditions.

Transient transfection and luciferase assay

Cells to be transfected were seeded in 96-well plates. The cells were co-transfected with promoter constructs $(CAGA)_{12}$-luc (Smad3 responsive), ARE-luc/Fast-1 (Smad2 responsive) or $(Bre)_2$-luc (Smad 1/5 responsive), kindly provided by Dr. Peter ten Dijke (Leiden University Medical Center, the Netherlands), together with pRL-TK (Renilla Luciferase control, Promega, Madison, WI) plasmid using Fugene HD transfection reagent (Roche, Basel, Switzerland). The transfection, cell lysis and the measurement of the luciferase activity were performed as described in Tamminen et al. 2012 [26]. The cells were stimulated for 24 hours under serum-free conditions where indicated.

RNA isolation and quantitative RT-PCR

Total cellular RNA was isolated using RNeasy Mini kit (Qiagen, Hilden, Germany) and reverse transcribed to cDNA using iScript cDNA synthesis Kit (Bio-Rad, Hercules, CA) according to the manufacturer's instructions. The quantitative RT-PCR was performed as previously described [26].

SDS-PAGE and Western blotting

Cells were lysed and protein concentrations were measured as described earlier [26]. Equal amounts of protein were separated by SDS-PAGE using 4-20% gradient Tris-glycine gels (Bio-Rad). Conditioned media from mesothelioma cell cultures were collected during 2 days, concentrated using Amicon Ultra 10K centrifugal filters (Millipore, Merck, Darmstadt, Germany) and separated by SDS-PAGE. The transfer of the proteins to Protran nitrocellulose membranes (Whatman, Springfield Mill, UK**),** Western blotting and final detection of the proteins were performed as described previously [26]. Relative band densities were quantified using ImageJ software (National Institutes of Health, Bethesda, MA, USA).

Cell migration assays

The migratory capacity of the cell lines was analyzed using Incucyte ZOOM 2013A kinetic live cell imaging system (Essen Bioscience, Hertfordshire, UK) according to the manufacturer's instructions. Briefly, the cells were plated on 96-well plates and the next day a wound was applied using a woundmaker (Essen Bioscience). The media was replaced with serum-free media supplemented with sActR2B-Fc where indicated. Two distinct pictures were taken of each well every 2 hours for 48 hours. Data were analyzed with Incucyte ZOOM 2013A software and the relative wound density was used as a measure of the wound closure. Alternatively, cells were seeded on 12-well plates and wounds were made in confluent monolayers using a P200 pipette tip. The media was replaced with serum-free media supplemented with DMSO, PD98059 or sActR2B-

Fc where indicated. Two pictures per well were taken after 0, 6, 24 and 48 hours using Nikon Eclipse TS 100 and Digital Sight DS-L2 (Nikon). The wound density was quantified using Image ProPlus 7.0 software (Media Cybernetics, Inc., Rockville, MD) and is shown as % area occupied by cells relative to % wound area and has been normalized to wound density data at the 0 hour time point. The control treated wound density has been set to one.

3D invasive growth assay

The lower Matrigel gel (BD Biosciences, San Jose, CA) was laid on the bottom of the well on a 96-well plate and allowed to solidify at 37˚C for 45 minutes. Next, 3000-4000 cells per well were seeded and allowed to attach for 1 hour after which the media was carefully removed and replaced with the top gel. Before seeding, the cells were pre-treated with sActR2B-Fc, sAMHR2-Fc, DMSO or PD98059 for 15 minutes where indicated. The top gel was allowed to solidify for 30 minutes after which media was added. Inhibitors were also added to Matrigel and cell culture media on top of the gel.

Statistical analyses

Data were analyzed using PASW Statistics 21 program for Windows (SPSS, Chicago, IL). Statistical difference between two independent groups was evaluated using nonparametric Mann-Whitney U-test. Statistical difference between more than two independent groups was evaluated using nonparametric Kruskal-Wallis test. A p-value of less than 0.05 was considered statistically significant.

RESULTS

Activin-A and -B are highly expressed in malignant mesothelioma

Activins are known regulators of inflammation and tissue repair processes [5,27]. Activin expression has also been linked to malignant and fibrotic conditions [7]. To analyze the expression of activin-A and -B in mesothelioma, tissue biopsies from patients were stained with specific antibodies against inhibin β_A and β_B subunits. Immunoreactivity for both activins was abundantly detected in mesothelioma tumors (Fig. 1A). All tumor samples (n=10) were positive for both activins. In 8 out of 10 samples the immunoreactivity of activin-A was stronger compared to the immunoreactivity of activin-B (Table 2). The immunoreactivity localized into the mesothelioma tumor cells, while the stroma was mainly negative. Capillary endothelium in the stroma was found positive. In addition, normal and reactive pleura showed immunoreactivity for both activins (not shown). Tumor cells were also positive for follistatin immunoreactivity, which was observed in a more heterogeneous pattern (Table 2). In addition to tumor cells, follistatin was detected in the stroma, endothelium and strongly in normal and reactive pleura (not shown).

We have previously described isolation and culture of primary mesothelioma cells from patients' pleural effusion samples [25]. The cells retain gene expression characteristics of the tumor at early passage cultures. The mRNA expression levels of activin-A (*INHBA*) and -B (*INHBB*) in primary cells were analyzed using quantitative RT-PCR. Met5A cells, immortalized but non-tumorigenic mesothelial cells that were used as controls, expressed both activin-A and -B. The levels of activin-

A were about 10-fold higher than activin-B levels (Fig. 1B). All primary mesothelioma cells expressed considerably higher levels of activins when compared to Met5A cells (Fig. 1B). Primary cells that overexpressed mainly activin-A were isolated from a patient with biphasic mesothelioma (JP4), while the other primary cells were from patients with epithelioid type mesothelioma. We also analyzed activin expression levels in established mesothelioma cell lines (211H, H2052, H28, H2452) and found that there was more heterogeneity in the expression levels of activin subunits compared to primary cells (Fig. 1C). In general, activin mRNA expression levels were significantly higher, especially in 211H and H2052 cell lines, than in Met5A cells. Interestingly, similar to what was found in JP4 primary cells we observed specific upregulation of the activin-A subunit in the 211H cell line, which is also isolated from a patient with biphasic mesothelioma. Secretion of activin subunits into the culture media was analyzed by Western blot analysis and found to correlate with the mRNA expression data (Fig. 1D).

Follistatin and follistatin like-3 (FSTL-3) are extracellular inhibitors of TGF-β family growth factors. They can bind to all activins and inhibit their biological functions [10]. The mRNA expression levels of FST and FSTL3 in mesothelioma cells were analyzed next. In primary mesothelioma cells FST expression levels were downregulated, in some cells (JP1 and JP4) more clearly than in others. FSTL3 mRNA expression levels were elevated in 3 out of 4 primary mesothelioma cells (Fig. 1E). In the established mesothelioma cell lines FST and FSTL3 expression levels showed more variability. FST levels were downregulated in H28 and H2452 cell lines, while upregulated in 211H and H2052 cell lines (Fig. 1F). FSTL3 mRNA expression levels tended to decrease, which is in contrast to what was observed in the primary cells. Secretion of FST into the culture media was analyzed by Western blot analysis and found to correlate with the mRNA expression data (Fig. 1D).

ALK7 and ACVR2A are overexpressed in mesothelioma cells

The cells' sensitivity to activins and other TGF-β superfamily growth factors is defined by cell surface receptor expression and the specificity of the signal is defined by the type 1 receptor [12]. Both activin-A and -B activate Smad2/3 pathway through ALK4 [12]. In addition, activin-B can activate Smad2/3 pathway through ALK7 [13,14] and Smad1/5/8 pathway through ALK3 [15]. The activin receptor mRNA expression levels were analyzed using quantitative RT-PCR. Met5A cells expressed activin type 1 receptors ALK3 and ALK4 and very low levels of ALK7 (Fig. 2A). Overall, ALK3 and ALK4 mRNA expression levels were not consistently altered in primary mesothelioma cells or in established mesothelioma cell lines (Fig. 2A and C). However, ALK7 receptor expression was highly increased in primary mesothelioma cells (Fig. 2B). In addition, all the established mesothelioma cell lines showed higher levels of ALK7 when compared to Met5A cells (Fig. 2D).

Met5A cells expressed both activin type 2 receptors ACVR2A and ACVR2B. The levels of receptor 2B were about 3-fold higher than receptor 2A expression levels (Fig. 2E and F). This is in contrast to what was observed in all primary mesothelioma cells. The 2A receptor expression levels increased significantly, while receptor 2B levels decreased (~13-fold higher level of receptor 2A

compared to receptor 2B on average) (Fig. 2E), suggesting that there is a switch in the predominant type 2 receptor in mesothelioma cells. This was also noted in 3 out of 4 established mesothelioma cell lines (Fig. 2F). The H28 cell line was the only one showing elevated levels of both type 2 receptors.

Mesothelioma cells have altered Smad activation in response to activins

Activin-A and -B induced Smad responses were studied in mesothelioma cells using transient transfection of Smad3 responsive [$(CAGA)_{12}$-luc], Smad2 responsive [ARE-luc] or Smad1/5 responsive [$(Bre)_2$-luc] promoter-luciferase constructs followed by overnight stimulation by activin-A or -B (see Methods). Basal Smad3 activity was somewhat higher in primary cells (JP5) compared to established mesothelioma cell lines or Met5A cells (Fig. 3A). Smad3 activity increased ~80-fold in activin-A and ~60-fold in activin-B treated Met5A cells (Fig. 3B). The H28 mesothelioma cell line showed similar responses. In contrast, H2052 and 211H cell lines as well as JP5 primary cells had strongly attenuated activin induced Smad3 activation.

Basal Smad2 activity differed between the cells. Significantly lower basal Smad2 activity was observed in 211H and H2052 cells (Fig. 3C). Both activins induced Smad2 activity in Met5A cells. Induction of activity was also observed in 211H cells, whereas H2052 and H28 cells showed only a moderate 2-fold increase in Smad2 activity in response to activin-A and -B (Figure 3D). In JP5 primary cells activins failed to induce Smad2 activity.

A tendency towards higher basal Smad1/5 activity levels were noted in JP5 primary cells as well as in 211H and H2052 cells compared to Met5A cells (Fig. 3E). H28 cell line showed significantly increased basal level Smad1/5 activity. Interestingly, activin-B increased Smad1/5 activity in this particular cell line, but not in any other cells tested (Fig. 3F).

Mesothelioma cells differ in migratory capacity

To analyze the migratory capacity of established mesothelioma cell lines, a scratch-wound assay was performed. Cell migration was monitored using a live-cell imaging system (see Methods). Clear differences in mesothelioma cell migration were observed (Fig. 4A). H2052 and 211H cells migrated efficiently to close the wound. These two cell lines exhibited increased mRNA and protein expression of activin-A as well as altered Smad3 signaling responses. H2452 cells were less migratory and H28 cells were able to close the wound only after extended periods of time (Fig. 4A). Migration of 211H cells reduced with addition of a soluble activin inhibitor (sActR2B-Fc), suggesting that endogenous activins contribute to 211H mesothelioma cell migration (Fig. 4B and C). The migratory capacity of JP5 primary cells was measured using a scratch-wound assay and imaging at 0, 6, 24 and 48 hour time points. JP5 cells were also found to migrate rapidly. Treatment with the activin inhibitor sActR2B-Fc clearly delayed wound closure (Fig. 4 D and E). Similar to what was observed in 211H cells the inhibition was clearly detectable at 24 hours (Fig. 4D) and was sustained at 48 hours, when sActR2B-Fc treated wounds were approximately half as dense as the untreated control wounds (Fig. 4E).

Migratory mesothelioma cells also show invasive growth in 3D

To analyze the invasive growth of mesothelioma cell lines, they were seeded into 3D matrices and monitored for 36 hours (see Methods). The highly migratory cell lines 211H and H2052 were able to form irregular shaped spheroids and invade through the Matrigel forming a network of sprouts (Fig. 5A), whereas H28 and H2452 cells were unable to do this. Next we analyzed whether activin signals contribute to invasive growth. The cells were pretreated with sActR2B-Fc, which binds and inhibits the action of both activin-A and -B, before they were seeded into Matrigel. Interestingly, addition of sActR2B-Fc was able to inhibit the invasive growth of 211H and H2052 mesothelioma cell lines (Fig. 5B, C) as well as JP5 primary cells (Fig. 5D). Addition of a soluble anti-Müllerian hormone receptor (sAMHR2-Fc), which was used as a control treatment, had no impact on invasive growth (Fig. 5B). These results suggest that activins contribute to the invasive growth properties of mesothelioma cells.

ERK activity contributes to mesothelioma cell migration and invasive growth

Activins can also induce non-canonical signaling pathways. These include the ERK and JNK MAP kinase pathways, which have been shown to contribute to cell migration [17,20]. ERK phosphorylation, i.e., activation was analyzed by Western blotting after treatment of cells with activin-A or -B for 90 minutes. In Met5A control cells activins did not induce ERK phosphorylation, instead, pERK levels seemed to decrease. In contrast, in H2052 and JP5 primary cells activins induced robust ERK phosphorylation (Fig. 6A). Activin-A seemed to induce a stronger response than activin-B. To determine whether endogenous activins support ERK activation, mesothelioma cells were treated with the soluble activin inhibitor sActR2B-Fc. In all migratory and invasive mesothelioma cells (211H, H2052 and JP5) sActR2B-Fc treatment reduced ERK phosphorylation levels significantly (Fig. 6B and C). Due to a limited possibility to do experiments with early passage primary cells (n=2), the decrease in JP5 cells did not, however, reach statistical significance. In the other cell lines (Met5A, H28 or H2452) treatment with sActR2B-Fc did not lead to similar reduction in ERK phosphorylation (not shown). No significant changes in JNK1/2 phosphorylation in response to activin stimulation were detected (not shown).

To analyze the involvement of ERK activity in mesothelioma cell migration a scratch-wound assay was performed in the presence or absence of an inhibitor of the upstream kinase MEK (PD98059). In JP5 primary cells as well as in 211H and H2052 cells wound closure was considerably delayed by the MEK inhibitor (Fig. 6D and E). Compared to DMSO treated control cells, in MEK inhibitor treated 211H and JP5 primary cells a significantly delayed wound closure was observed at 48 hours. In H2052 cells the delay in wound closure was significant already at 6 hours when the wounds were approximately half as dense as the control wounds (Fig. 6E). Unlike in the DMSO treated control, H2052 wounds remained open in the presence of the MEK inhibitor at 24 hours (Fig. 6D). Activin-A increased H2052 cell migration. After six hours, the wounds were approximately twice as dense as the control wounds (Fig. 6F and G). Treatment with the MEK inhibitor significantly delayed the wound closure also in activin-A stimulated cells (Fig. 6F and G).

The contribution of ERK pathway activity to the invasive growth of mesothelioma cells was analyzed next. Cells were pretreated with the MEK inhibitor or DMSO, after which the cells were seeded into 3D matrices. Inhibition of ERK pathway activity significantly inhibited invasive growth of 211H and JP5 primary cells (Fig. 6 H). This was similar to what was observed with sActR2B-Fc. In addition, H2052 cells showed a similar trend of decreased ability for invasive growth (not shown). However, this observation was not so clear due to the sensitivity of H2052 cells to DMSO control treatment in a three-dimensional setting. Taken together, our data suggest that inhibition of ERK activity efficiently prevents mesothelioma cell invasive growth.

DISCUSSION

TGF-β family growth factors have an important role during development and adult tissue homeostasis. There is also ample evidence linking aberrant growth factor activity to cancer progression [28]. TGF-β activity has been linked to mesothelioma, but the role of activins is less well understood. There is one study showing overexpression of activin-A in mesothelioma and suggesting a function in the regulation of mesothelioma cell proliferation [8]. Here, we provide evidence that activin-A and activin-B are important regulators of mesothelioma cell migration and invasive growth properties. By blocking activin activity using a soluble inhibitor, we can efficiently inhibit invasive growth in a three-dimensional culture system. Mesothelioma cells showed a clear difference in signaling responses to activins, which may be a key mechanism for the invasive growth inducing activity. Similar to what has been described for TGF-β [29,30], we speculate that increased activin production and altered signaling responses in malignant cells mediate a switch in their function from a tumor suppressor to a tumor promoter. Interestingly, suppression of Smad activity and concomitant increase in ERK activation has been suggested to mediate the switch in TGF-β function during tumor progression [31].

All mesothelioma tumors showed consistently high immunoreactivity for activin-A, which is in agreement with a previous report [8]. In addition, activin-B immunoreactivity was observed in all tumors. Immunoreactivity for the activin inhibitor follistatin, on the other hand, was more variable and not consistently altered in tumors. We have analyzed primary mesothelioma tumor cells isolated from pleural effusion samples [25] and found very consistent changes in the activin signaling pathway. Established mesothelioma cell lines showed clearly more heterogeneity, which suggests that it is important to use cell lines with similar characteristics as the primary tumors in mechanistic studies. Primary mesothelioma cells and migratory and invasive mesothelioma cell lines showed increased expression of activin-A, activin-B, ALK7 and ACVR2A, as well as ERK activation and attenuated Smad2/3 signaling responses. These alterations were clearly associated with a migratory and invasive growth phenotype, which could be blocked using a soluble activin inhibitor (sActR2B-Fc) or MEK inhibitor.

Activins can use different receptor heterodimers to mediate signaling. We found a significant upregulation of ALK7 receptor in mesothelioma. As ALK7 is an activin-B preferring receptor coexpression of ACVR2 and ALK7 should provide sensitivity to activin-B. In addition to activin-B also Nodal is a ligand for ALK7 [32]. Nodal is a developmental morphogen, which has been linked

to cancer stem cell phenotype, epithelial-to-mesenchymal transition and invasion in other malignancies [33]. The possible role of Nodal in mesothelioma remains to be elucidated. Another interesting finding was a switch from a predominant expression of type 2 receptor ACVR2B to ACVR2A. This may lead to changes in activin mediated intracellular signaling and function as an adaptation mechanism required for cells to escape growth/invasion limiting actions of activins. Since activin type 2 receptors are involved in a variety of receptor signaling complexes, the switch of the predominantly expressed receptor may also alter responses to other TGF-β family ligands. We observed a clear association of type 2 receptor expression profile with loss of Smad3 responsiveness and migratory and invasive phenotype. H28 mesothelioma cells did not show this receptor swich, were sensitive to Smad3 activation and did not show high migratory or invasive growth phenotype. H28 cells have been shown to lack β-catenin [34], which is not a typical feature of mesothelioma [35]. This suggests that H28 is a unique mesothelioma cell line.

Activins can induce inhibition of proliferation and apoptosis [5]. Cancer cells can avoid these suppressive functions through various mechanisms. Loss of the CDKN2A/ARF locus is the most common genetic alteration in mesothelioma and leads to inactivation of the $p16^{INK4a}$ tumor suppressor gene [36]. This may also reduce activin induced apoptotic responses [37]. Smad-mediated signaling is also crucial for activin induced growth arrest [38]. We have shown here a clear transformation in activin induced intracellular signaling cascades in mesothelioma cells. Smad3 activation, measured using a promoter assay, was almost lost in migratory and invasive mesothelioma cells, while Smad2 activation was partially retained in some cell lines. In addition, TGF-β was still able to induce Smad3 activation (our unpublished data), suggesting an activin specific loss of responsiveness. Higher follistatin expression levels in established mesothelioma cell lines could not explain the loss of responsiveness, since activins induced a robust ERK activation in H2052 cells. Furthermore, JP5 primary cells had low levels of follistatin expression but attenuated Smad3 activation. We have previously shown high P-Smad2 immunoreactivity in mesothelioma tumor samples [39], but P-Smad3 levels *in vivo* have not been specifically analyzed and remain to be determined.

Previously it has been observed that activin-B induces skin wound re-epithelialization through Smad3-independent mechanisms [40]. This is also demonstrated by accelerated wound healing in Smad3 knockout mice [41]. The ERK pathway has been found important for activin induced epithelial wound healing [40]. The migratory and invasive growth phenotype in mesothelioma cells was also clearly associated with activin induced ERK activity, since inhibition of both activin-A and -B by using a soluble type 2 receptor reduced levels of ERK phosphorylation and migration and invasive growth in 3D matrix. Similar effects were observed when ERK phosphorylation was blocked with an inhibitor of the upstream kinase MEK. ERK is one of the well-known activators of cyclin D [42]. Our results are in agreement with a report by Hoda et al. (2012) [8] suggesting that activin-A can also function through cyclin D in mesothelioma. The ERK pathway is involved in the regulation of cell cycle progression, apoptosis and differentiation. It is also commonly activated in tumors [43]. ERK is known to be highly activated in mesothelioma [44] and central to mesothelioma cell migration, proliferation as well as tumor development and chemoresistance [45]. In addition to TGF-β family ligands, receptor tyrosine kinases can contribute to ERK pathway

activity in mesothelioma cells. Fibroblast growth factor receptor (FGFR)1 was recently found upregulated in mesothelioma cells and in patient samples [46]. Inhibition of growth caused by FGFR inhibition was associated with downregulation of basal ERK activity [46].

The exact molecular mechanism of the swich from Smad3 signaling to ERK pathway signaling in activin responsive mesothelioma cells remains to be elucidated. Changes in activin type 2 receptor expression profile may contribute to this switch. Downregulation of TGF-β type 2 receptor has been implicated in the loss of responsiveness to the anti-proliferative effects of TGF-β in lung cancer cells [47]. In addition to changes in receptor expression, it has been suggested that a specific isoform of PP2A is differentially recruited to TGF-β type 1 receptor in normal and malignant cells leading to differential activation of ERK [31]. Similar mechanisms may play a role in the observed activin pathway alterations.

Mesotheliomas are characterized with aggressive and locally invasive phenotypes. Understanding of the mechanisms that the tumor invasion is vital for the development of treatment strategies. Cancer cells and the tumor microenvironment both contribute to the invasive phenotype of the tumors. We have shown here that mesothelioma cells produce activin-A and -B, which both contribute to the invasive and migratory phenotype of the cancer cells. High expression levels of activins are associated with attenuation of the canonical Smad3 signaling and increase in non-canonical ERK signaling responses. Similar changes in the signaling pathways have been associated with the function of TGF-β as a tumor promoter in cancer cells [31]. In conclusion, inhibition of activin or ERK activity, or both, represents a therapeutic approach for inhibition of invasive mesothelioma tumors. Novel inhibitors of activin signaling are under development for clinical use, which makes activins a plausible target for adjunctive therapy in mesothelioma.

ACKNOWLEDGEMENTS

We thank Emma Paasikivi and Sami Starast for excellent technical assistance and the Biomedicum Imaging Unit for imaging support.

REFERENCES

[1] Mossman BT, Shukla A, Heintz NH, Verschraegen CF, Thomas A, Hassan R, New insights into understanding the mechanisms, pathogenesis, and management of malignant mesotheliomas, Am J Pathol. 182 (2013) 1065-1077.

[2] Huuskonen MS, Rantanen J, Finnish Institute of Occupational Health (FIOH): prevention and detection of asbestos-related diseases, 1987-2005, Am J Ind Med. 49 (2006) 215-220.

[3] Vorobiof DA, Mafafo K, Malignant pleural mesothelioma: medical treatment update, Clin Lung Cancer. 10 (2009) 112-117.

[4] Vale W, Wiater E, Gray P, Harrison C, Bilezikjian L, Choe S, Activins and inhibins and their signaling, Ann N Y Acad Sci. 1038 (2004) 142-147.

[5] Antsiferova M, Werner S, The bright and the dark sides of activin in wound healing and cancer, J Cell Sci. 125 (2012) 3929-3937.
[6] Panopoulou E, Murphy C, Rasmussen H, Bagli E, Rofstad EK, Fotsis T, Activin A suppresses neuroblastoma xenograft tumor growth via antimitotic and antiangiogenic mechanisms, Cancer Res. 65 (2005) 1877-1886.
[7] Hedger MP, de Kretser DM, The activins and their binding protein, follistatin-Diagnostic and therapeutic targets in inflammatory disease and fibrosis, Cytokine Growth Factor Rev. 24 (2013) 285-295.
[8] Hoda MA, Munzker J, Ghanim B, Schelch K, Klikovits T, Laszlo V, Sahin E, Bedeir A, Lackner A, Dome B, Setinek U, Filipits M, Eisenbauer M, Kenessey I, Torok S, Garay T, Hegedus B, Catania A, Taghavi S, Klepetko W, Berger W, Grusch M, Suppression of activin A signals inhibits growth of malignant pleural mesothelioma cells, Br J Cancer. 107 (2012) 1978-1986.
[9] Walton KL, Makanji Y, Harrison CA, New insights into the mechanisms of activin action and inhibition, Mol Cell Endocrinol. 359 (2012) 2-12.
[10] Schneyer A, Sidis Y, Xia Y, Saito S, del Re E, Lin HY, Keutmann H, Differential actions of follistatin and follistatin-like 3, Mol Cell Endocrinol. 225 (2004) 25-28.
[11] Tsuchida K, Arai KY, Kuramoto Y, Yamakawa N, Hasegawa Y, Sugino H, Identification and characterization of a novel follistatin-like protein as a binding protein for the TGF-β family, J Biol Chem. 275 (2000) 40788-40796.
[12] Itoh S, Itoh F, Goumans MJ, Ten Dijke P, Signaling of transforming growth factor-β family members through Smad proteins, Eur J Biochem. 267 (2000) 6954-6967.
[13] Bernard DJ, Lee KB, Santos MM, Activin B can signal through both ALK4 and ALK7 in gonadotrope cells, Reprod Biol Endocrinol. 4 (2006) 52.
[14] Tsuchida K, Nakatani M, Yamakawa N, Hashimoto O, Hasegawa Y, Sugino H, Activin isoforms signal through type I receptor serine/threonine kinase ALK7, Mol Cell Endocrinol. 220 (2004) 59-65.
[15] Besson-Fournier C, Latour C, Kautz L, Bertrand J, Ganz T, Roth MP, Coppin H, Induction of activin B by inflammatory stimuli up-regulates expression of the iron-regulatory peptide hepcidin through Smad1/5/8 signaling, Blood. 120 (2012) 431-439.
[16] Moustakas A, Heldin CH, Non-Smad TGF-β signals, J Cell Sci. 118 (2005) 3573-3584.
[17] Huang HM, Chang TW, Liu JC, Basic fibroblast growth factor antagonizes activin A-mediated growth inhibition and hemoglobin synthesis in K562 cells by activating ERK1/2 and deactivating p38 MAP kinase, Biochem Biophys Res Commun. 320 (2004) 1247-1252.
[18] Zhang L, Deng M, Parthasarathy R, Wang L, Mongan M, Molkentin JD, Zheng Y, Xia Y, MEKK1 transduces activin signals in keratinocytes to induce actin stress fiber formation and migration, Mol Cell Biol. 25 (2005) 60-65.
[19] Zhang M, Liu NY, Wang XE, Chen YH, Li QL, Lu KR, Sun L, Jia Q, Zhang L, Activin B promotes epithelial wound healing in vivo through RhoA-JNK signaling pathway, PLoS One. 6 (2011) e25143.
[20] Zhang M, Sun L, Wang X, Chen S, Jia Q, Liu N, Chen Y, Kong Y, Zhang L, Zhang AL, Activin B promotes BM-MSC-mediated cutaneous wound healing by regulating cell migration via the JNK-ERK signaling pathway, Cell Transplant. (2013).
[21] Thompson TB, Cook RW, Chapman SC, Jardetzky TS, Woodruff TK, Beta A versus beta B: is it merely a matter of expression?, Mol Cell Endocrinol. 225 (2004) 9-17.
[22] Hulmi JJ, Oliveira BM, Silvennoinen M, Hoogaars WM, Ma H, Pierre P, Pasternack A, Kainulainen H, Ritvos O, Muscle protein synthesis, mTORC1/MAPK/Hippo signaling, and capillary density are altered by blocking of myostatin and activins, Am J Physiol Endocrinol Metab. 304 (2013) E41-50.
[23] Leppäranta O, Sens C, Salmenkivi K, Kinnula VL, Keski-Oja J, Myllärniemi M, Koli K, Regulation of TGF-β storage and activation in the human idiopathic pulmonary fibrosis lung, Cell Tissue Res. 348 (2012) 491-503.
[24] Ke Y, Reddel RR, Gerwin BI, Reddel HK, Somers AN, McMenamin MG, LaVeck MA, Stahel RA, Lechner JF, Harris CC, Establishment of a human in vitro mesothelial cell model system for investigating mechanisms of asbestos-induced mesothelioma, Am J Pathol. 134 (1989) 979-991.
[25] Tamminen JA, Parviainen V, Rönty M, Wohl AP, Murray L, Joenväära S, Varjosalo M, Leppäranta O, Ritvos O, Sengle G, Renkonen R, Myllärniemi M, Koli K, Gremlin-1 associates with fibrillin microfibrils in vivo and regulates mesothelioma cell survival through transcription factor slug, Oncogenesis. 2 (2013) e66.
[26] Tamminen JA, Myllärniemi M, Hyytiäinen M, Keski-Oja J, Koli K, Asbestos exposure induces alveolar epithelial cell plasticity through MAPK/ Erk signaling, J Cell Biochem. 113 (2012) 2234-2247.
[27] Apostolou E, Stavropoulos A, Sountoulidis A, Xirakia C, Giaglis S, Protopapadakis E, Ritis K, Mentzelopoulos S, Pasternack A, Foster M, Ritvos O, Tzelepis GE, Andreakos E, Sideras P, Activin-A overexpression in the murine lung causes pathology that simulates acute respiratory distress syndrome, Am J Respir Crit Care Med. 185 (2012) 382-391.
[28] Wakefield LM, Hill CS, Beyond TGFβ: roles of other TGFβ superfamily members in cancer, Nat Rev Cancer. 13 (2013) 328-341.

[29] de Caestecker MP, Piek E, Roberts AB, Role of transforming growth factor-β signaling in cancer, J Natl Cancer Inst. 92 (2000) 1388-1402.
[30] Drabsch Y, ten Dijke P, TGF-β signalling and its role in cancer progression and metastasis, Cancer Metastasis Rev. 31 (2012) 553-568.
[31] Zhang Q, Yu N, Lee C, Mysteries of TGF-beta Paradox in Benign and Malignant Cells, Front Oncol. 4 (2014) 94.
[32] Tsuchida K, Nakatani M, Uezumi A, Murakami T, Cui X, Signal transduction pathway through activin receptors as a therapeutic target of musculoskeletal diseases and cancer, Endocr J. 55 (2008) 11-21.
[33] Quail DF, Siegers GM, Jewer M, Postovit LM, Nodal signalling in embryogenesis and tumourigenesis, Int J Biochem Cell Biol. 45 (2013) 885-898.
[34] Shigemitsu K, Sekido Y, Usami N, Mori S, Sato M, Horio Y, Hasegawa Y, Bader SA, Gazdar AF, Minna JD, Hida T, Yoshioka H, Imaizumi M, Ueda Y, Takahashi M, Shimokata K, Genetic alteration of the β-catenin gene (CTNNB1) in human lung cancer and malignant mesothelioma and identification of a new 3p21.3 homozygous deletion, Oncogene. 20 (2001) 4249-4257.
[35] Abutaily AS, Collins JE, Roche WR, Cadherins, catenins and APC in pleural malignant mesothelioma, J Pathol. 201 (2003) 355-362.
[36] Sekido Y, Molecular pathogenesis of malignant mesothelioma, Carcinogenesis. 34 (2013) 1413-1419.
[37] Chen YG, Lui HM, Lin SL, Lee JM, Ying SY, Regulation of cell proliferation, apoptosis, and carcinogenesis by activin, Exp Biol Med (Maywood). 227 (2002) 75-87.
[38] Ten Dijke P, Goumans MJ, Itoh F, Itoh S, Regulation of cell proliferation by Smad proteins, J Cell Physiol. 191 (2002) 1-16.
[39] Vehviläinen P, Koli K, Myllärniemi M, Lindholm P, Soini Y, Salmenkivi K, Kinnula VL, Keski-Oja J, Latent TGF-β binding proteins (LTBPs) 1 and 3 differentially regulate transforming growth factor-β activity in malignant mesothelioma, Hum Pathol. 42 (2011) 269-278.
[40] Deng M, Chen WL, Takatori A, Peng Z, Zhang L, Mongan M, Parthasarathy R, Sartor M, Miller M, Yang J, Su B, Kao WW, Xia Y, A role for the mitogen-activated protein kinase kinase kinase 1 in epithelial wound healing, Mol Biol Cell. 17 (2006) 3446-3455.
[41] Ashcroft G S, Yang X, Glick AB, Weinstein M, Letterio J L, Mizel DE, Anzano M, Greenwell-Wild T, Wahl SM, Deng C, Roberts AB, Mice lacking Smad3 show accelerated wound healing and an impaired local inflammatory response, Nat Cell Biol. 1 (1999) 260-266.
[42] Klein EA, Assoian RK, Transcriptional regulation of the cyclin D1 gene at a glance, J Cell Sci. 121 (2008) 3853-3857.
[43] McCubrey JA, Steelman LS, Chappell WH, Abrams SL, Wong EW, Chang F, Lehmann B, Terrian DM, Milella M, Tafuri A, Stivala F, Libra M, Basecke J, Evangelisti C, Martelli AM, Franklin RA, Roles of the Raf/MEK/ERK pathway in cell growth, malignant transformation and drug resistance, Biochim Biophys Acta. 1773 (2007) 1263-1284.
[44] de Melo M, Gerbase MW, Curran J, Pache JC, Phosphorylated extracellular signal-regulated kinases are significantly increased in malignant mesothelioma, J Histochem Cytochem. 54 (2006) 855-861.
[45] Shukla A, Hillegass JM, MacPherson MB, Beuschel SL, Vacek PM, Pass HI, Carbone M, Testa JR, Mossman BT, Blocking of ERK1 and ERK2 sensitizes human mesothelioma cells to doxorubicin, Mol Cancer. 9 (2010) 314.
[46] Marek LA, Hinz TK, von Massenhausen A, Olszewski KA, Kleczko EK, Boehm D, Weiser-Evans MC, Nemenoff RA, Hoffmann H, Warth A, Gozgit JM, Perner S, Heasley LE, Nonamplified FGFR1 Is a Growth Driver in Malignant Pleural Mesothelioma, Mol Cancer Res. 12 (2014) 1460-1469.
[47] Halder SK, Cho YJ, Datta A, Anumanthan G, Ham AJ, Carbone DP, Datta PK, Elucidating the mechanism of regulation of transforming growth factor β Type II receptor expression in human lung cancer cell lines, Neoplasia. 13 (2011) 912-922.

FIGURE LEGENDS

Fig. 1
Activins are abundantly expressed in mesothelioma tumor tissue as well as in cultured mesothelioma cells. (A) Immunohistochemical staining of mesothelioma tumor samples using activin-A, activin-B or follistatin antibodies. See Table 2 for scoring of the staining intensity in tumors. The mRNA expression levels of activin-A (*INHBA*) and activin-B (*INHBB*) were analyzed in primary mesothelioma cells (B) and mesothelioma cell lines (C) using quantitative RT-PCR. The expression levels were normalized to the expression levels of TATA-binding protein and are shown relative to the expression levels of activin-A in Met5A cells. (D) Mesothelioma cell conditioned media were analyzed using Western blotting. The ~15 kDa activin-A monomer as well as ~55 kDa prodomain and ~30 kDa dimer of activin-B and follistatin (FST) are shown. Recombinant proteins used as positive controls (pos. ctrl) and molecular weight markers are shown on the right. The mRNA levels of follistatin (*FST*) and follistatin-like 3 (*FSTL3*) were analyzed in primary mesothelioma cells (E) and mesothelioma cell lines (F). The expression levels were normalized to the expression levels of TATA-binding protein and are shown relative to the expression levels of *FST* in Met5A cells. Error bars represent standard deviation (n=3).

Fig. 2
The expression of *ACVR2A* and *ALK7* is increased in mesothelioma cells. The mRNA expression levels of activin type 1 (*ALK3*, *ALK4* and *ALK7*) and type 2 (*ACVR2A* and *ACVR2B*) receptors were analyzed in primary mesothelioma cells (A, B, E) and in mesothelioma cell lines (C, D, F). The expression levels were normalized to the expression levels of TATA-binding protein and are shown relative to the expression levels of *ALK4* (A, C), *ALK7* (B, D) or *ACVR2A* (E, F) in Met5A cells. Error bars represent standard deviation (n=2). * $p \leq 0.025$ Kruskal-Wallis Test.

Fig. 3
Activin induced Smad3 activation is attenuated in mesothelioma cells. Met5A and mesothelioma cells were transfected with Smad3 (A, B), Smad2 (C, D) or Smad1/5 (E, F) responsive promoters and stimulated overnight with activin-A or -B. Promoter activity is shown relative to the level in Met5A cells. (A) Basal Smad3 activity was somewhat elevated in primary mesothelioma cells (JP5, n=2). (B) Activin induced Smad3 activation was dramatically decreased in primary mesothelioma cells and in 211H and H2052 cell lines (n=2). (C) Basal Smad2 activity was downregulated significantly in 211H and H2052 mesothelioma cells [**p=0.007 Kruskal-Wallis Test comparing all samples; *p=0.008 Mann-Whitney Test comparing two groups (Met5A vs. 211H and Met5A vs. H2052) ($n \geq 3$)]. (D) Activin-A and -B induced robust Smad2 activation in Met5A and 211H cells whereas other cells showed attenuated Smad2 response ($n \geq 2$). (E) Basal Smad1/5 activity was significantly increased in H28 cells and slightly increased in other mesothelioma cells [**p=0.006 Kruskal-Wallis Test ($n \geq 2$); *p=0.007 Mann-Whitney Test comparing two groups (Met5A vs. H28) ($n \geq 3$)]. (F) Activin-B induced Smad1/5 activation only in H28 cell line ($n \geq 3$). Error bars represent standard deviation.

Fig. 4
Inhibition of activin activity reduces mesothelioma cell migration. Cell migration was analyzed using a scratch-wound assay and monitored by 48-hour live cell imaging (A-C) or imaging at 0, 6, 24 and 48 hour time points (D, E). The results are presented as relative wound density. H2052 and 211H mesothelioma cells were found to rapidly close the wound. Inhibition of activin signaling using a soluble type 2 receptor (sActR2B-Fc) delayed wound closure in 211H cells. Error bars represent standard deviation (n=2). (C) Representative pictures of 211H cells at the 24 hour time point are shown. (D, E) Representative pictures of JP5 primary mesothelioma cell scratch-wound assay. Inhibition of activin signaling (by sActR2B-Fc) delayed wound closure in primary cells [p=0.1 Mann-Whitney Test, (n=3)]. Error bars represent standard deviation.

Fig. 5
Invasive growth of mesothelioma cells was analyzed in three-dimensional matrix. (A) 211H and H2052 cells, but not H28 and H2452 cells, embedded in Matrigel were able to form irregular shaped spheroids as well as invade and sprout through the surrounding matrix. (B-D) Inhibition of activin signaling (by sActR2B-Fc) prevented invasive growth of 211H, H2052 and JP5 primary cells. Soluble anti-Müllerian hormone receptor (sAMHR2-Fc) was used as a negative control and had no effect on invasive growth. Representative pictures are shown. Original magnification 100x. Inset: high magnification picture.

Fig. 6
ERK activity is essential for activin induced mesothelioma cell migration and invasive growth. (A) Cells were stimulated with activin-A or -B for 90 minutes and analyzed for ERK phosphorylation using Western blotting. (B, C) When mesothelioma cells were treated with sActR2B-Fc (90 minutes) to inhibit activin signaling, ERK phosphorylation levels decreased significantly [*p=0.029 Mann-Whitney Test (n=4); JP5 primary cells (n=2)]. (D) Representative pictures of 211H (48h), H2052 (24h) and JP5 (48h) scratch-wound assay are shown. (E) Compared to DMSO treated control cells MEK-inhibitor (PD98059) significantly delayed wound closure. H2052 cell wound density was analyzed at the 6 hour time point. JP5 primary and 211H cell wound density was analyzed at the 48 hour time point [*p=0.029 Mann-Whitney Test (n=4); JP5 primary cells, (n=3)]. Error bars represent standard deviation. (F) Representative pictures of H2052 scratch wound assay are shown. (G) H2052 cell wound density was analyzed at the 6 hour time point. The wound density in activin-A stimulated cells was twice as high compared to the DMSO treated control cells. The MEK-inhibitor (PD98059) significantly delayed wound closure in activin-A stimulation cells [*p=0.029 Mann-Whitney Test (n=4)]. (H) The effect of inhibition of ERK activity to mesothelioma cell invasive growth in three-dimensional matrix was analyzed using the MEK-inhibitor (PD98059). PD98059 prevented invasive growth of 211H and JP5 primary cells. Representative pictures are shown.

TABLES

Table 1. Mesothelioma patient characteristics.

Patient	Type	Location	Age	Gender
JP1	epithelial	pleura	53	male
JP2	biphasic	pleura	71	male
JP3	epithelial	pleura	63	male
JP4	biphasic	peritoneum	72	female
JP5	epithelial	pleura	69	female
JP6	biphasic	pleura	71	female
JP7	epithelial	pleura	62	male
JP8	epithelial	pleura	63	male
JP9	epithelial	pleura	54	male
JP10	epithelial	pleura	75	male
JP11	epithelial	pleura	65	male
JP12	epithelial	pleura	60	male

Table 2. Scoring of activin-A, activin-B and follistatin immunoreactivity in mesothelioma patient samples.

Patient	activin-A	activin-B	follistatin
JP2	+++	+++	++
JP3	+	+	++
JP5	+++	++	+
JP6	+++	+	++
JP7	+++	++	++
JP8	+++	+	++
JP9	++++	+++	+++
JP10	++	+	++
JP11	++++	++	+
JP12	++++	++	++

Extent of staining (score): no staining (0), weak staining (+), moderate staining (++), strong staining (+++) and very strong staining (++++).

Figure 1

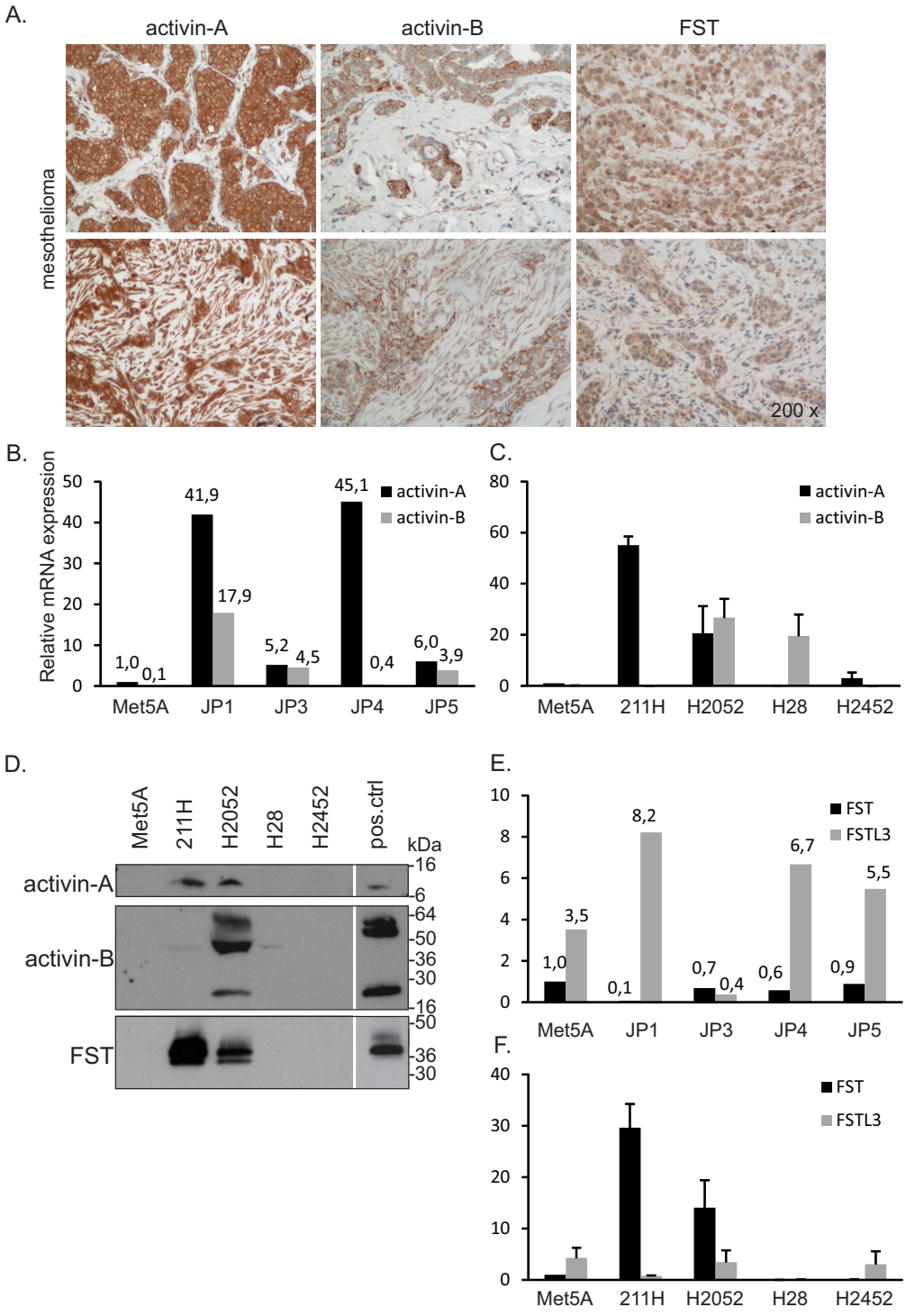
A.
activin-A
activin-B
FST
mesothelioma
200 x
B.
Relative mRNA expression
activin-A
activin-B
1,0
0,1
41,9
17,9
5,2
4,5
45,1
0,4
6,0
3,9
Met5A
JP1
JP3
JP4
JP5
C.
activin-A
activin-B
Met5A
211H
H2052
H28
H2452
D.
Met5A
211H
H2052
H28
H2452
pos.ctrl
kDa
activin-A
activin-B
FST
E.
FST
FSTL3
1,0
3,5
0,1
8,2
0,7
0,4
0,6
6,7
0,9
5,5
Met5A
JP1
JP3
JP4
JP5
F.
FST
FSTL3
Met5A
211H
H2052
H28
H2452

Figure 2

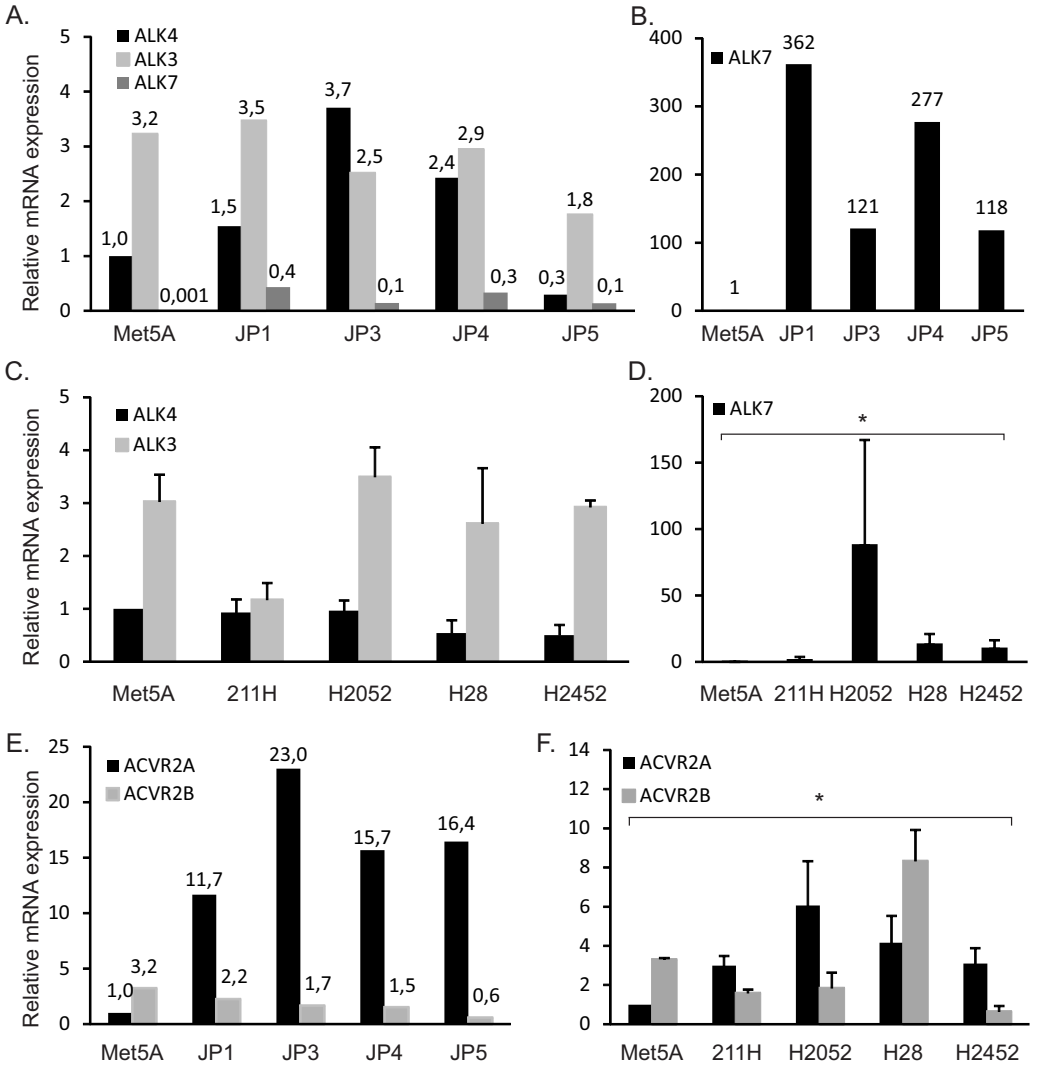
A.
ALK4
ALK3
ALK7
Relative mRNA expression
1,0
3,2
0,001
1,5
3,5
0,4
3,7
2,5
0,1
2,4
2,9
0,3
0,3
1,8
0,1
Met5A
JP1
JP3
JP4
JP5
B.
ALK7
1
362
121
277
118
Met5A
JP1
JP3
JP4
JP5
C.
ALK4
ALK3
Relative mRNA expression
Met5A
211H
H2052
H28
H2452
D.
ALK7
*
Met5A
211H
H2052
H28
H2452
E.
ACVR2A
ACVR2B
Relative mRNA expression
1,0
3,2
11,7
2,2
23,0
1,7
15,7
1,5
16,4
0,6
Met5A
JP1
JP3
JP4
JP5
F.
ACVR2A
ACVR2B
*
Met5A
211H
H2052
H28
H2452

Figure 3

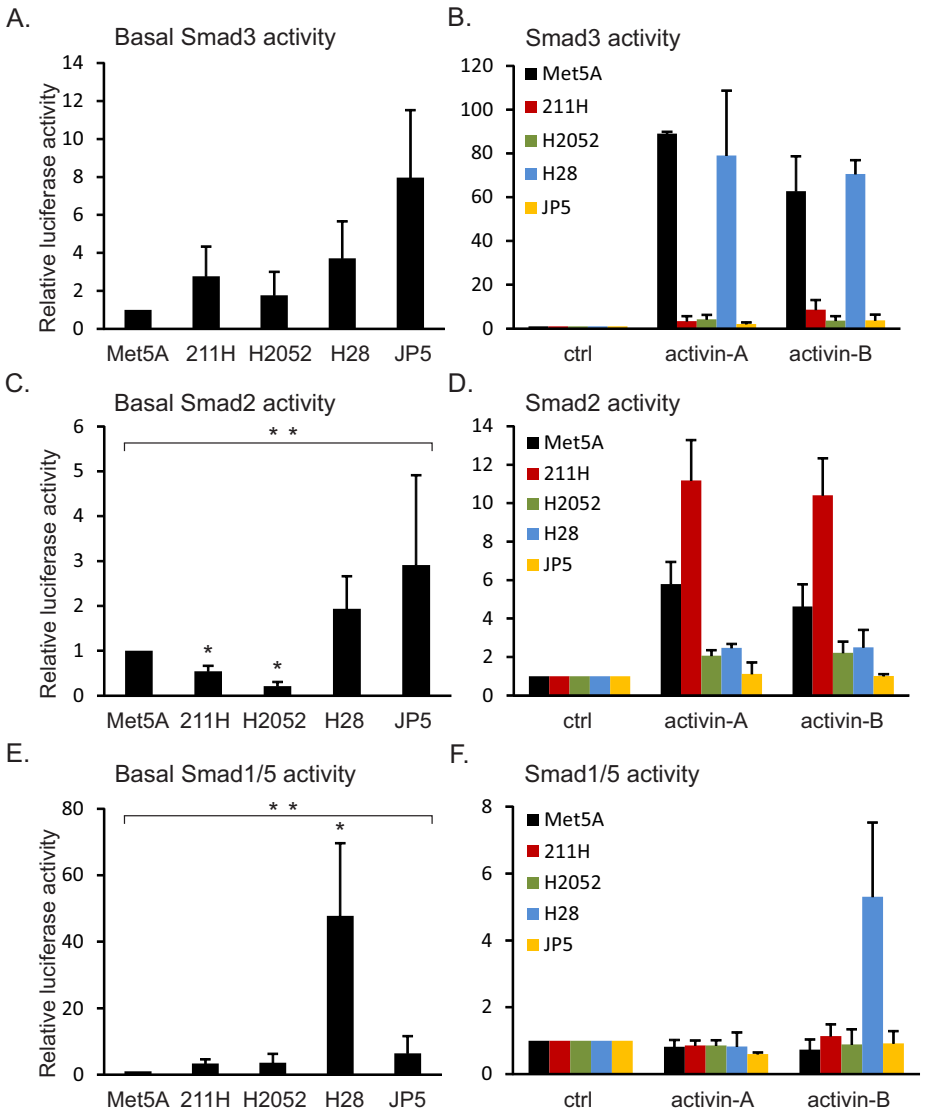
A.
Basal Smad3 activity
Relative luciferase activity
14
12
10
8
6
4
2
0
Met5A
211H
H2052
H28
JP5
B.
Smad3 activity
120
100
80
60
40
20
0
Met5A
211H
H2052
H28
JP5
ctrl
activin-A
activin-B
C.
Basal Smad2 activity
Relative luciferase activity
6
5
4
3
2
1
0
* *
*
*
Met5A
211H
H2052
H28
JP5
D.
Smad2 activity
14
12
10
8
6
4
2
0
Met5A
211H
H2052
H28
JP5
ctrl
activin-A
activin-B
E.
Basal Smad1/5 activity
Relative luciferase activity
80
60
40
20
0
* *
*
Met5A
211H
H2052
H28
JP5
F.
Smad1/5 activity
8
6
4
2
0
Met5A
211H
H2052
H28
JP5
ctrl
activin-A
activin-B

Figure 4

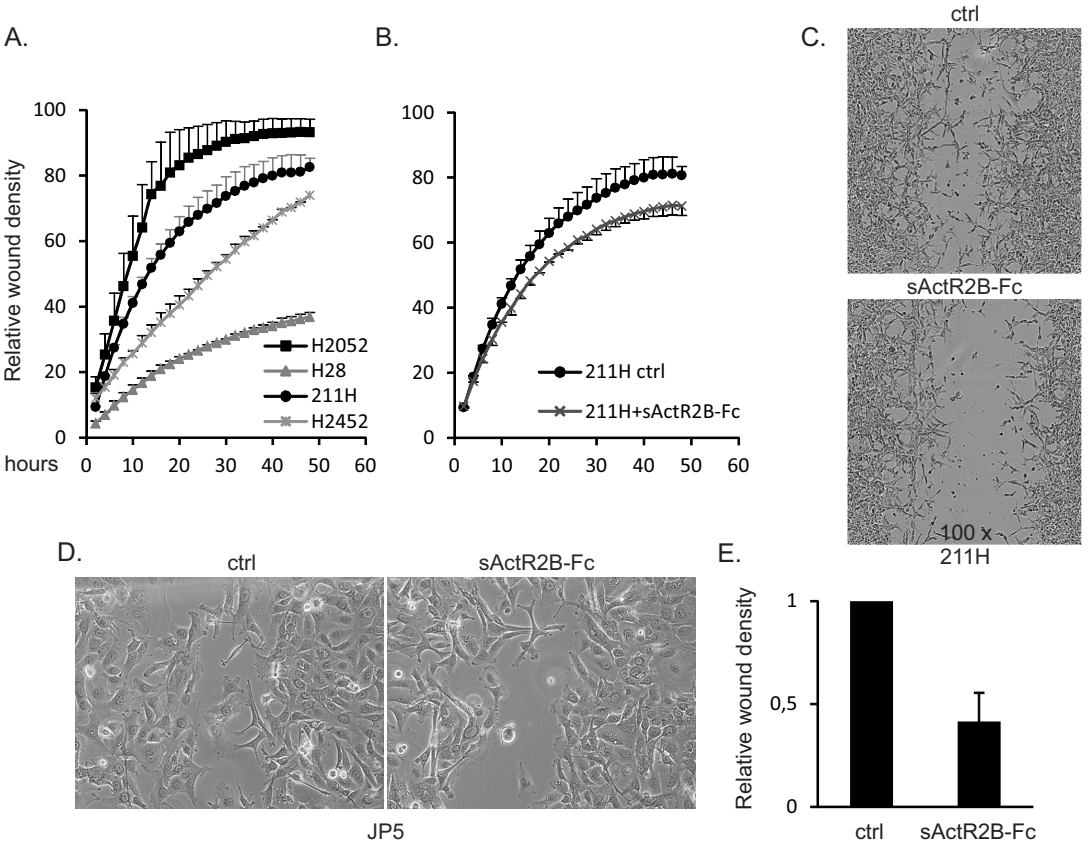
A.
B.
C.
ctrl
sActR2B-Fc
100 x
211H
Relative wound density
hours
H2052
H28
211H
H2452
211H ctrl
211H+sActR2B-Fc
D.
ctrl
sActR2B-Fc
JP5
E.
Relative wound density
ctrl
sActR2B-Fc

Figure 5

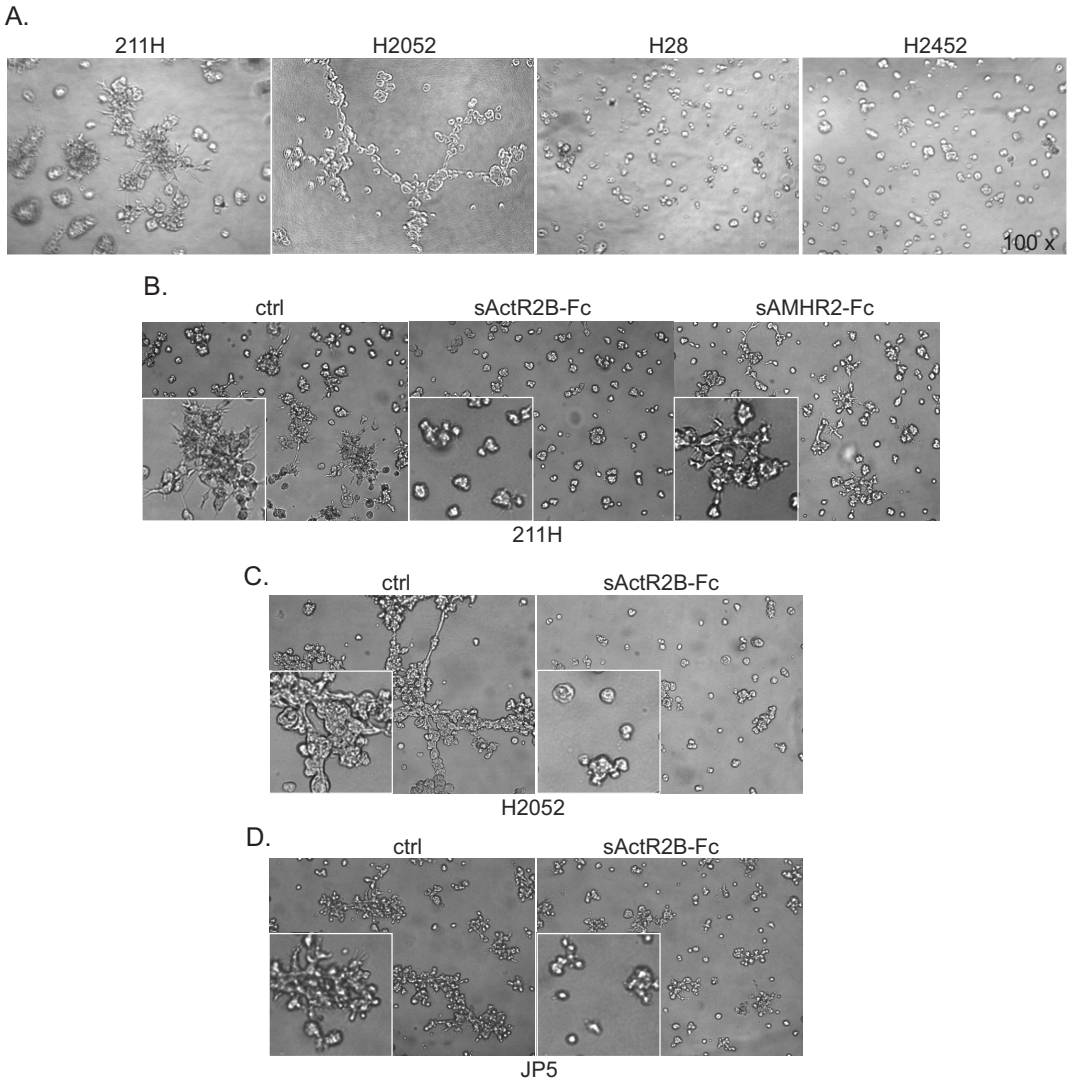
A.
211H
H2052
H28
H2452
100 x
B.
ctrl
sActR2B-Fc
sAMHR2-Fc
211H
C.
ctrl
sActR2B-Fc
H2052
D.
ctrl
sActR2B-Fc
JP5

Figure 6

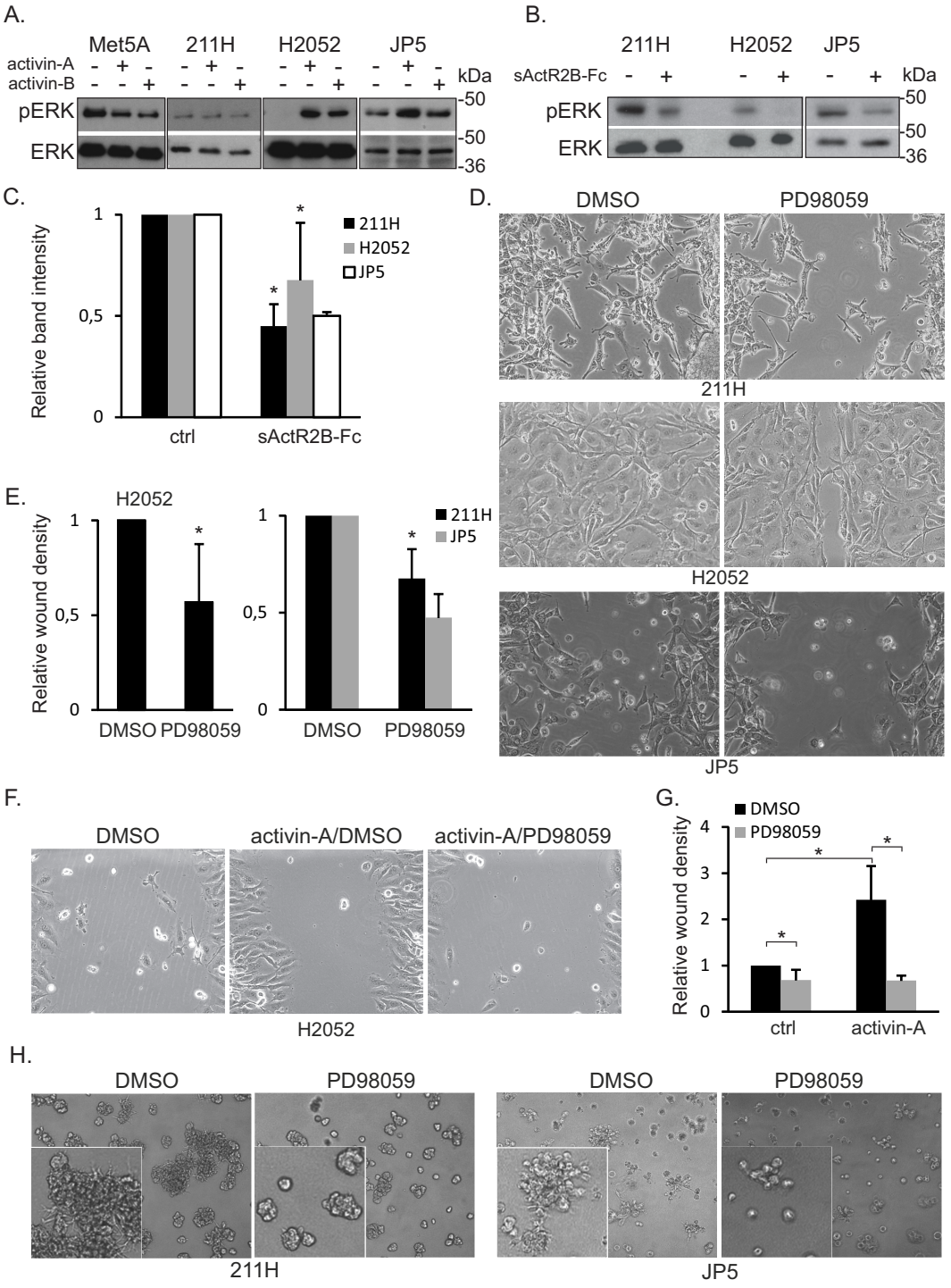
A.
Met5A
211H
H2052
JP5
activin-A
activin-B
kDa
pERK
ERK
50
50
36
B.
211H
H2052
JP5
sActR2B-Fc
kDa
pERK
ERK
50
50
36
C.
Relative band intensity
1
0,5
0
211H
H2052
JP5
ctrl
sActR2B-Fc
D.
DMSO
PD98059
211H
H2052
JP5
E.
H2052
Relative wound density
1
0,5
0
DMSO
PD98059
211H
JP5
DMSO
PD98059
F.
DMSO
activin-A/DMSO
activin-A/PD98059
H2052
G.
DMSO
PD98059
Relative wound density
4
3
2
1
0
ctrl
activin-A
H.
DMSO
PD98059
DMSO
PD98059
211H
JP5